MAX-PLANCK-INSTITUT

Topology, Magnetism und Chirality

Claudia Felser, MPI CPfS
felser@cpfs.mpg.de

Claudia Felser, Johannes Gooth, Topology and Chirality, arXiv:2205.05809

topology

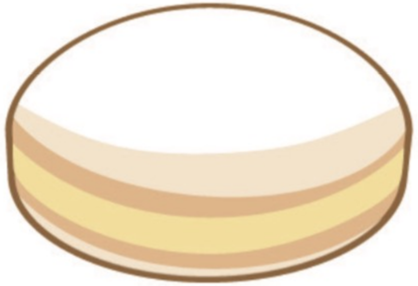

Genius g = 0

g = 1

g = 3

Gauss–Bonnet Theorem:

$$\chi = 2(1 - g) = \frac{1}{2\pi}\int K.dS$$

C. F. Gauss, , Werke , 8 , K. Gesellschaft Wissenschaft. Göttingen (1900)
O. Bonnet, J. École Polytechnique , 19 (1848) pp. 1–146
J. Kroder, et al., Chemie in unserer Zeit 56 (2022) 12–20

topology

from molecule to solid

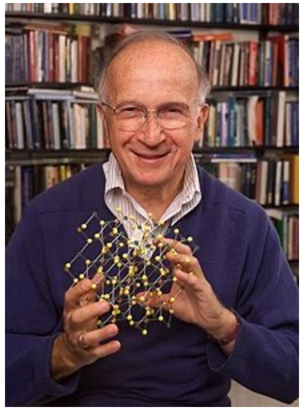

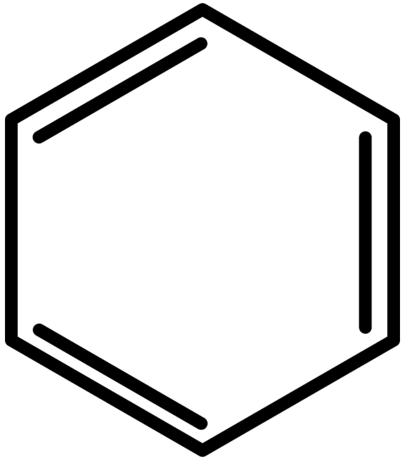

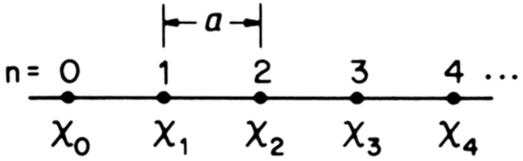

$$\psi_k = \sum_n e^{ikna} \chi_n$$

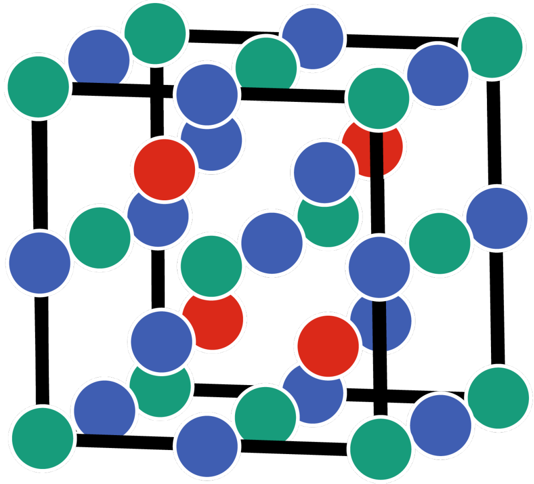

from orbitals to bands

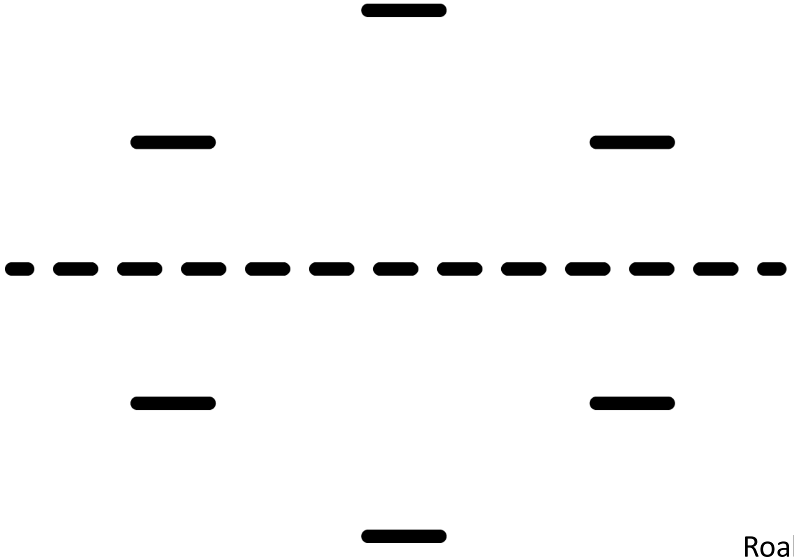

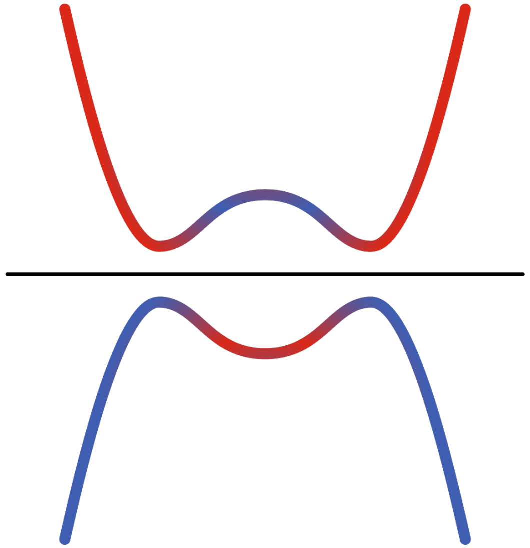

Roald Hoffmann Angewandte. Chem. 26 (1987) 846

from benzen to graphene

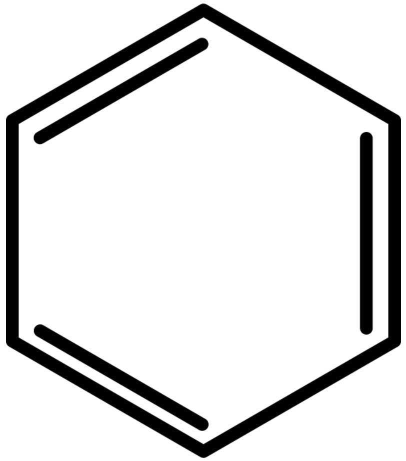

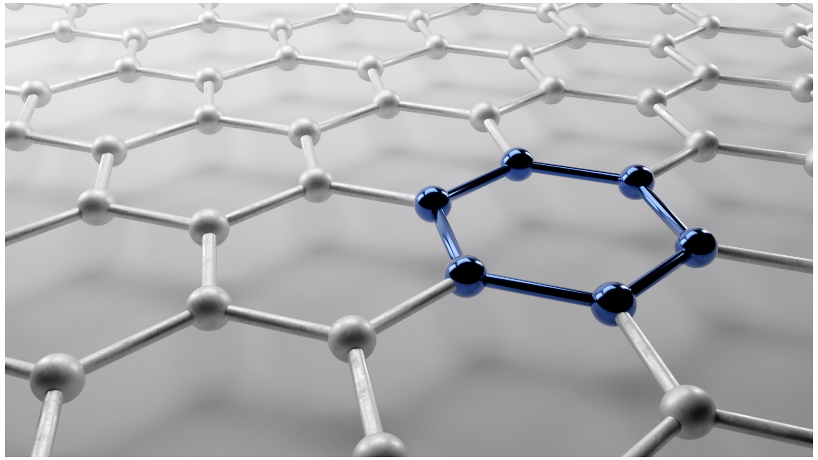

from bonds to bands

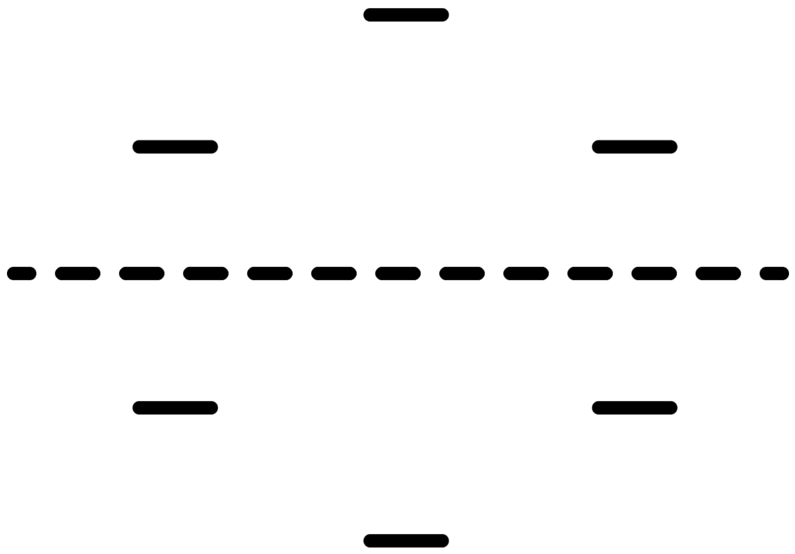

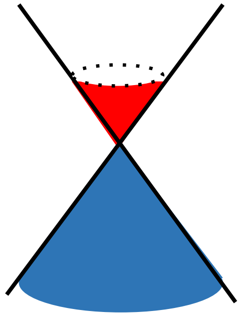

Dirac cone

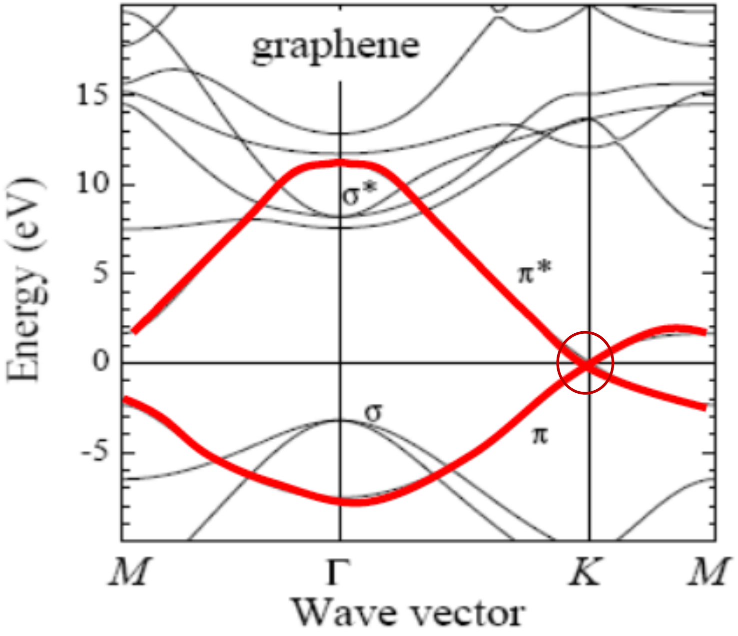

electronic structure

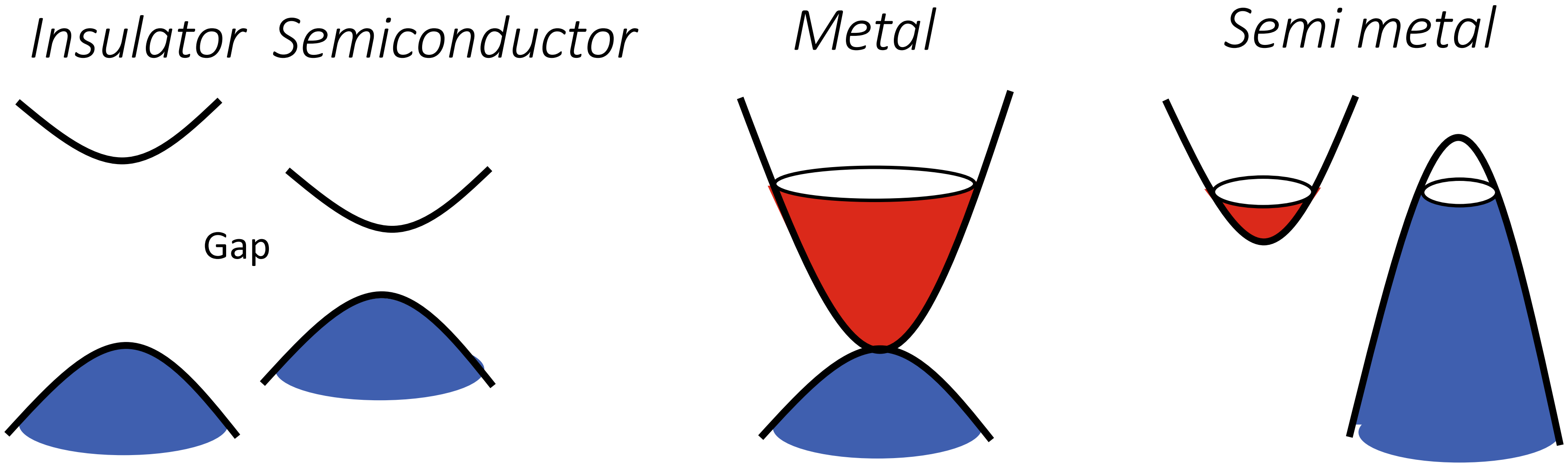

J. Gooth, J. Kübler, C. Felser, Physik Journal 20 (2021) 29.

black box of the electronic structure

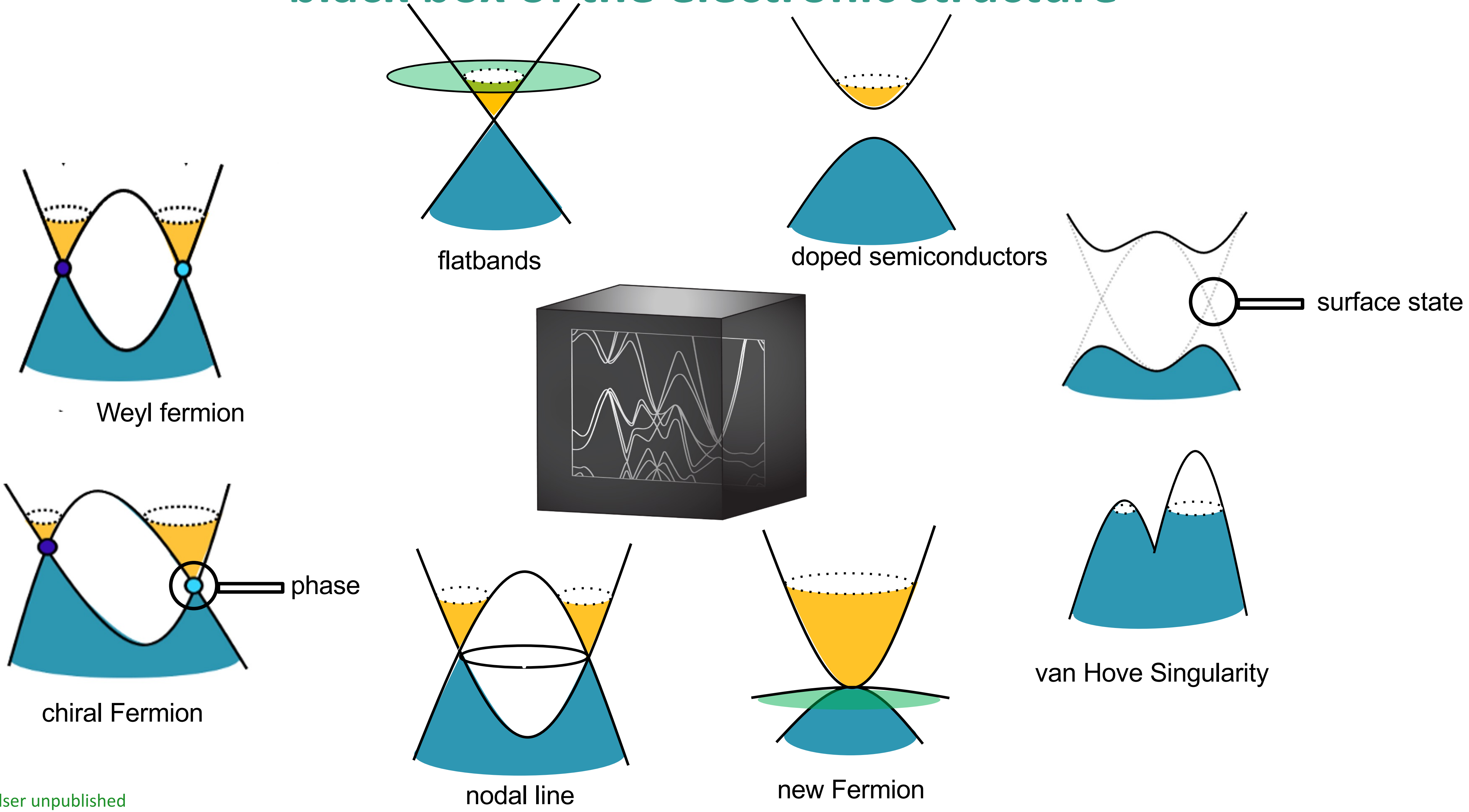

Gooth, Felser unpublished

topological insulators

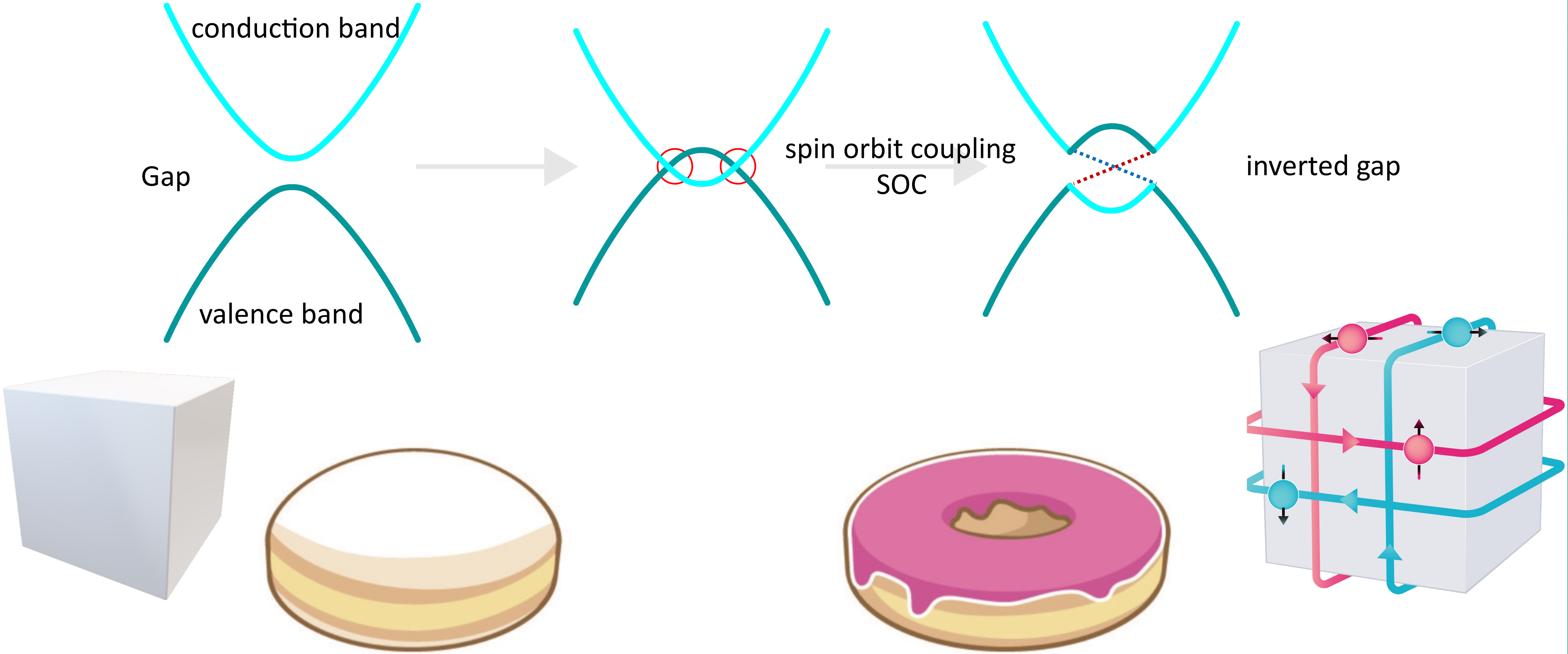

Topological Quantum Materials from the Viewpoint of Chemistry, Nitesh Kumar, Satya N. Guin, Kaustuv Manna, Chandra Shekhar, and Claudia Felser, doi.org/10.1021/acs.chemrev.0c00732

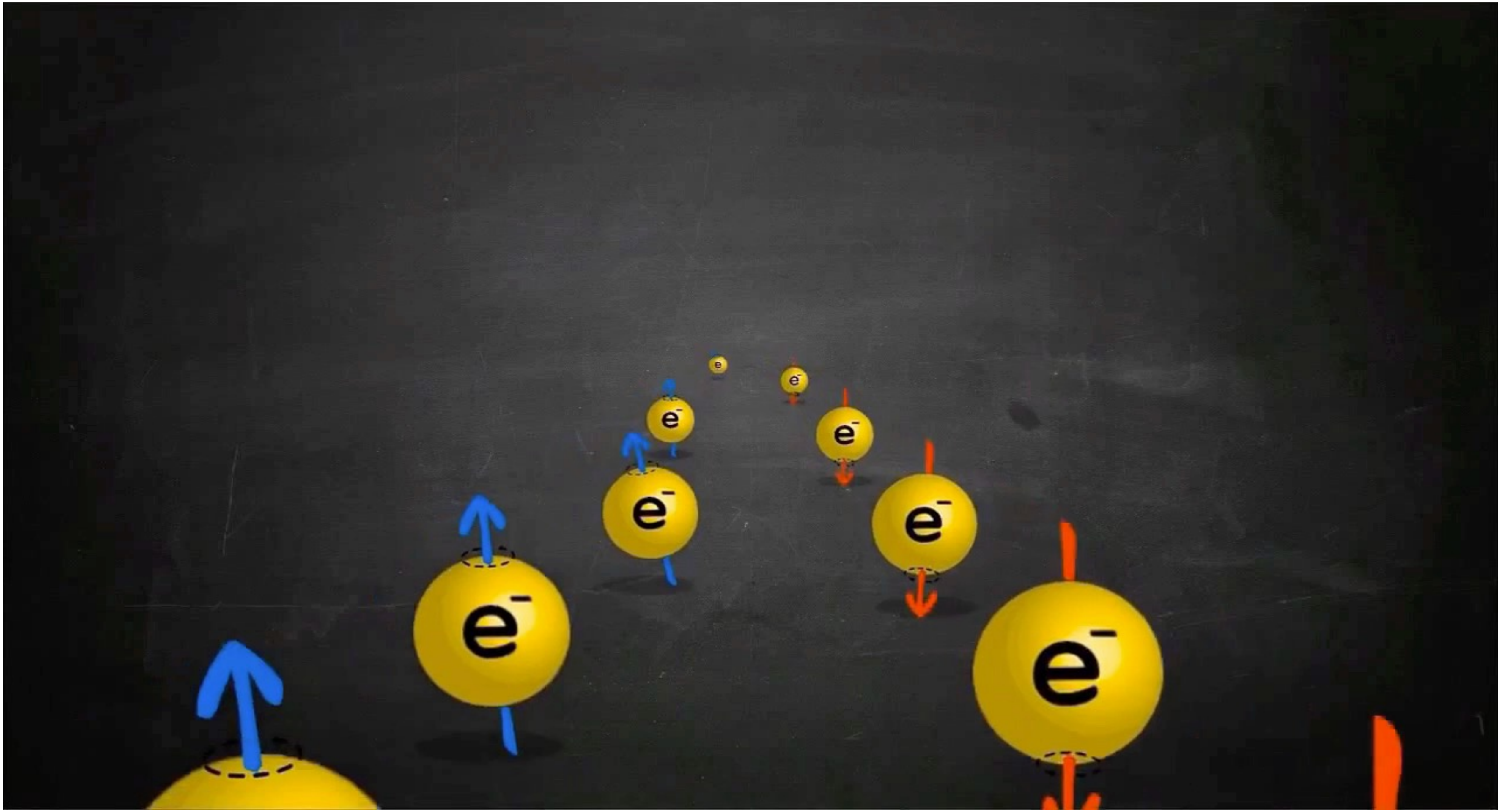
e⁻

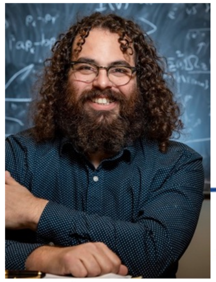

from all 250 000 known inorganic compounds 25% are topological

https://doi.org/10.1038/

A complete catalogue of high-qualit[y] topological materials

8,9* & Zhijun Wang[7,1

https://doi.org/10.1038/s41586-019-0937-5

TICLE

Topological

Barry Bradlyn[1*], L. Elcoro[2*], Jennifer

RESEARCH

RESEARCH ARTICLE SUMMARY

TOPOLOGICAL MATTER

All topological bands of all nonmagnetic stoichiometric materials

Maia G. Vergniory*†, Benjamin J. Wieder*†, Luis Elcoro, Stuart S. P. Parkin, Claudia Felser, B. Andrei Bernevig, Nicolas Regnault*

opological
indicators

https://doi.org/10.1038/s41586-019-0944-6

ectronic

ng[1,4], Hongming Weng[1,5,6,7,8*] &

s of magnetic

topological materials

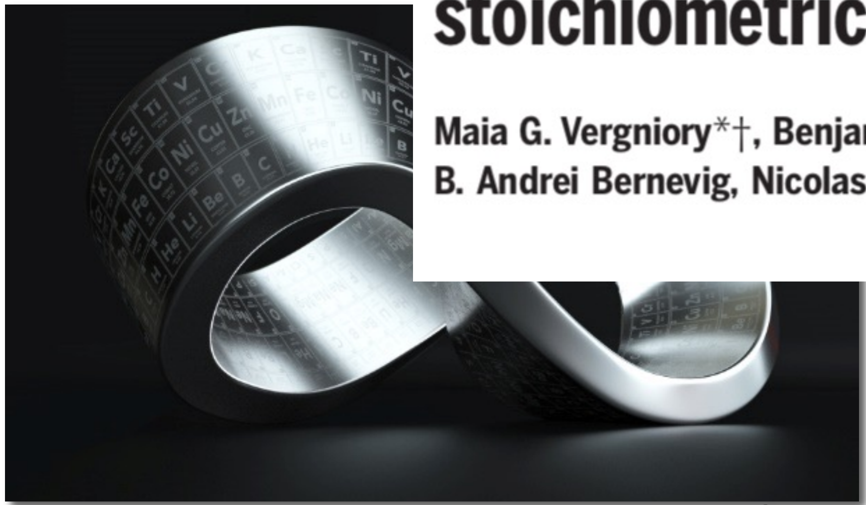

© Nature

https://doi.org/10.1038/s41586-020-2837-0
Received: 27 January 2020
Accepted: 24 August 2020

Yuanfeng Xu[1], Luis Elcoro[2], Zhida Song[3], Benjamin J. Wieder[3,4,5], M. G. Vergniory[6,7], Nicolas Regnault[3,8], Yulin Chen[9,10,11,12], Claudia Felser[13,14] & B. Andrei Bernevig[1,3,15]

https://doi.org/10.1038/s41586-020-2837-0

topologicalquantumchemistry.org

37 Rb	38 Sr	39 Y	40 Zr	41 Nb	42 Mo	43 Tc	44 Ru	45 Rh	46 Pd	47 Ag	48 Cd	49 In	50 Sn	51 Sb	52 Te	53 I	54 Xe
55 Cs	56 Ba	57 La	72 Hf	73 Ta	74 W	75 Re	76 Os	77 Ir	78 Pt	79 Au	80 Hg	81 Tl	82 Pb	83 Bi	84 Po	85 At	86 Rn
87 Fr	88 Ra	89 Ac	104 Rf	105 Db	106 Sg	107 Bh	108 Hs	109 Mt	110 Ds	111 Rg	112 Cn	113 Nh	114 Fl	115 Mc	116 Lv	117 Ts	118 Og
			58 Ce	59 Pr	60 Nd	61 Pm	62 Sm	63 Eu	64 Gd	65 Tb	66 Dy	67 Ho	68 Er	69 Tm	70 Yb	71 Lu	
			90 Th	91 Pa	92 U	93 Np	94 Pu	95 Am	96 Cm	97 Bk	98 Cf	99 Es	100 Fm	101 Md	102 No	103 Lr	

12 Entries found for **Hf, Te**, showing:

ALL (12) | **TI (5)** | **SM (1)** | **Trivial (6)**

Compound	Symmetry Group	Topological Indices	Crossing Type	Type
Hf1 Te2	164 (*P*-3*m*1)		Line	ES
Hf1 Te3	11 ($P2_1/m$)			LCEBR
Hf1 Te5	63 (*Cmcm*)	Z_4=3, $Z_{2w,1}$=1, $Z_{2w,2}$=1		NLC

chemistry

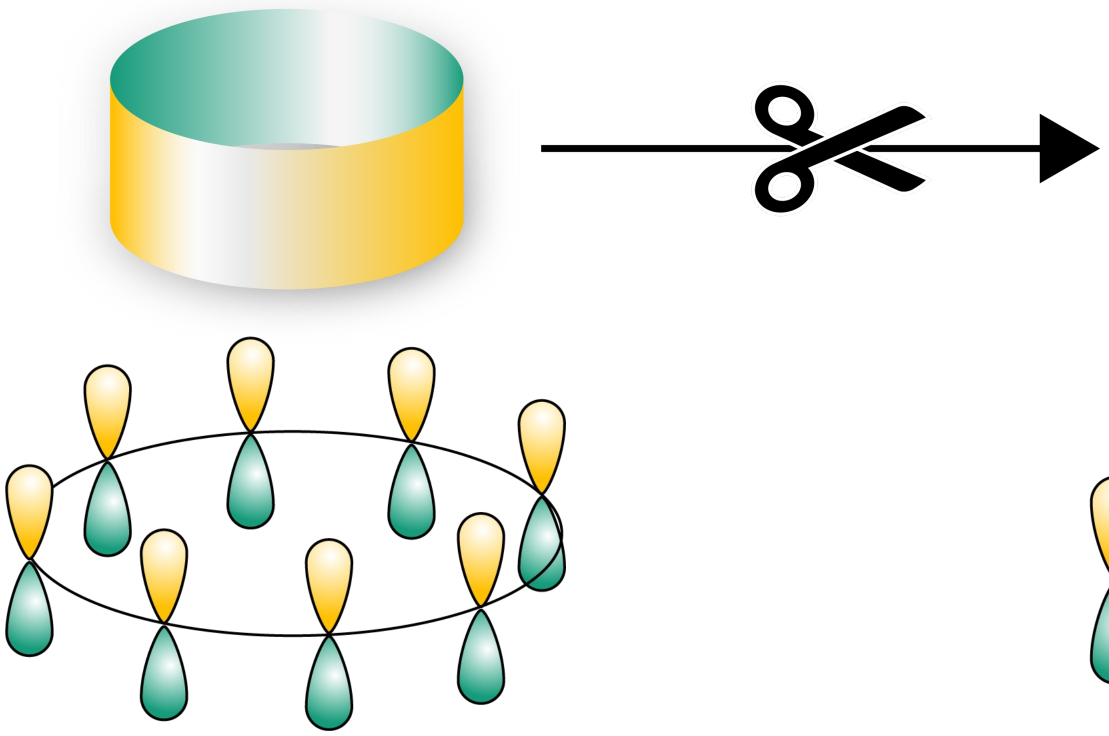

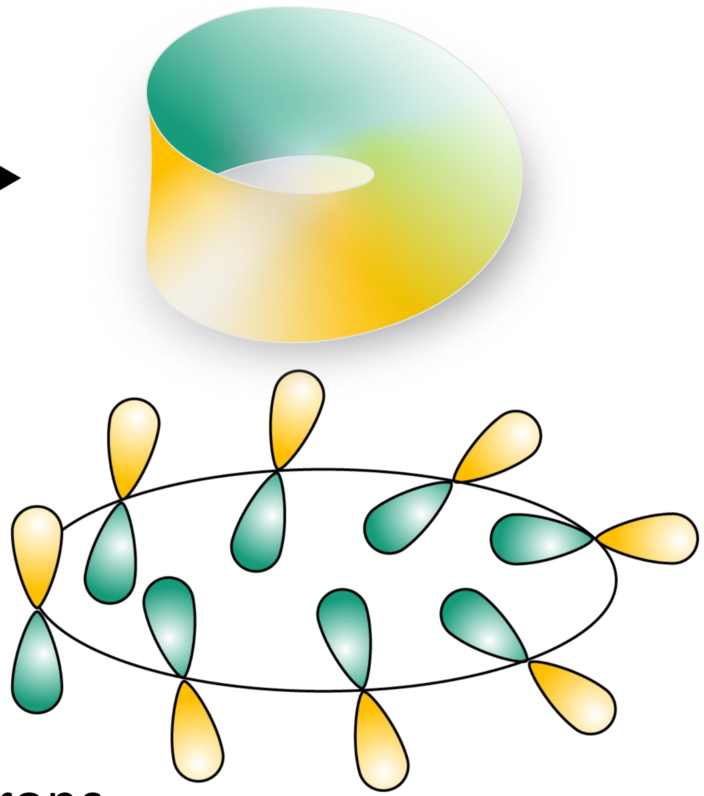

<u>magic electron numberof π-electrons</u>

Hückel:
4n+2 aromatic
4n antiaromatic

Möbius:
4n aromatic
4n+2 antiaromatic

topology in chemistry

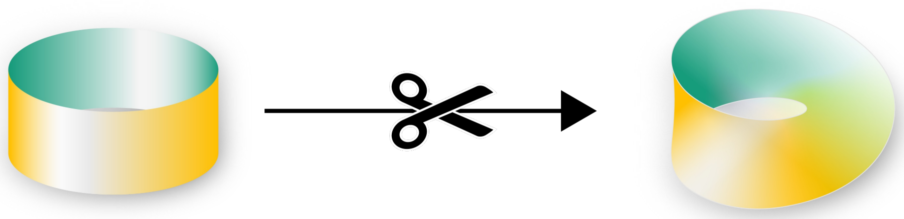

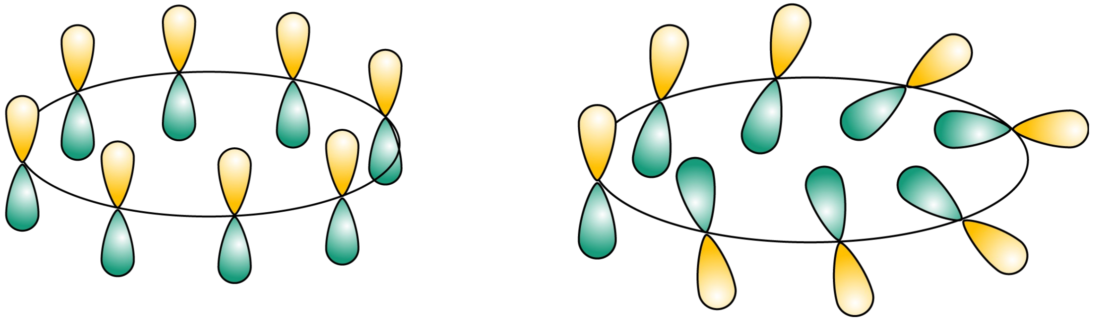

Magic electron numbers

Hückel:

4n+2 aromatic

4n antiaromatic

Möbius:

4n aromatic

4n+2 antiaromatic

ORGANIC CHEMISTRY

Aromatics with a twist

Rainer Herges

The properties of flat aromatic molecules are well known to chemists, but some non-planar aromatics remain a mystery. A molecule that can twist into a Möbius band on command might shed light on their features.

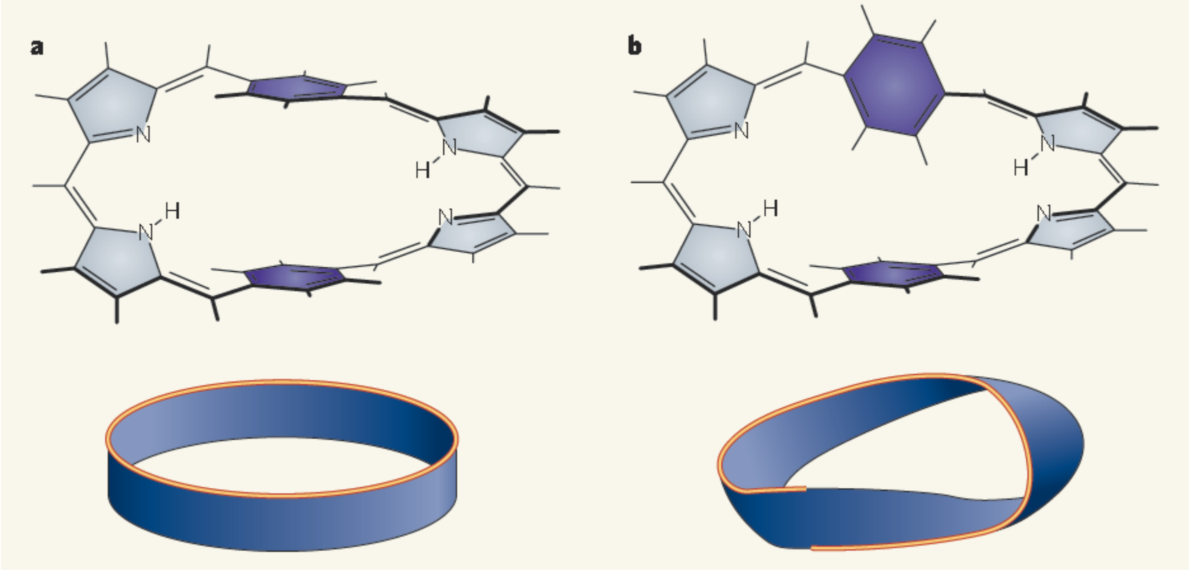

Figure 2 | A molecular topological switch. Latos-Grażyński and colleagues[1] have made a compound that is antiaromatic in nonpolar solvents, but not in polar solvents. **a**, In nonpolar solvents, the two benzene rings (purple) in the molecule are parallel, and the molecule is a two-sided, non-twisted band. **b**, In polar solvents, the upper benzene ring twists by 90°, so that the molecule becomes a one-sided, Möbius structure. This conformational change alters the aromaticity of the molecule.

graphene – the twist

Physics

TREND

Bilayer Graphene's Wicked, Twisted Road

Superconductivity, magnetism, and other forms of interacting electron behavior—bilayers of graphene seem to have it all. Researchers are now using this pristine material to unlock the secrets of interacting-electron phenomena with unprecedented control and tunability.

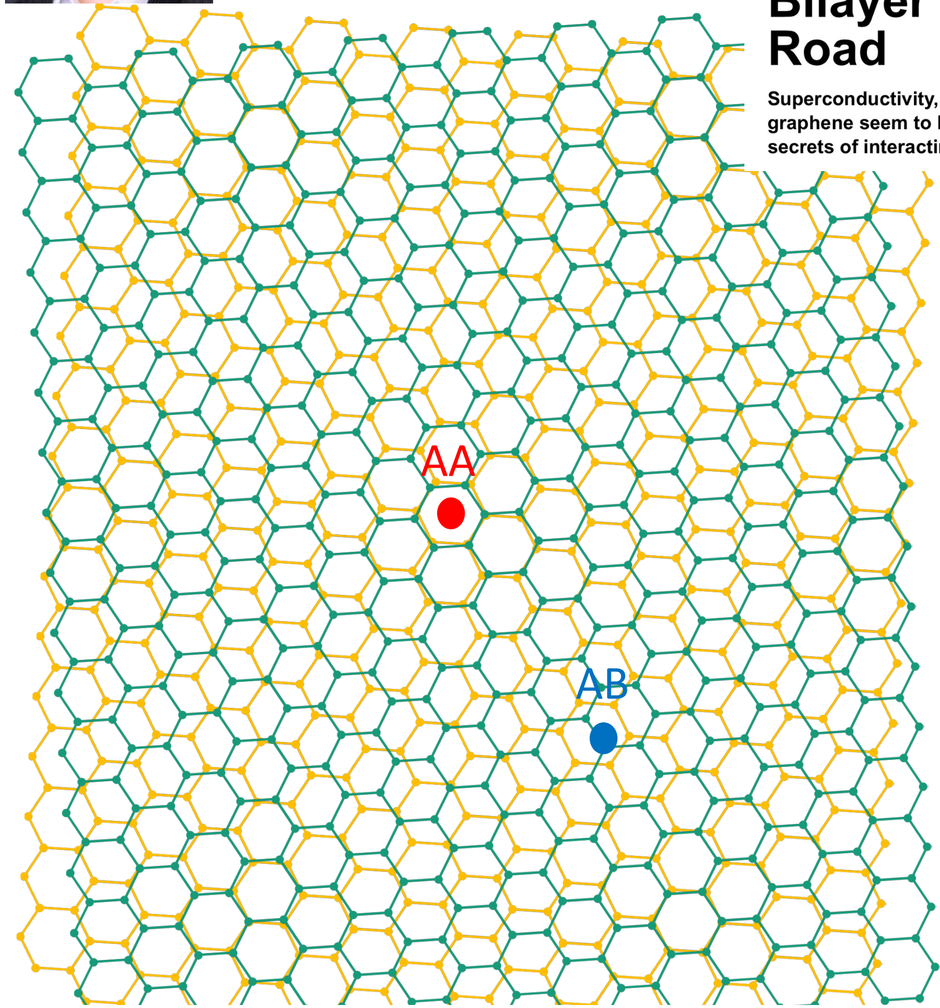

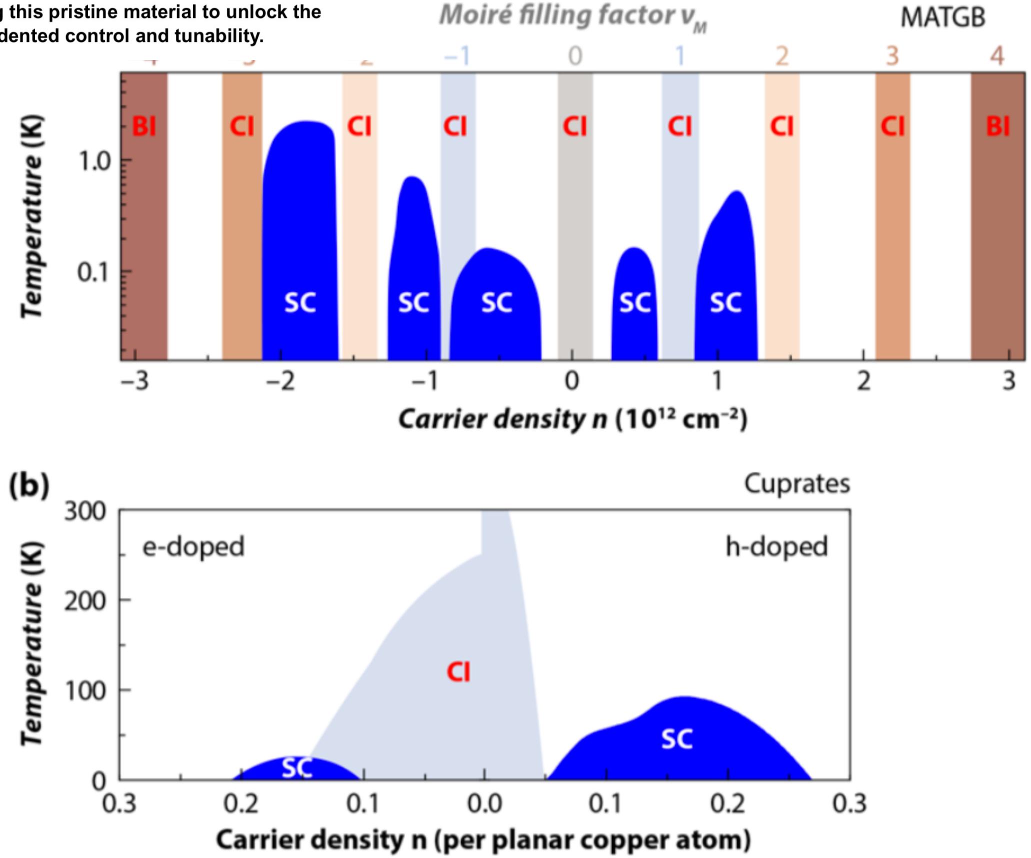

Unconventional superconductivity in magic-angle …, Y Cao, , et al., Nature 556 (2018), 43-50, Spectroscopy of Twisted Bilayer Graphene …, Dumitru Călugăru et al., arXiv:2110.15300

graphene – the twist

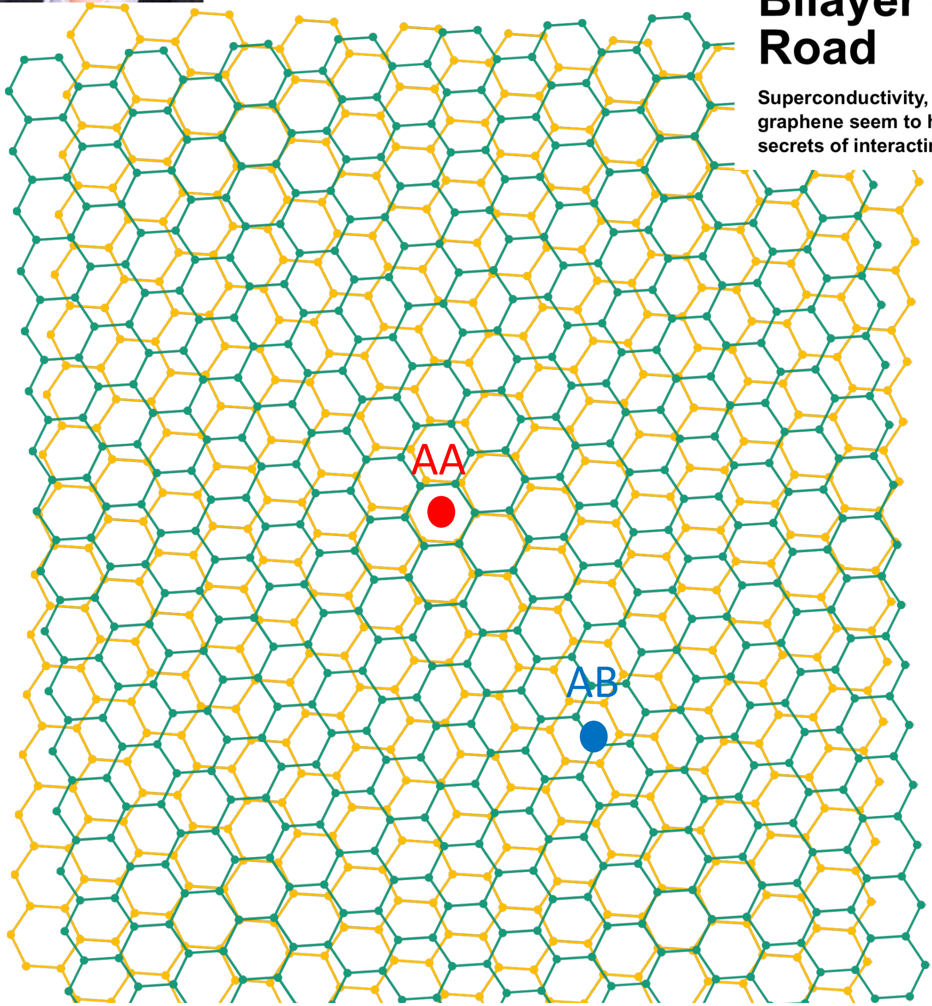

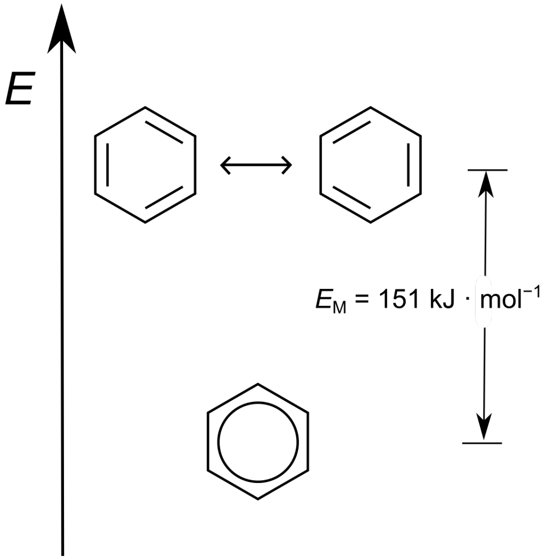

Spectroscopy with STM

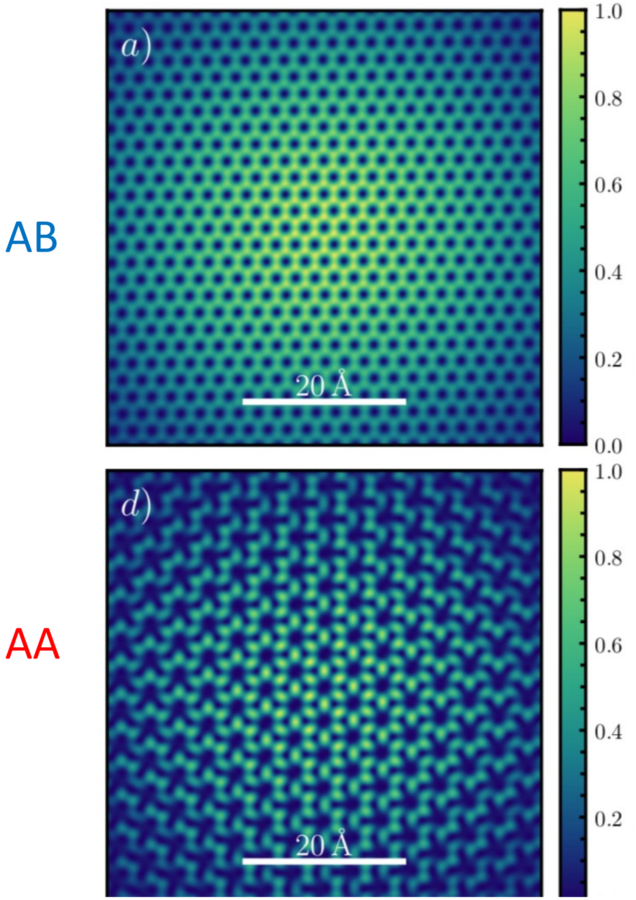

AA π-elektrons localised
AB π-electrons delocalised

Unconventional superconductivity in magic-angle ..., Y Cao, , et al., Nature 556 (2018), 43-50, Spectroscopy of Twisted Bilayer Graphene ..., Dumitru Călugăru et al., arXiv:2110.15300

graphene – the twist

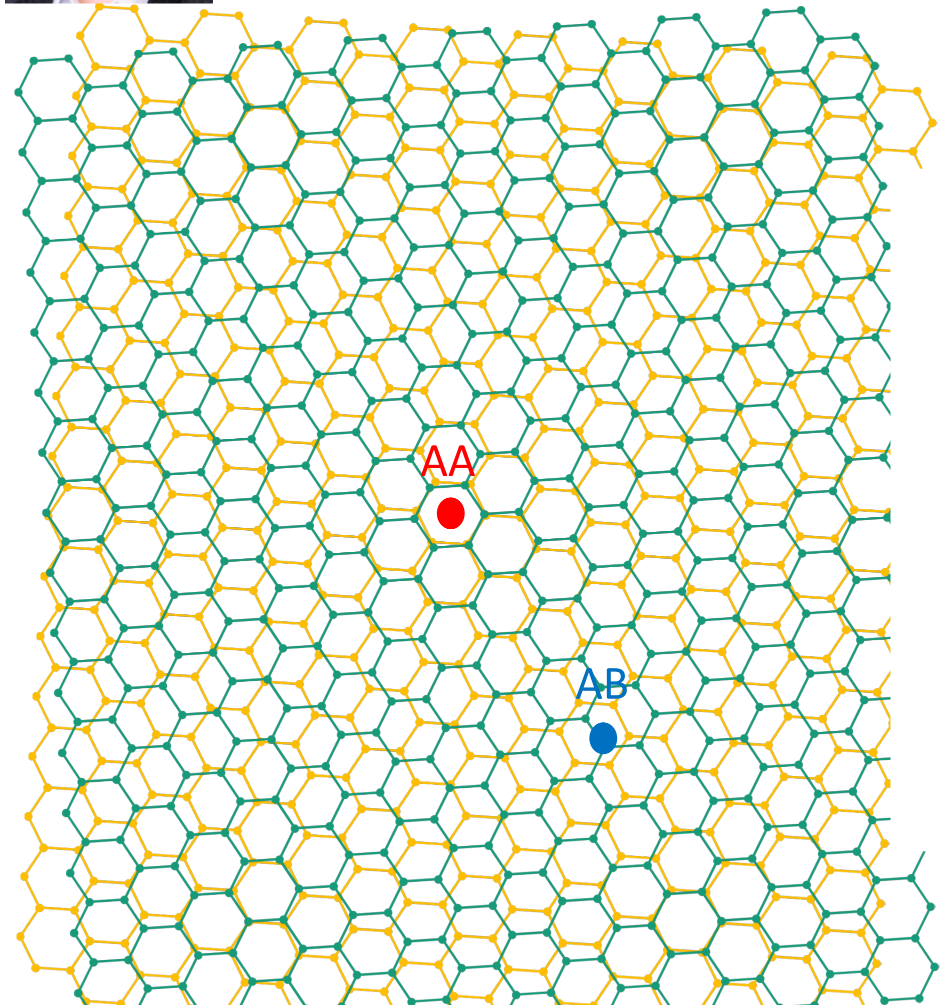

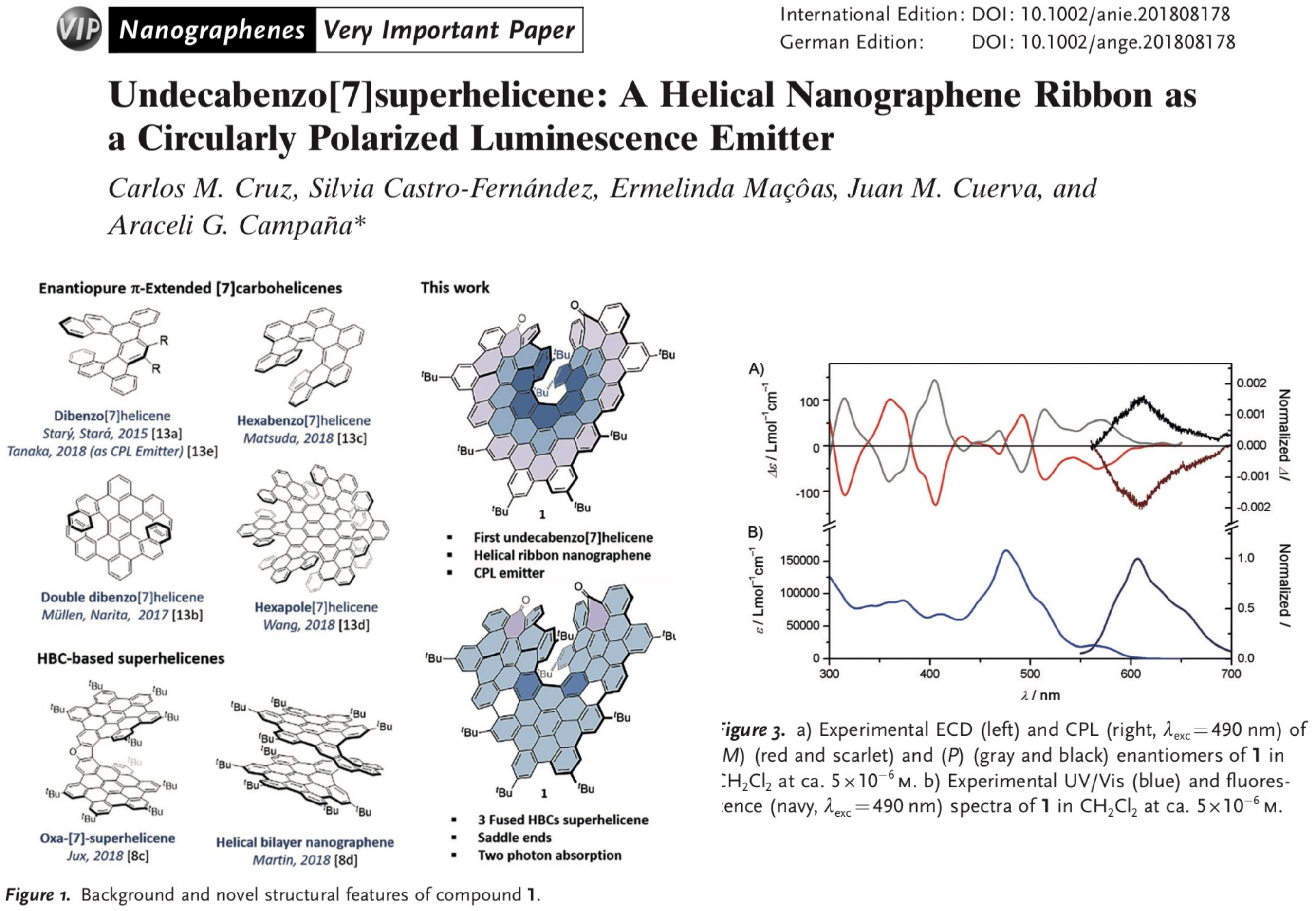
VIP Nanographenes Very Important Paper
International Edition: DOI: 10.1002/anie.201808178
German Edition: DOI: 10.1002/ange.201808178

Undecabenzo[7]superhelicene: A Helical Nanographene Ribbon as a Circularly Polarized Luminescence Emitter

*Carlos M. Cruz, Silvia Castro-Fernández, Ermelinda Maçôas, Juan M. Cuerva, and Araceli G. Campaña**

Figure 1. Background and novel structural features of compound **1**.

Figure 3. a) Experimental ECD (left) and CPL (right, $\lambda_{exc} = 490$ nm) of (M) (red and scarlet) and (P) (gray and black) enantiomers of **1** in CH_2Cl_2 at ca. 5×10^{-6} M. b) Experimental UV/Vis (blue) and fluorescence (navy, $\lambda_{exc} = 490$ nm) spectra of **1** in CH_2Cl_2 at ca. 5×10^{-6} M.

twisted graphene – aromatic – antiaromatic ???

Unconventional superconductivity in magic-angle …, Y Cao, , et al., Nature 556 (2018), 43-50, Spectroscopy of Twisted Bilayer Graphene …, Dumitru Călugăru et al., arXiv:2110.15300

topological insulators

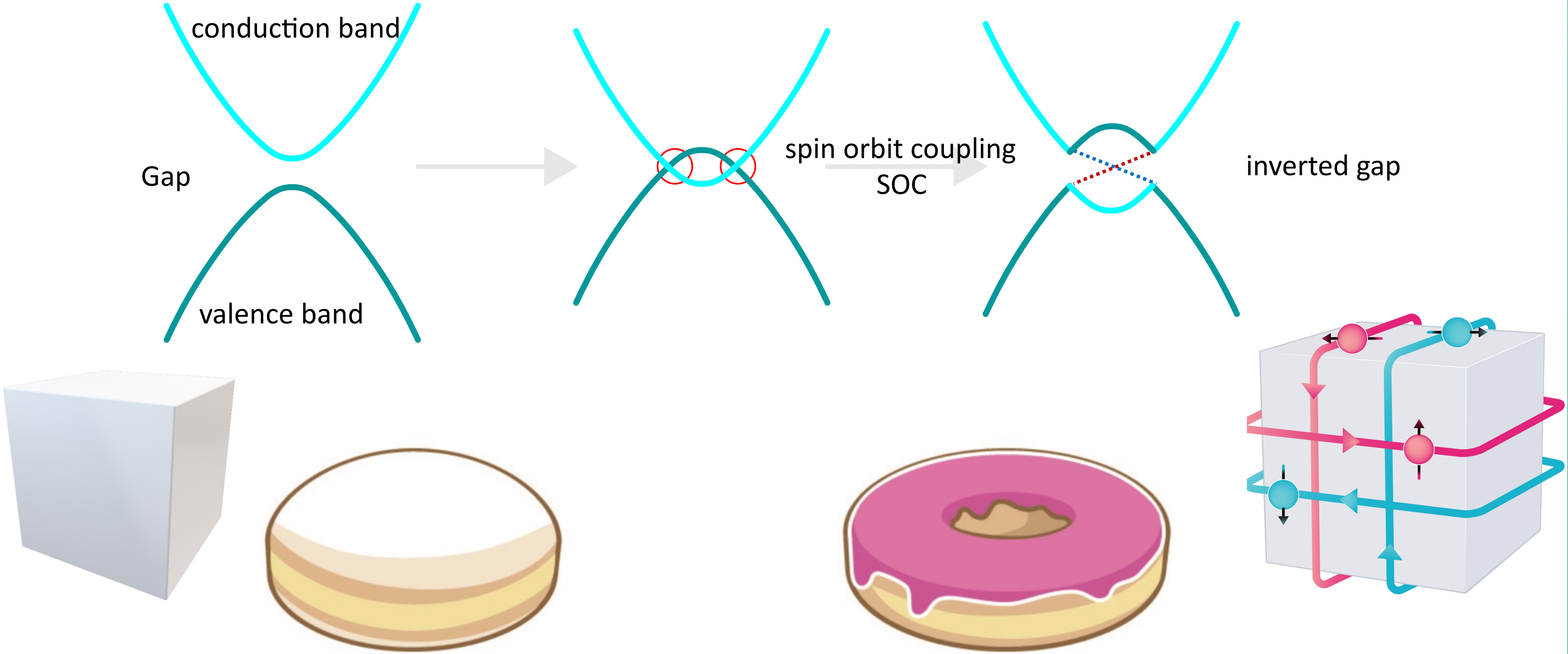

Topological Quantum Materials from the Viewpoint of Chemistry, Nitesh Kumar, Satya N. Guin, Kaustuv Manna, Chandra Shekhar, and Claudia Felser, doi.org/10.1021/acs.chemrev.0c00732

semiconductor

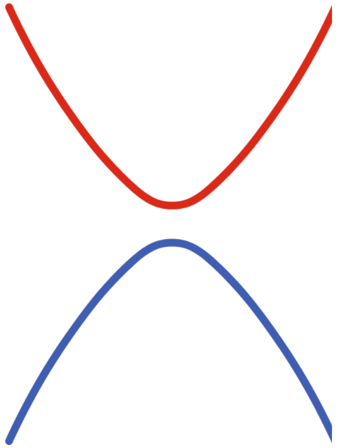

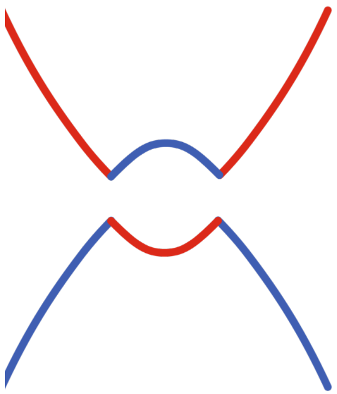

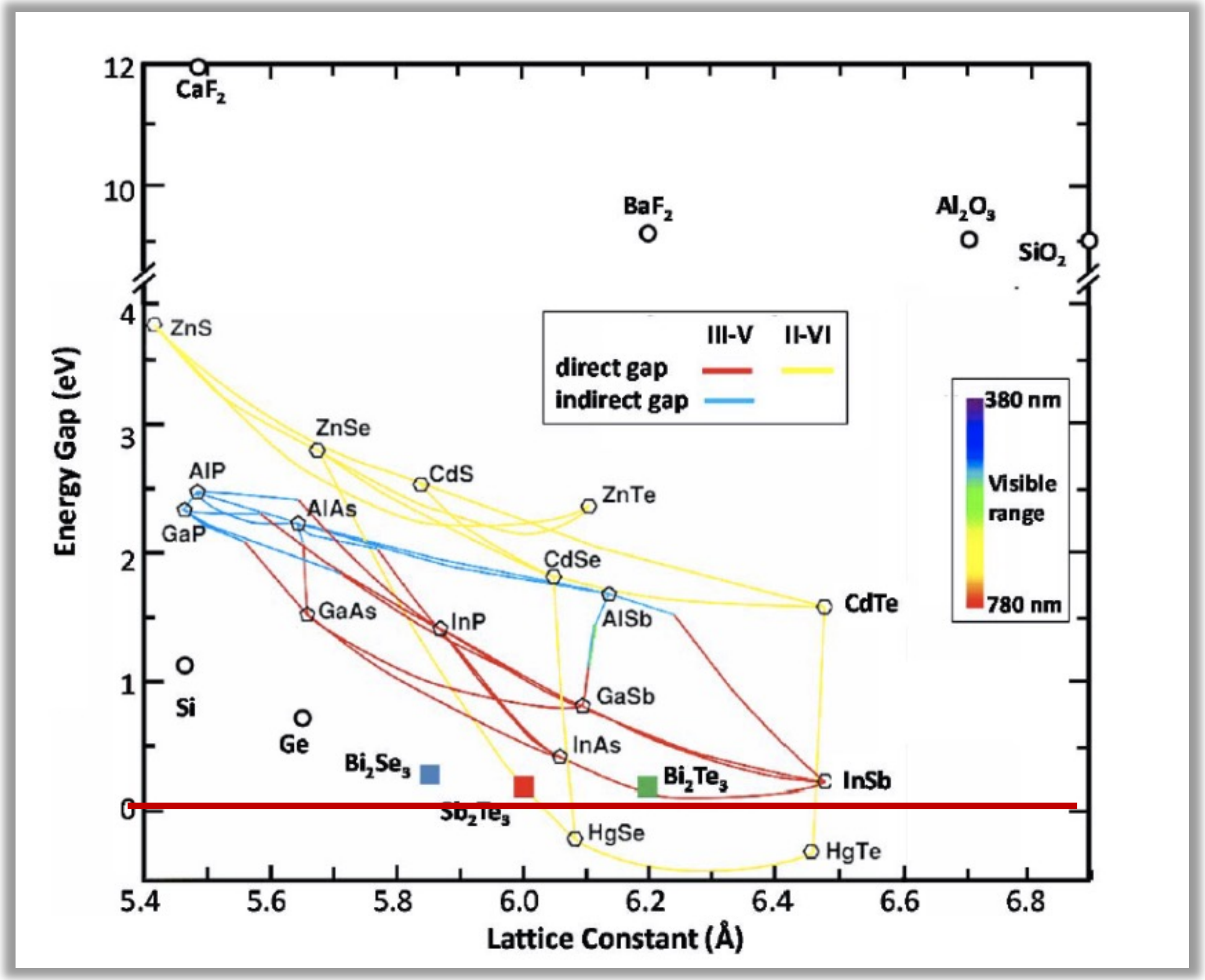

XZ

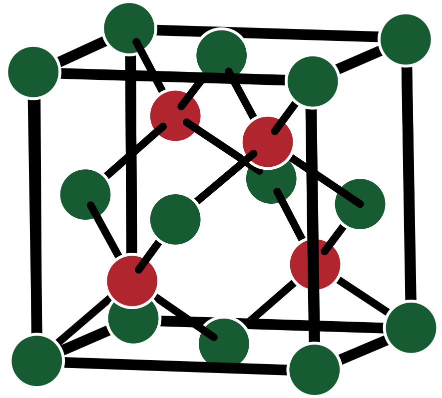

J. Kroder, G. Fecher, C. Felser, Chemie in unserer Zeit 56 (2022) 12–20

N. Kumar, Satya N. Guin, Kaustuv Manna, Chandra Shekhar, and Claudia Felser, Chem. Rev. 2021, 121, 5, 2780–2815

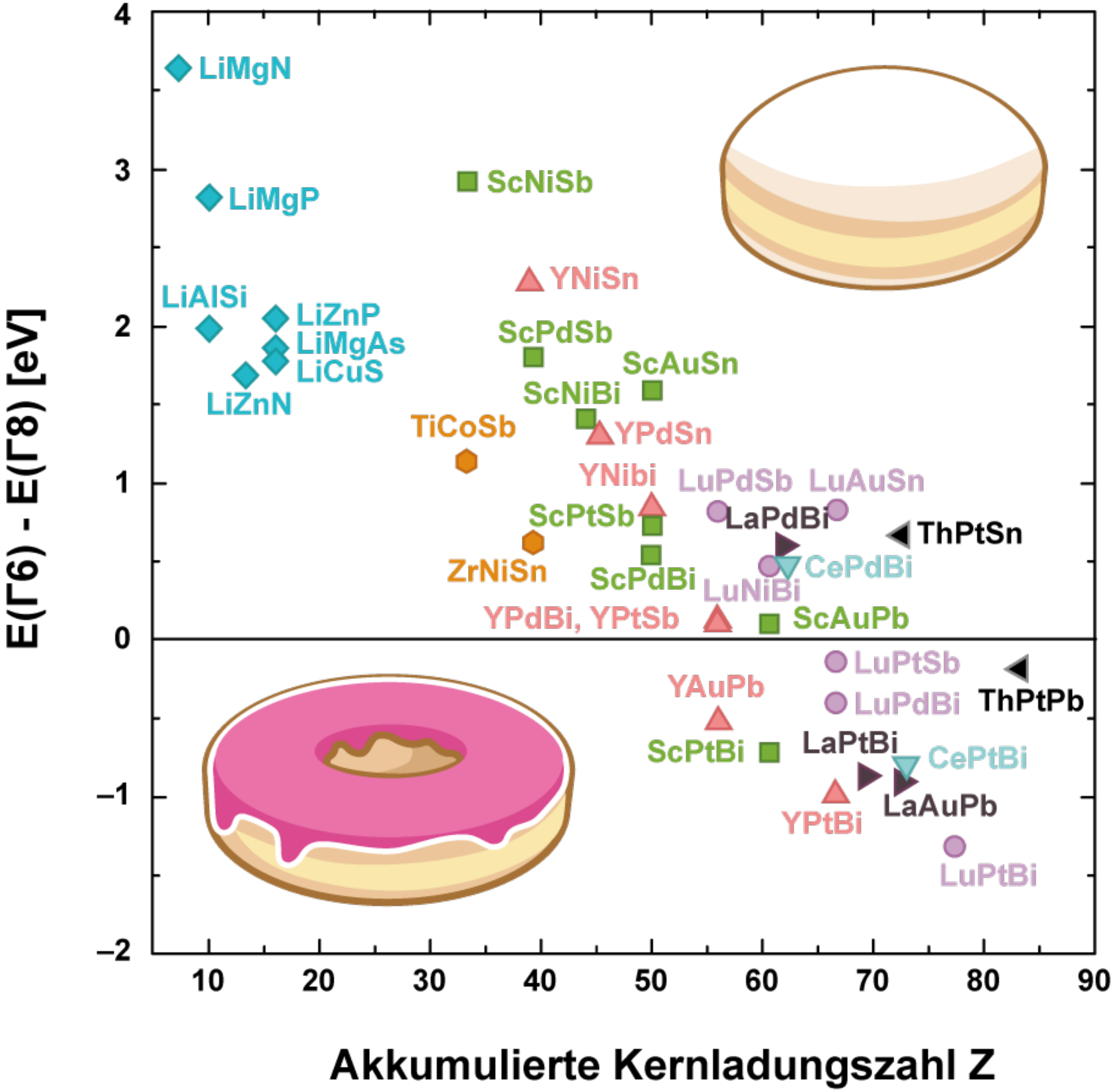
LiMgN
LiMgP
LiAlSi
LiZnP
LiMgAs
LiCuS
LiZnN
ScNiSb
YNiSn
ScPdSb
ScAuSn
ScNiBi
TiCoSb
YPdSn
YNibi
LuPdSb
LuAuSn
ScPtSb
LaPdBi
ThPtSn
ZrNiSn
ScPdBi
CePdBi
LuNiBi
YPdBi, YPtSb
ScAuPb
LuPtSb
ThPtPb
YAuPb
LuPdBi
ScPtBi
LaPtBi
CePtBi
LaAuPb
YPtBi
LuPtBi
E(Γ6) - E(Γ8) [eV]
Akkumulierte Kernladungszahl Z
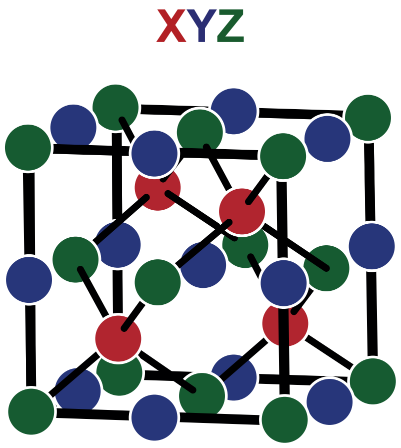
XYZ
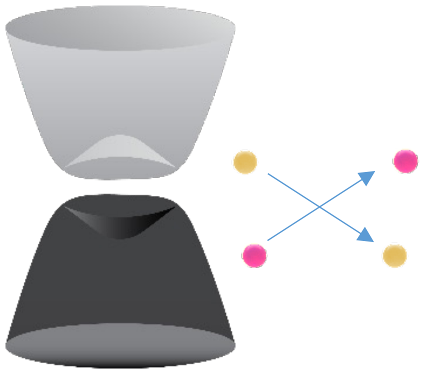

ternary semiconductor

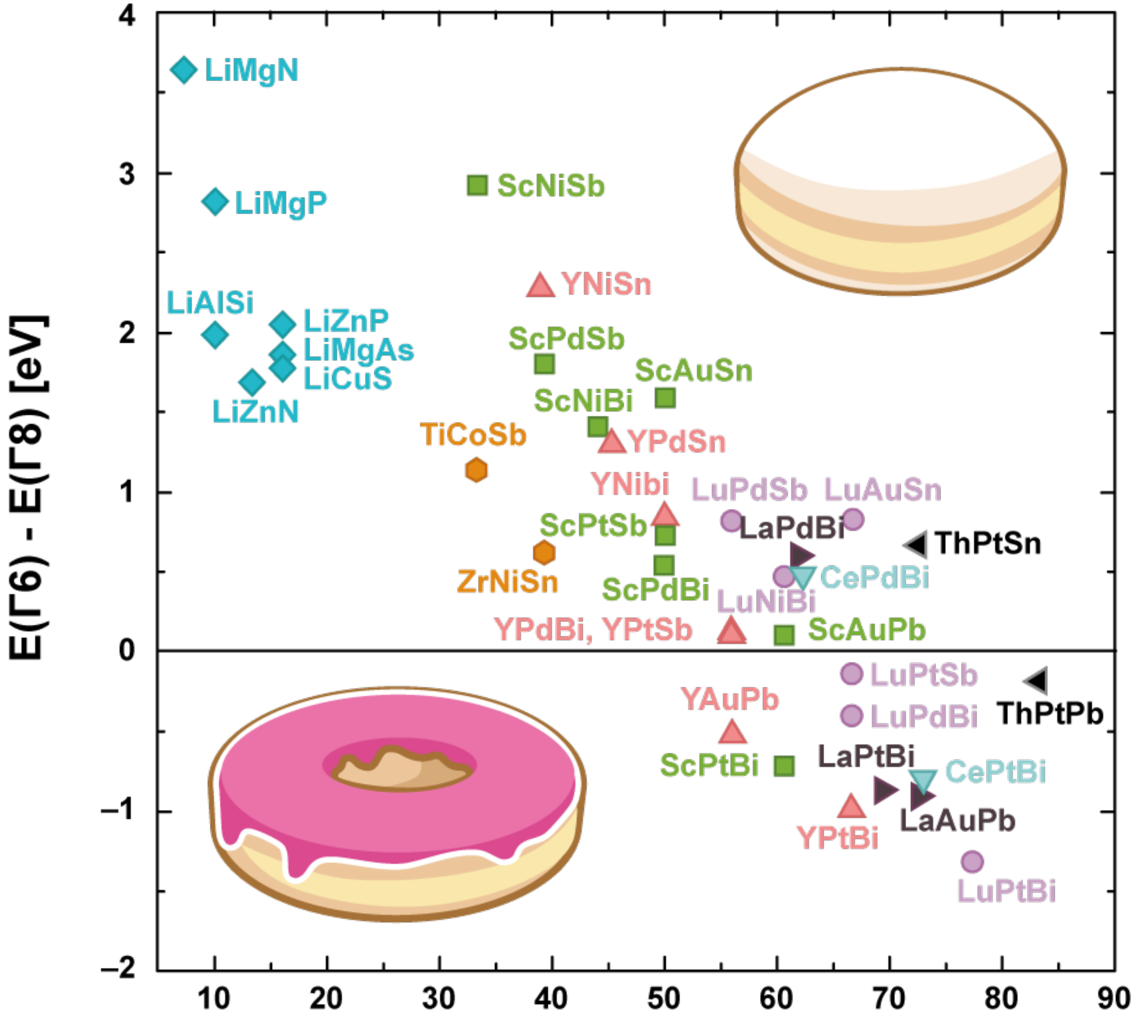

average nuclear charge Z

half Heusler compounds are ternary semiconductors

XYZ

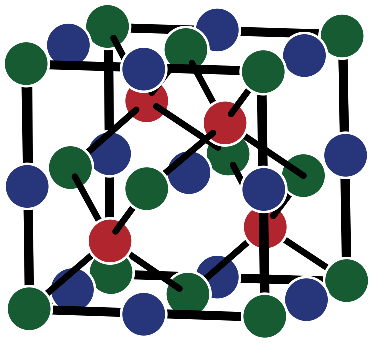

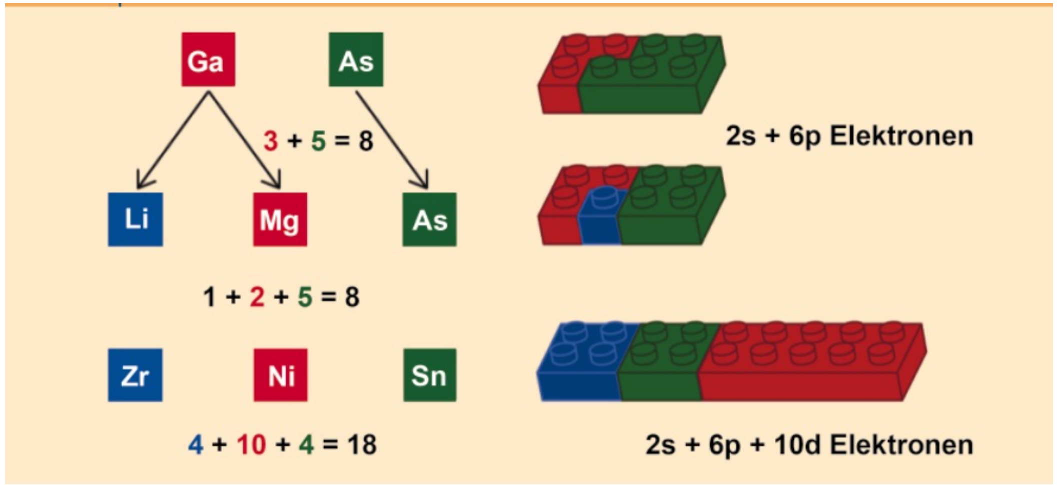

J. Kroder, G. Fecher, C. Felser, , Chem. Unserer Zeit 56 (2022) 12–20
S Chadov, et al., Nature materials 9 (2010) 541-545

gold: a topological metal

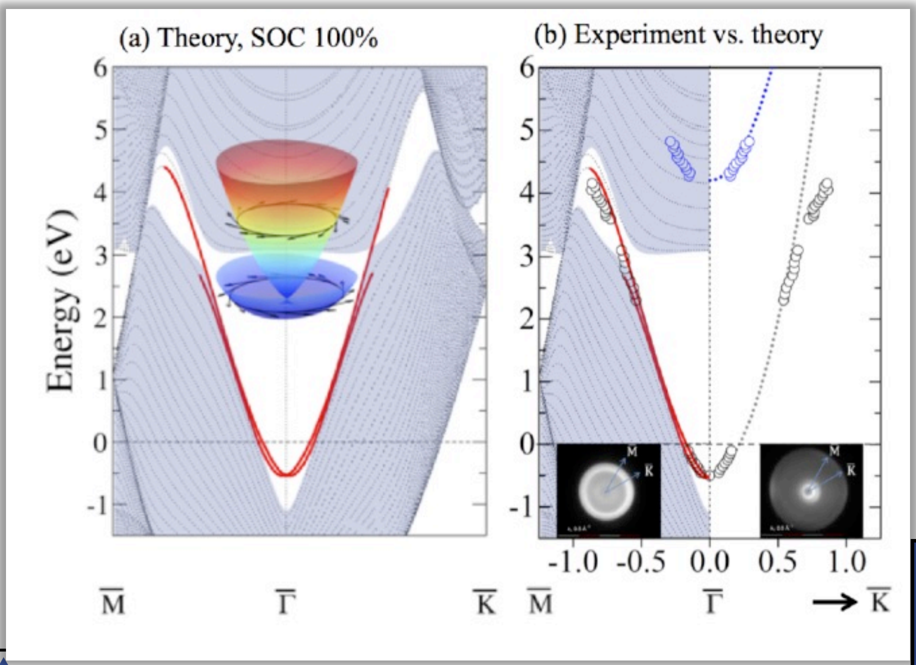

Inert pair effect

contraction of the 1s-orbital =
higher s orbitals will be „core“ like

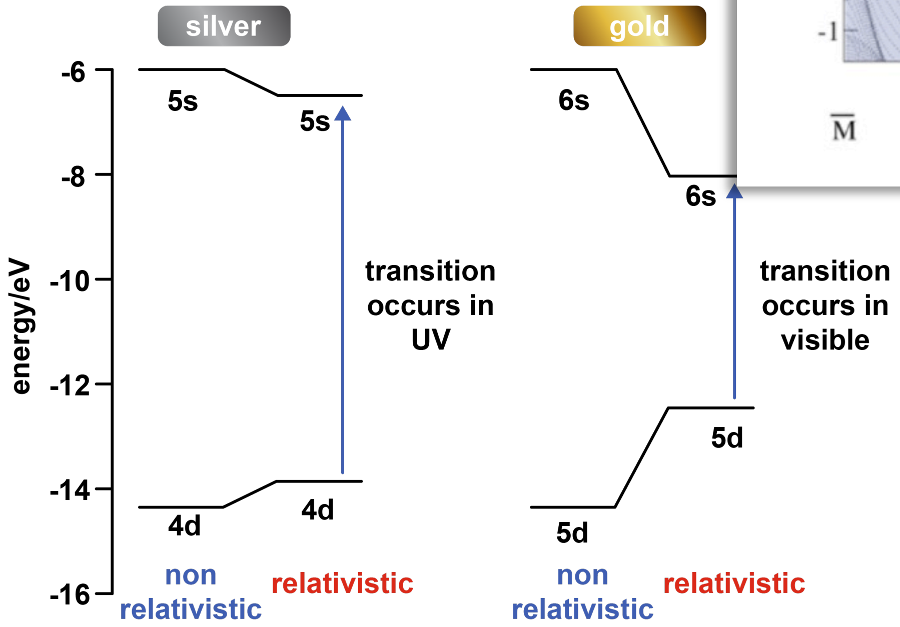

In^{+} In^{3+}	Sn^{2+} Sn^{4+}	Sb^{3+} Sb^{5+}
Tl^{+} Tl^{3+}	Pb^{2+} Pb^{4+}	Bi^{3+} Bi^{5+}

Binghai Yan at al., Nature Communications 6 (2015) 10167

measurements

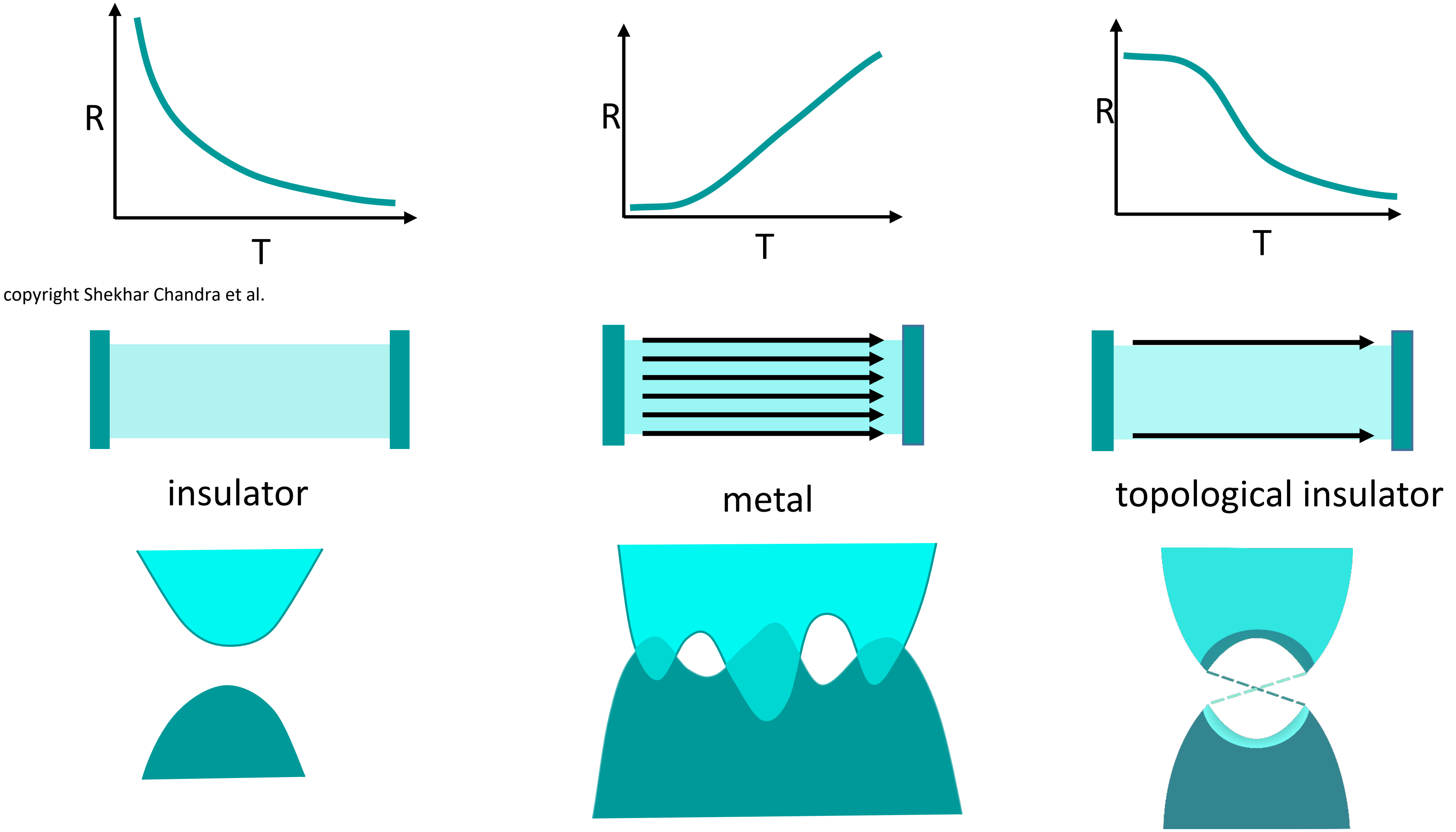

Nitesh Kumar, Satya N. Guin, Kaustuv Manna, Chandra Shekhar, and Claudia Felser, Chem. Rev. 121 (2021) 2780.

Hall-measurements of semiconductors

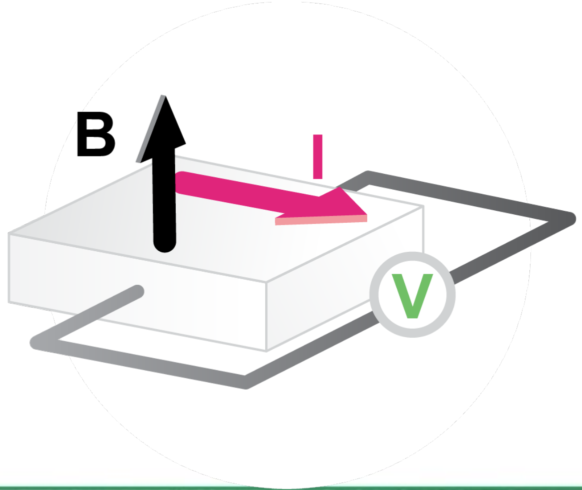

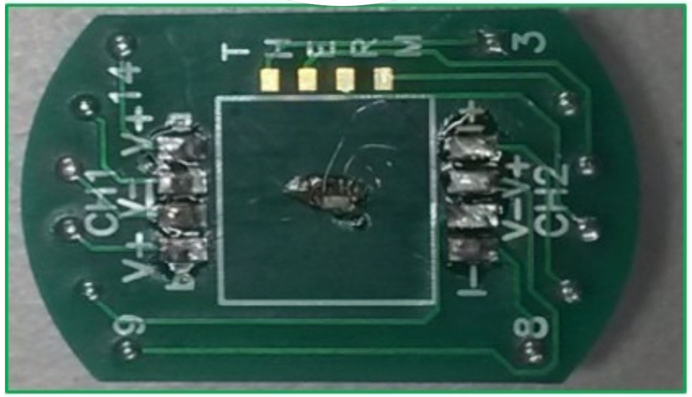

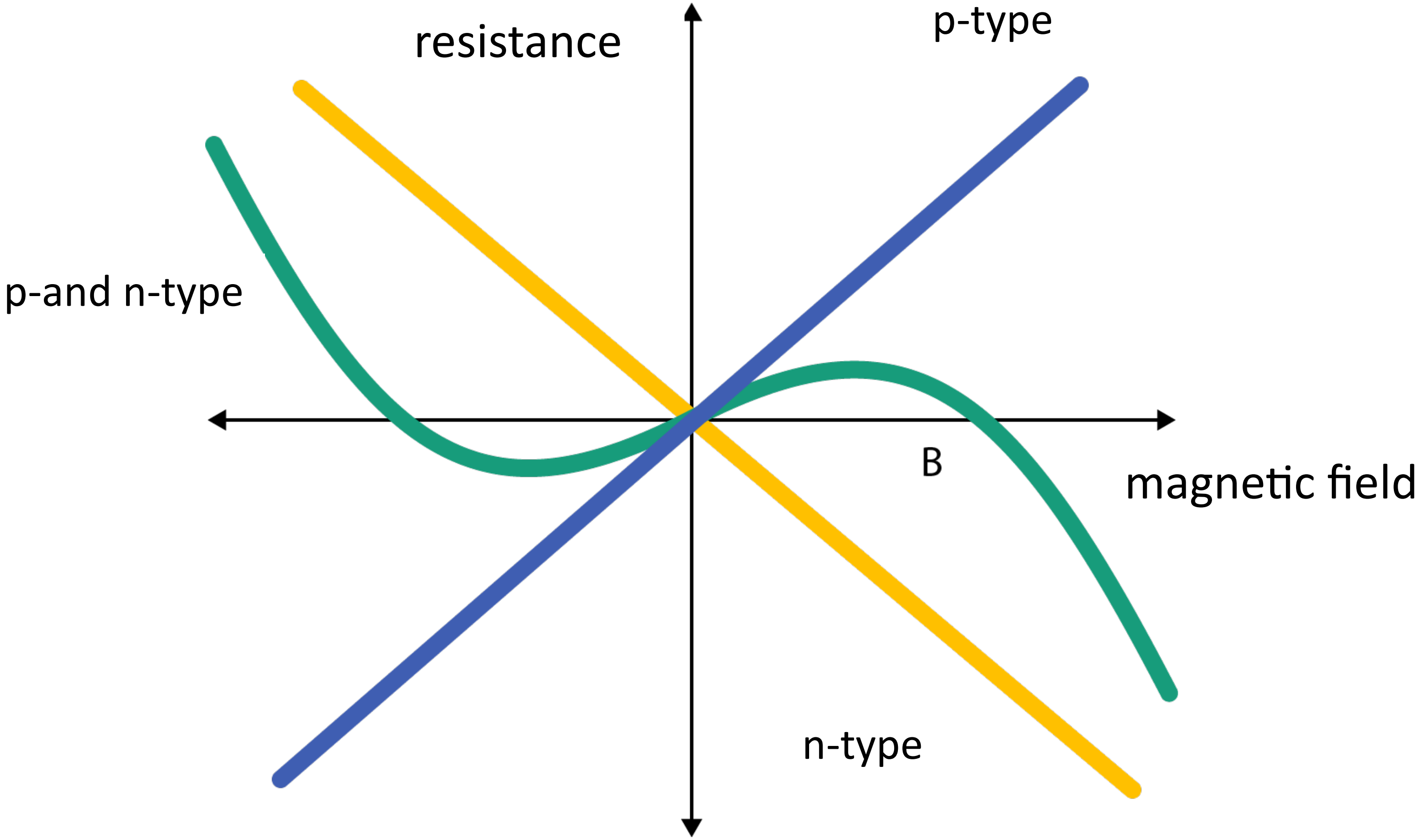

quantum Hall effect

Klaus von Klitzing
©mpg

or the beginning

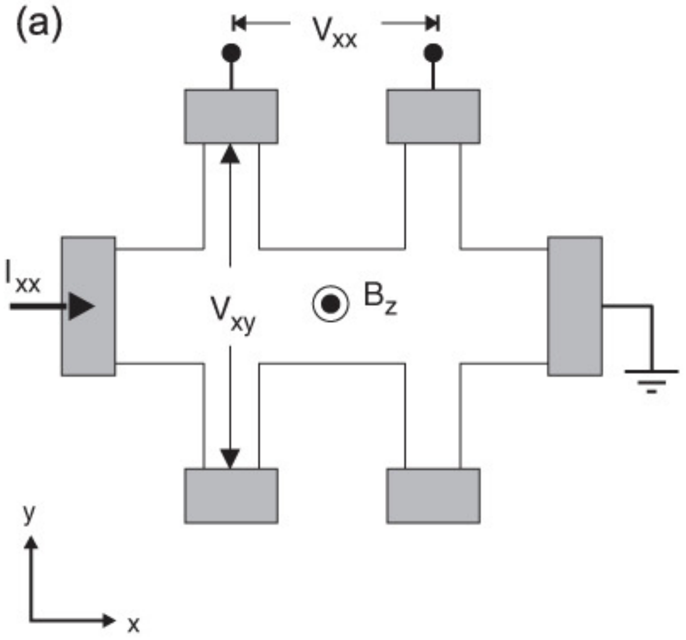

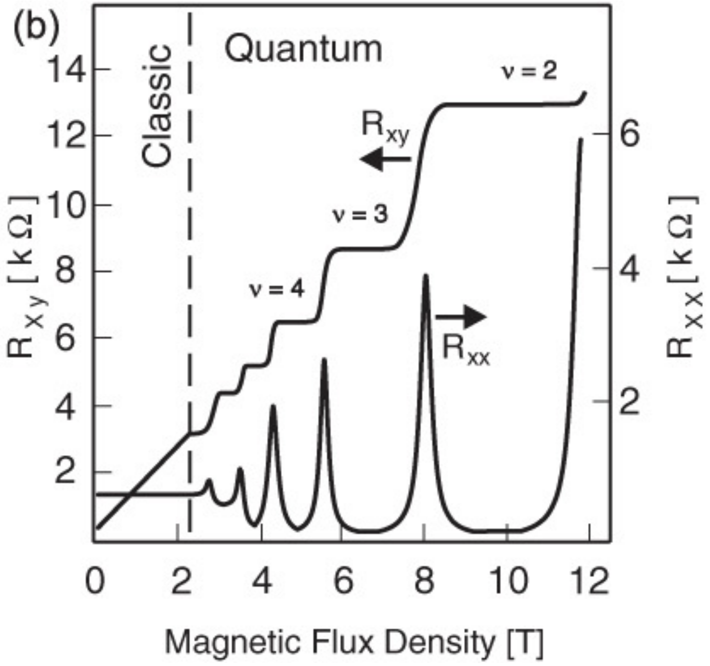

quantum Hall effect:

- exotic effect
- in complex layer systems of semiconductors
- precisely adjusted charge carrier concentration
- high magnetic fields
- low temperature

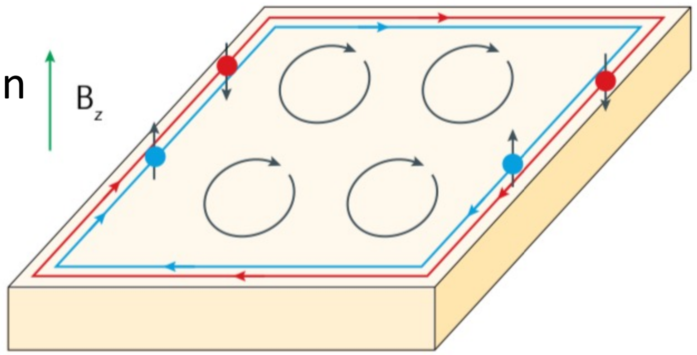

Klaus von Klitzing, et al., , Nature Reviews Physics 2 (2020) 397

T. Janssen et al., 2013 Rep. Prog. Phys. **76** 104501

quantum Hall effect in a crystal

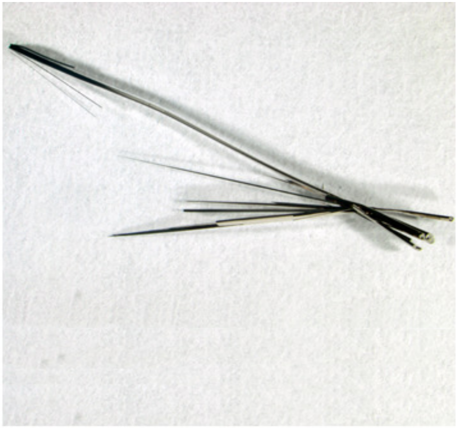

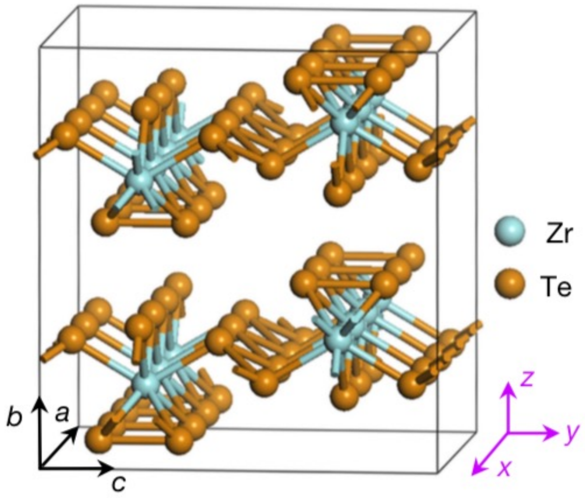

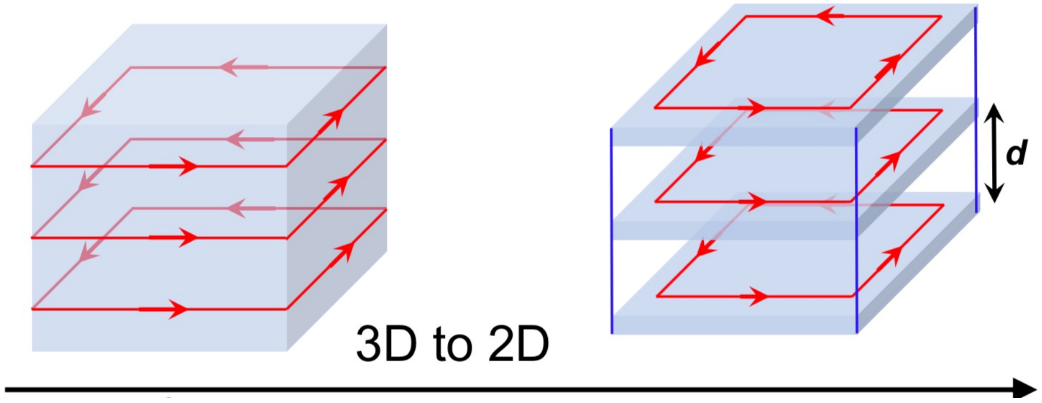

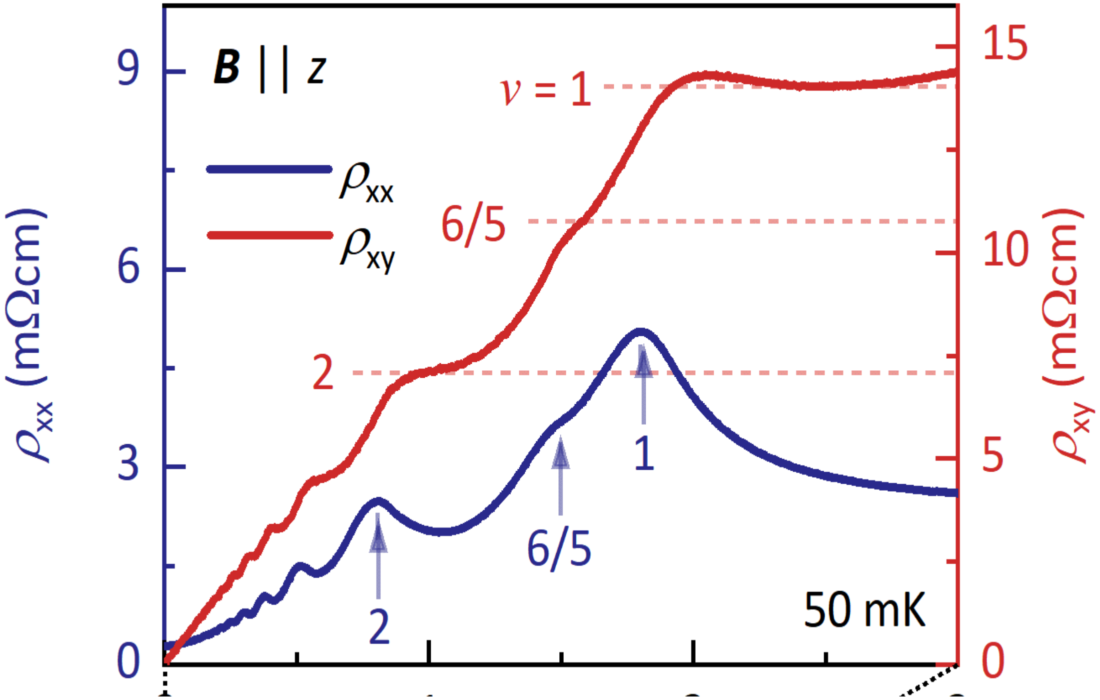

J. Gooth et al., Nature Communications 12 (2021) 3197, Fangdong Tang, et al., Nature 569 (2019) 537

quantum anomalous Hall – quantum spin Hall

VOLUME 61, NUMBER 18 PHYSICAL REVIEW LETTERS 31 OCTOBER 1988

Model for a Quantum Hall Effect without Landau Levels: Condensed-Matter Realization of the "Parity Anomaly"

F. D. M. Haldane
Department of Physics, University of California, San Diego, La Jolla, California 92093

Topological Quantum Matter

Nobel Lecture, December 8, 2016

Z_2 Topological Order and the Quantum Spin Hall Effe

C. L. Kane and E. J. Mele
Department of Physics and Astronomy, University of Pennsylvania, Philadelphia, Pennsylvania 19104, USA
(Received 22 June 2005; published 28 September 2005)

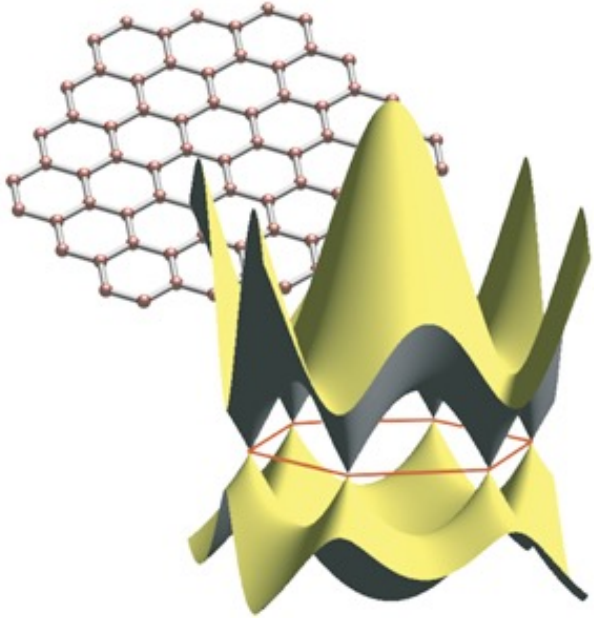

Prediction of the quantum anomalous Hall effect without magnetic field

Solution: Magnetic materials

Prediction of the quantum spin Hall effect

Solution: materials with large spin orbit coupling

Haldane, PRL 61, 2015 (1988)

Kane and Mele, PRL 95, 146802 (2005)

topological insulators – quantum spin Hall

Z_2 **Topological Order and the Quantum Spin Hall Effect**

C. L. Kane and E. J. Mele
Department of Physics and Astronomy, University of Pennsylvania, Philadelphia, Pennsylvania 19104, USA

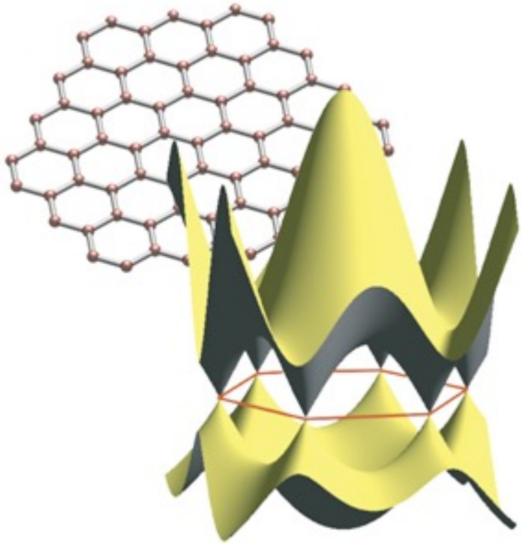

Heavy insulating elements?

Strained α-Sn and Bi-bilayer

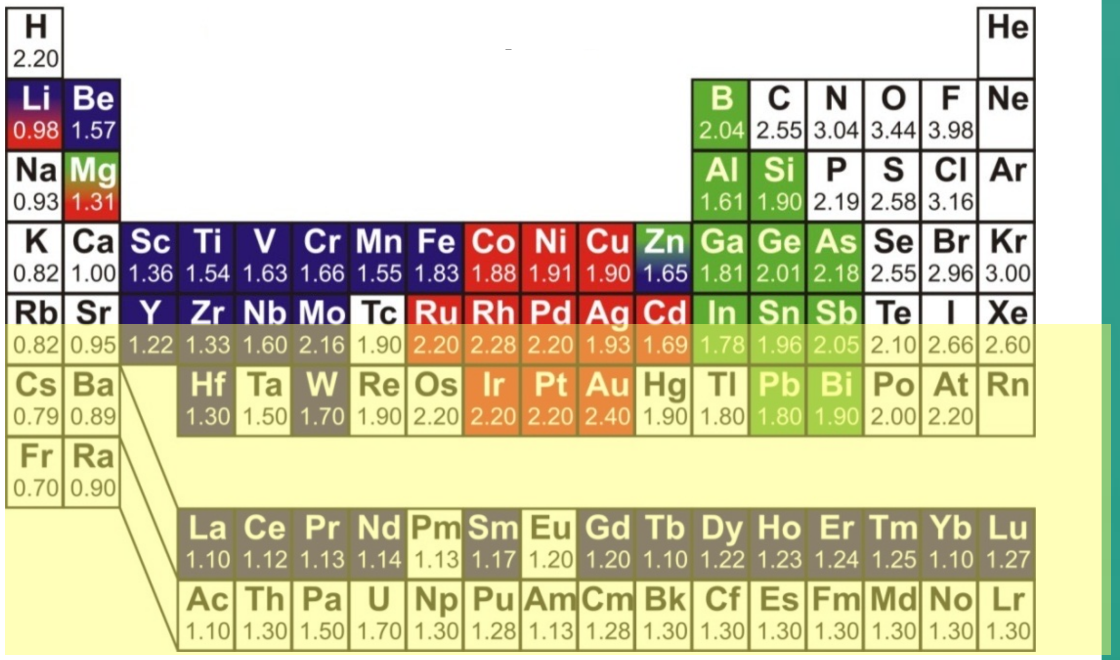

Prediction of the quantum spin Hall effect

Solution: materials with large spin orbit coupling

$\lambda_{SOC} \sim Z^2$ **for valence shells**

Kane and Mele, PRL 95, 146802 (2005)

topological insulators

Element Bismuth
Bi-Sb alloys
Bi_2Se_3 and related structures

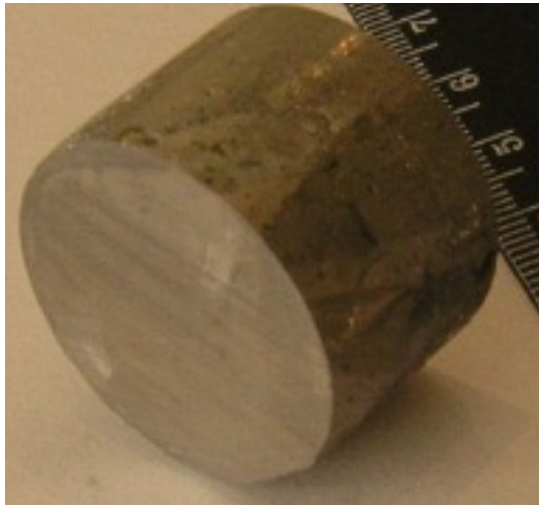

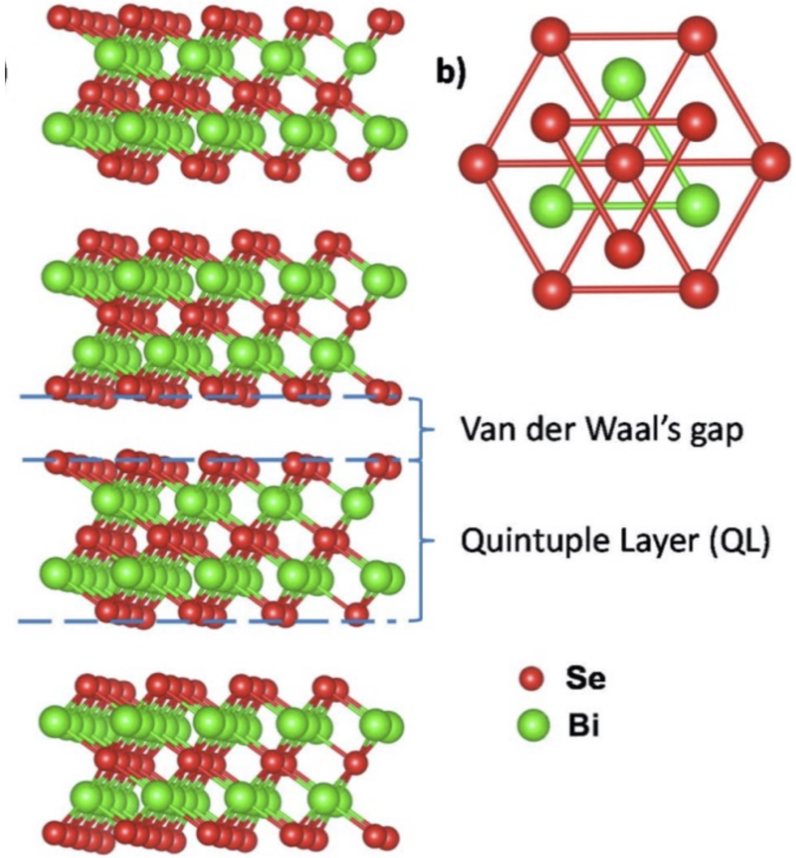

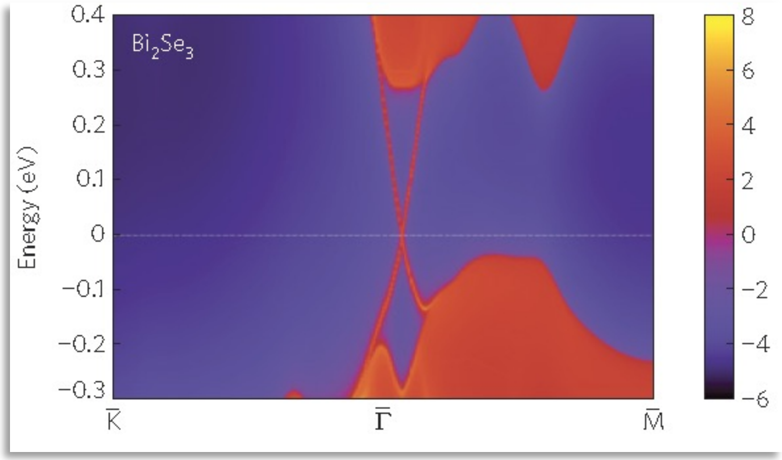

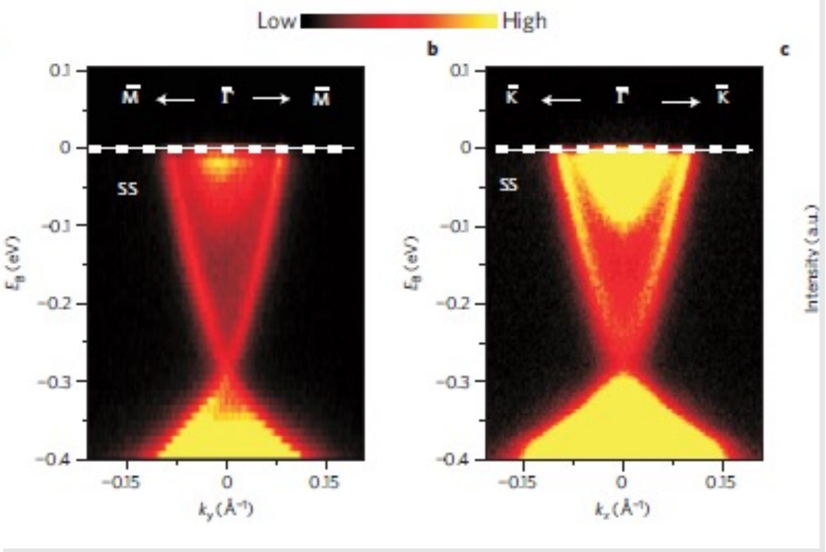

Moore and Balents, PRB 75, 121306(R) (2007)
Fu and Kane, PRB 76, 045302 (2007)
Murakami, New J. Phys. 9, 356 (2007)
Hsieh, et al., Science 323, 919 (2009)
Xia, et al., Nature Phys. 5, 398 (2009); Zhang, et al., Nature Phys. 5, 438 (2009)

measurements

- protected surface states
- quantized effects
- large effects in response to
    - the magnetic field, …

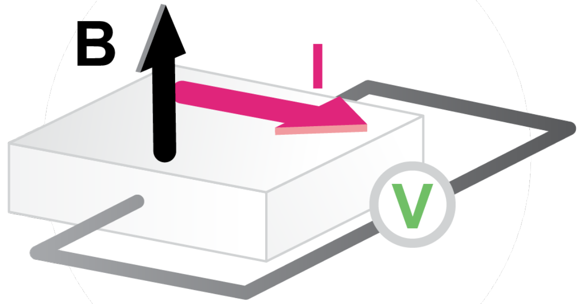

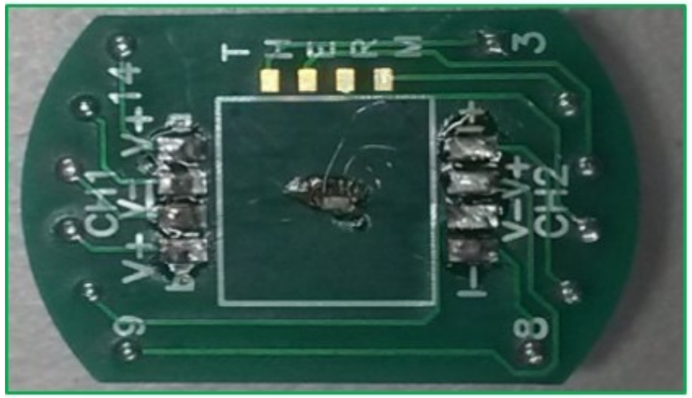

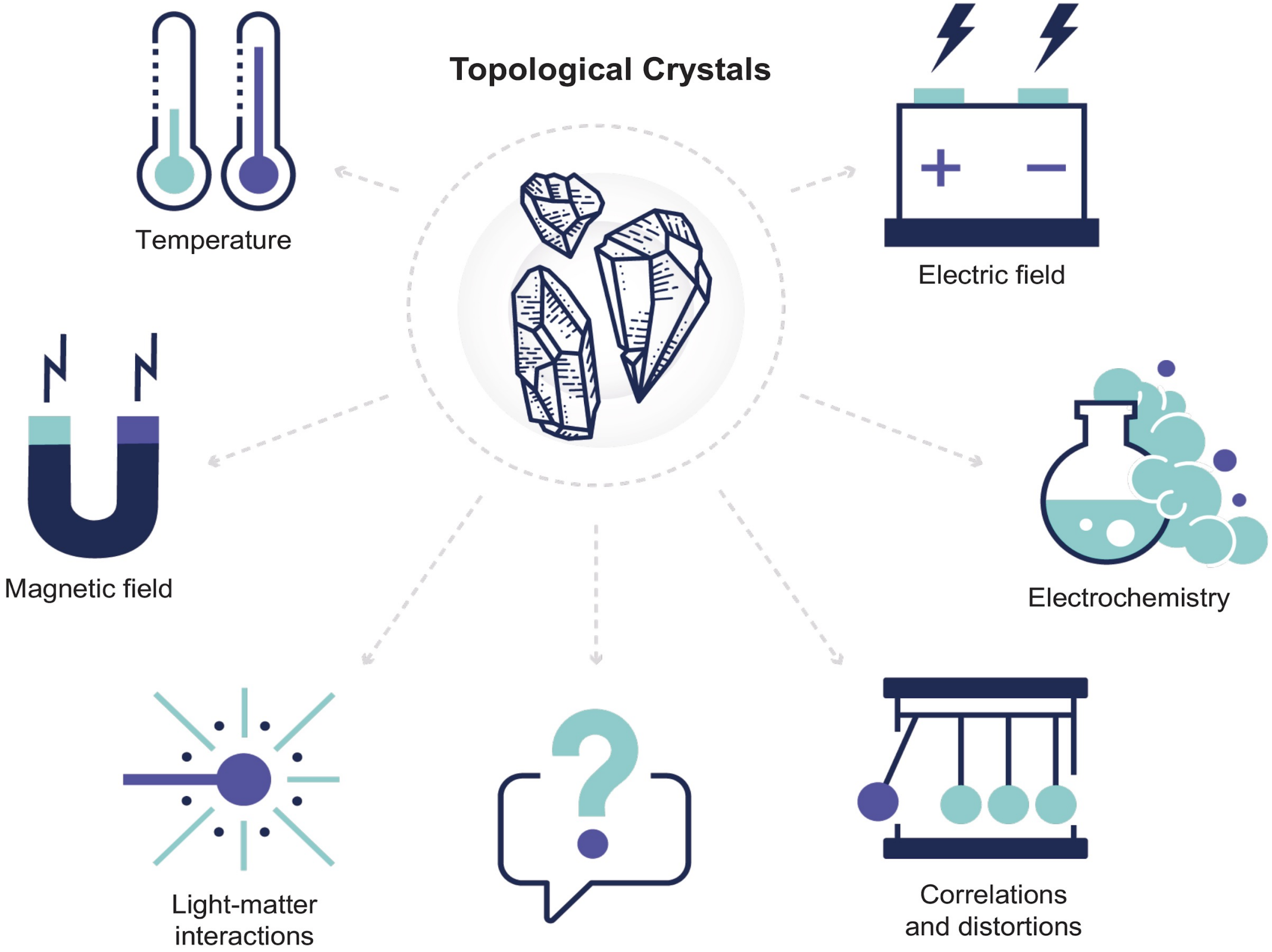

topologic or trivial

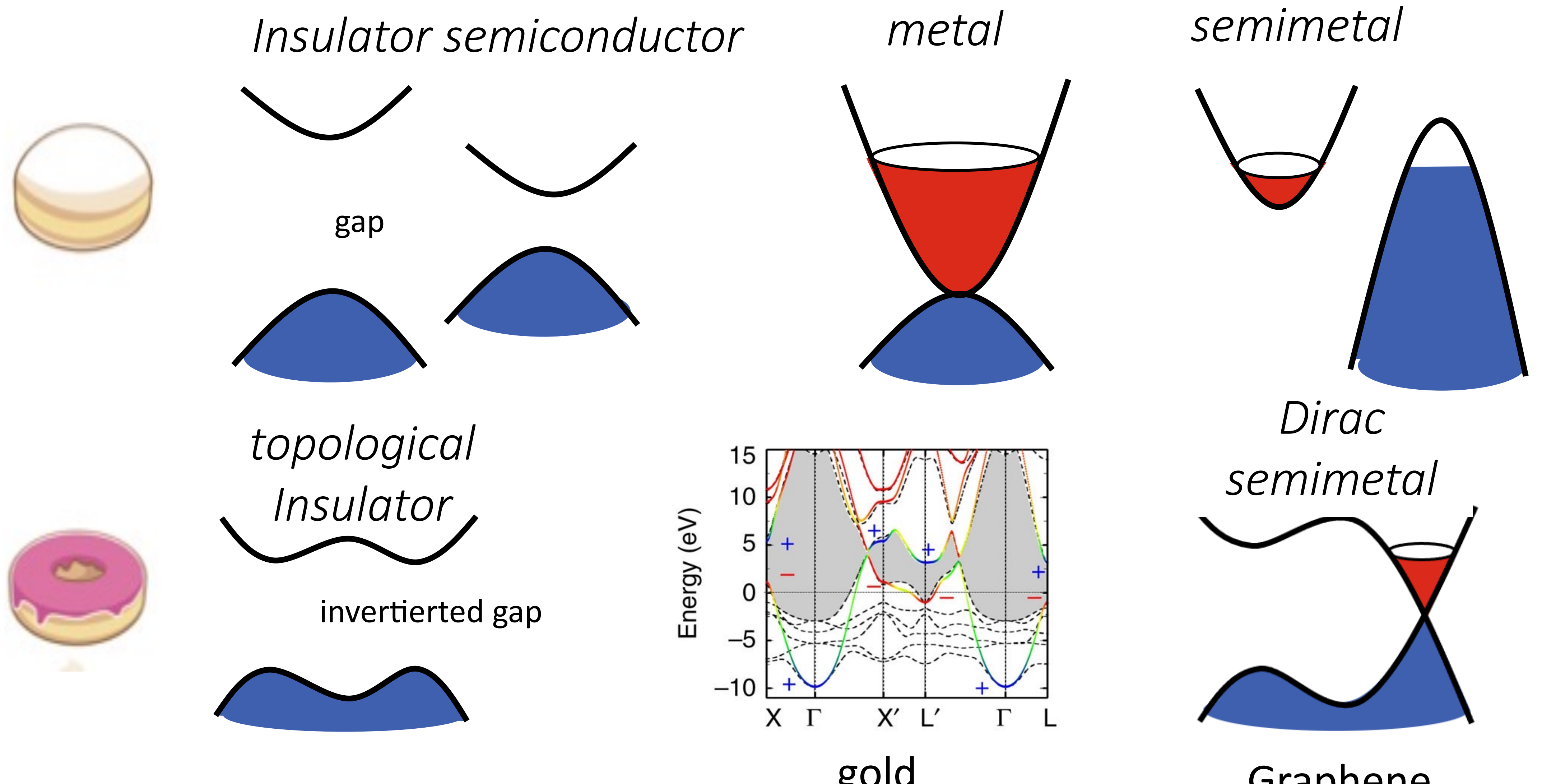

J. Gooth, J. Kübler, C. Felser, Physik Journal 20 (2021) 29.

from insulator to semimetal

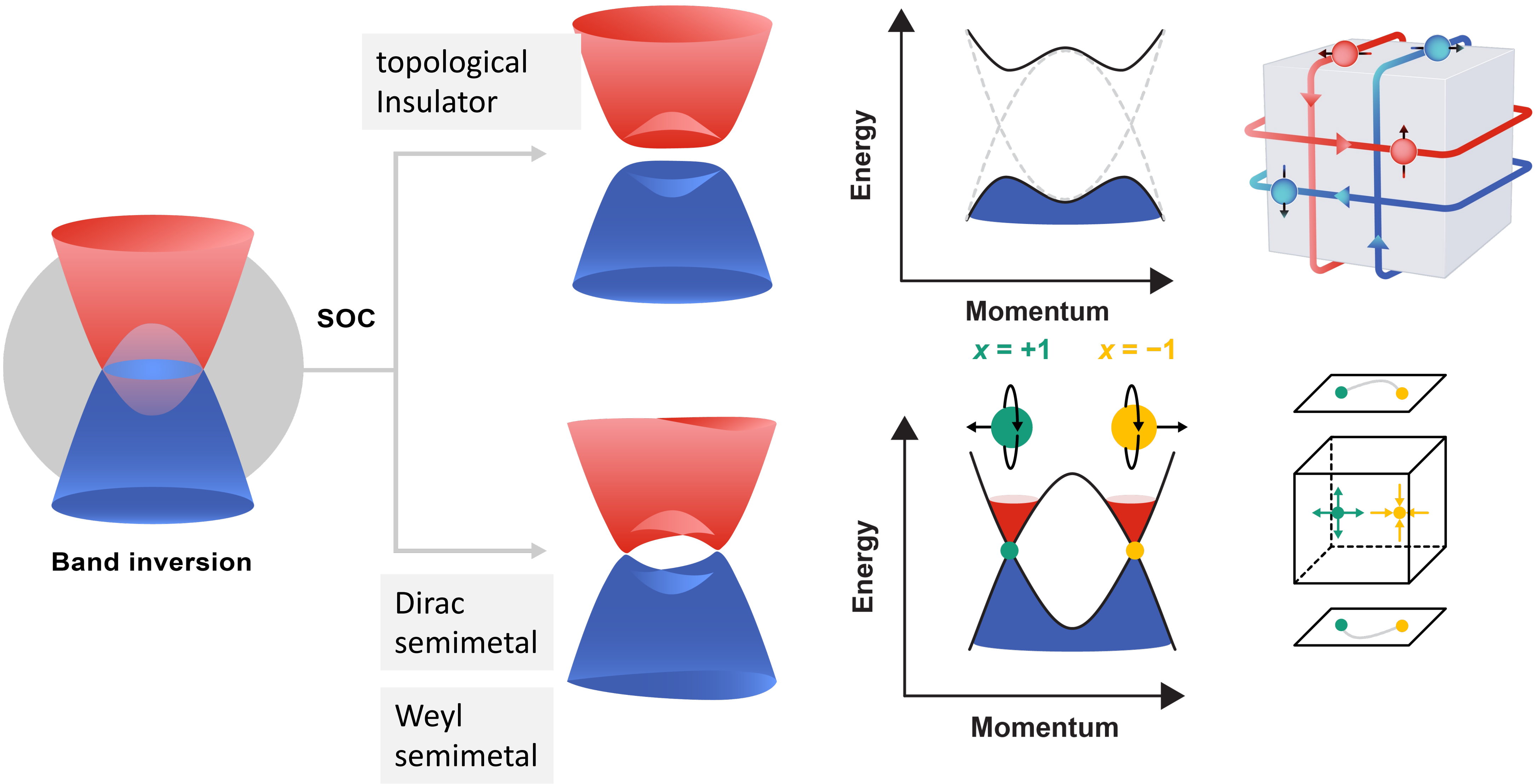

Binghai Yan and Claudia Felser, Annual Review Condensed Matter Physics **8** (2017) 337, Prineha Narang, Christina A. C. Garcia and Claudia Felser, Nature Materials **20** (2021) 293

semimetals are common

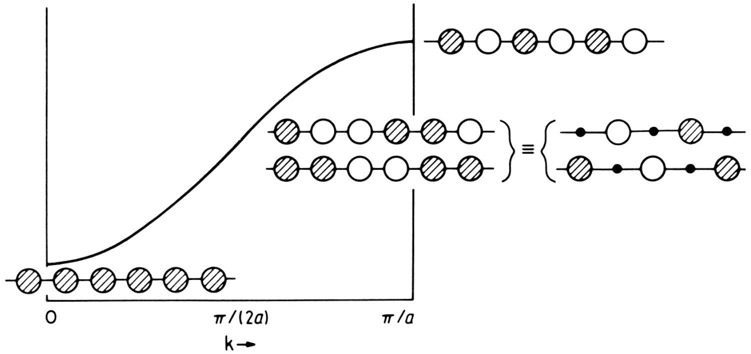

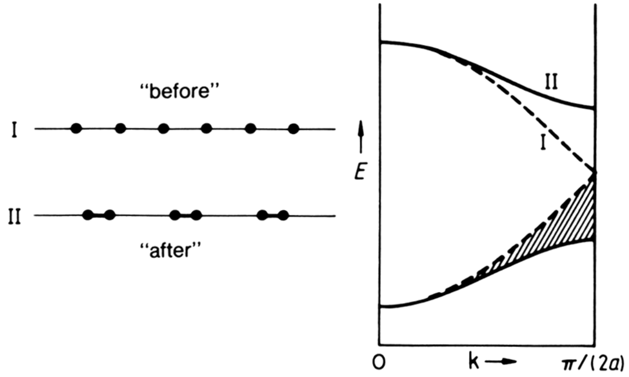

a‘= 2a
k= π/2a

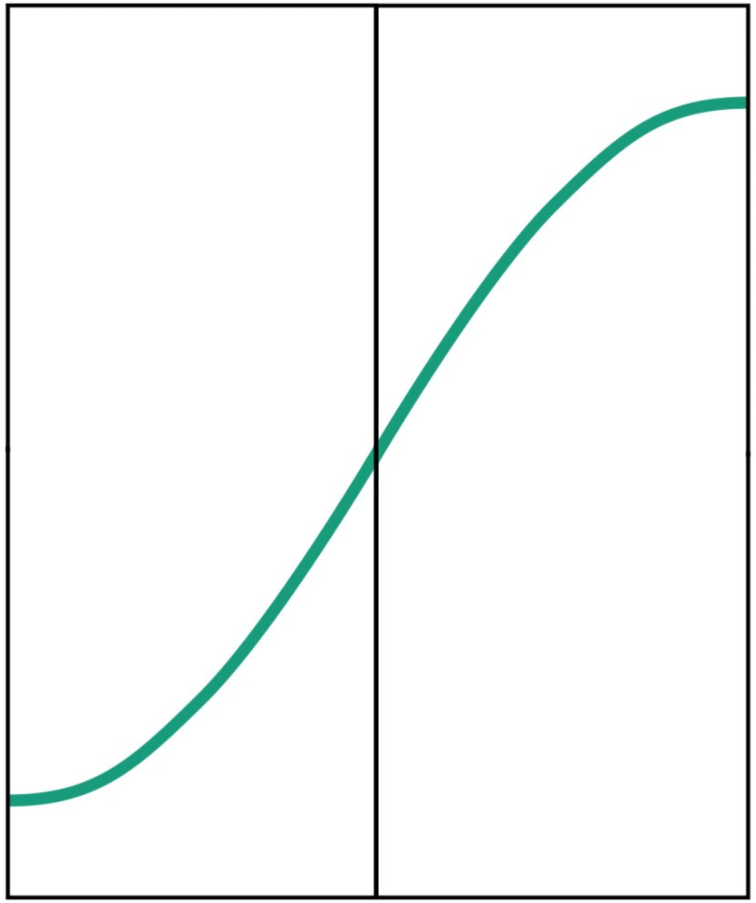

Roald Hoffmann Angewandte. Chem. 26 (1987) 846

chiral electrons

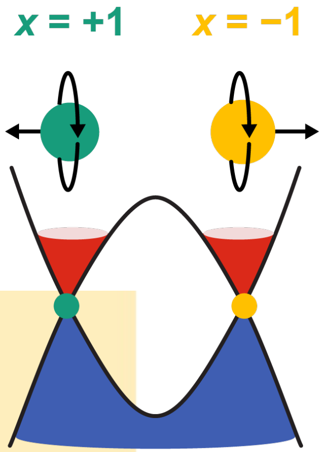

in bulk

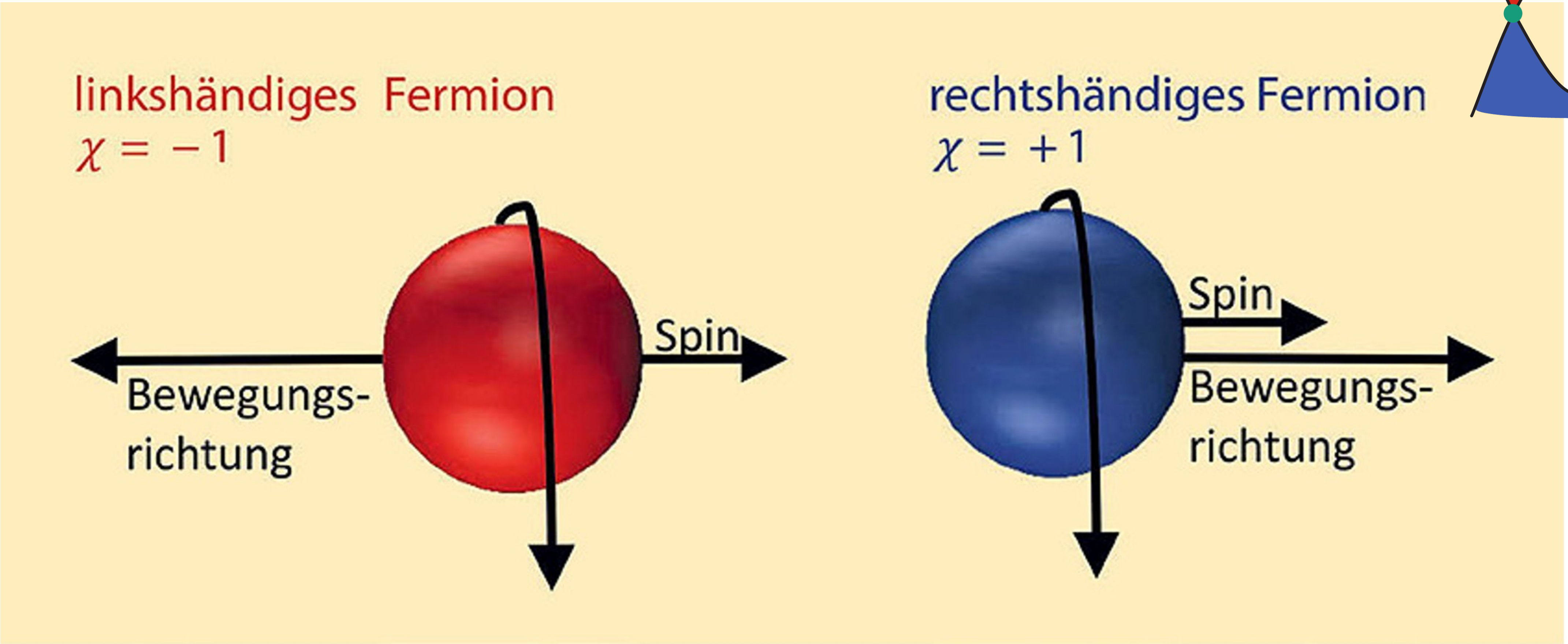

A. C. Niemann, et al., Physik in unserer Zeit 49 (2018) 168-175

chirality

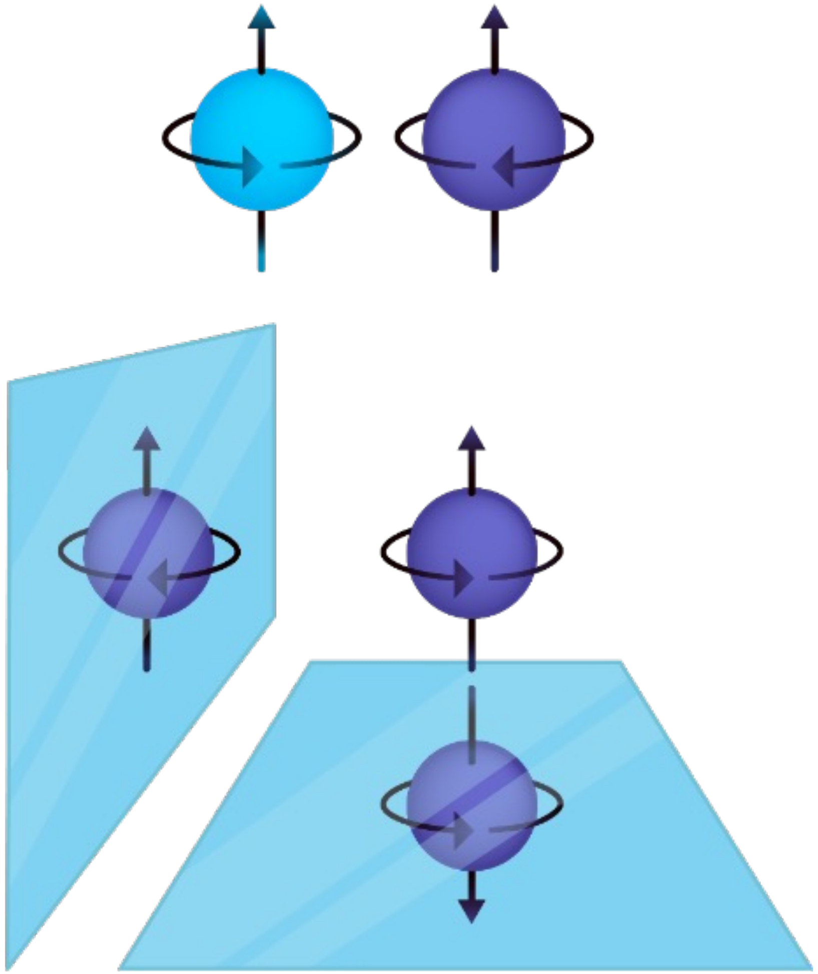

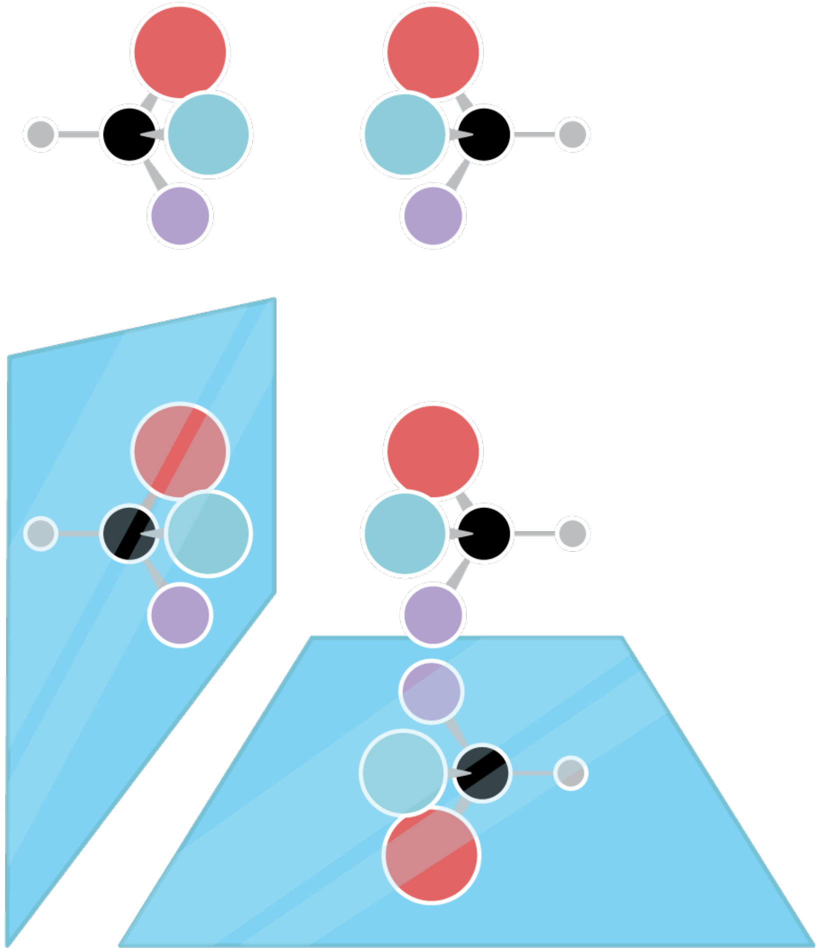

Nobel Symposium 167 on Chiral matter

June 28 – July 1, 2021

Lidingö, Sweden

NOBEL SYMPOSIA

synthesis

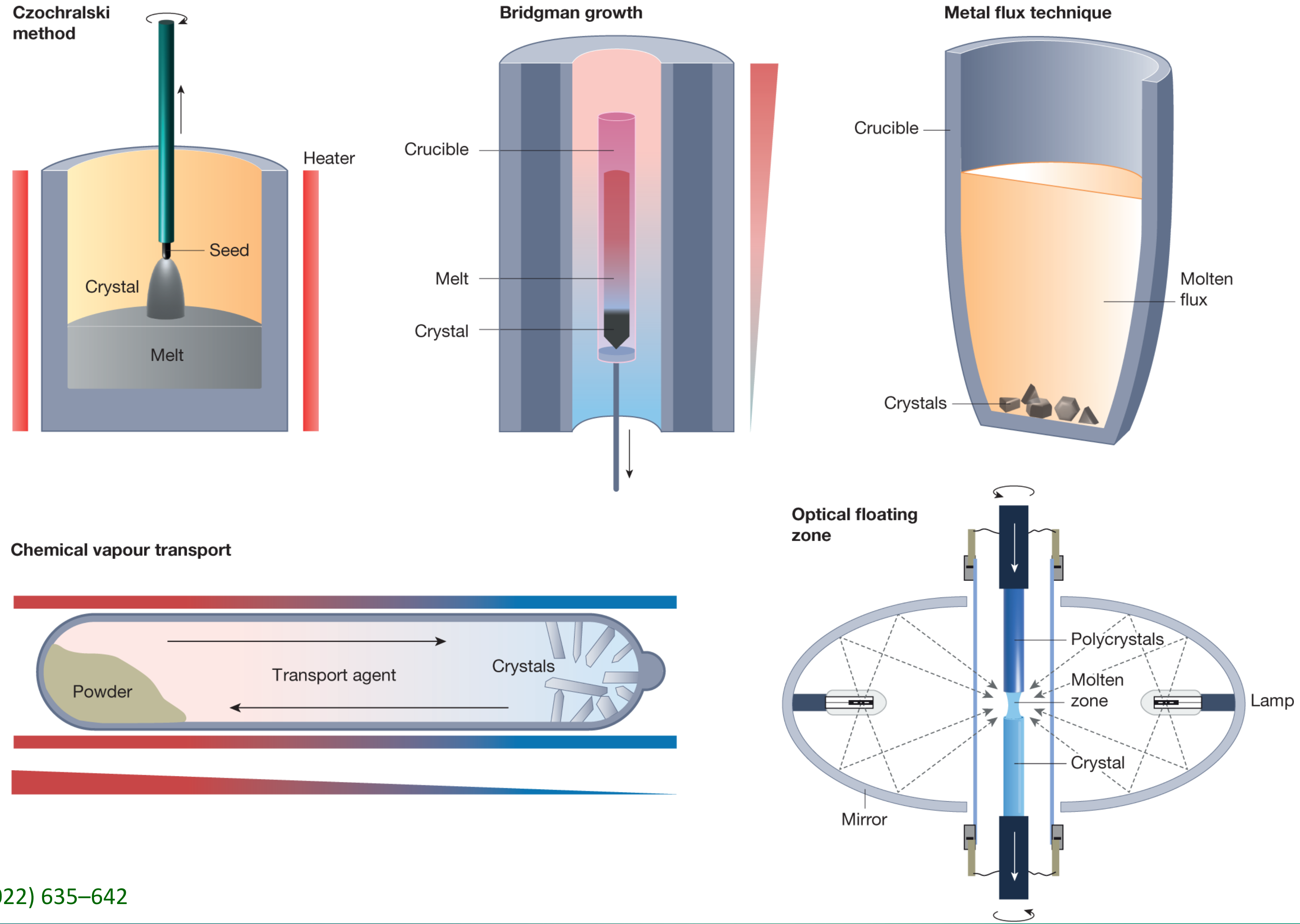

M. Scheffler et al., Nature 604 (2022) 635–642

chiral anomaly

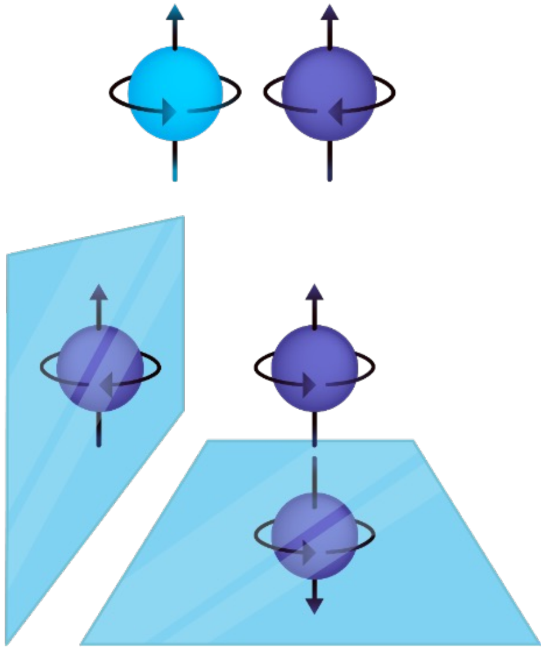

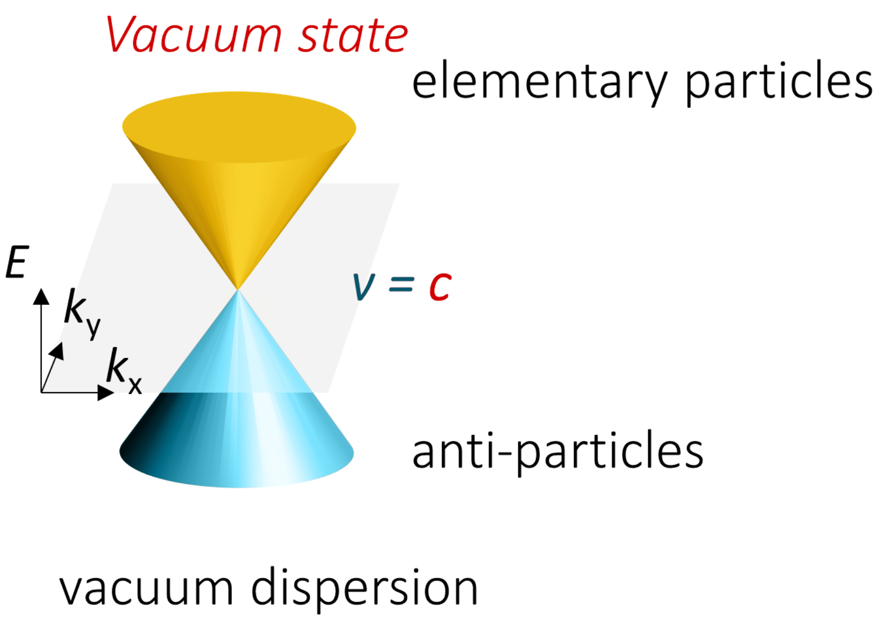

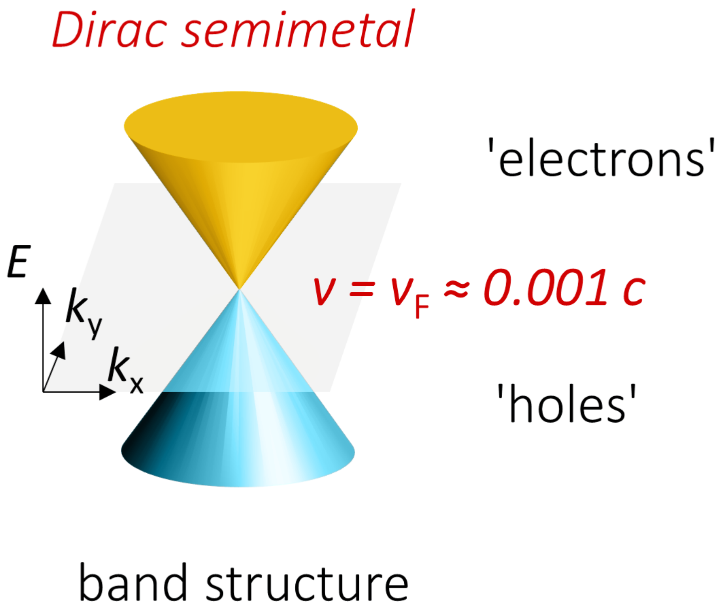

Chiral anomaly is the **anomalous non-conservation** of a chiral current.

A sealed box with equal numbers of positive and negative charged particles is found when it is opened to have more positive than negative particles, or vice-versa.
Prohibited from classical conservation laws, but can be **broken in a quantum world**.
Universe contains more matter than antimatter

Wikipedia

Adler, Phys. Rev. **177**, 2426 (1969)
Bell and. Jackiw, Nuovo Cim. **A60**, 47 (1969)
Zyuzin, Burkov - Physical Review B (2012)

Burkov, Balents, PRL **107**, 12720 (2012)
Burkov, J. Phys.: Condens. Matter **27**, 113201 (2015)
Volovik, The Universe in a Helium Droplet (International Series of Monographs on Physics, Band 117) ISBN: 9780199564842

Weyl semimetals

3D topological Weyl - transport measurements:

1. Giant responses to an external stimuli
2. Fermi arc
3. Chiral anomaly
4. Axial gravitational anomaly

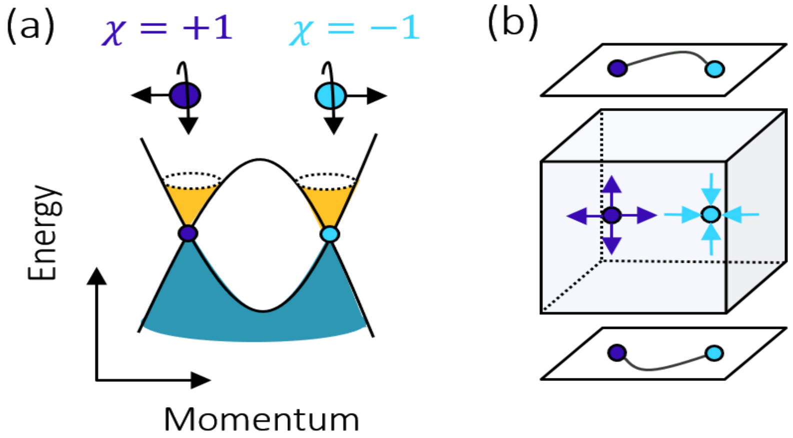

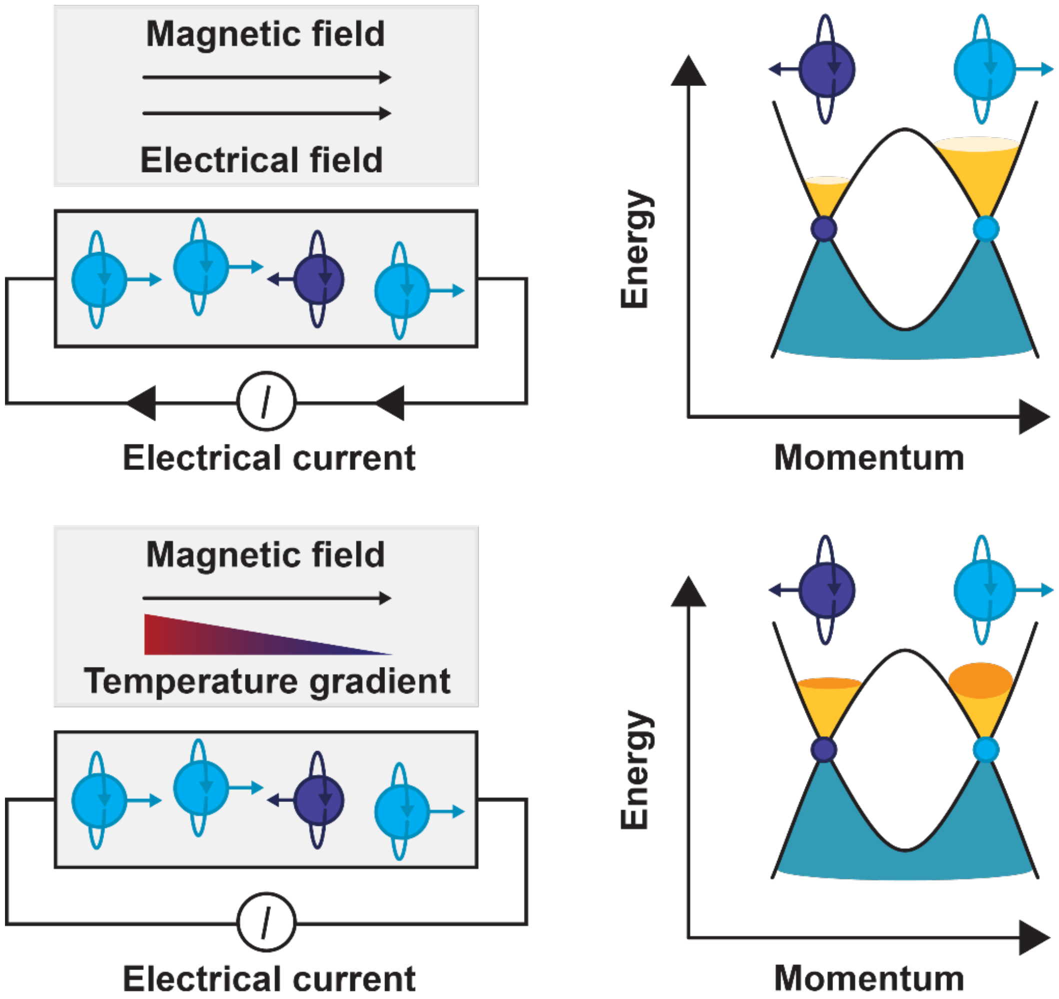

Burkov, Balents, PRL **107** 12720 (20

Burkov, arXiv:1704.05467v2

Burkov, J. Phys.: Condens. Matter **27** (2015) 113201

Johannes Gooth et al., Nature 547 (2017) 324

chiral anomaly

$$A = -\left(\frac{L^2}{2\pi\ell_B^2}\right)\left(\frac{Le\dot{k}_z}{2\pi}\right) = -V\frac{e^3}{4\pi^2\hbar^2}\mathbf{E}.\mathbf{B}$$

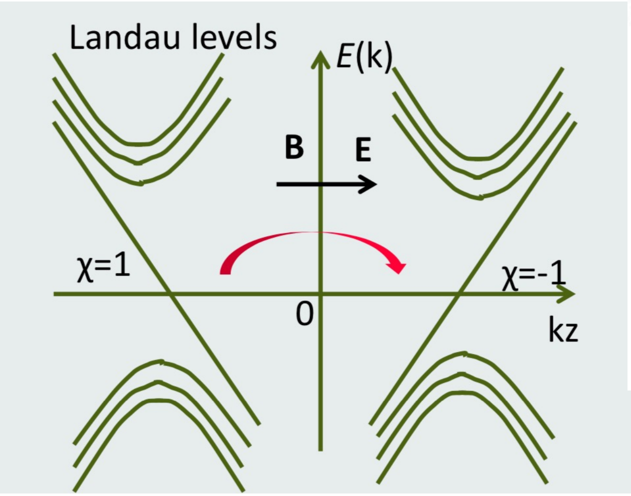

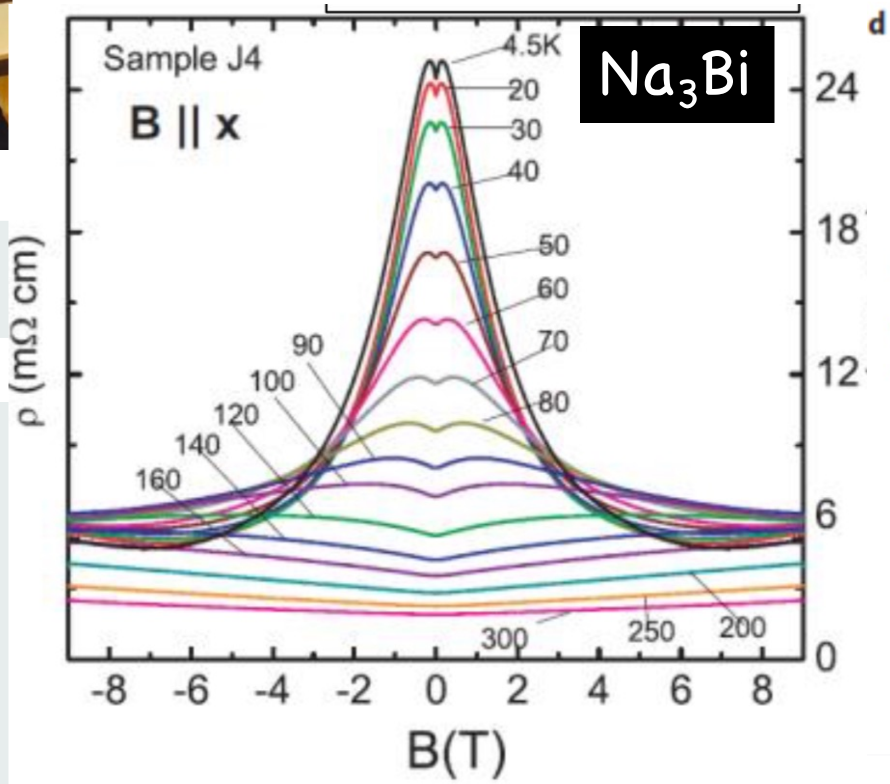

Jun Xiong, S. Kushwaha et al., *Science* 2015

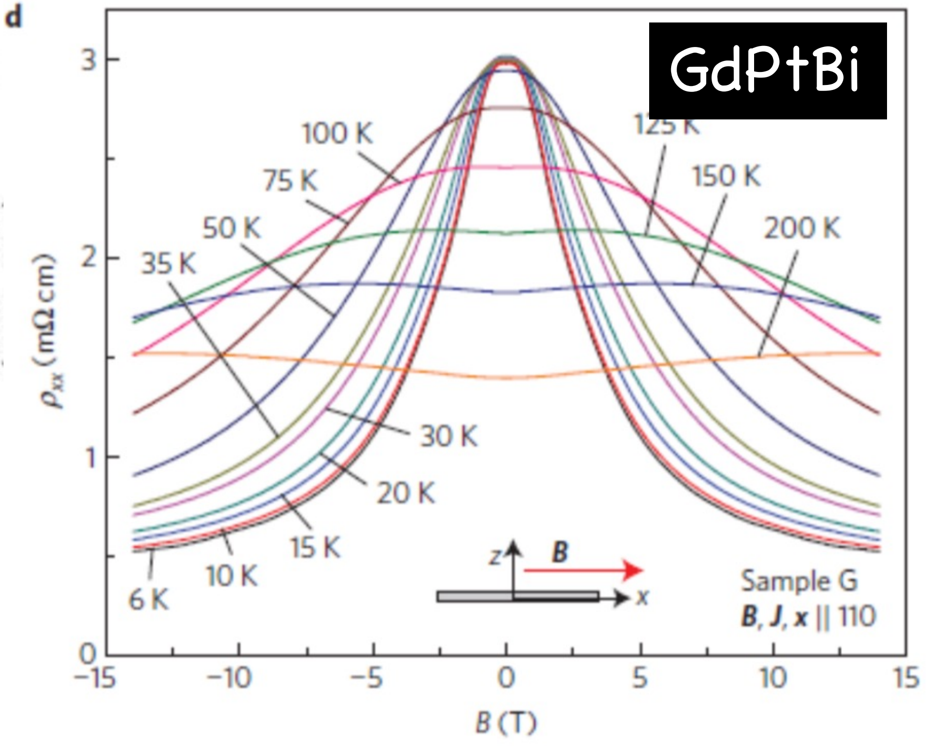

Hirschberger et al., *Nature Materials*, 2016

S. L. Adler, Phys. Rev. 177, 2426 (1969)
J. S. Bell and R. Jackiw, Nuovo Cim. A60, 47 (1969)
AA Zyuzin, AA Burkov - Physical Review B (2012)

Weyl semimetals

NbP, NbAs, TaP, TaAs

Weyl Semimetal Phase in Noncentrosymmetric Transition-Metal Monophosphides

Hongming Weng, Chen Fang, Zhong Fang, B. Andrei Bernevig, and Xi Dai

Phys. Rev. X **5**, 011029 – Published 17 March 2015

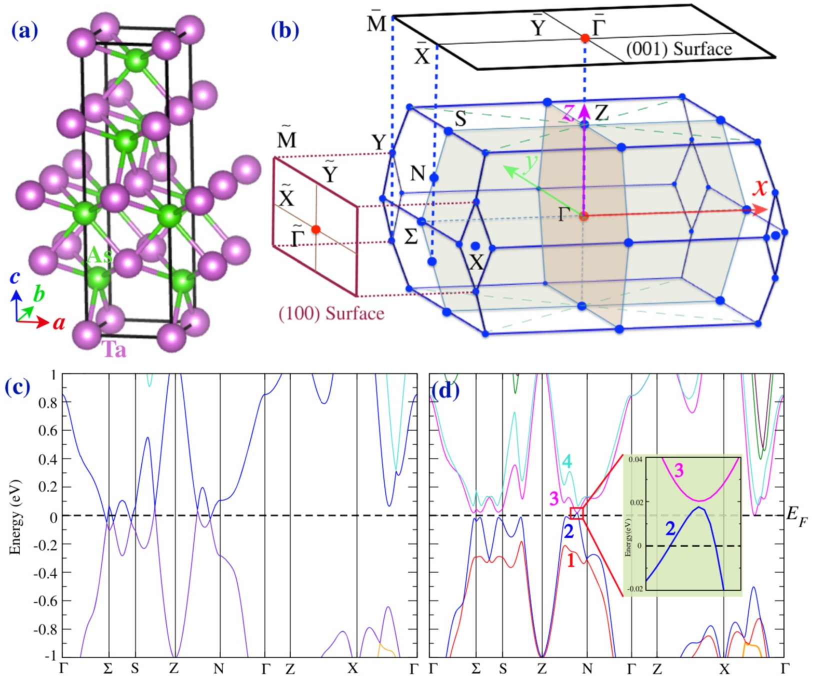

ARTICLE

Received 24 Nov 2014 | Accepted 30 Apr 2015 | Published 12 Jun 2015

DOI: 10.1038/ncomms8373

OPEN

A Weyl Fermion semimetal with surface Fermi arcs in the transition metal monopnictide TaAs class

Shin-Ming Huang[1,2,*], Su-Yang Xu[3,4,*], Ilya Belopolski[3,4,*], Chi-Cheng Lee[1,2], Guoqing Chang[1,2], BaoKai Wang[1,2,5], Nasser Alidoust[3,4], Guang Bian[3], Madhab Neupane[3,4,6], Chenglong Zhang[7], Shuang Jia[7,8], Arun Bansil[5], Hsin Lin[1,2] & M. Zahid Hasan[3,4,9]

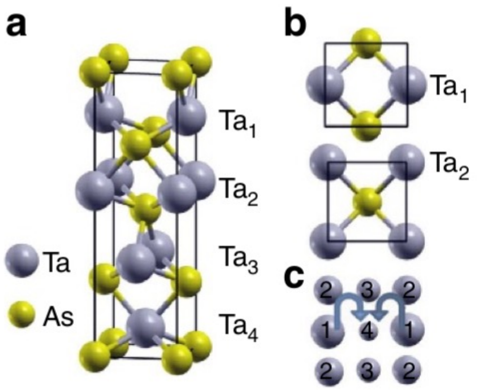

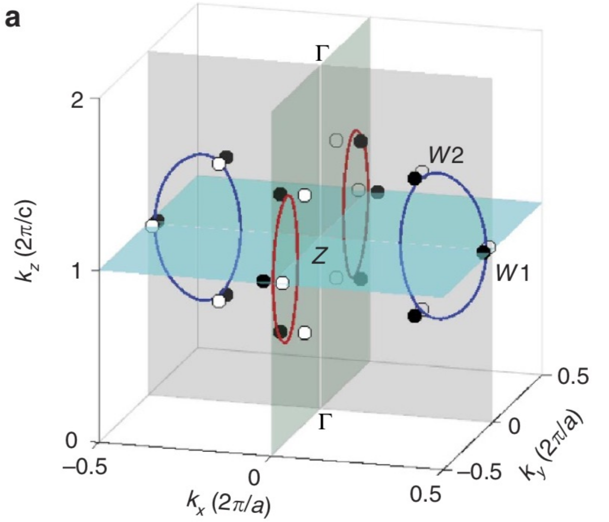

Weyl semimetals

NbP, NbAs, TaP, TaAs

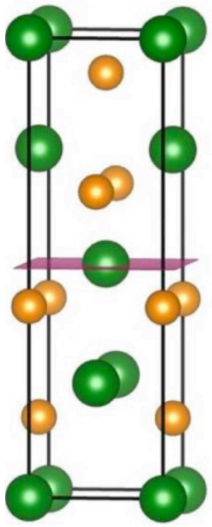

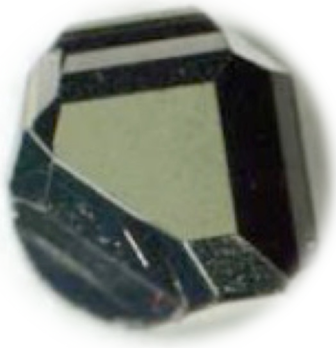

angle resolved Photoemission

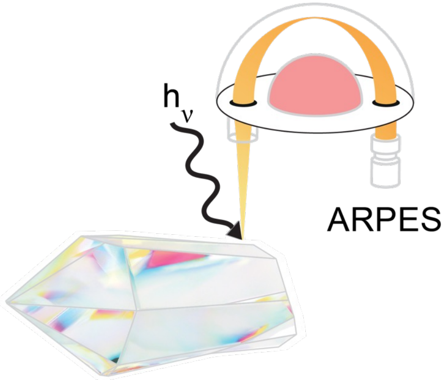

chemical vapor transport

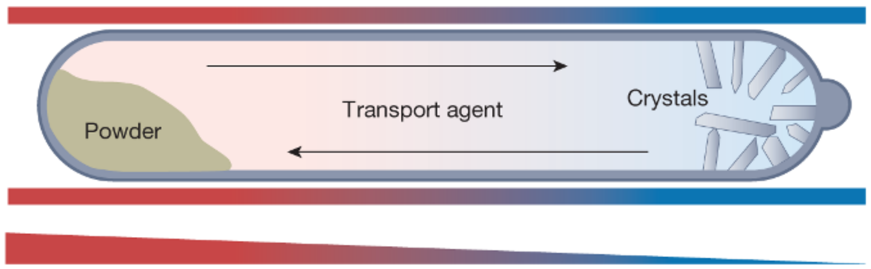

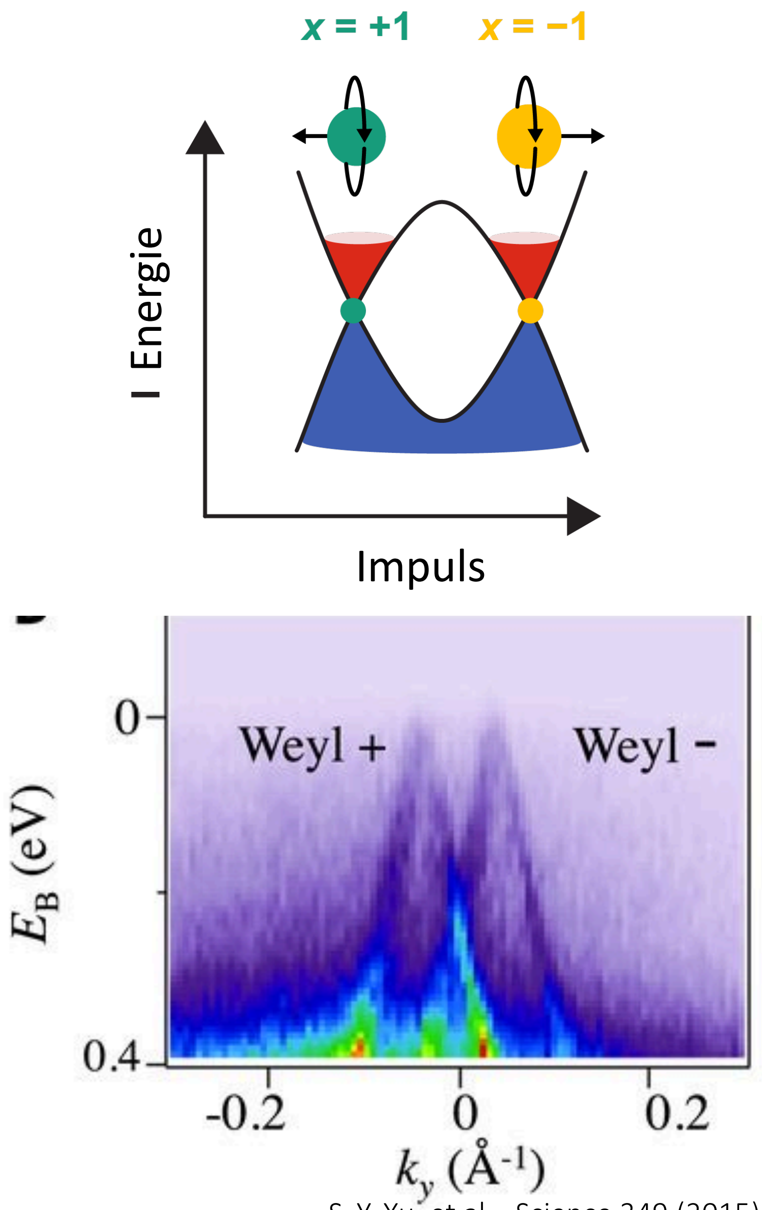

Weng, et al. Phys. Rev. X 5, 11029 (2015)
Huang et al. preprint arXiv:1501.00755

S.-Y. Xu, et al., Science 349 (2015) 613

Weyl semimetals

NbP, NbAs, TaP, TaAs

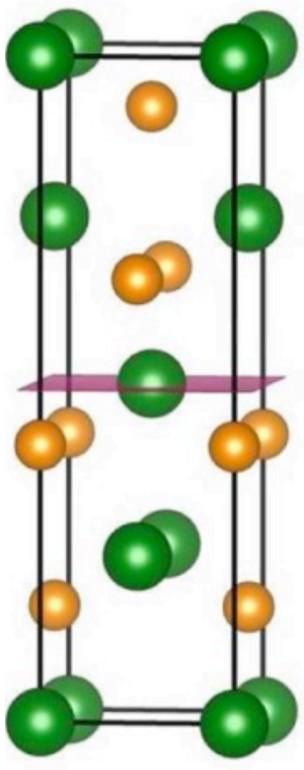

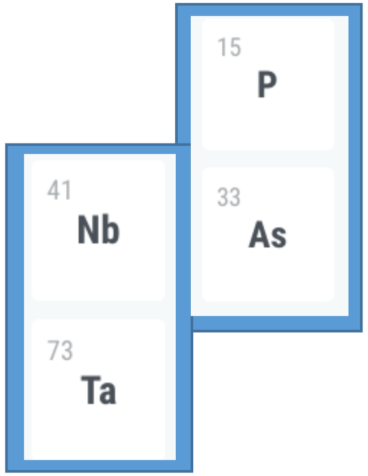

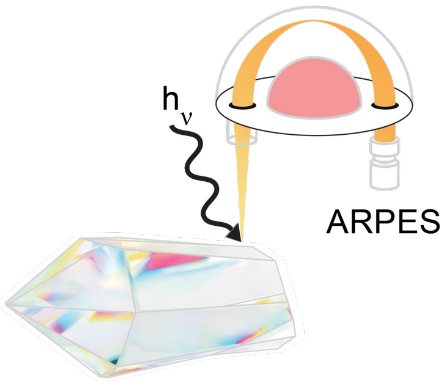

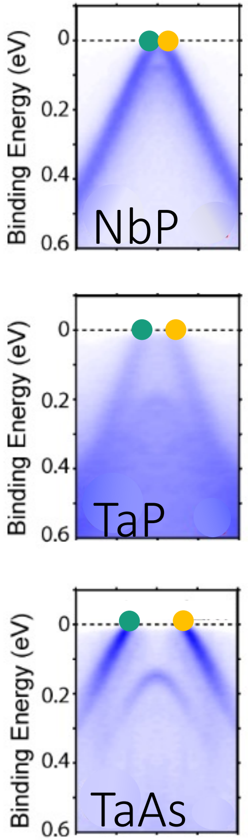

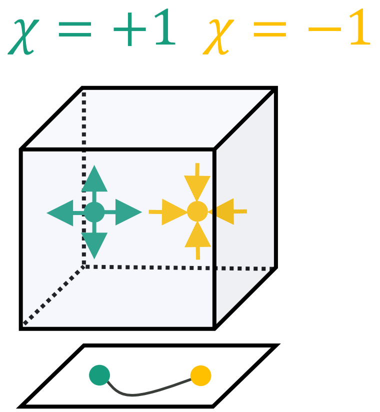

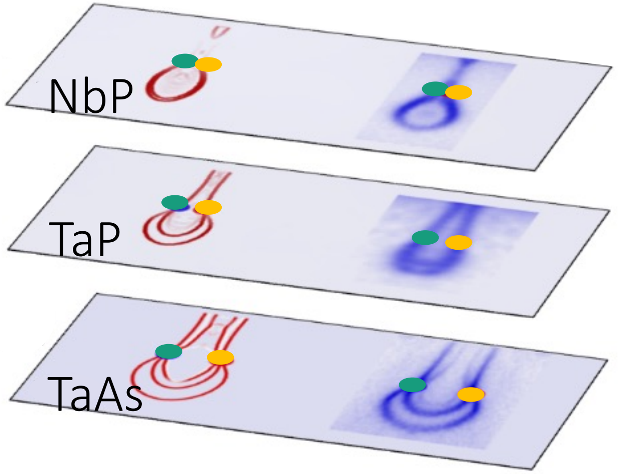

Weng, et al. Phys. Rev. X 5, 11029 (2015)
Huang et al. preprint arXiv:1501.00755

Shekhar, et al. , Nature Physics 11 (2015) 645
Frank Arnold, et al. Nature Communication 7 (2016) 11615

Weyl semimetals

NbP, NbAs, TaP, TaAs

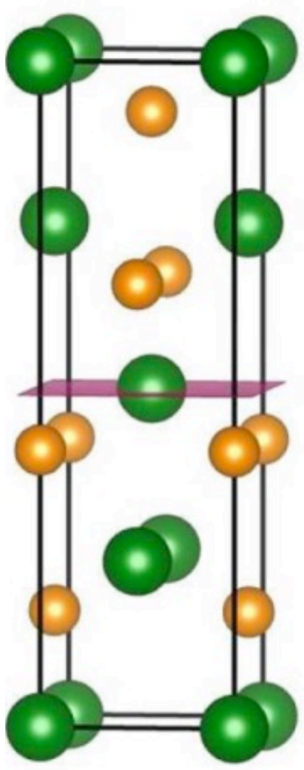

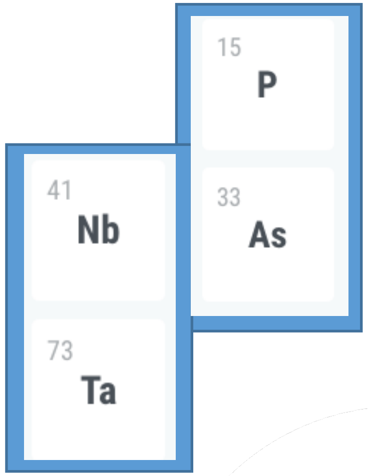

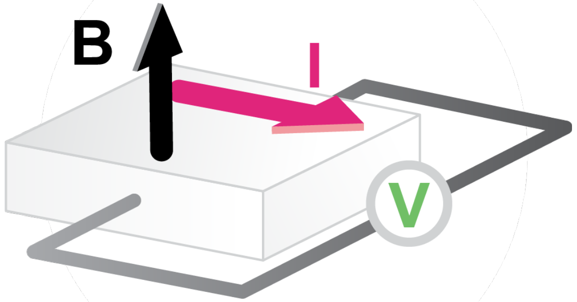

giant magnetoresistance

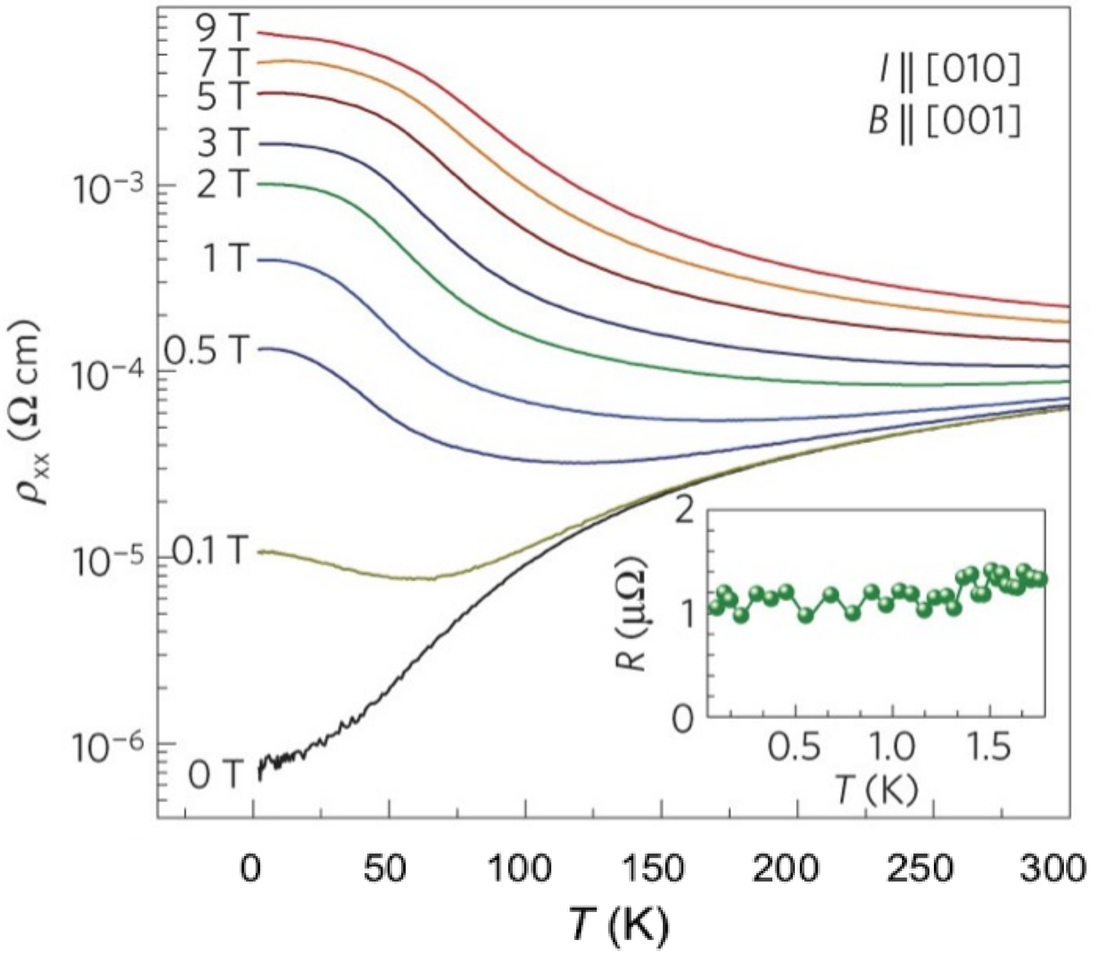

Weng, et al. Phys. Rev. X 5, 11029 (2015)
Huang et al. preprint arXiv:1501.00755

Shekhar, et al. , Nature Physics 11 (2015) 645
Frank Arnold, et al. Nature Communication 7 (2016) 11615

Weyl semimetals

NbP, NbAs, TaP, TaAs

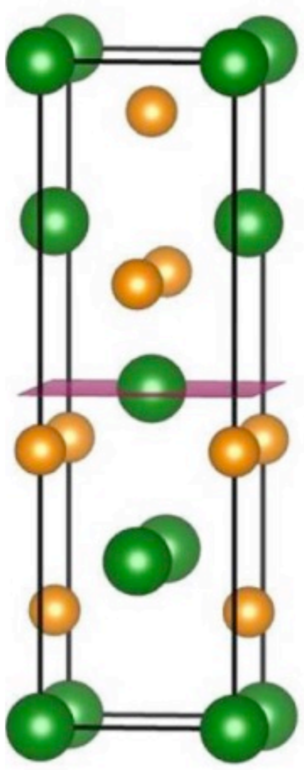

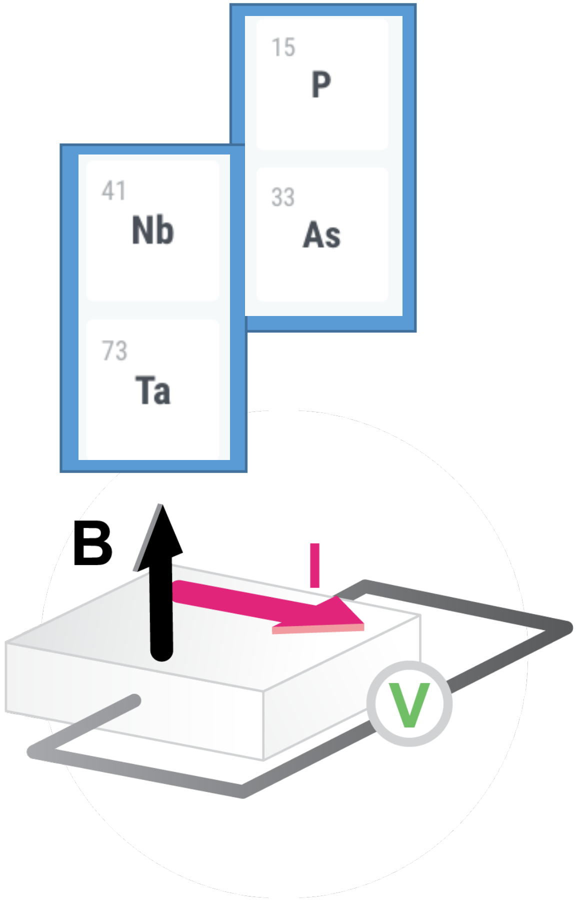

giant mobility

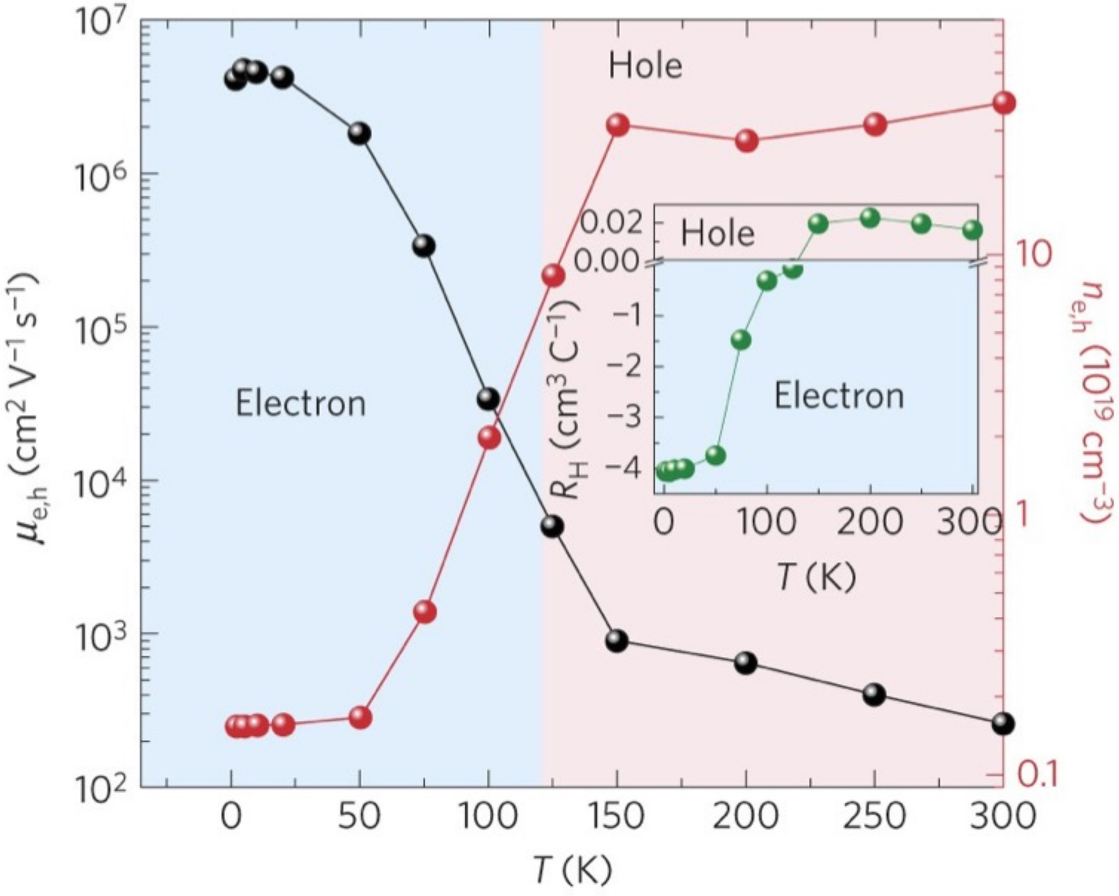

Weng, et al. Phys. Rev. X 5, 11029 (2015)
Huang et al. preprint arXiv:1501.00755

Shekhar, et al. , Nature Physics 11 (2015) 645
Frank Arnold, et al. Nature Communication 7 (2016) 11615

chiral anomaly

conservation of chirality

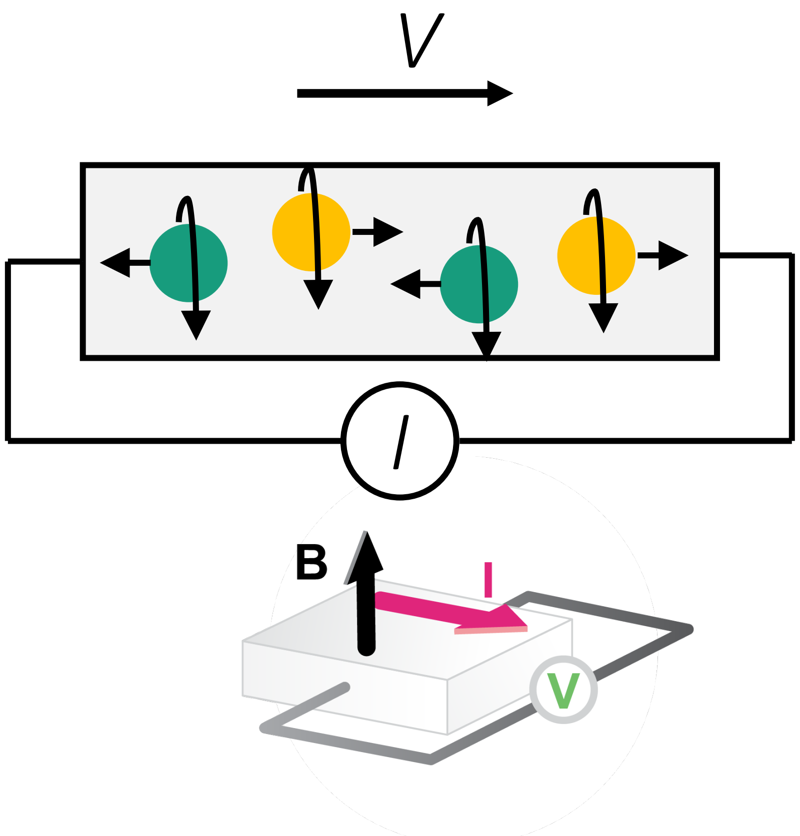

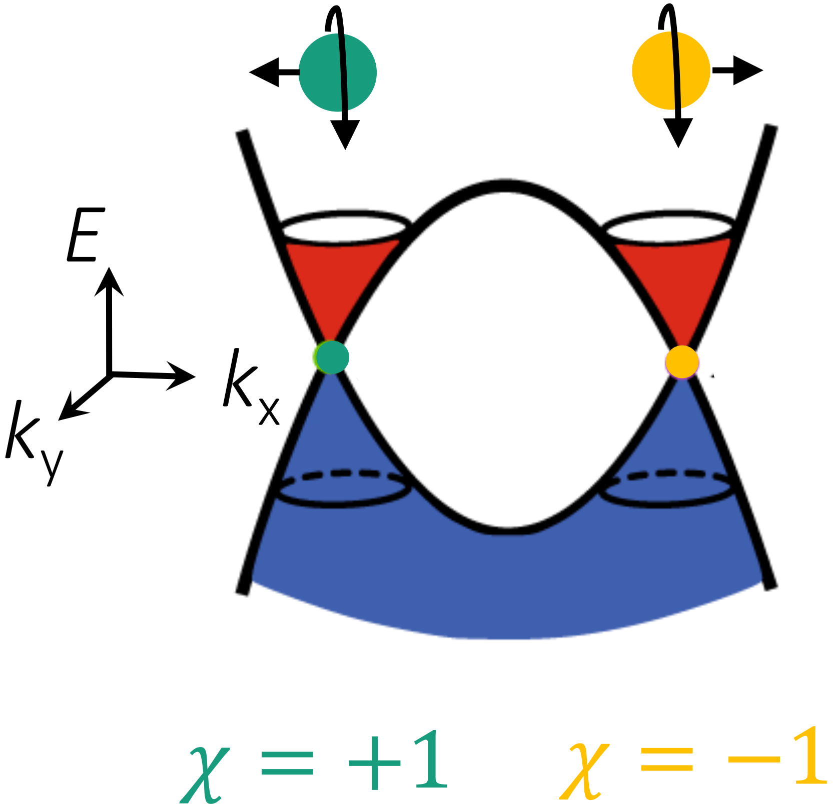

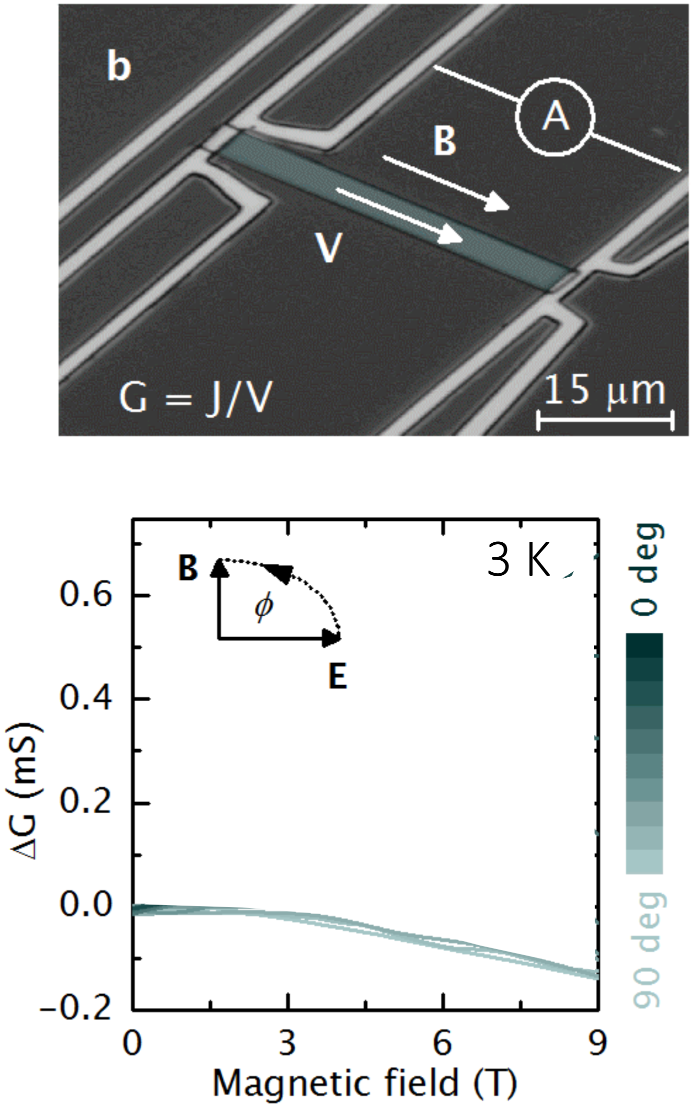

J. Gooth et al., Nature 547 (2017) 324 arXiv:1703.10682.
J. Gooth, J. Kübler, C. Felser, Physik Journal 20 (2021) 29.
Lucas, A., Davison, R. A. & Sachdev, S. PNAS **113**, 9463–9468 (2016).
Landsteiner K., et al. Gravitational anomaly and transport phenomena. Phys. Rev. Lett. **107**, 021601 (2011). URL
Jensen, et al. Thermodynamics, gravitational anomalies and cones. Journal of High Energy Physics **2013**, 88 (2013).

chirale Anomalie

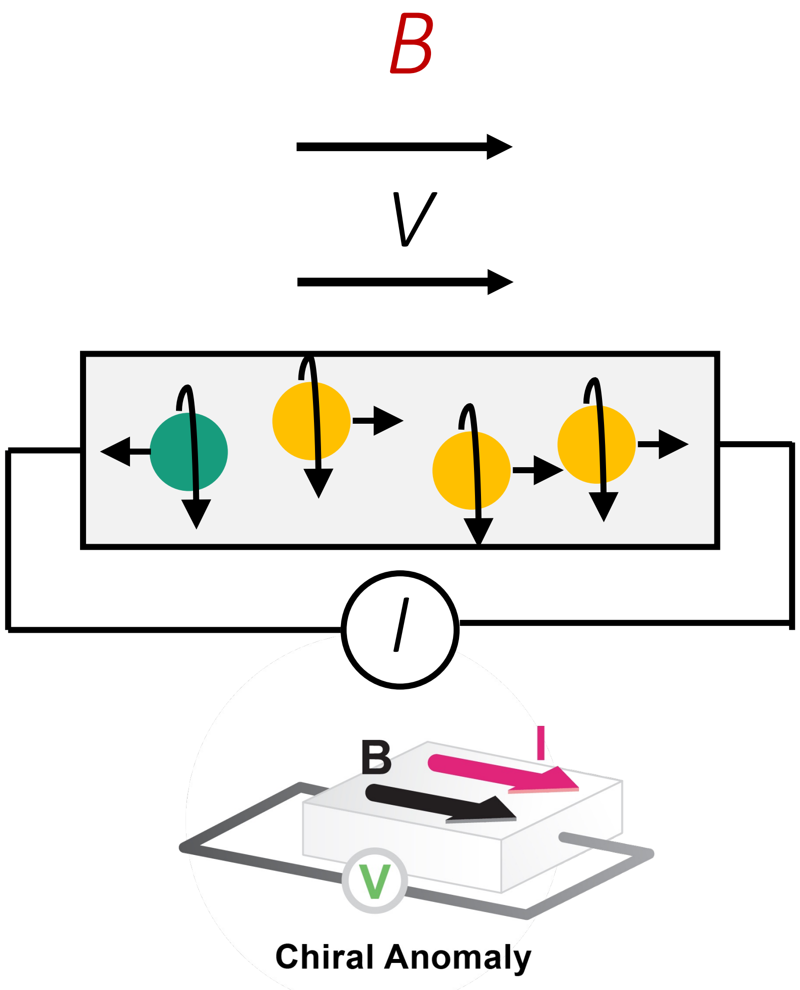

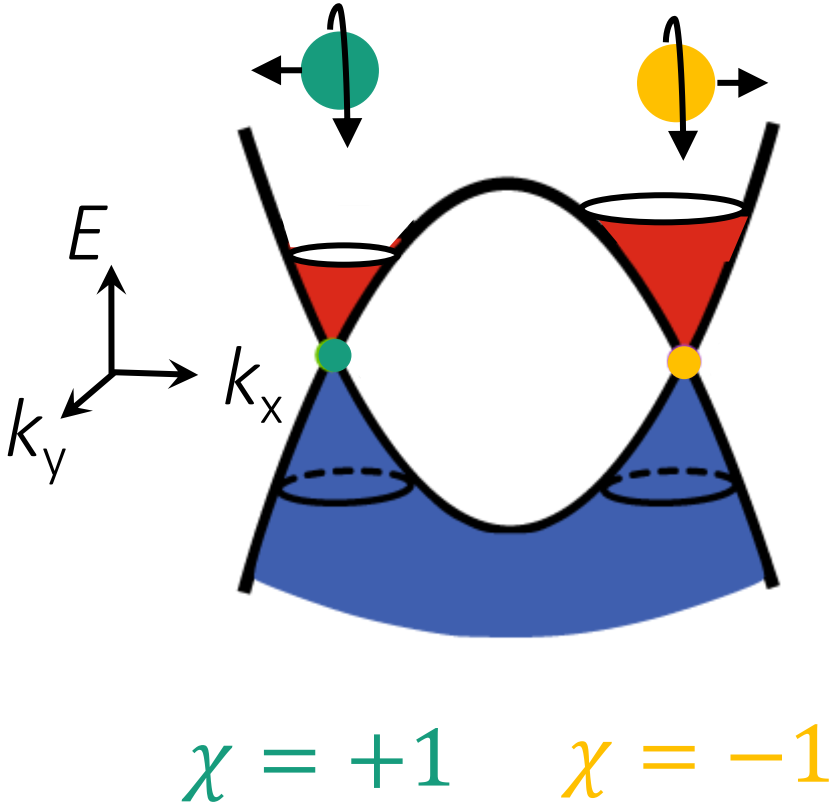

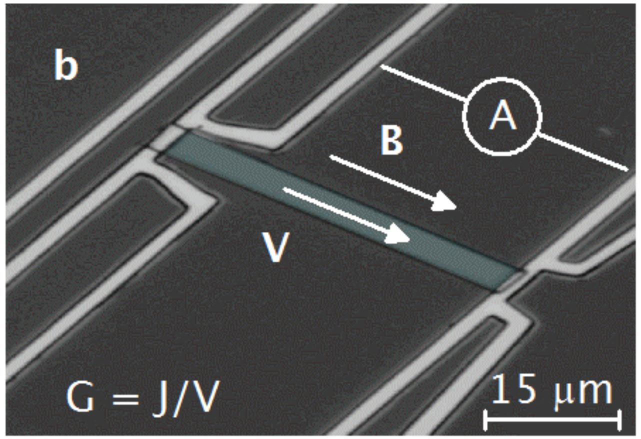

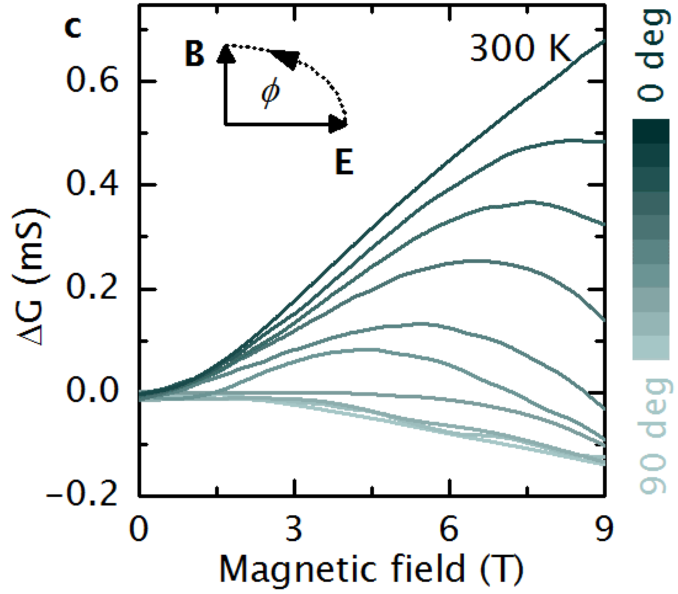

J. Gooth et al., Nature 547 (2017) 324 arXiv:1703.10682.
J. Gooth, J. Kübler, C. Felser, Physik Journal 20 (2021) 29.
Lucas, A., Davison, R. A. & Sachdev, S. PNAS **113**, 9463–9468 (2016).
Landsteiner K., et al. Gravitational anomaly and transport phenomena. Phys. Rev. Lett. **107**, 021601 (2011). URL
Jensen, et al. Thermodynamics, gravitational anomalies and cones. Journal of High Energy Physics **2013**, 88 (2013).

chiral anomaly

Erhaltung der Chiralität

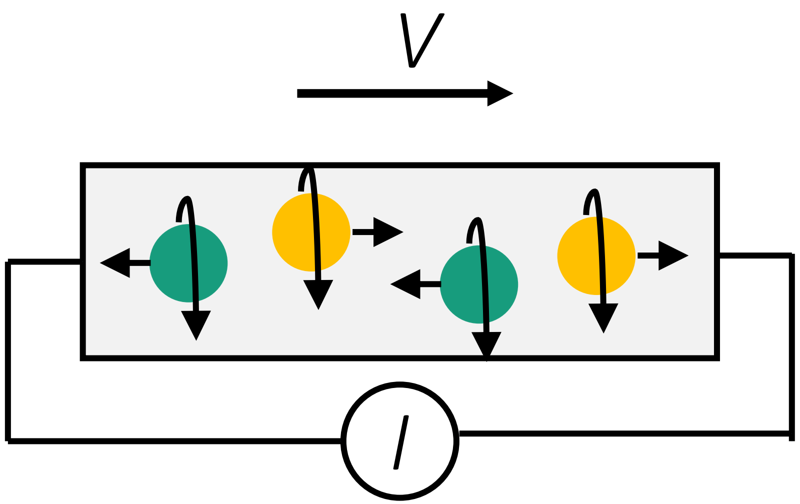

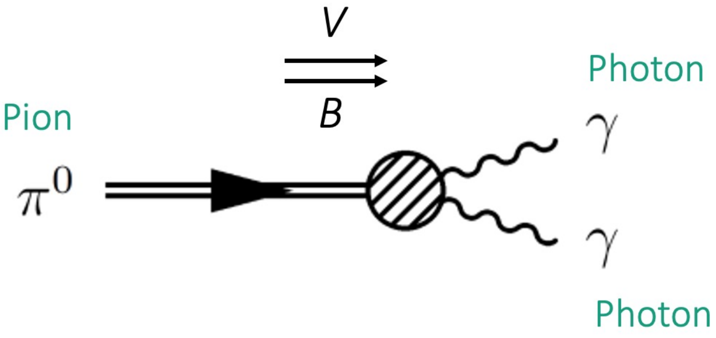

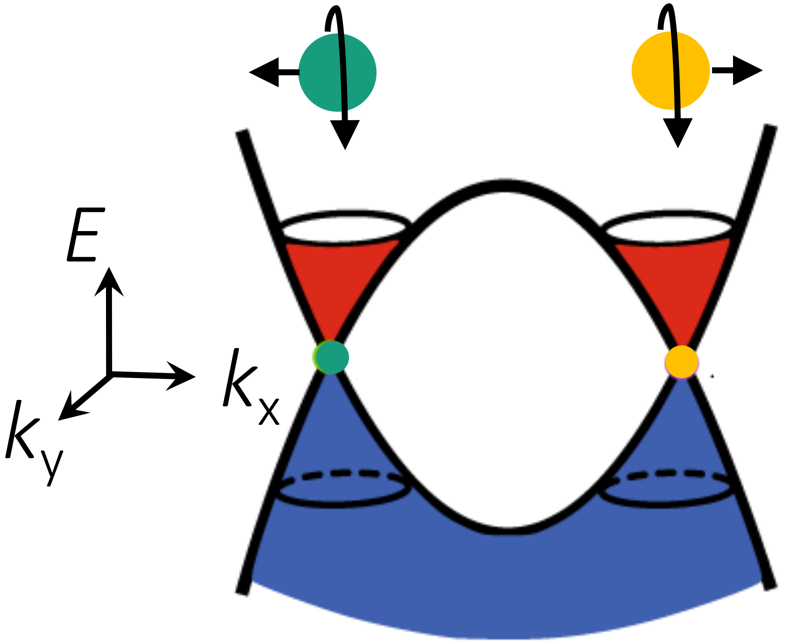

$\chi = +1$ $\chi = -1$

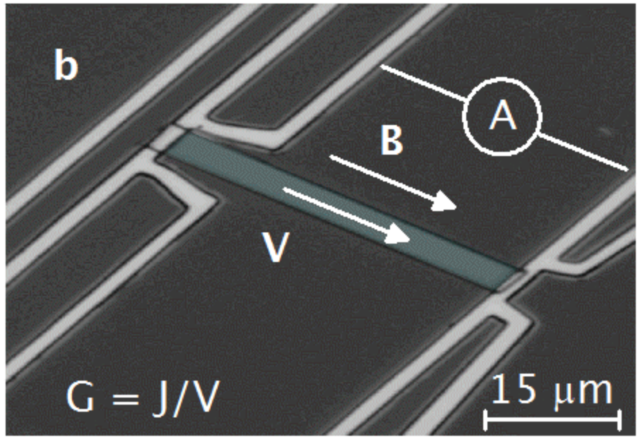

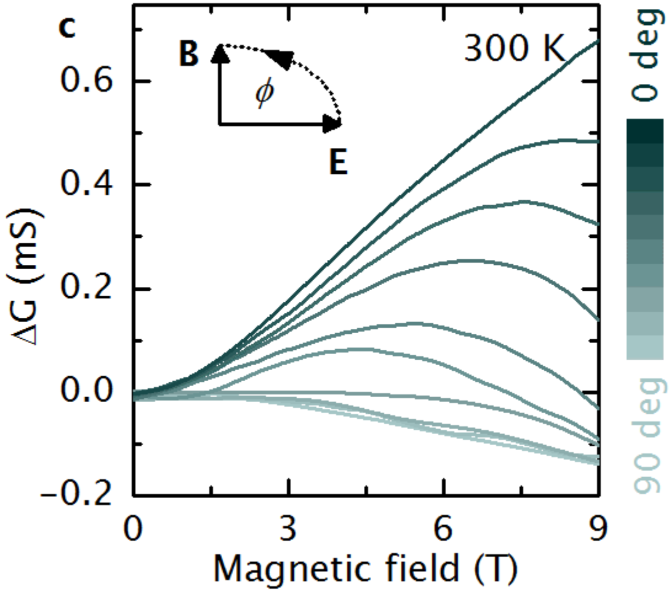

Johannes Gooth et al., Nature 547 (2017) 324 arXiv:1703.10682

axial gravitational anomaly

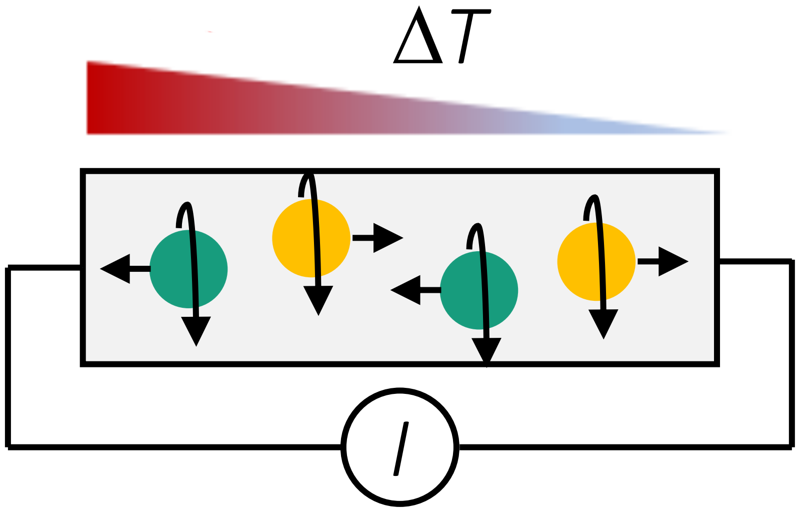

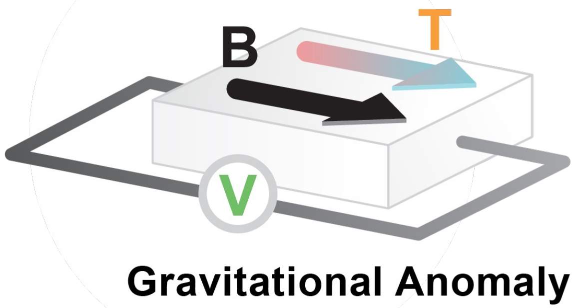

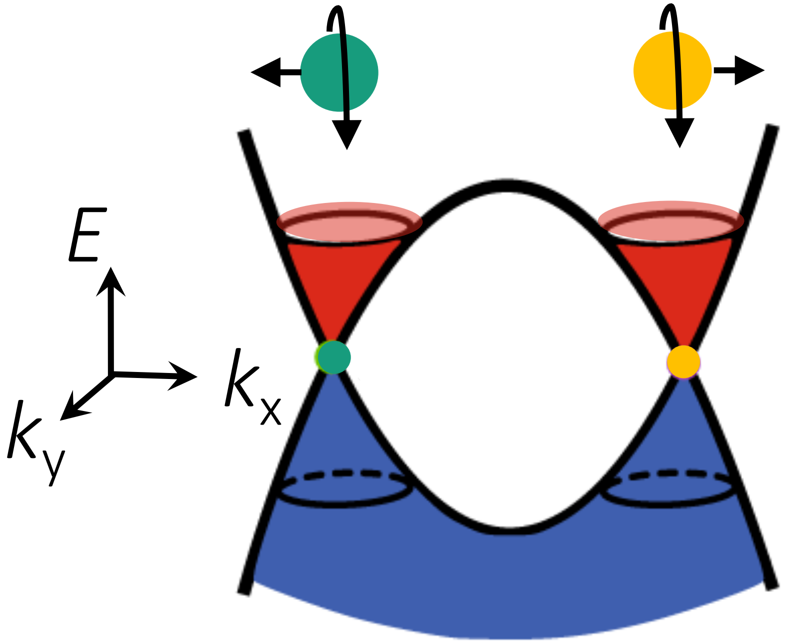

$\chi = +1$ $\chi = -1$

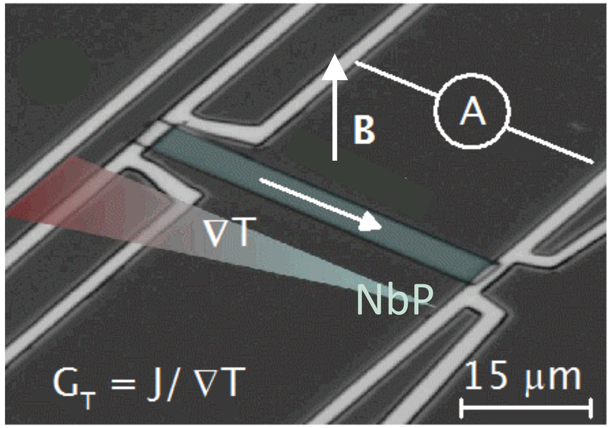

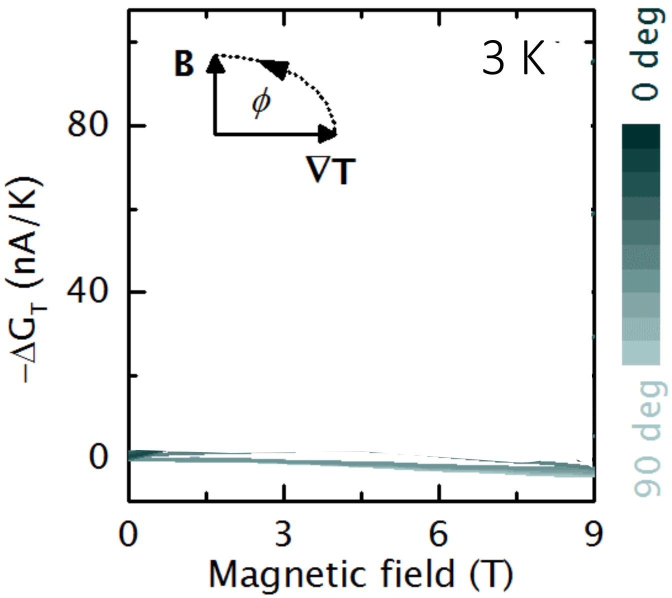

Johannes Gooth et al., Nature 547 (2017) 324 arXiv:1703.10682

Lucas, A., Davison, R. A. & Sachdev, S. PNAS **113**, 9463–9468 (2016).

Landsteiner K., et al. Gravitational anomaly and transport phenomena. Phys. Rev. Lett. **107**, 021601 (2011). URL

Jensen, et al. Thermodynamics, gravitational anomalies and cones. Journal of High Energy Physics **2013**, 88 (2013).

axial gravitational anomaly

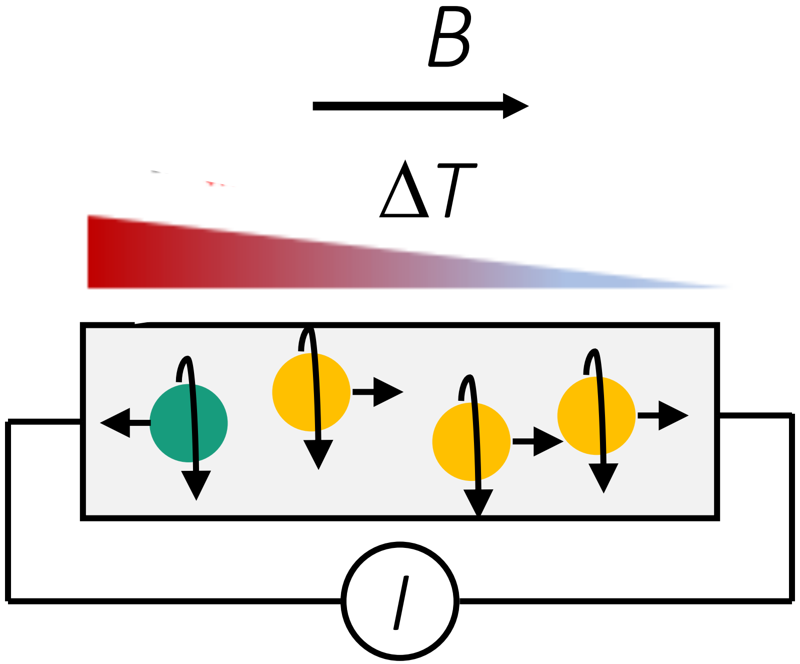

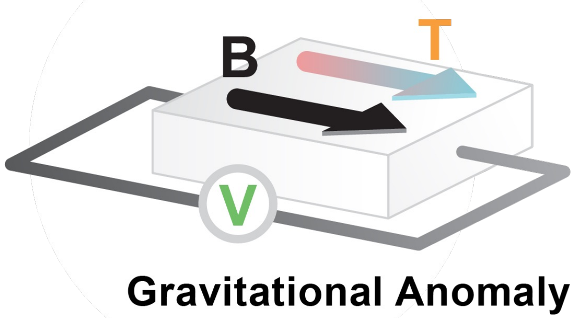

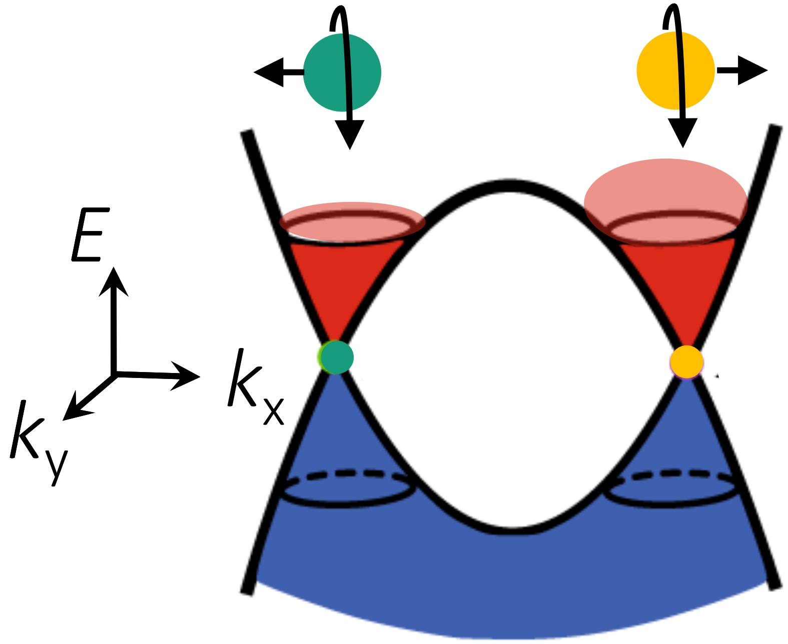

$\chi = +1$ $\chi = -1$

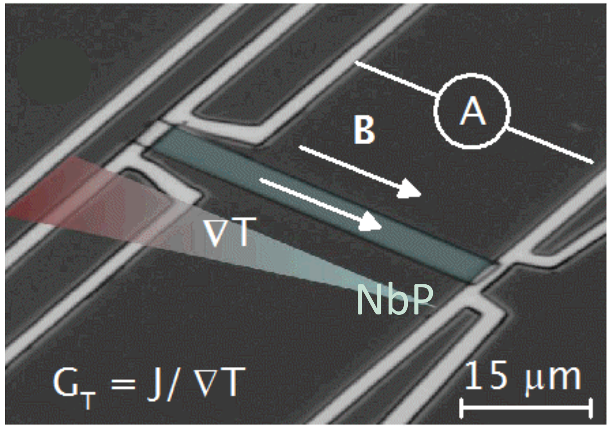

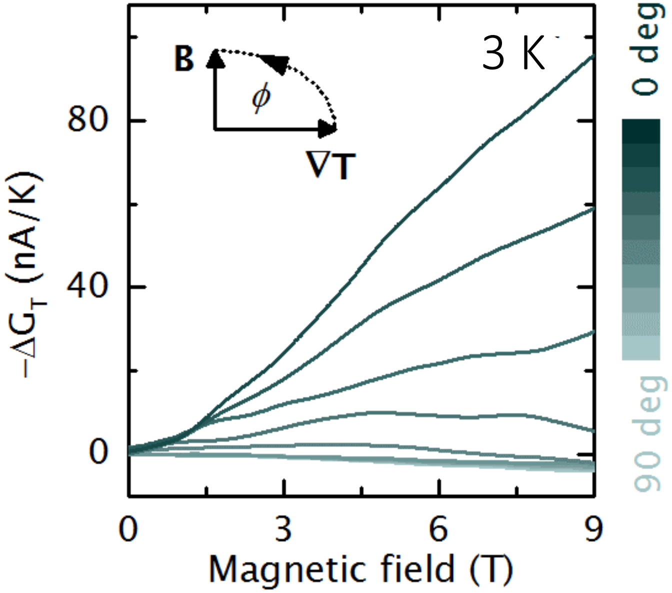

J. Gooth et al., Nature 547 (2017) 324 arXiv:1703.10682.
J. Gooth, J. Kübler, C. Felser, Physik Journal 20 (2021) 29.

chiral anomaly

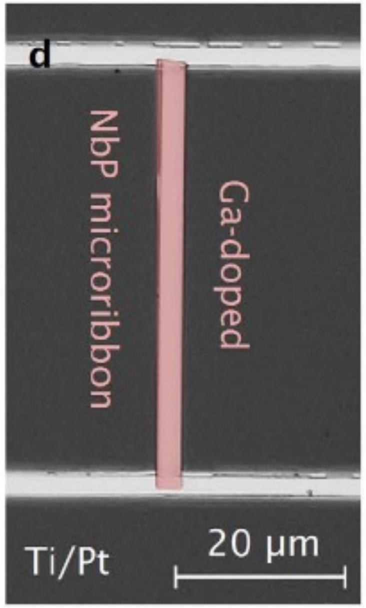

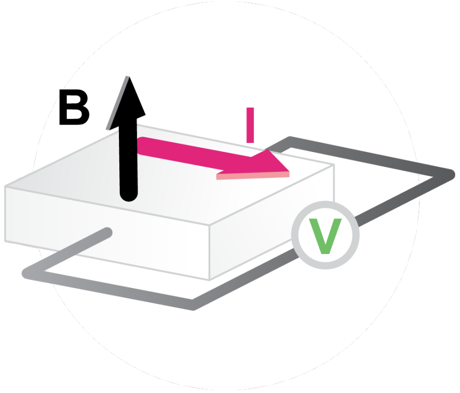

NbP

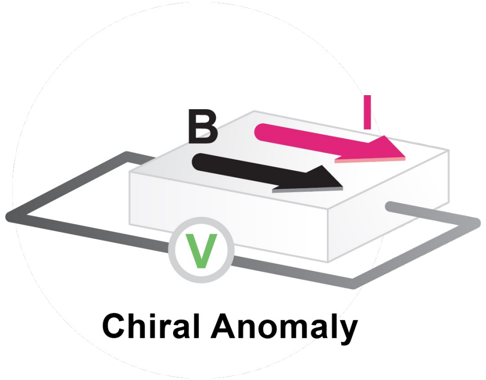

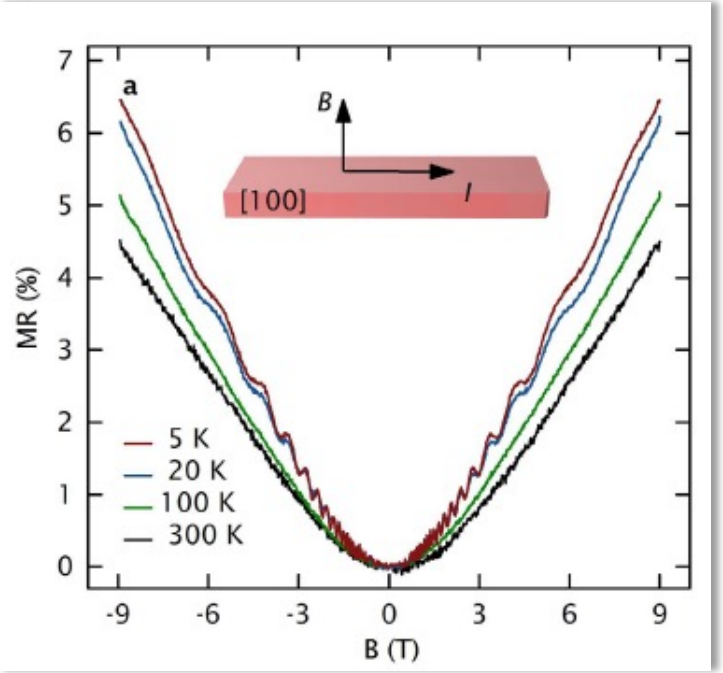

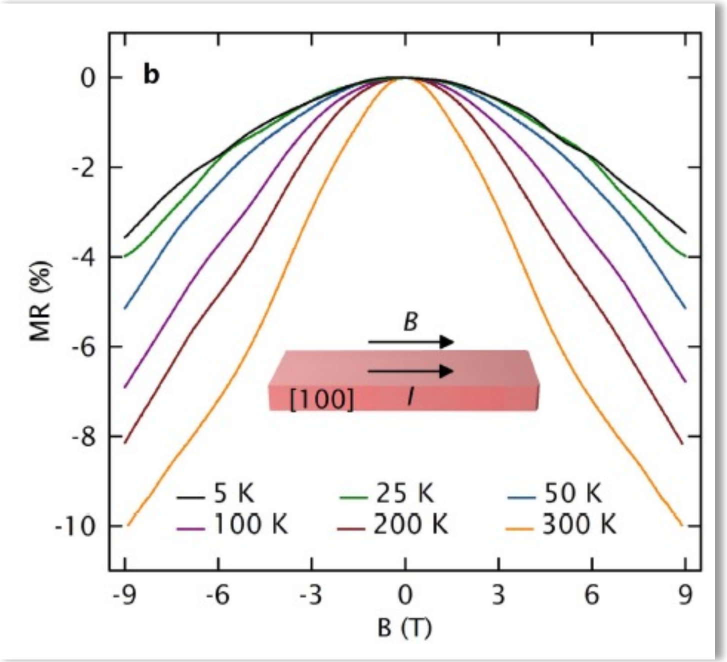

Ga-doping relocates the Fermi energy in NbP close to the W2 Weyl points

Therefore, we observe a negative MR as a signature of the chiral anomaly, that survives up to room temperature

Anna Corinna Niemann, Johannes Gooth et al. Scientific Reports **7** (2017) 43394 doi:10.1038/srep4339 preprint arXiv:1610.01413

chiral and axial gravitational anomaly

NbP

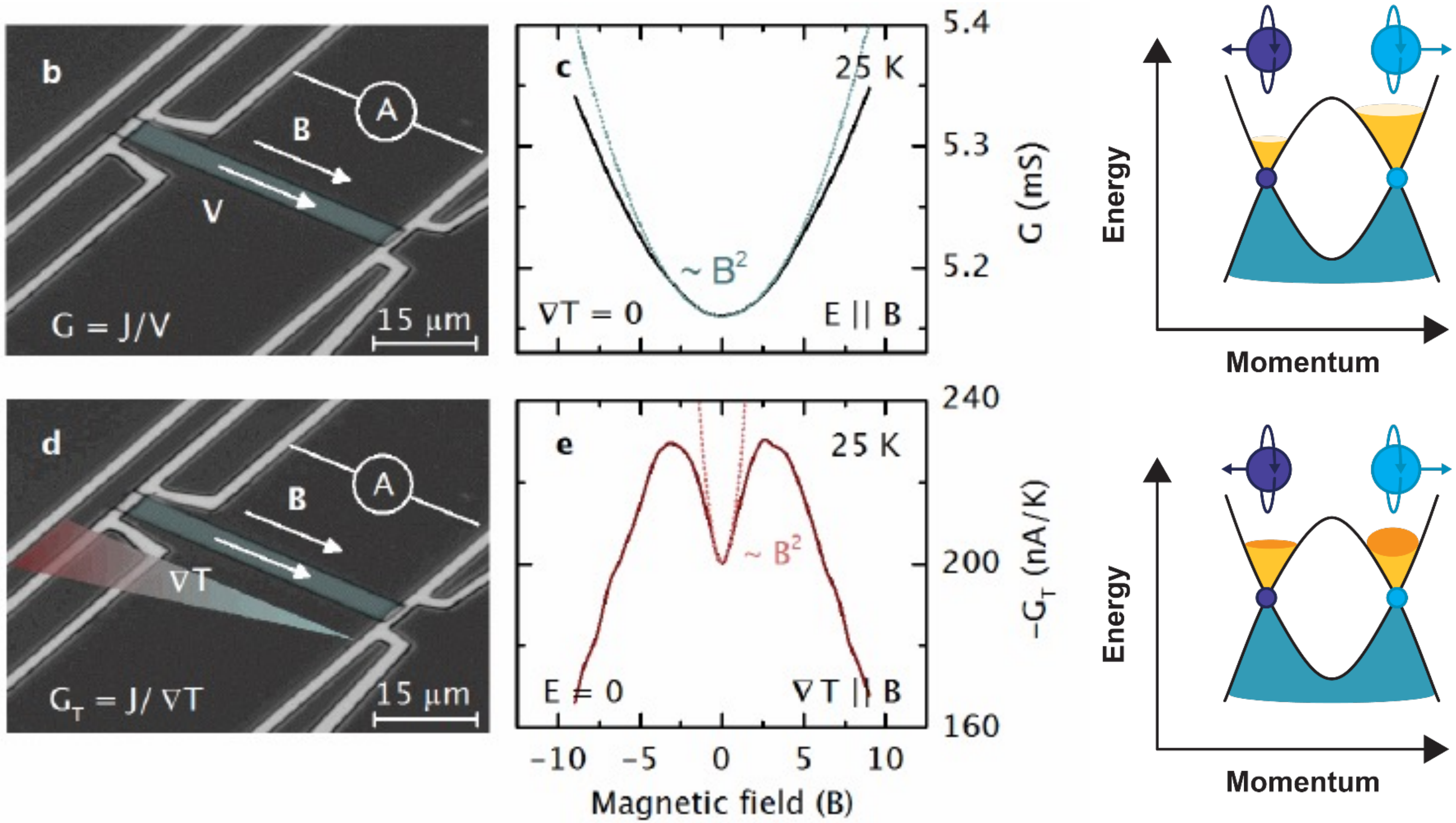

A positive longitudinal **magneto-thermoelectric conductance (PMTC) in the Weyl semimetal NbP** for collinear temperature gradients and magnetic fields that vanishes in the ultra quantum limit.

Lucas, A., Davison, R. A. & Sachdev, S. PNAS **113**, 9463–9468 (2016).
Landsteiner K., et al. Gravitational anomaly and transport phenomena. Phys. Rev. Lett. **107**, 021601 (2011). URL
Jensen, et al. Thermodynamics, gravitational anomalies and cones. Journal of High Energy Physics **2013**, 88 (2013).
Johannes Gooth et al., Nature 547 (2017) 324 arXiv:1703.10682

chiral and axial gravitational anomaly

NbP

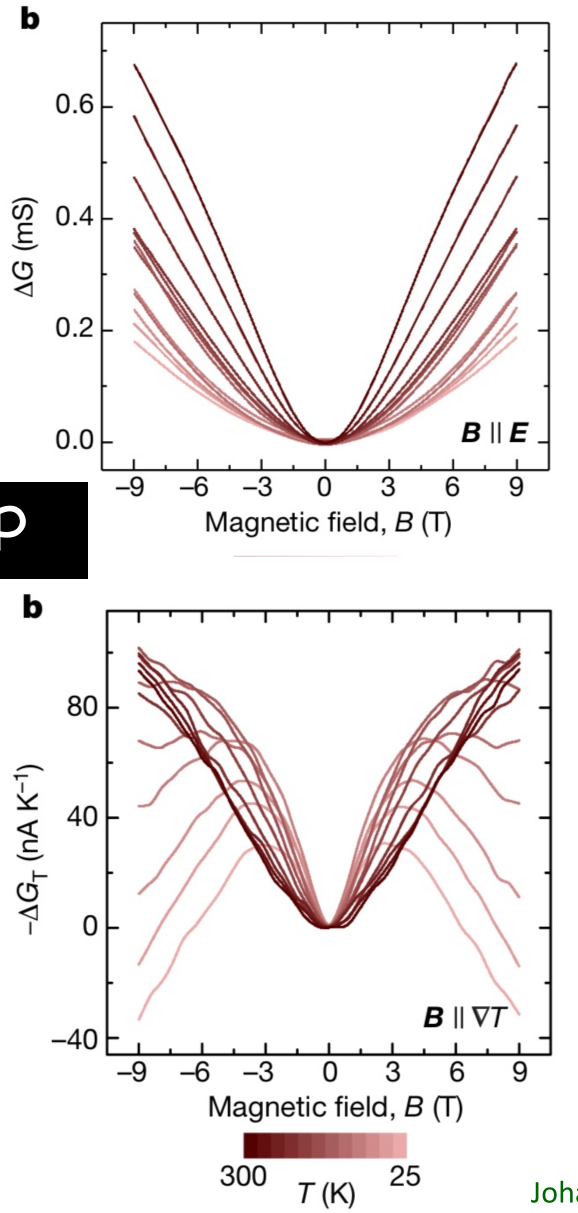

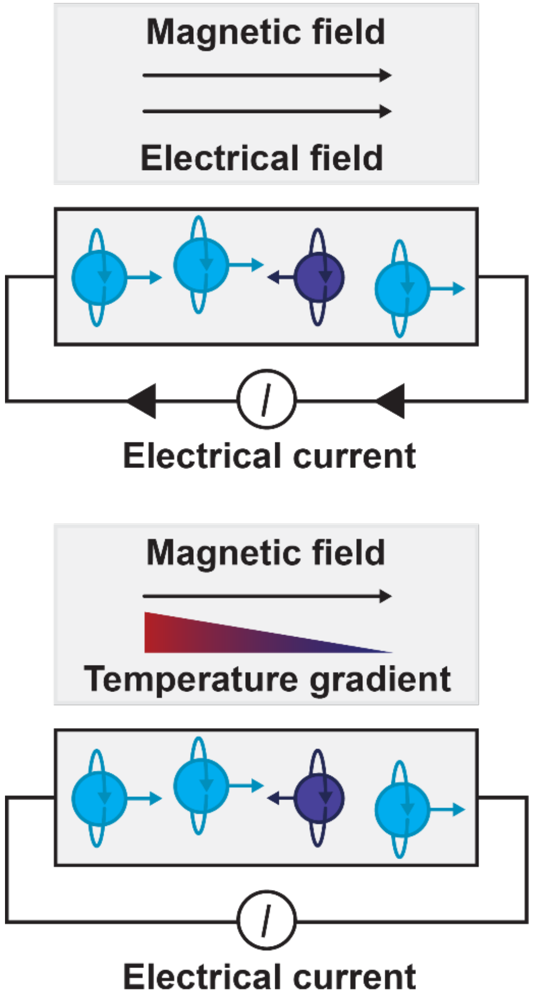

$Bi_{1-x}Sb_x$

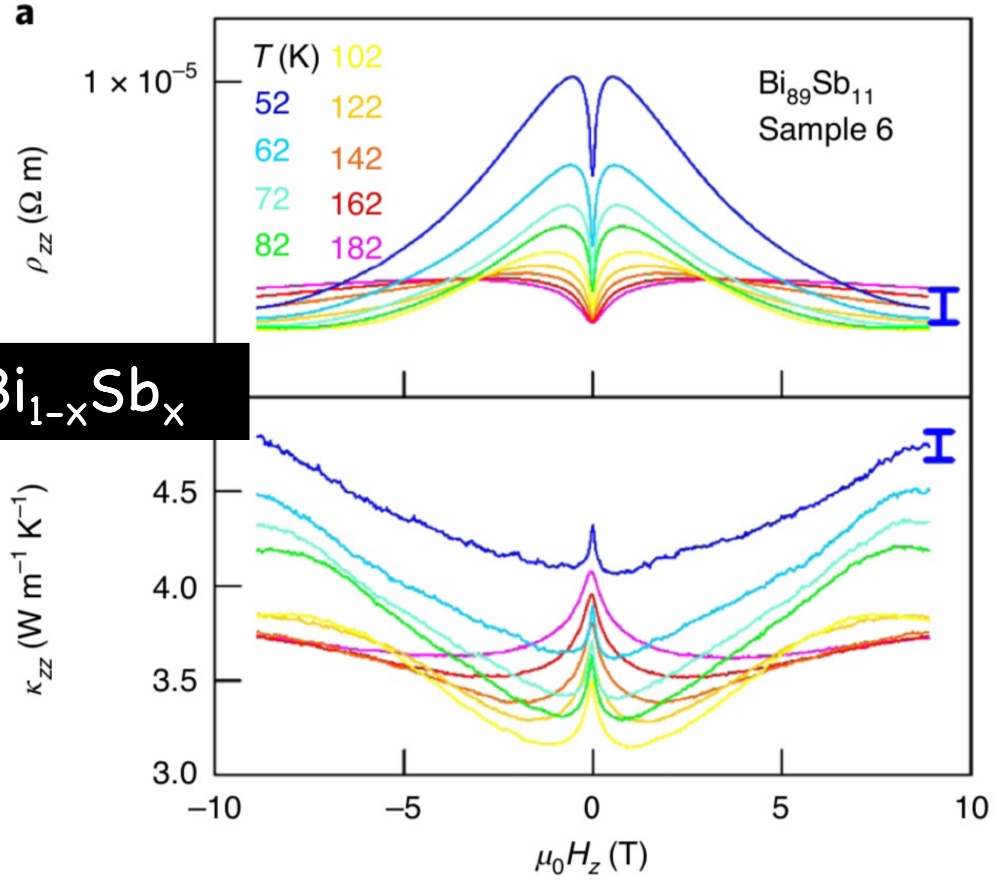

Johannes Gooth et al., Nature **547** (2017) 324.

Dung Vu, et al., Nature Materials **20** (2021) 1525–1531

the universe in a crystal

The New York Times | https://nyti.ms/2vCMCGi

SCIENCE

An Experiment in Zurich Brings Us Nearer to a Black Hole's Mysteries

By KENNETH CHANG JULY 19, 2017

magnetic Weyl

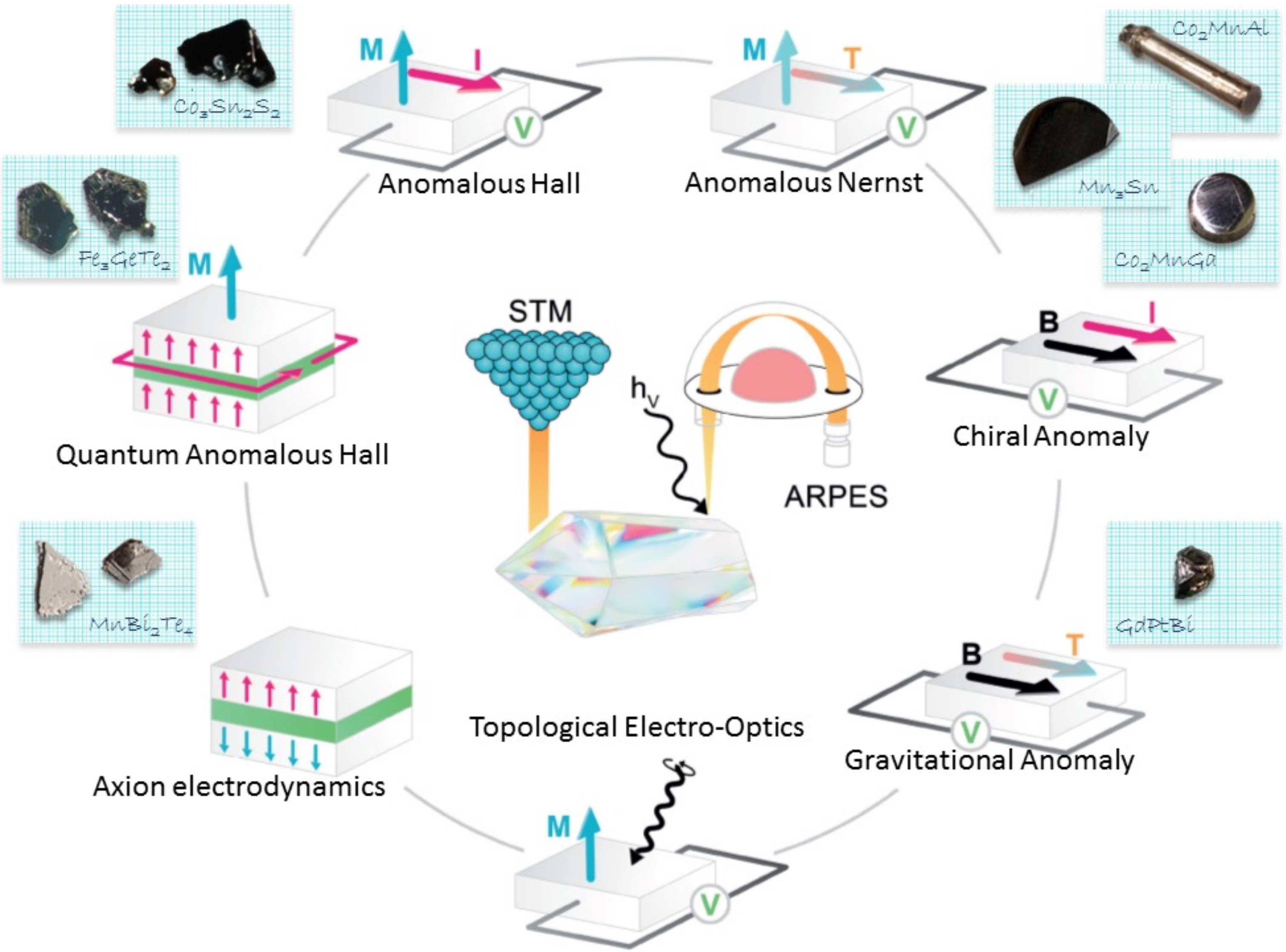

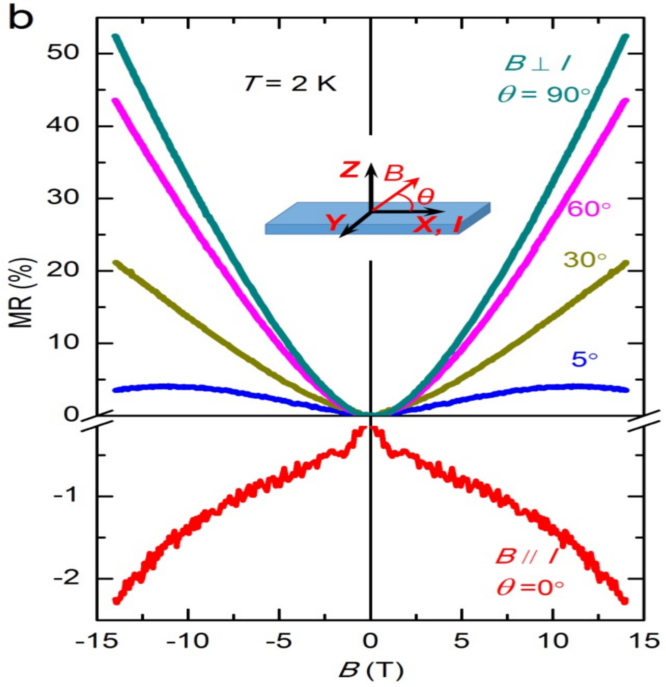

chiral anomaly in

$Co_3Sn_2S_2$

Andrei Bernevig, Claudia Felser, Haim Beidenkopf, Nature 588 (2022)

Liu, *et al*. Nature Physics **14** (2018) 1125

antiferromagnetic topological materials

Article

High-throughput calculations of magnetic topological materials

Table 3 | The magnetic topological materials identified in this work

Categories	Properties	Materials
I-A	Non-collinear manganese compounds	Mn_3GaC, Mn_3ZnC, Mn_3CuN, Mn_3Sn, Mn_3Ge, Mn_3Ir, Mn_3Pt, Mn_5Si_3
I-B	Actinide intermetallic	$UNiGa_5$, $UPtGa_5$, $NpRhGa_5$, $NpNiGa_5$
I-C	Rare-earth intermetallic	$NdCo_2$, $TbCo_2$, $NpCo_2$, PrAg DyCu, NdZn, TbMg, NdMg, Nd_5Si_4, Nd_5Ge_4, Ho_2RhIn_8, Er_2CoGa_8, Nd_2RhIn_8, Tm_2CoGa_8, Ho_2RhIn_8, $DyCo_2Ga_8$, $TbCo_2Ga_8$, Er_2Ni_2In, $CeRu_2Al_{10}$, $Nd_3Ru_4Al_{12}$, $Pr_3Ru_4Al_{12}$, $ScMn_6Ge_6$, YFe_4Ge_4, $LuFe_4Ge_4$, $CeCoGe_3$
II-A	Metallic iron pnictides	LaFeAsO, $CaFe_2As_2$, $EuFe_2As_2$, $BaFe_2As_2$, Fe_2As, $CaFe_4As_3$, LaCrAsO, Cr_2As, CrAs, CrN
II-B	Semiconducting manganese pnictides	$BaMn_2As_2$ $BaMn_2Bi_2$, $CaMnBi_2$, $SrMnBi_2$, $CaMn_2Sb_2$, CuMnAs, CuMnSb, Mn_2As
II-C	Rare-earth intermetallic compounds with the composition 1:2:2	$PrNi_2Si_2$, $YbCo_2Si_2$, $DyCo_2Si_2$, $PrCo_2P_2$, $CeCo_2P_2$, $NdCo_2P_2$, $DyCu_2Si_2$, $CeRh_2Si_2$, UAu_2Si_2, U_2Pd_2Sn, U_2Pd_2In, U_2Ni_2Sn, U_2Ni_2In, U_2Rh_2Sn
II-D	Rare-earth ternary compounds of the composition 1:1:1	CeMgPb, PrMgPb, NdMgPb, TmMgPb
III-A	Semiconducting actinides/ rare-earth pnictides	HoP, UP, UP_2, UAs, NpS, NpSe, NpTe, NpSb, NpBi, U_3As_4, U_3P_4
III-B	Metallic oxides	Ag_2NiO_2, $AgNiO_2$, $Ca_3Ru_2O_7$, Double perovskite Sr_3CoIrO_6
III-C	Metal-to-insulator transition compounds	NiS_2, $Sr_2Mn_3As_2O_2$
III-D	Semiconducting and insulating oxides, borates, hydroxides, silicates and phosphate	$LuFeO_3$, $PdNiO_3$, $ErVO_3$, $DyVO_3$, $MnGeO_3$, $Tm_2Mn_2O_7$, $Yb_2Sn_2O_7$, $Tb_2Sn_2O_7$, $Ho_2Ru_2O_7$, $Er_2Ti_2O_7$, $Tb_2Ti_2O_7$, $Cd_2Os_2O_7$, $Ho_2Ru_2O_7$, Cr_2ReO6, $NiCr_2O_4$, MnV_2O_4, Co_2SiO_4, Fe_2SiO_4, $PrFe_3(BO_3)_4$, $KCo_4(PO_4)_3$, $CoPS_3$, $SrMn(VO_4)(OH)$, $Ba_5Co_5ClO_{13}$, FeI_2

antiferromagnetic topological materials

III-A	Semiconducting actinides/ rare-earth pnictides	HoP, UP, UP_2, UAs, NpS, NpSe, NpTe, NpSb, NpBi, U_3As_4, U_3P_4

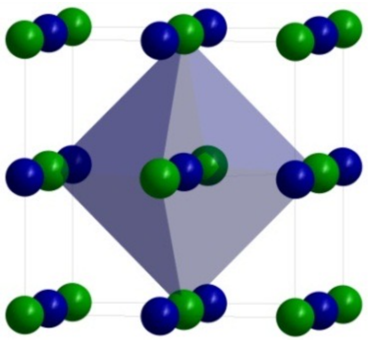

Strong interaction drives a quantum phase transition to a topological insulator phase

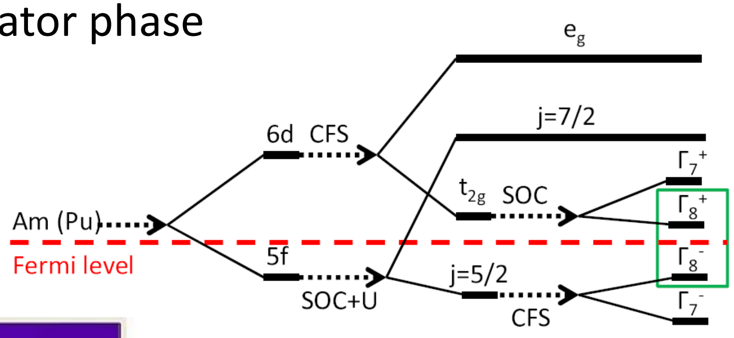

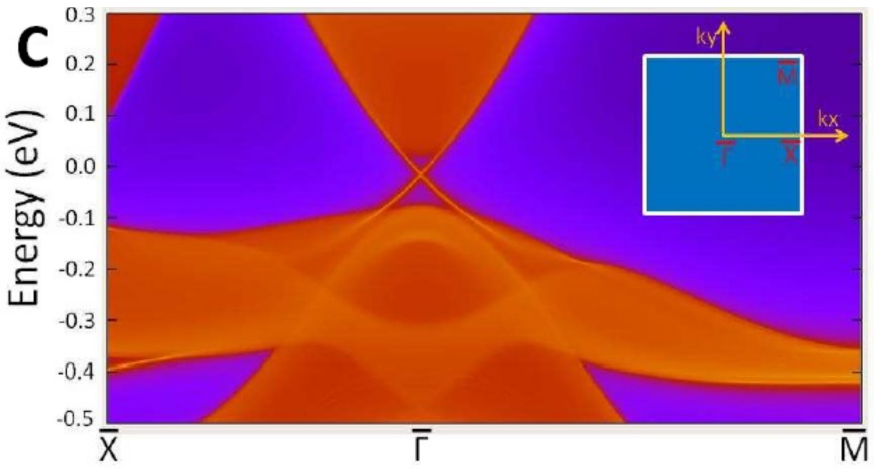

Band inversion between d and f bands of different parity

PuTe under pressure has a band gap up to 0.4 eV

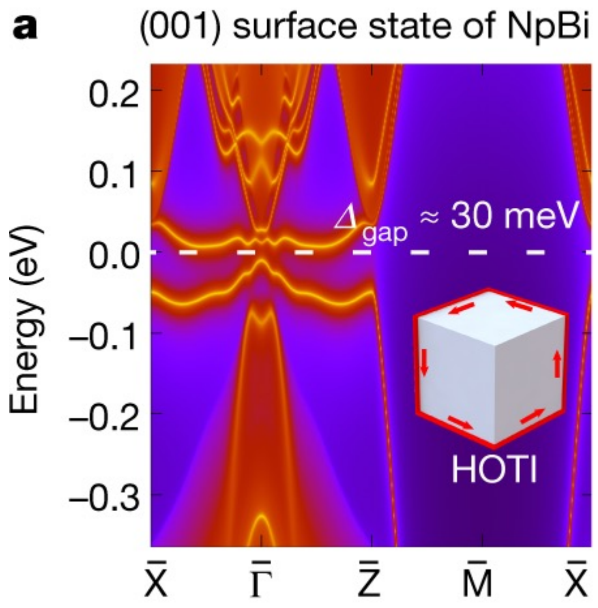

Higher Order topological insulator

Xiao Zhang, Haijun Zhang, Claudia Felser, Shou-Cheng Zhang, Science 335 (2012) 1464,

Y Xu, et al., Nature 586 (2020) 702

Heusler Verbindungen

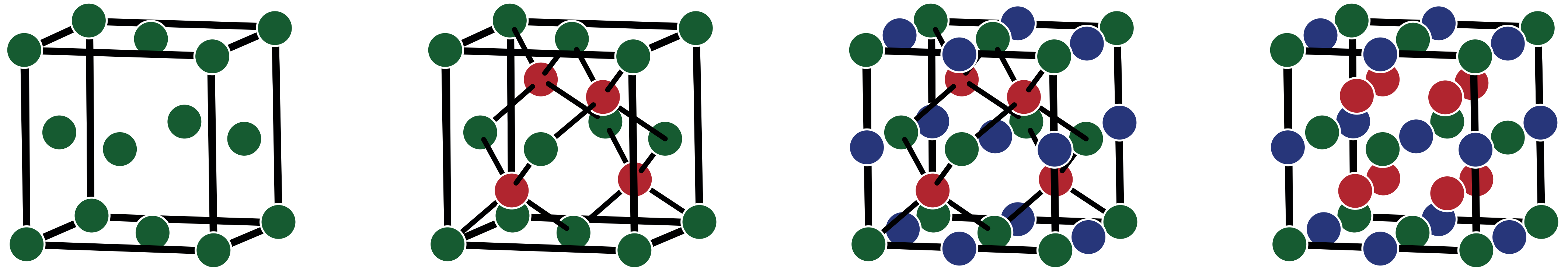

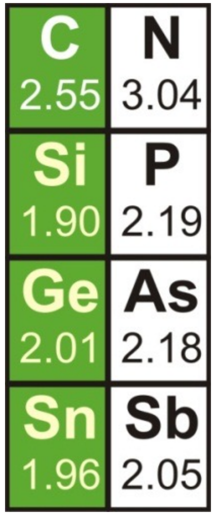

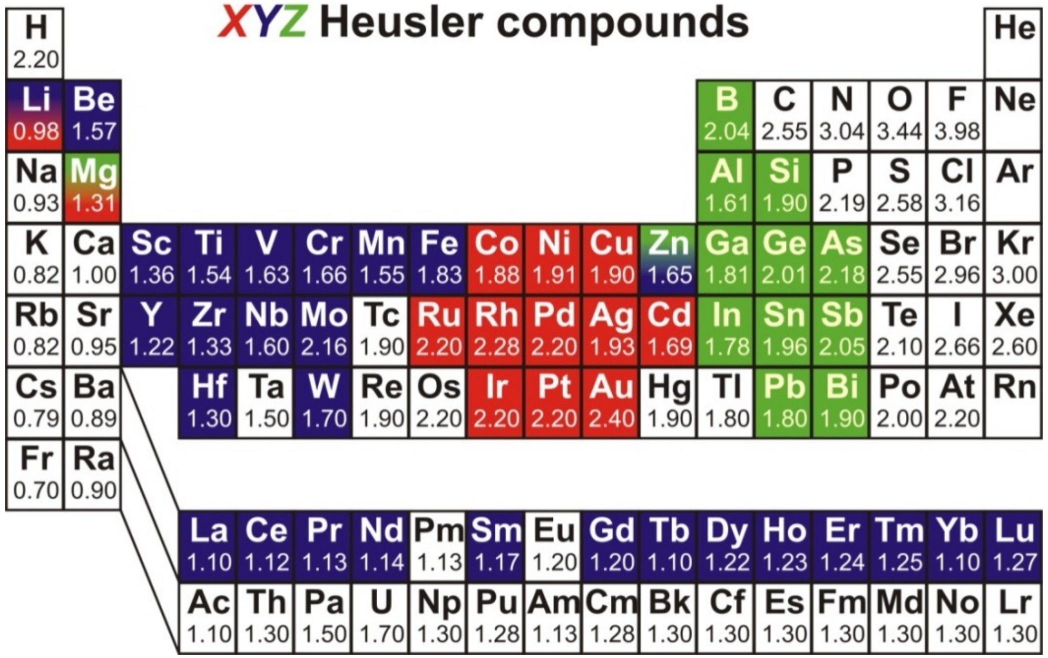

T. Graf, C. Felser, and S. S. P. Parkin, Prog. Solid State Chem. 39, 1 (2011)

Heusler compounds

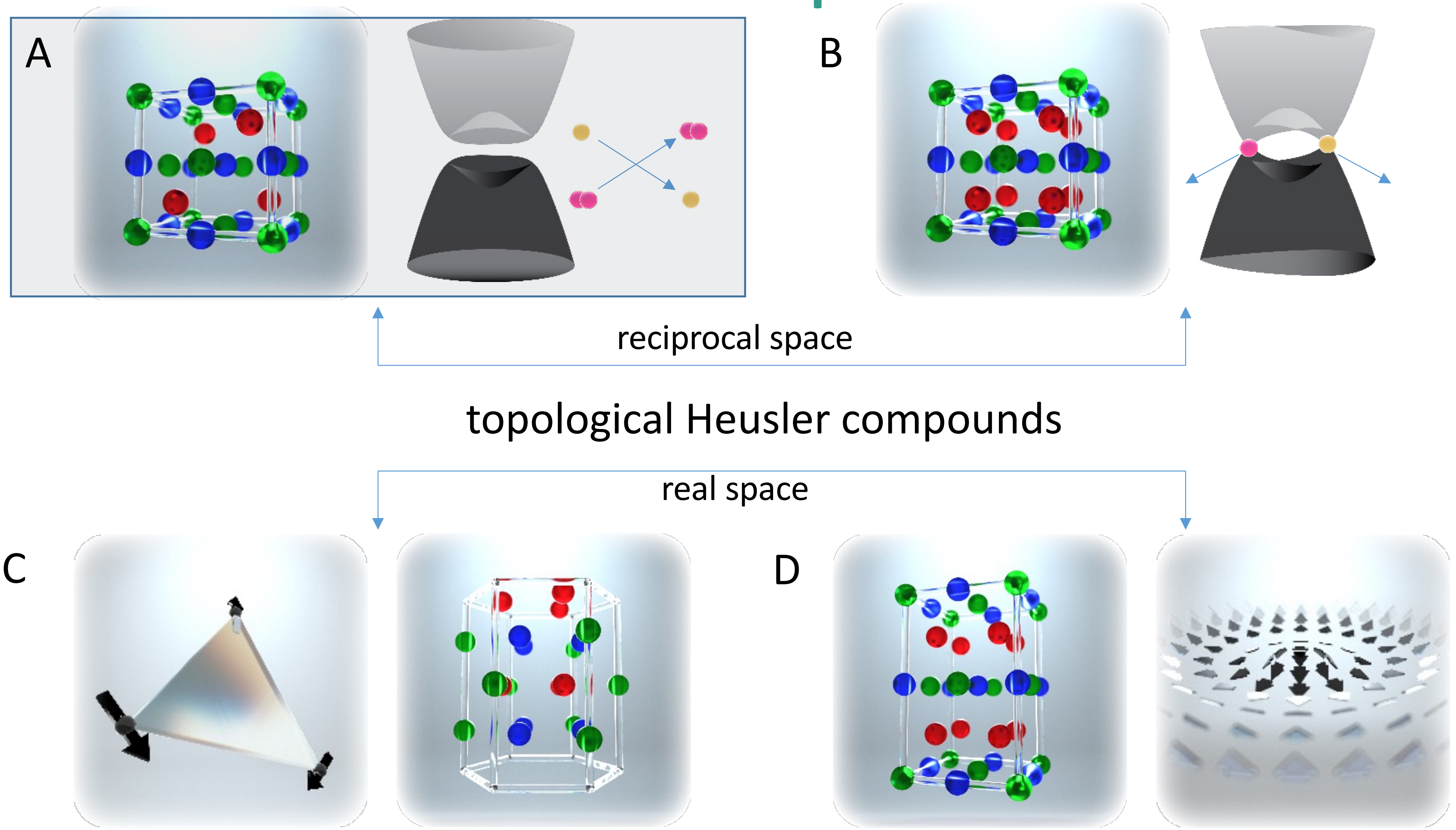

magnetic Weyl semimetals

Weyl points at low symmetry points

breaking time reversal symmetry

- magnetic field
- **all crossings in the band structure in ferromagnets are Weyl points**

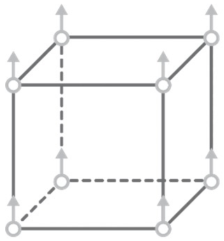

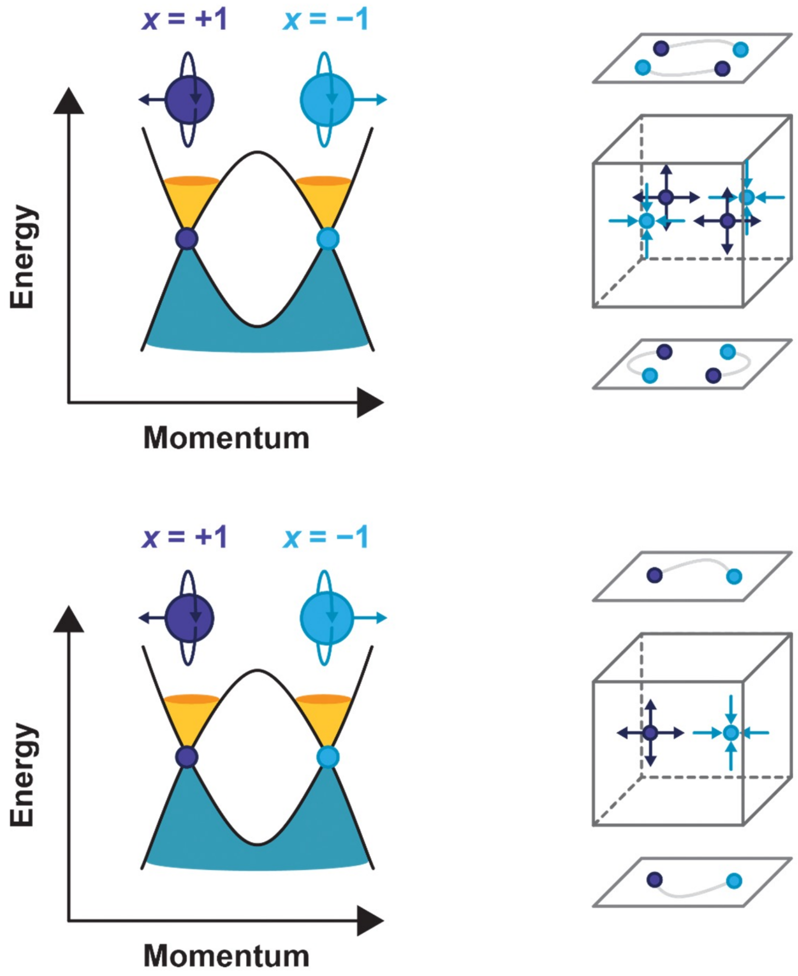

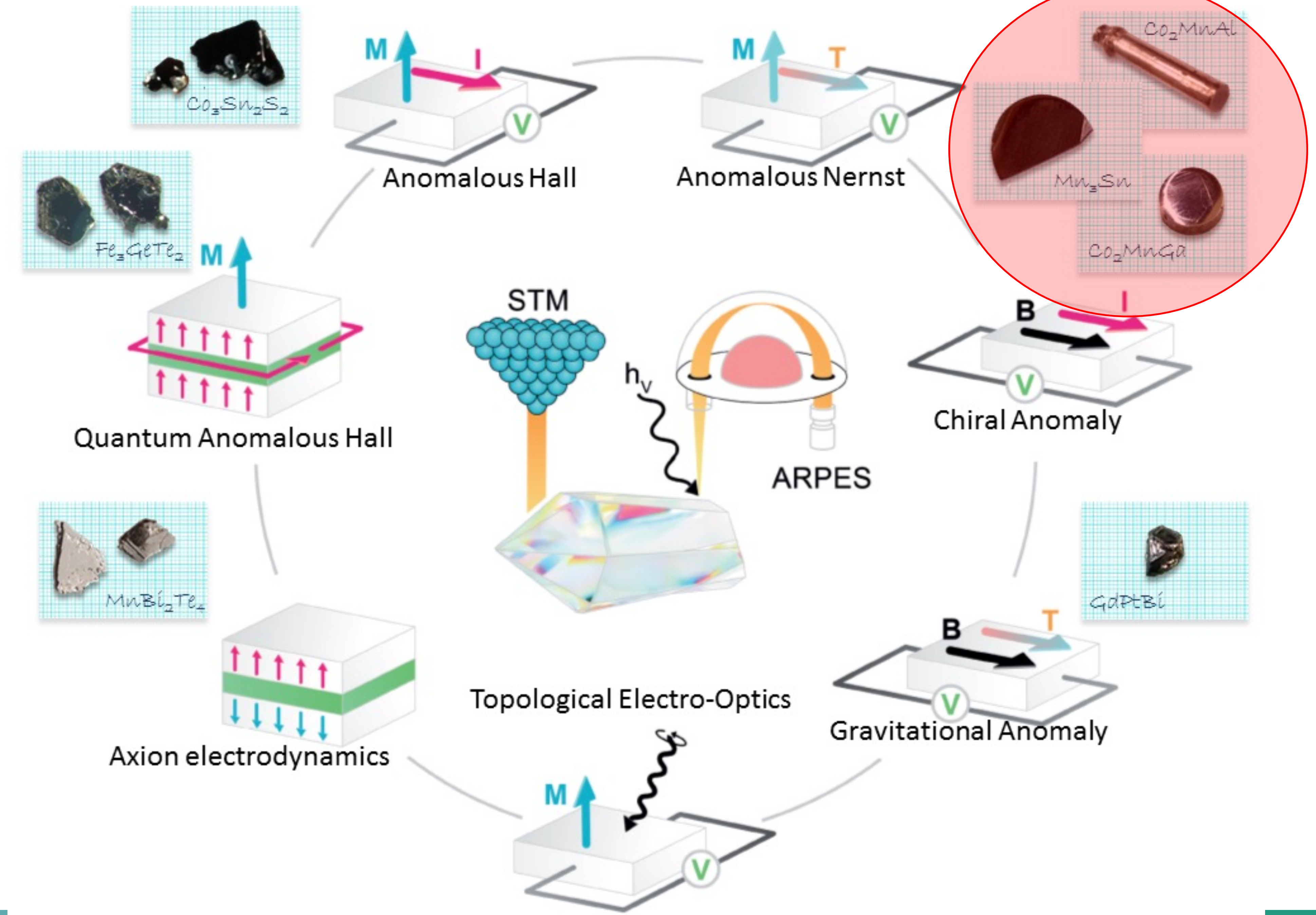

Co3Sn2S2
Fe3GeTe2
MnBi2Te4
Co2MnAl
Mn3Sn
Co2MnGa
GdPtBi
M
I
T
V
B
Anomalous Hall
Anomalous Nernst
Quantum Anomalous Hall
Chiral Anomaly
STM
ARPES
hv
Axion electrodynamics
Topological Electro-Optics
Gravitational Anomaly

Heusler compounds

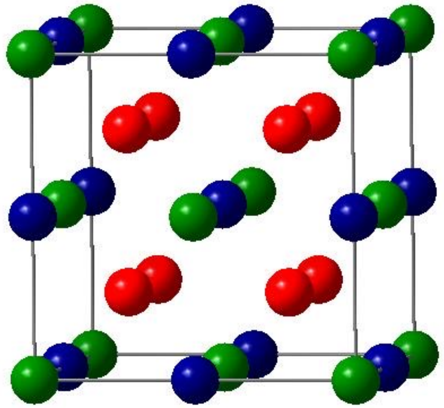

Heusler X_2YZ $L2_1$

T. Graf, C. Felser, and S. S. P. Parkin, Prog. Solid State Chem. 39, 1 (2011)

Heusler Verbindungen

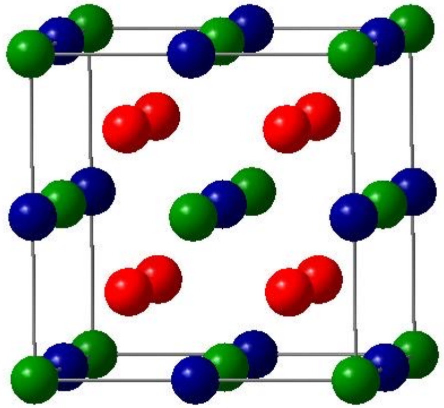

Heusler X_2YZ $L2_1$

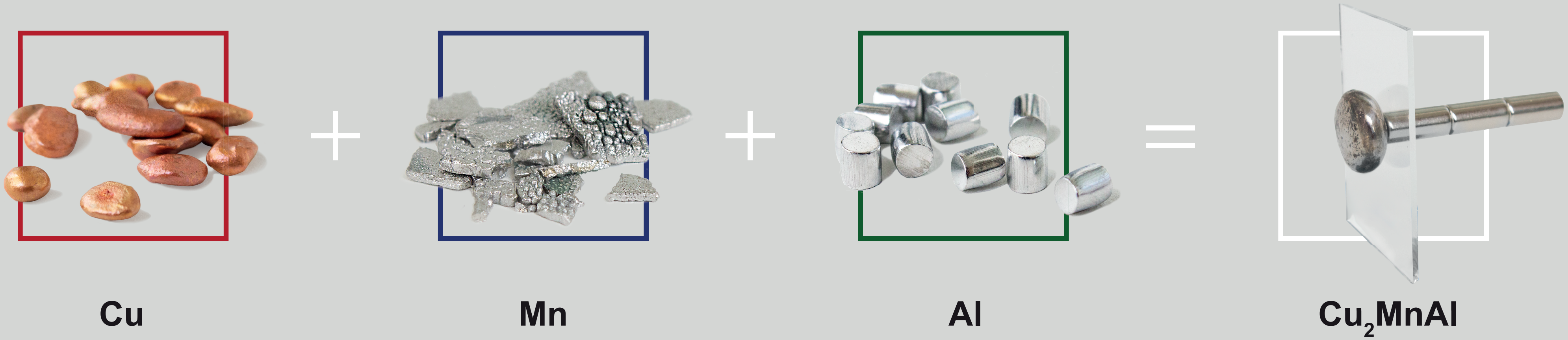

T. Graf, C. Felser, and S. S. P. Parkin, Prog. Solid State Chem. 39, 1 (2011)

Heusler compounds

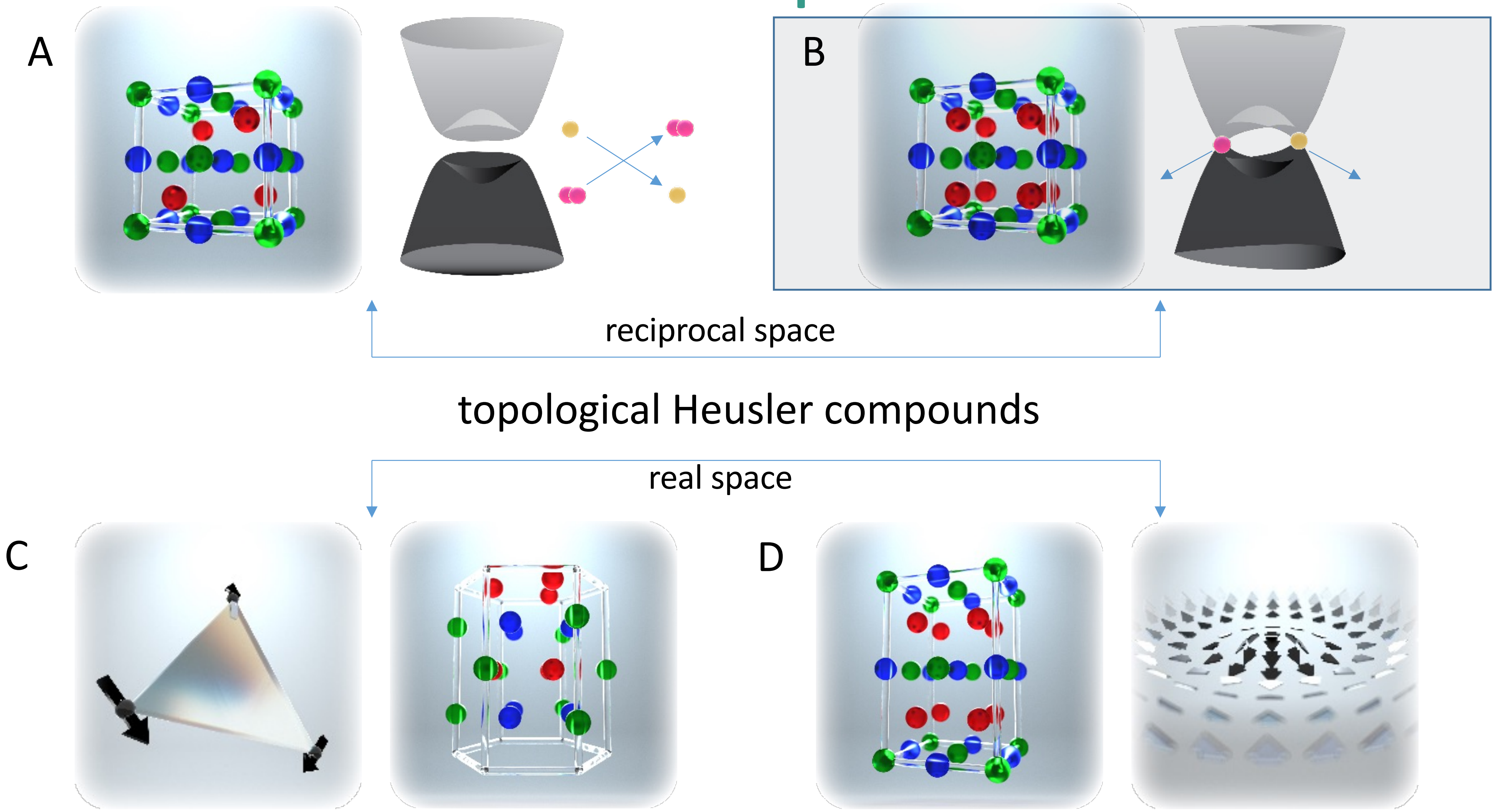

magnetic Heusler

X_2YZ

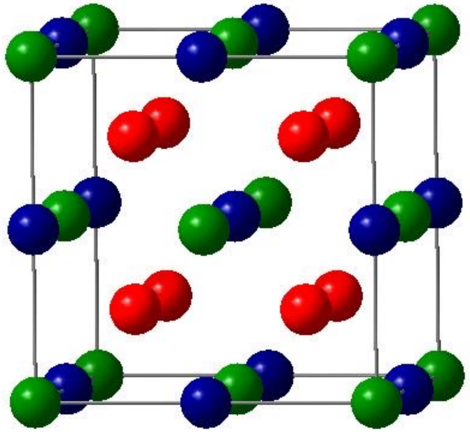

- magic valence electron number: 24
- valence electrons = 24 + magnetic moments

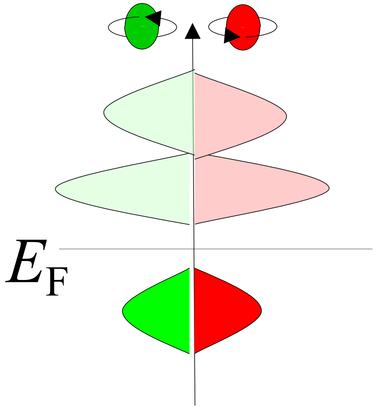

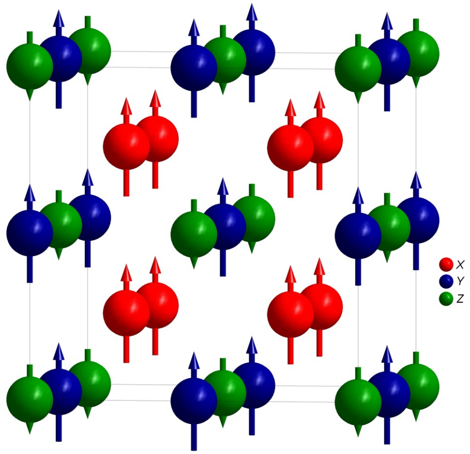

Fe_2	V	Al

Co_2	Mn	Ga

2 * 8 + 5 + 3 = 24

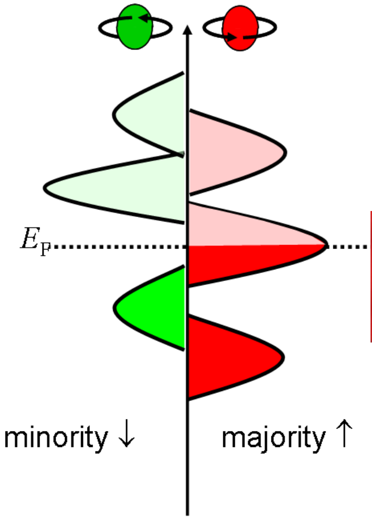

2 * 9 + 7 + 3 = 24 + 4

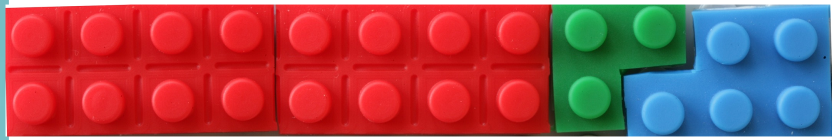

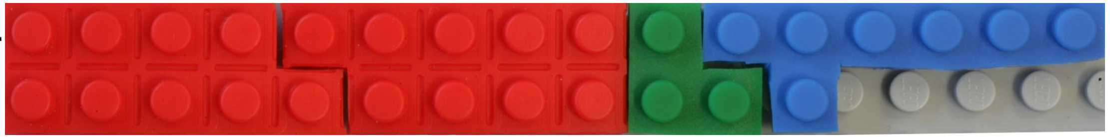

Kübler *et al.*, PRB **28**, 1745 (1983)
de Groot RA, et al. PRL **50** 2024 (1983)
Galanakis *et al.*, PRB **66**, 012406 (2002)

Kandpal et al., J. Phys. **D 40** (2007) 1507
Balke *et al.* Solid State Com. **150** (2010) 529
Kübler *et al.*, Phys. Rev. B **76** (2007) 024414

half metallic Heusler

X_2YZ

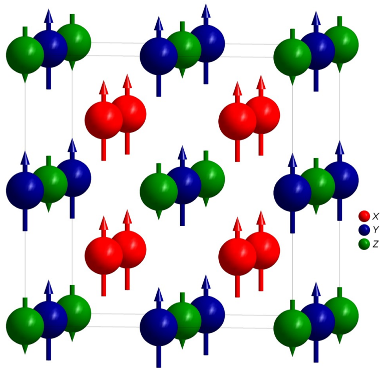

Co_2TiAl: 2×9 + 4 + 3 = 25 Ms = 1m_B

Co_2MnGa: 2×9 + 7 + 3= 28 Ms = 4m_B

Co_2FeSi: 2×9 + 8 + 4 = 30 Ms = 6m_B

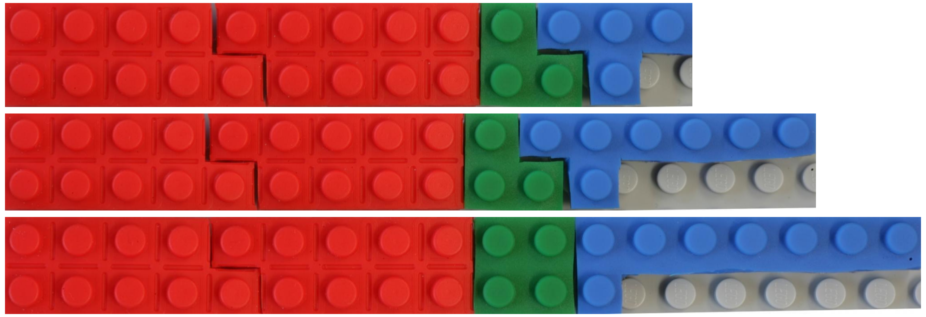

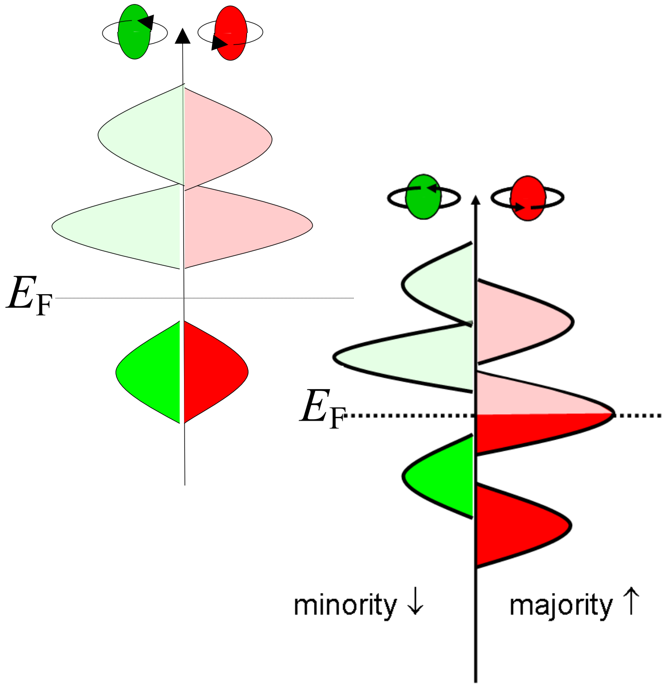

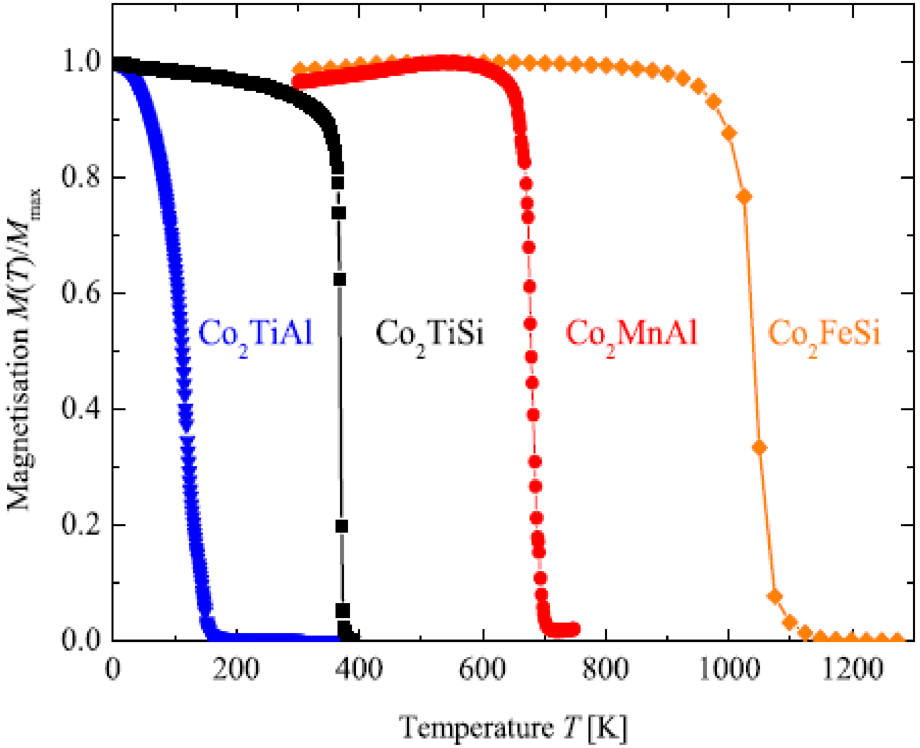

Kübler *et al.*, PRB **28**, 1745 (1983)
de Groot RA, et al. PRL **50** 2024 (1983)
Galanakis *et al.*, PRB **66**, 012406 (2002)

…l et al., J. Phys. **D 40** (2007) 1507
…t al. Solid State Com. **150** (2010) 529
Kübler *et al.*, Phys. Rev. B **76** (2007) 024414

Tunneling magnetoresistance effect in Heusler

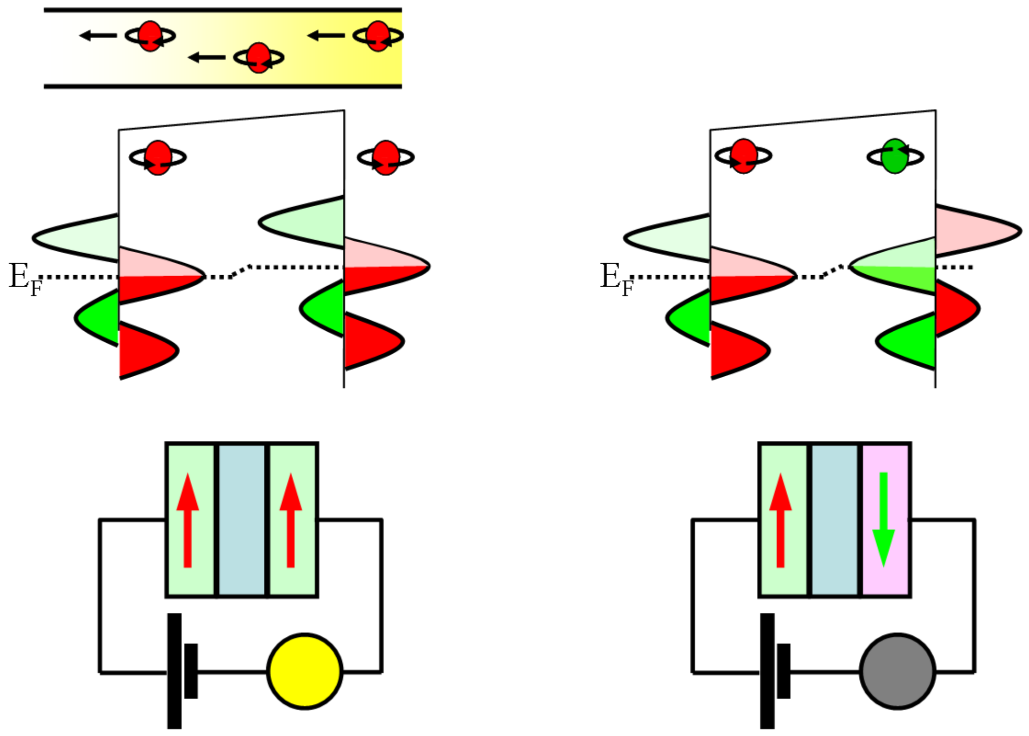

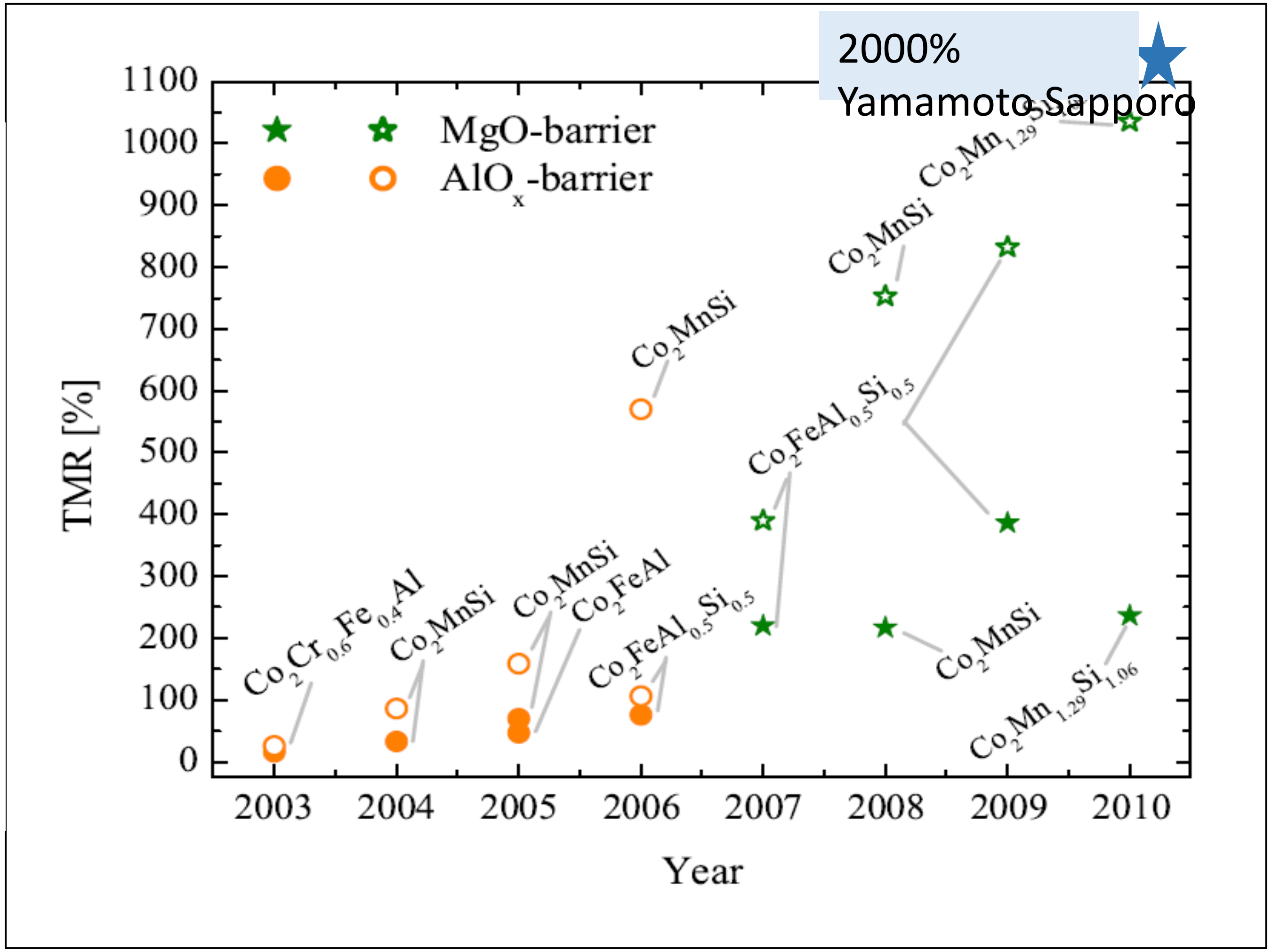

Read-Head Fabrication w/Heusler alloy

HITACHI
Inspire the Next

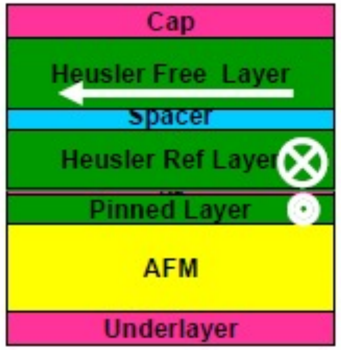

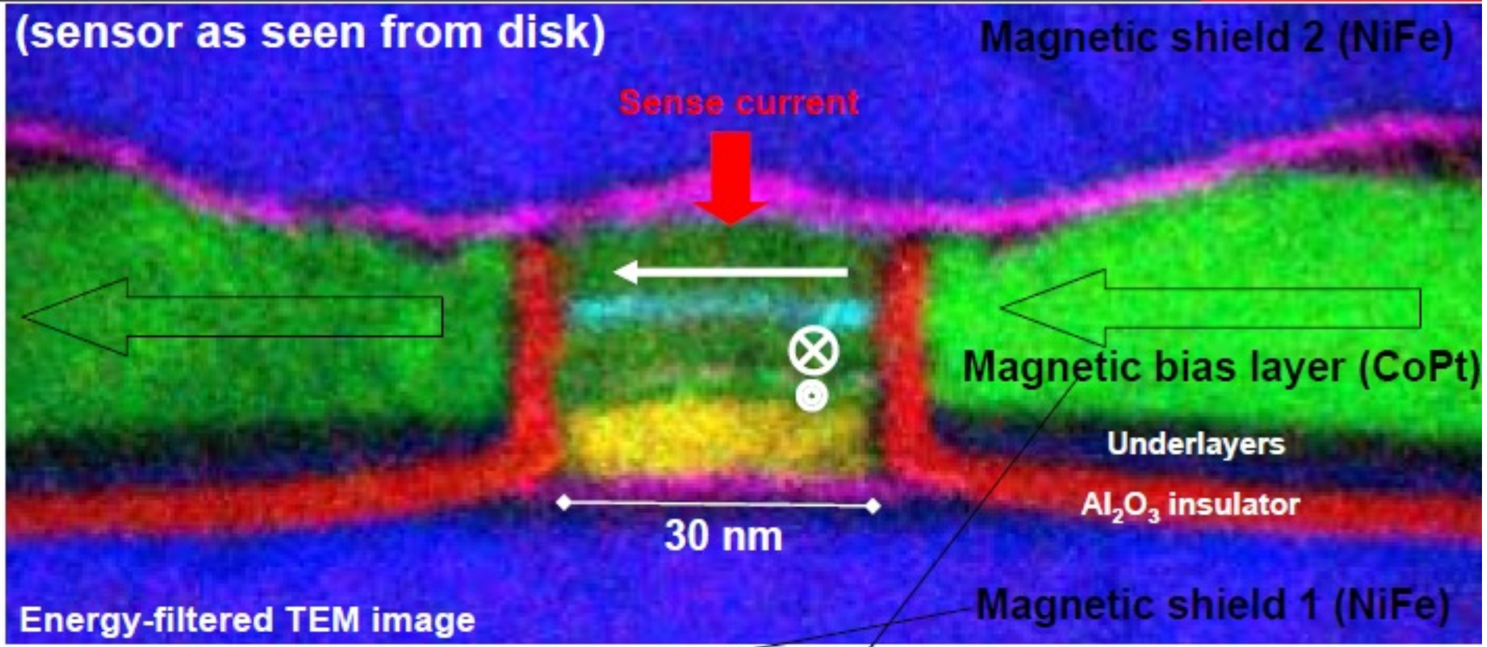

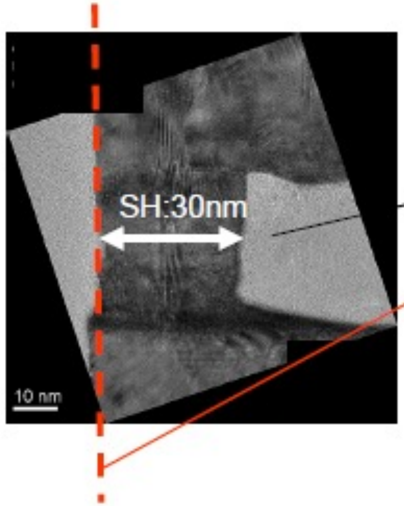

- Shielded sensor.
- Stabilized sensor through hard bias
- Stripe height defined through lapping.
- Air-bearing surface (ABS)

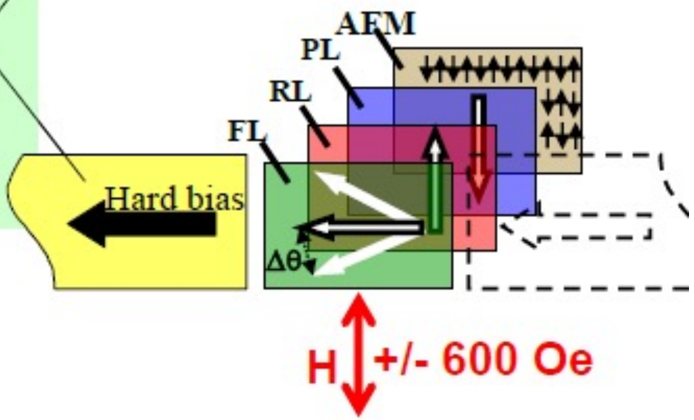

semimetallic Heusler compounds

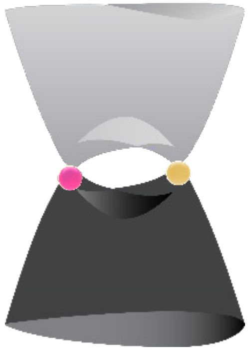

Co_2TiSn

Co_2TiSi: $2\times9 + 4 + 4 = 26$ $M_s = 2\mu_B$

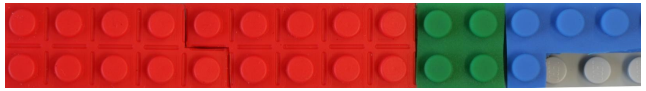

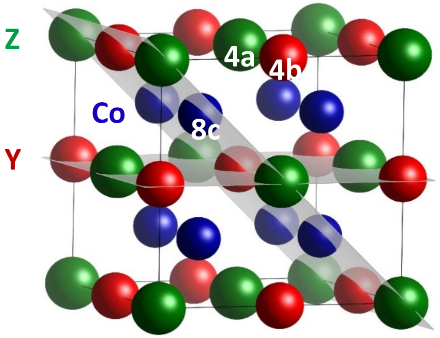

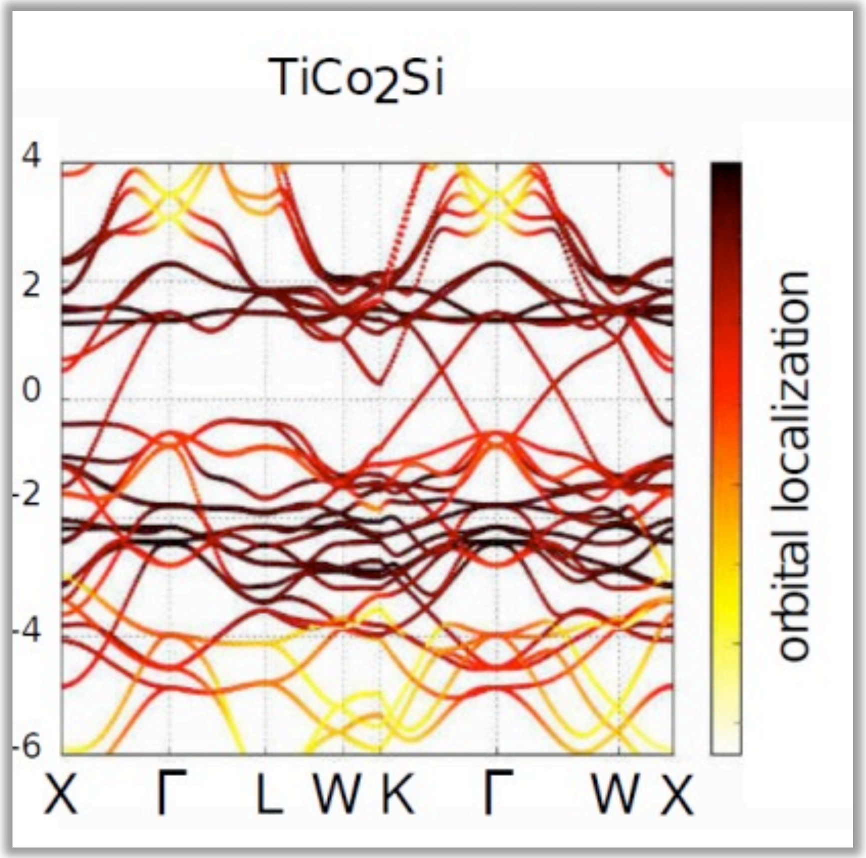

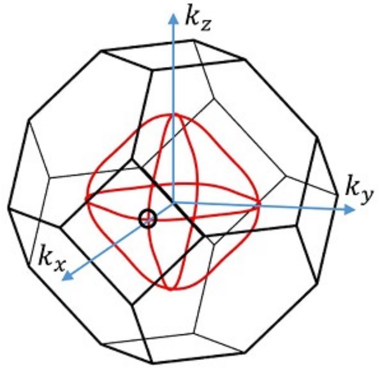

Symmetry and electronic structures depend on the magnetization direction

With SOC

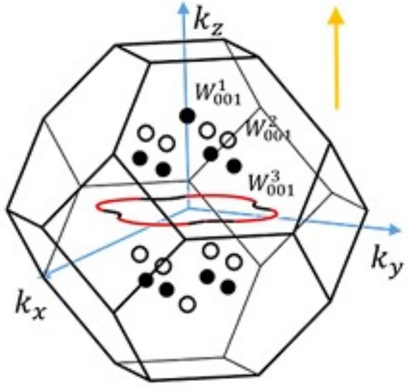

Phys. Rev. Lett. 117, 236401 (2016)
Sci. Rep. 6, 38839 (2016)

Heusler, Weyl and Berry

Giant AHE Co_2MnAl

$$\sigma_{xy} = 1800\,\mathrm{S/cm}\ \ \text{calc.}$$

$$\sigma_{xy} \approx 2000\,\mathrm{S/cm}\ \ \text{meas.}$$

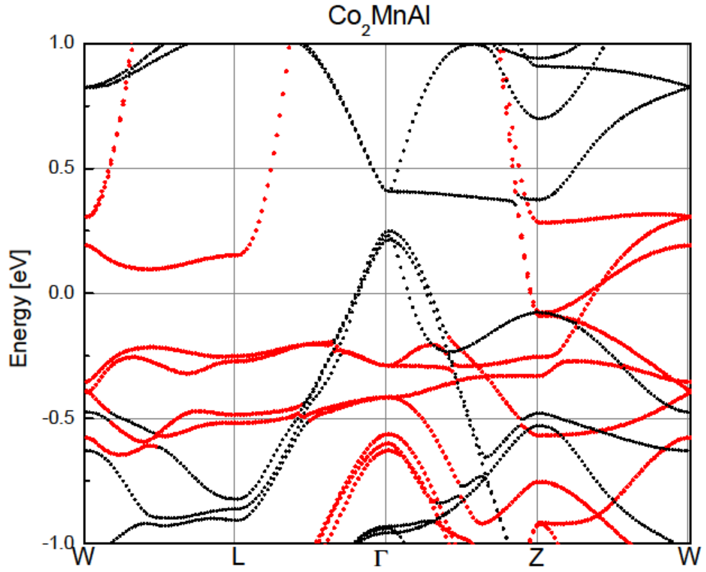

Nodal lines and Weyl points

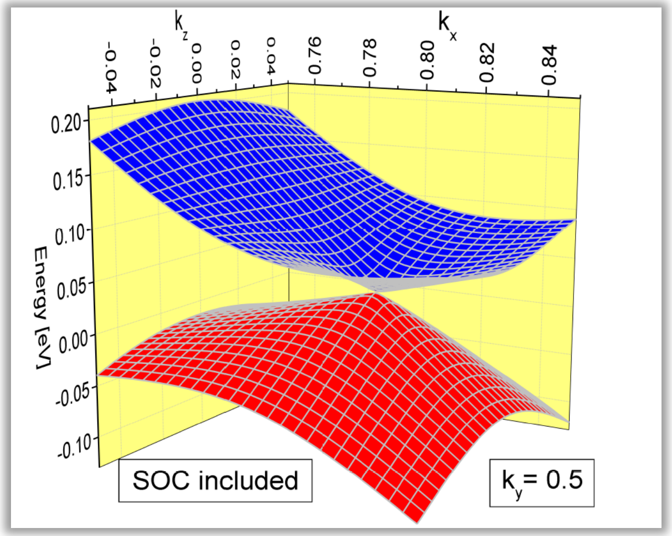

Berry curvature enhancement

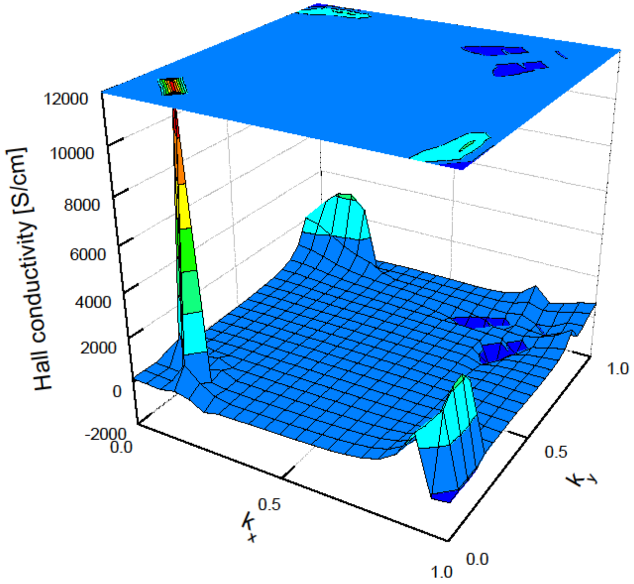

Kübler, Felser, PRB 85 (2012) 012405
Vidal et al., Appl .Phys. Lett. 99 (2011) 132509

Kübler, Felser, EPL 114 (2016) 47005.

Berry curvature and anomalous Nernst

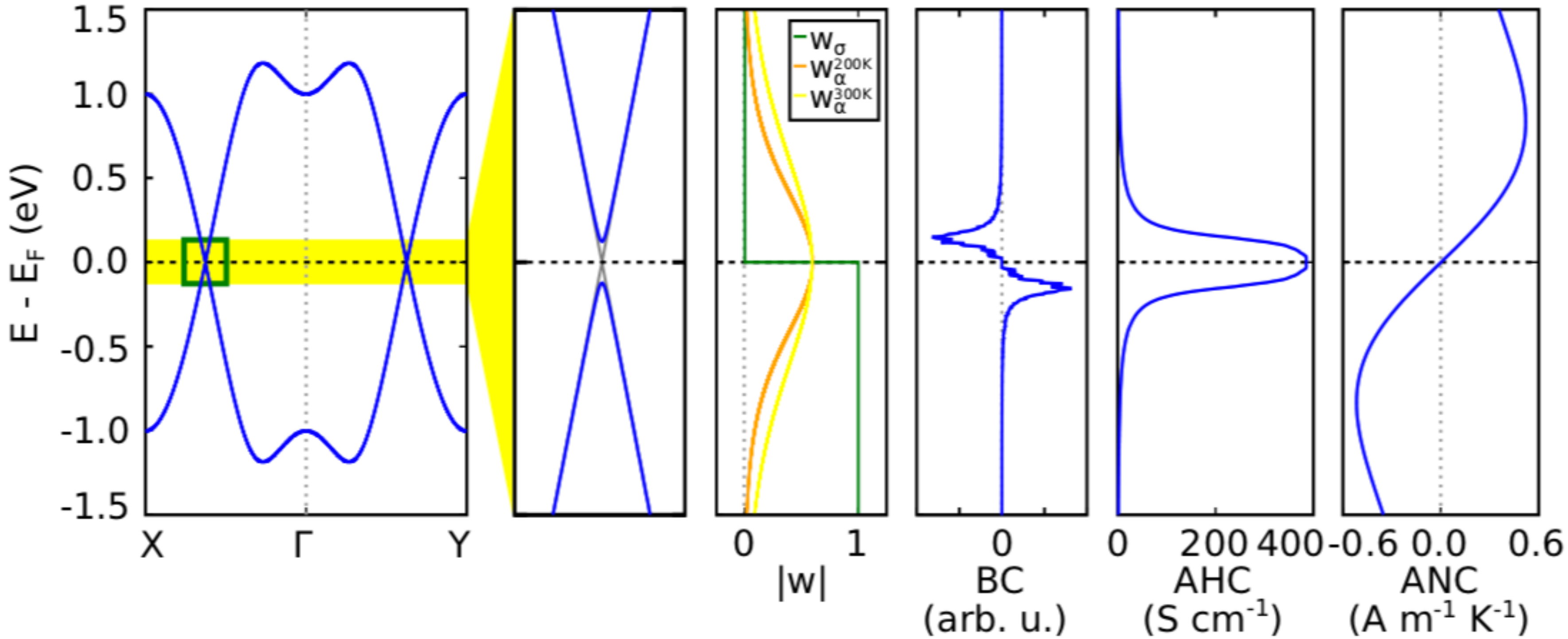

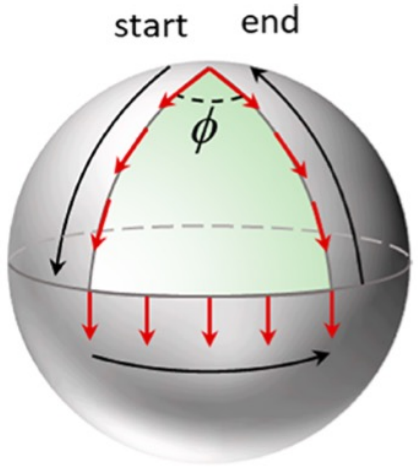

$$\sigma_{ij} = \frac{e^2}{\hbar} \sum_n \int \frac{d^3k}{(2\pi)^3} \Omega_{ij}^{nk} f_{nk}$$

$$\alpha_{ij} = \frac{e^2}{\hbar} \sum_n \int \frac{d^3k}{(2\pi)^3} \Omega_{ij}^{nk} \left(-\frac{1}{eT}\left[(E_{nk} - E_F) f_{nk} + k_B T \ln\left(1 + \exp\frac{E_{nk} - E_F}{-k_B T}\right)\right] \right)$$

Jonathan Noky, Claudia Felser, and Yan Sun, Physical Review B 99 (2019) 165117

Berry curvature design

Co_2MnGa

- giant anomalous Hall
- giant anomalous Nernst

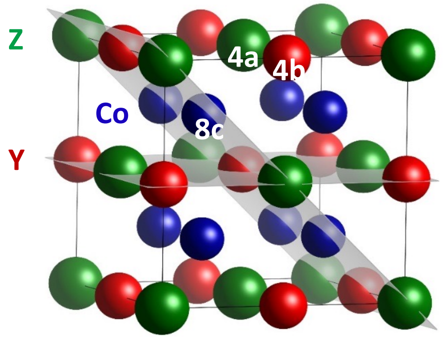

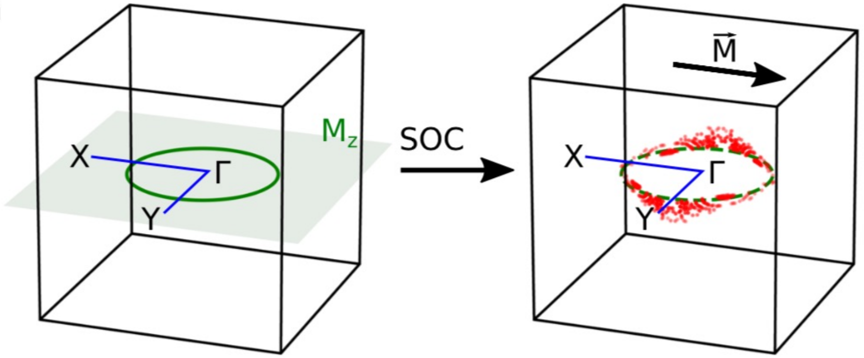

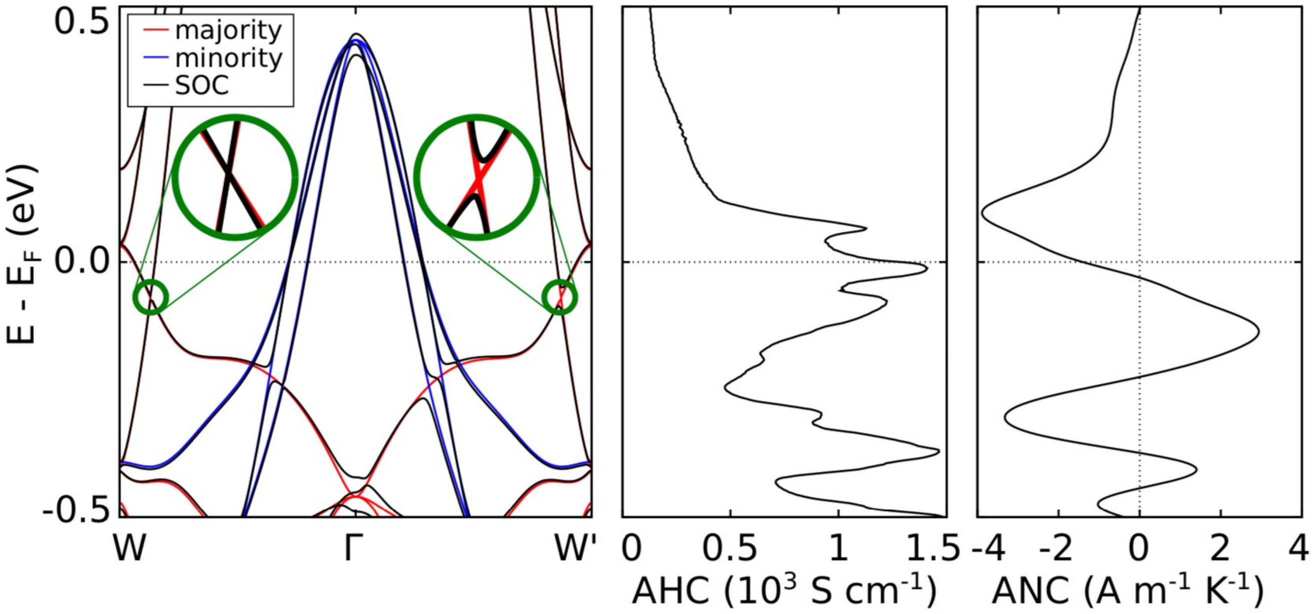

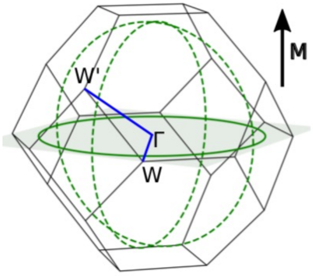

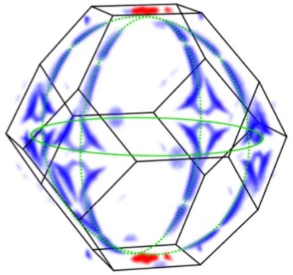

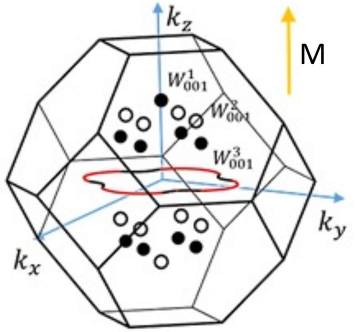

J. Noky et al., Phys. Rev. B 98, 241106(R) (2018), Fu et al., APL Mat. 8 (2020) 040913, Jonathan Noky, et al., npj Comput Mater 6 (2020) 77

ARPES

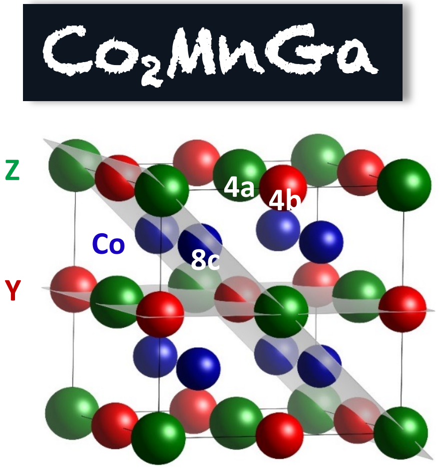

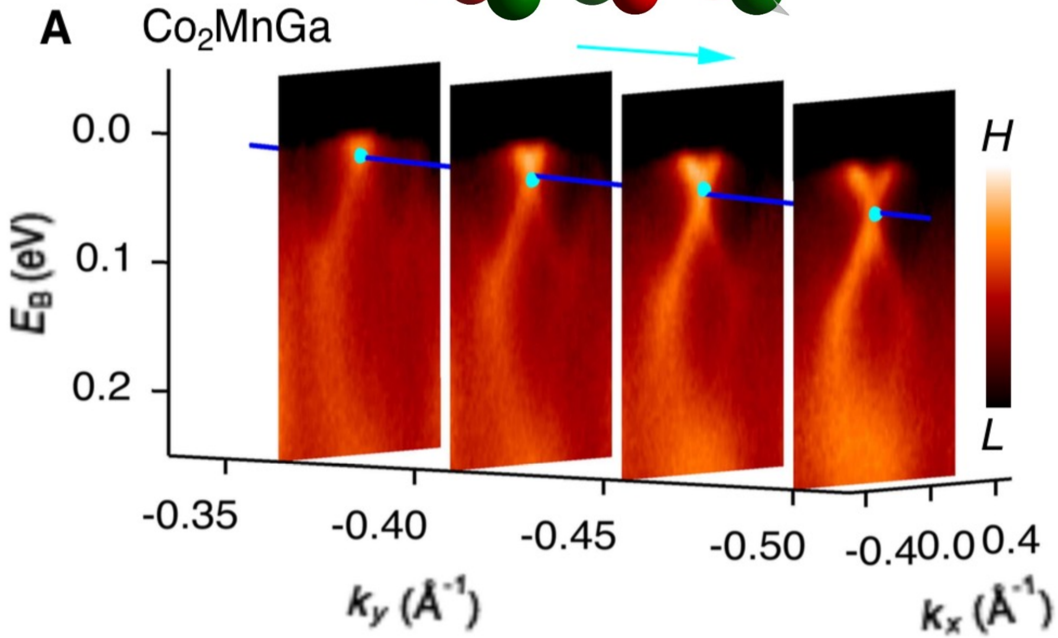

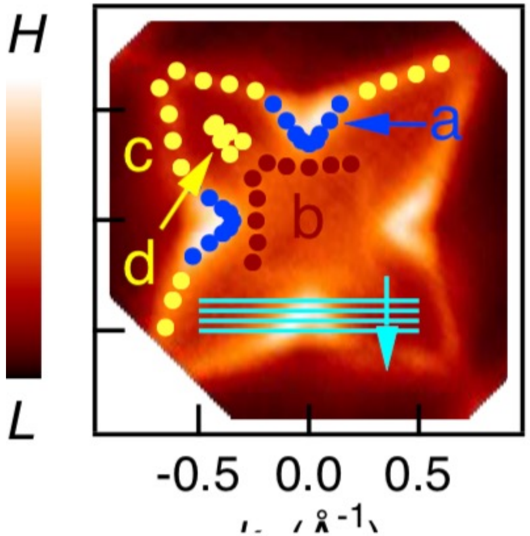

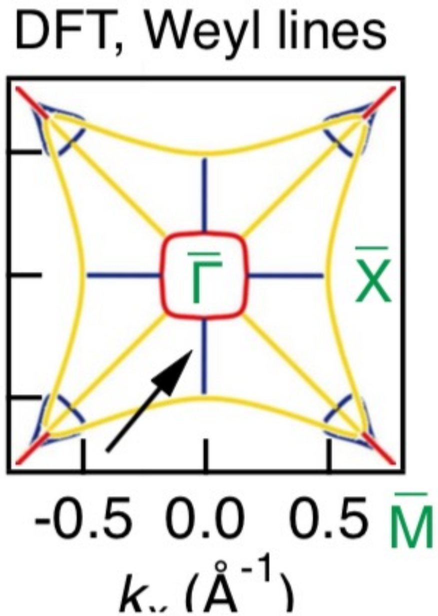

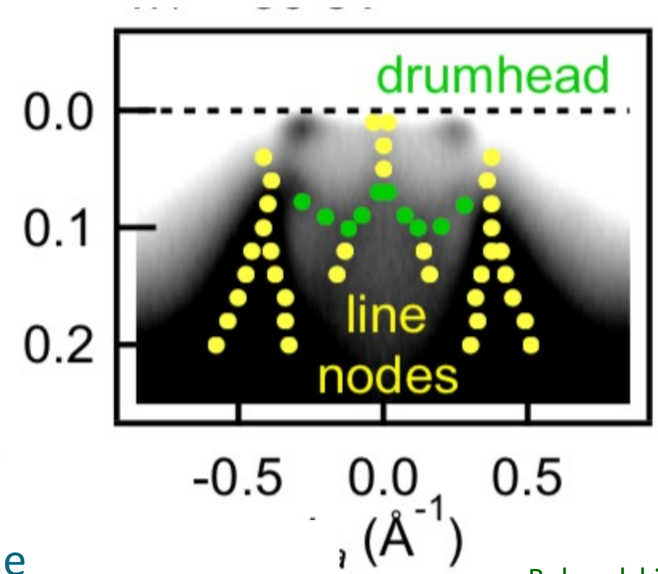

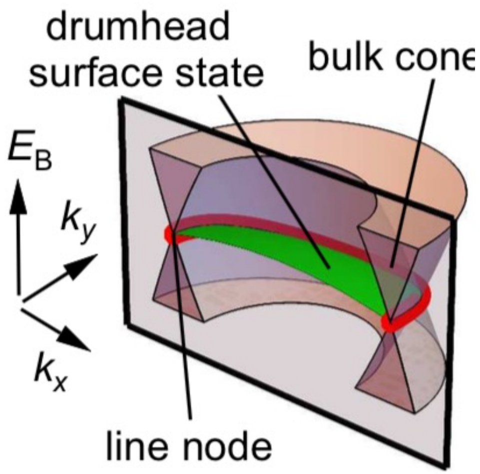

Series of ARPES cuts through the candidate line node

Belopolski, et al., Science (2019) preprint arXiv:1712.09992

Article

Observation of a linked-loop quantum state in a topological magnet

Co_2MnGa

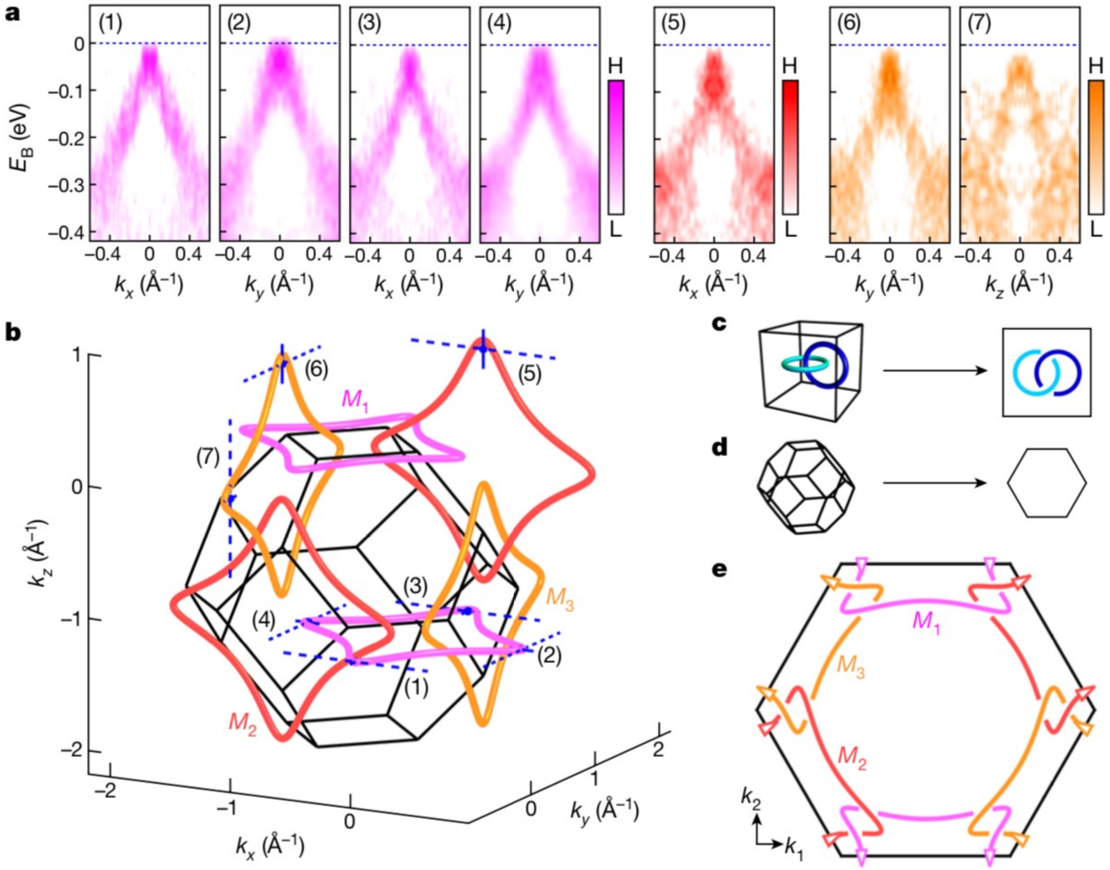

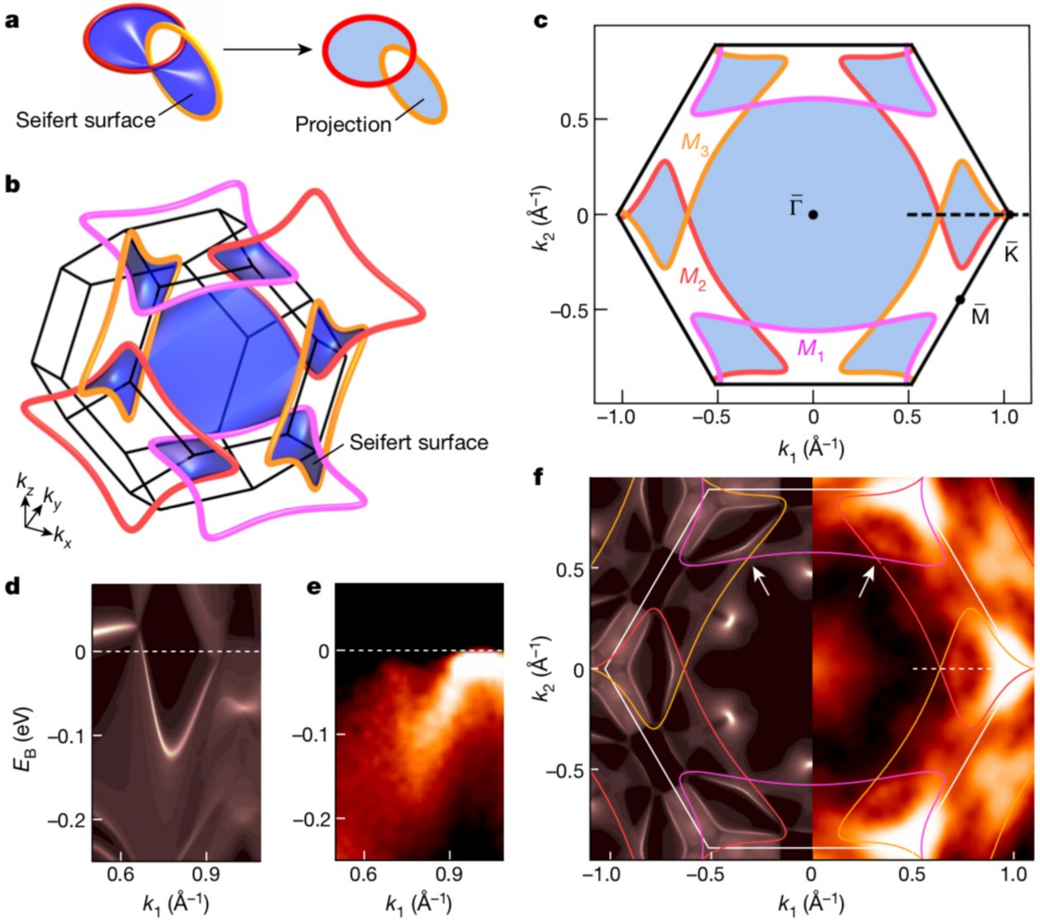

Belopolski, et al., Nature | Vol604 | 28April2022 | 647

Hall effect

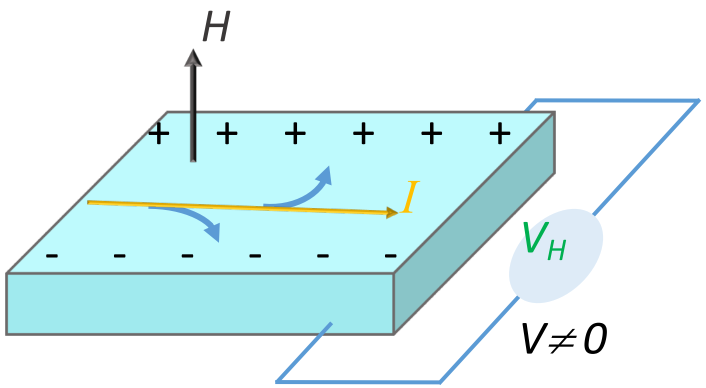

Hall Effect

diamagnetic semiconductor

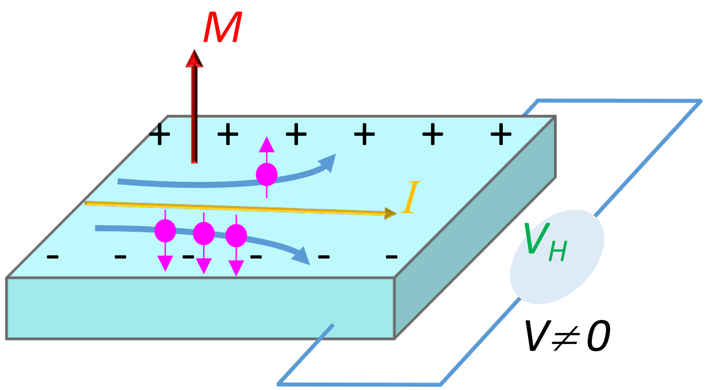

Anomalous Hall Effect

ferromagnetic material

-

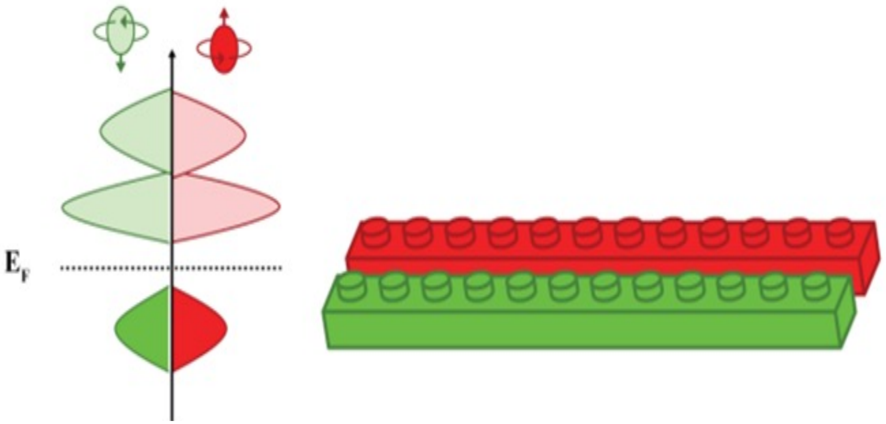

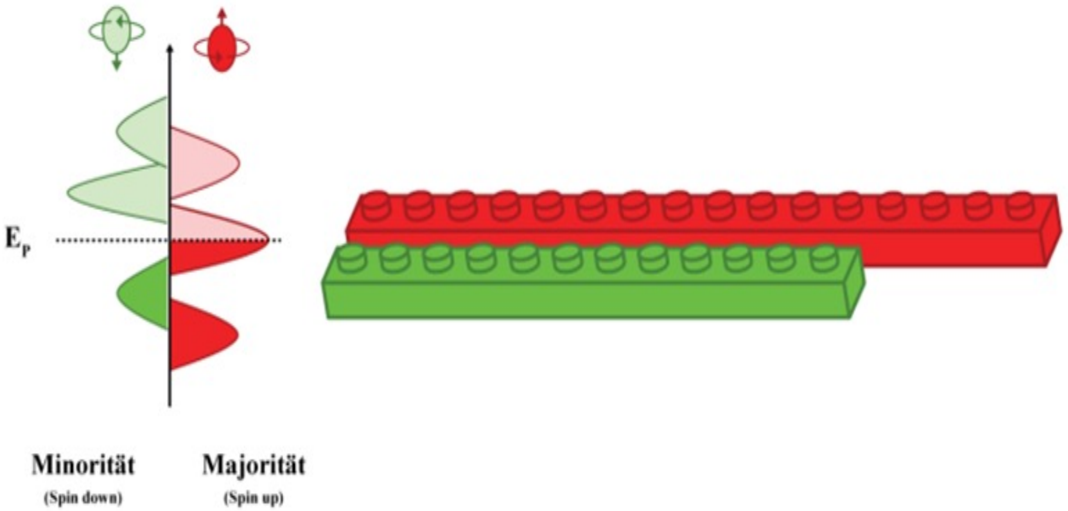

T. Graf, C. Felser, and S. S. P. Parkin, Prog. Solid State Chem. 39, 1 (2011)

Anomalous Hall

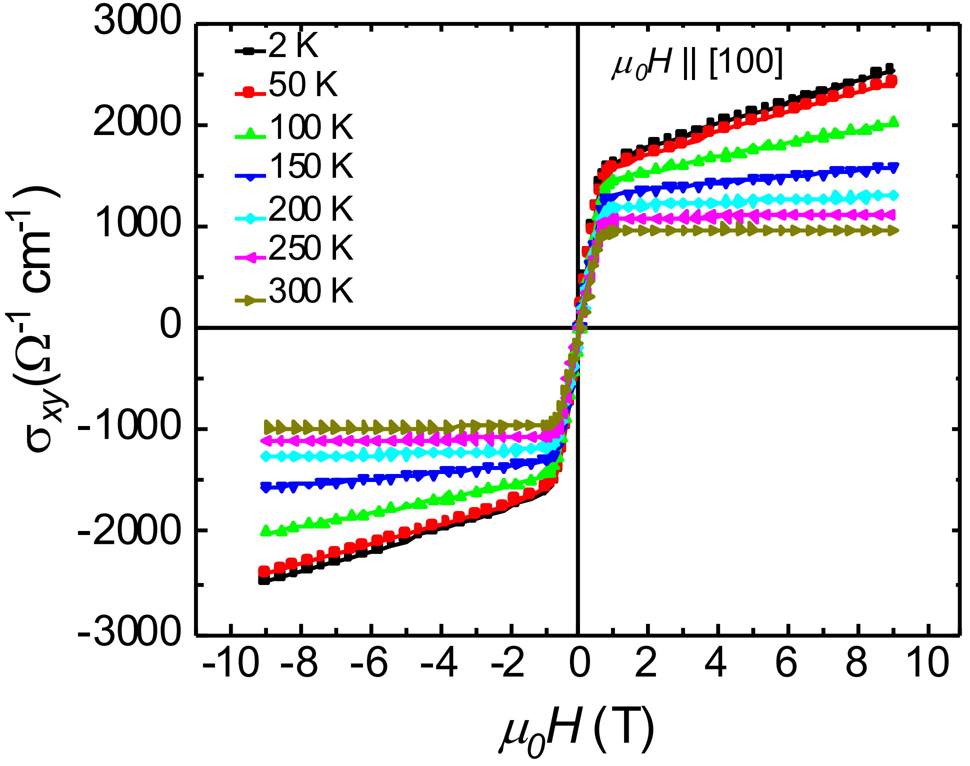

Co_2MnGa

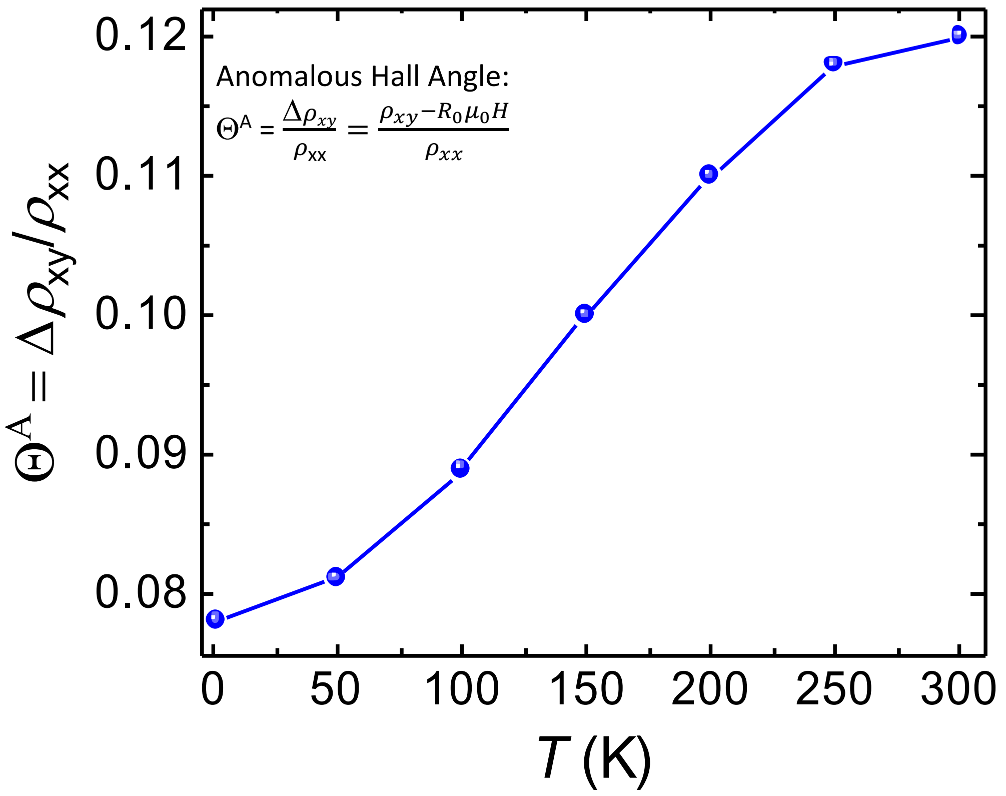

Kübler, Felser, PRB 85 (2012) 012405
Vidal et al., Appl .Phys. Lett. 99 (2011) 132509
Manna et al., Phys. Rev. X 8 (2018) 041045, arXiv:1712.10174

Anomalous Hall

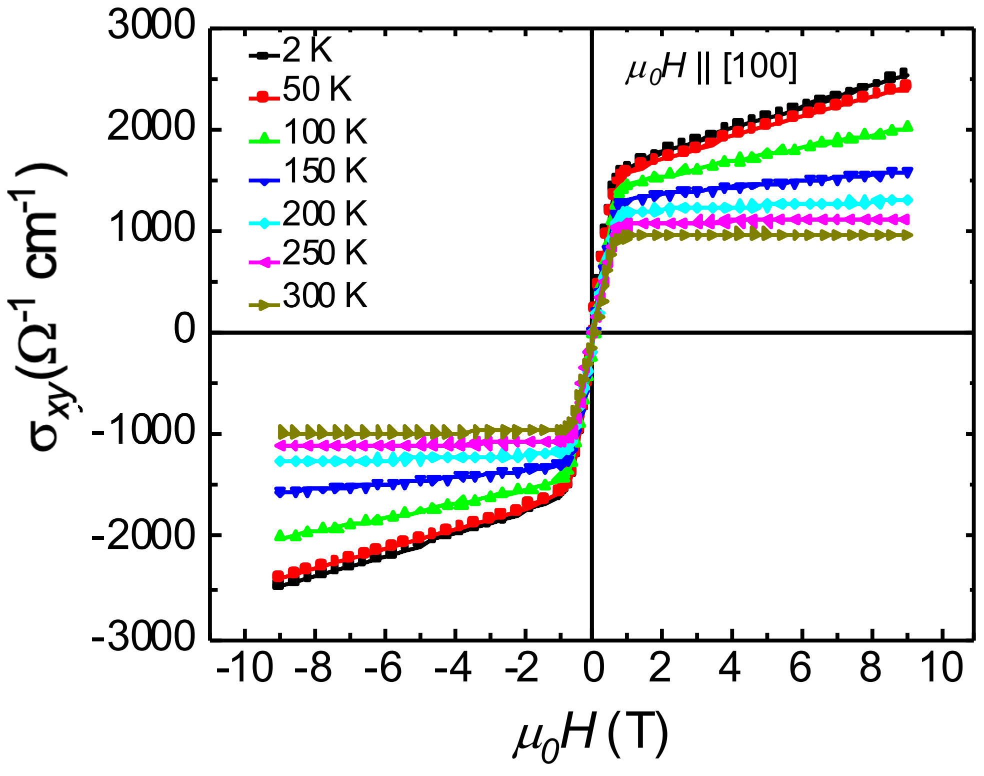

Co_2MnGa

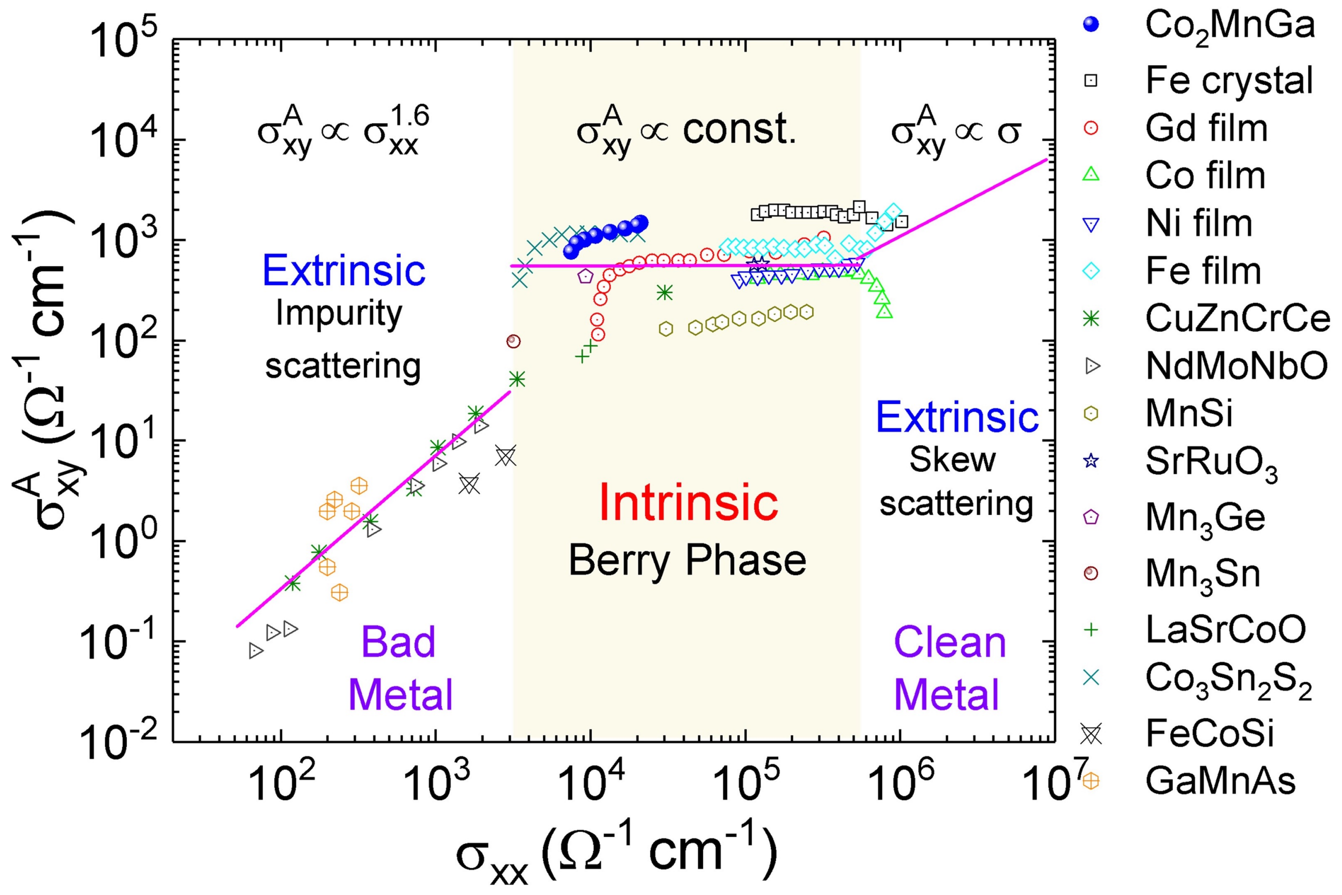

Naoto Nagaosa and Yoshinori Tokura 2012 Phys. Scr. 2012 014020

Kübler, Felser, PRB 85 (2012) 012405
Vidal et al., Appl .Phys. Lett. 99 (2011) 132509
Manna et al., Phys. Rev. X 8 (2018) 041045, arXiv:1712.10174

anomalous Nernst Effect

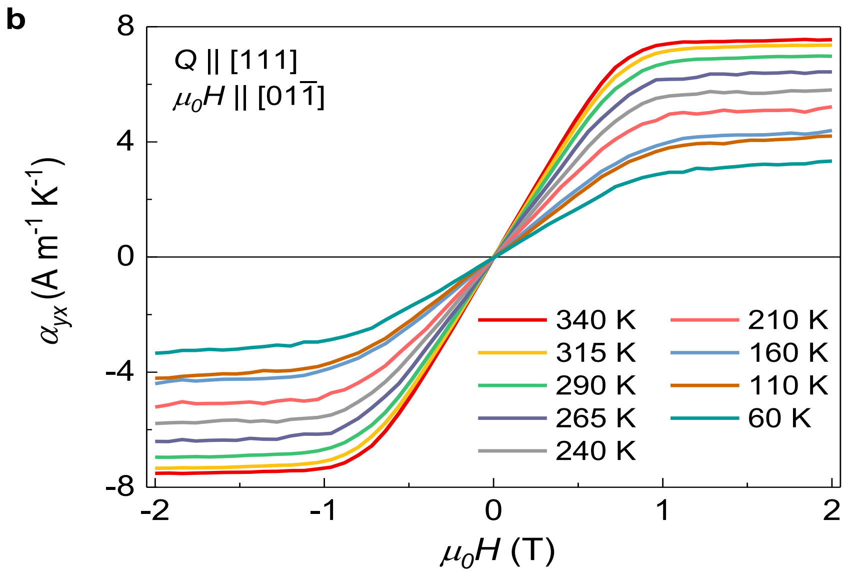

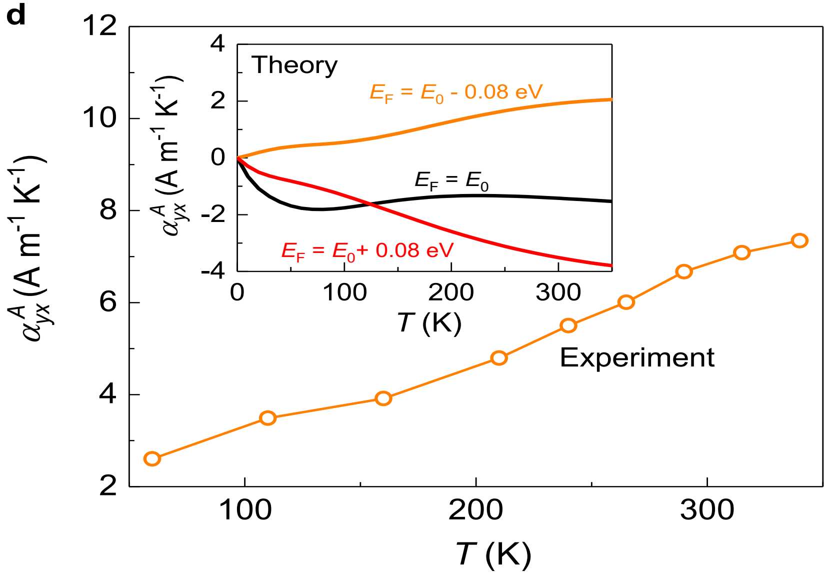

Co2MnGa

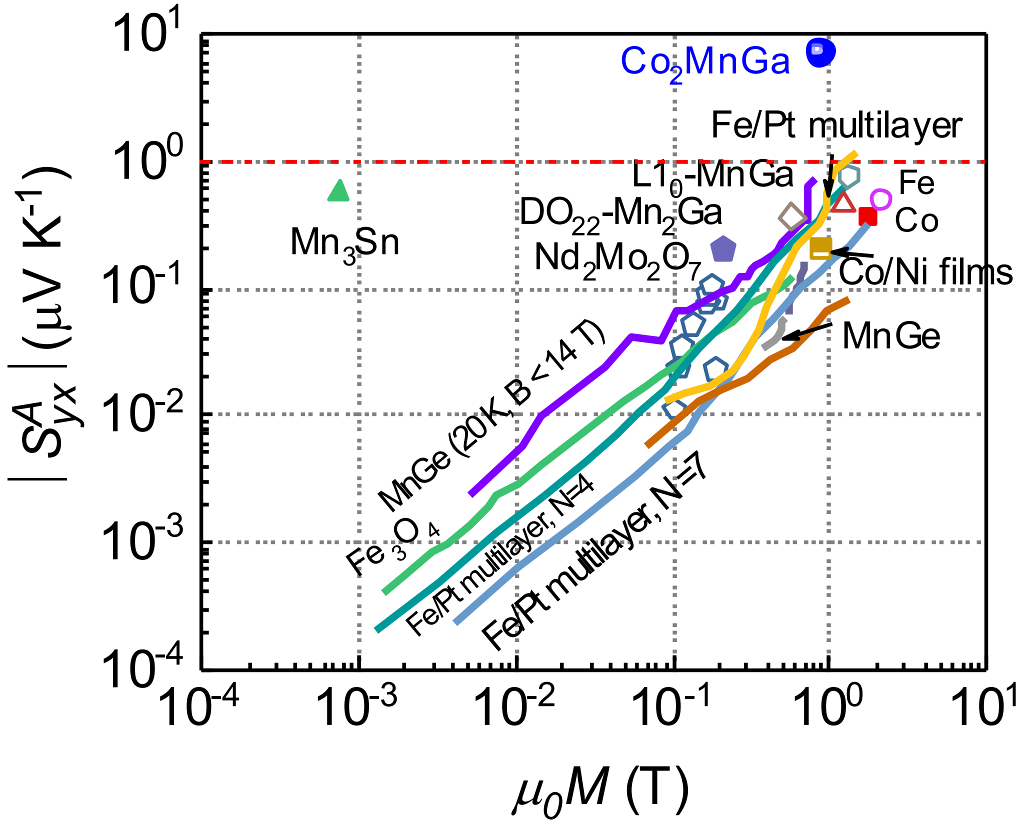

J. Noky et al., Phys. Rev. B 98, 241106(R) (2018)

Satya N. Guin, et al., NPG Asia Mater. 11, 16 (2019), arXiv:1806.06753

Sakain et al. Nature Physics 2018

Nernst Effect of iron compounds

Noky, J., Xu, Q., Felser, C. & Sun, Y. Large anomalous Hall and Nernst effects from nodal line symmetry breaking in Fe_2MnX (X = P, As, Sb). Phys. Rev. B 99, 165117 (2019).

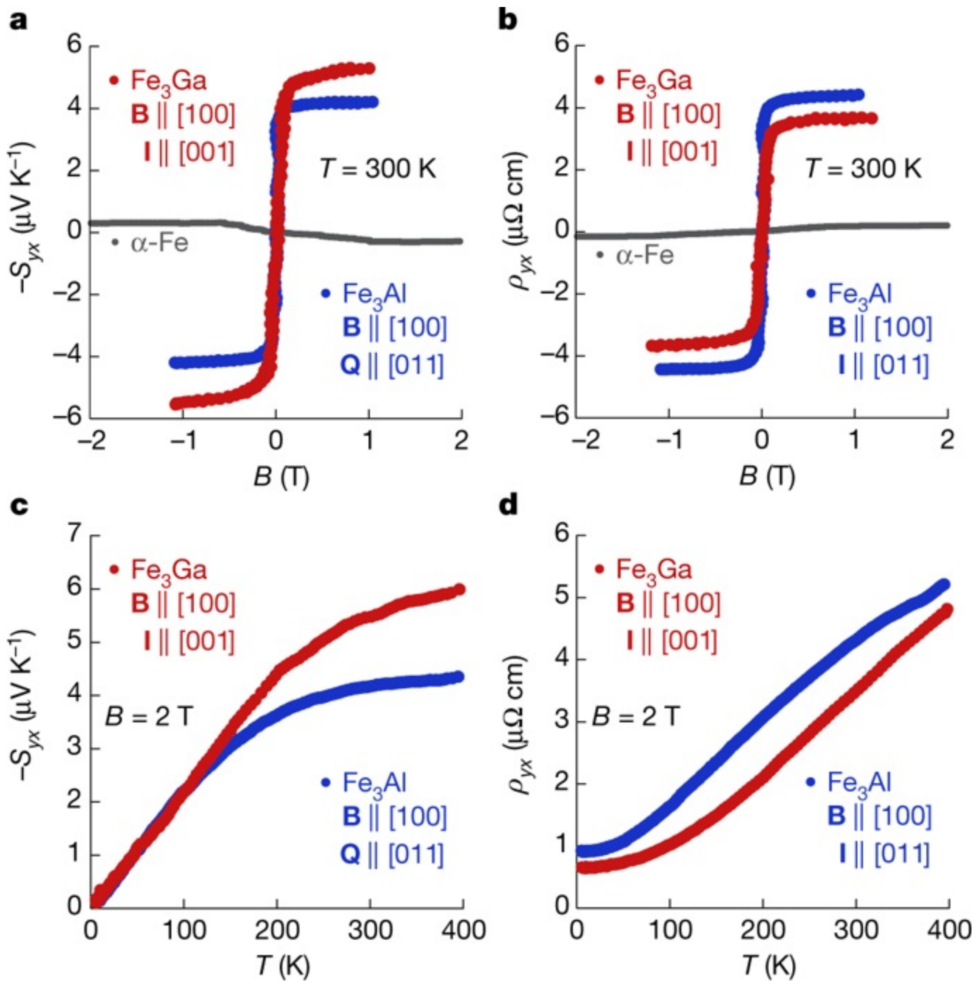

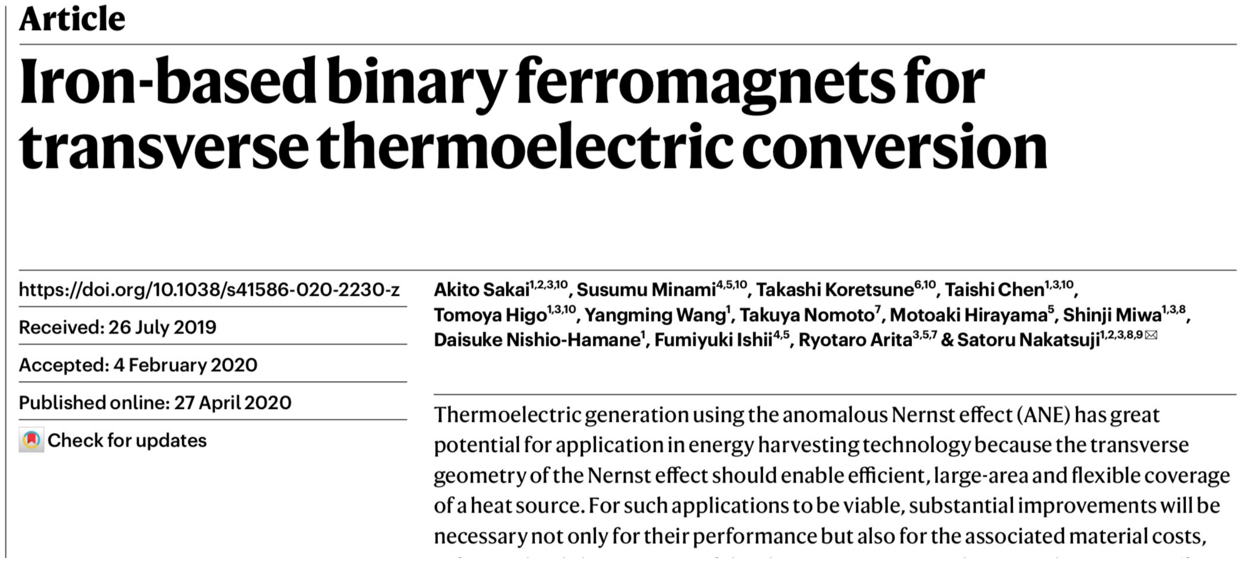

Article

Iron-based binary ferromagnets for transverse thermoelectric conversion

https://doi.org/10.1038/s41586-020-2230-z

Received: 26 July 2019

Accepted: 4 February 2020

Published online: 27 April 2020

Check for updates

Akito Sakai[1,2,3,10], Susumu Minami[4,5,10], Takashi Koretsune[6,10], Taishi Chen[1,3,10], Tomoya Higo[1,3,10], Yangming Wang[1], Takuya Nomoto[7], Motoaki Hirayama[5], Shinji Miwa[1,3,8], Daisuke Nishio-Hamane[1], Fumiyuki Ishii[4,5], Ryotaro Arita[3,5,7] & Satoru Nakatsuji[1,2,3,8,9]

Thermoelectric generation using the anomalous Nernst effect (ANE) has great potential for application in energy harvesting technology because the transverse geometry of the Nernst effect should enable efficient, large-area and flexible coverage of a heat source. For such applications to be viable, substantial improvements will be necessary not only for their performance but also for the associated material costs,

Heusler compounds

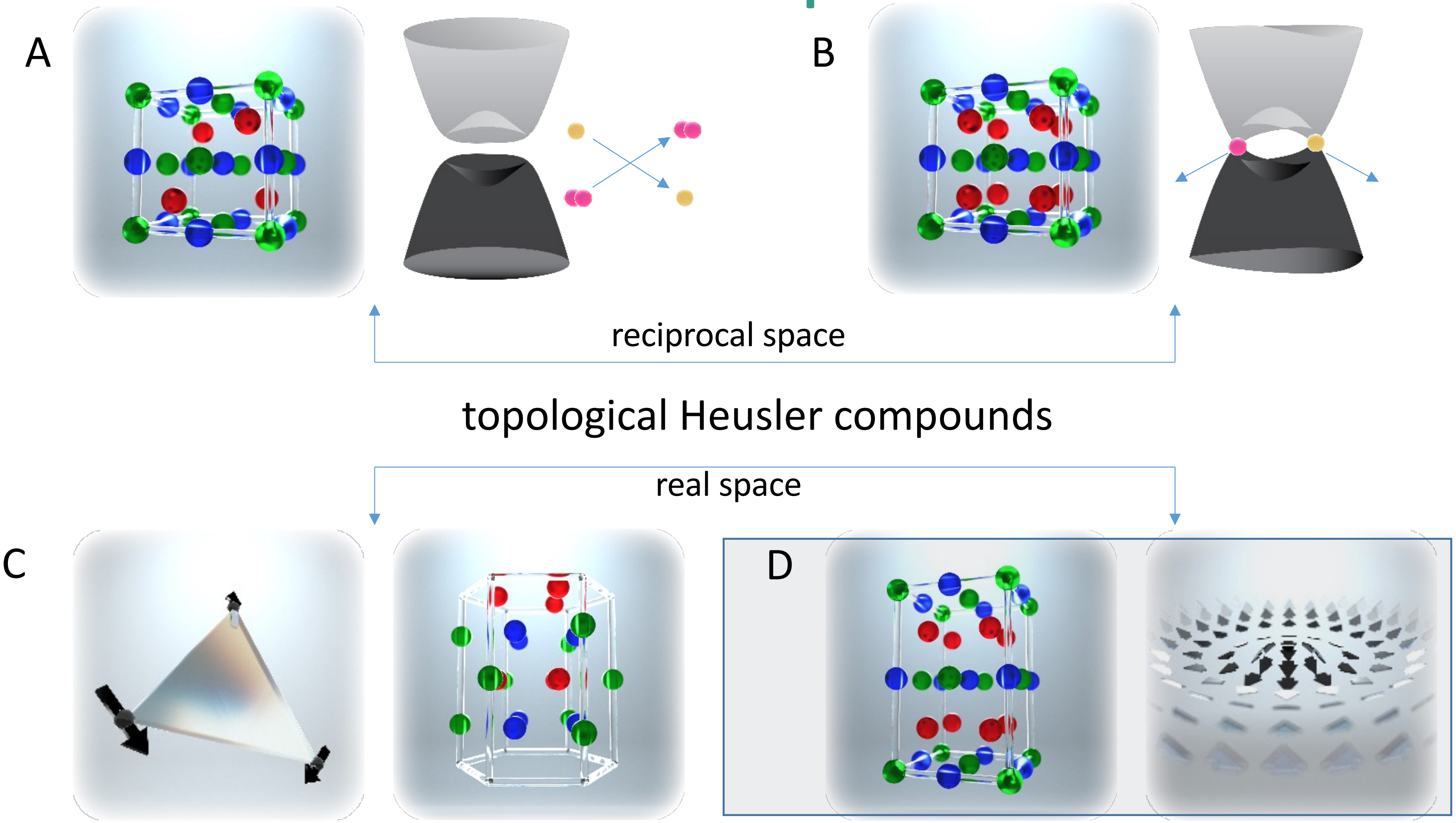

Heusler compounds with crystalline anisotropy

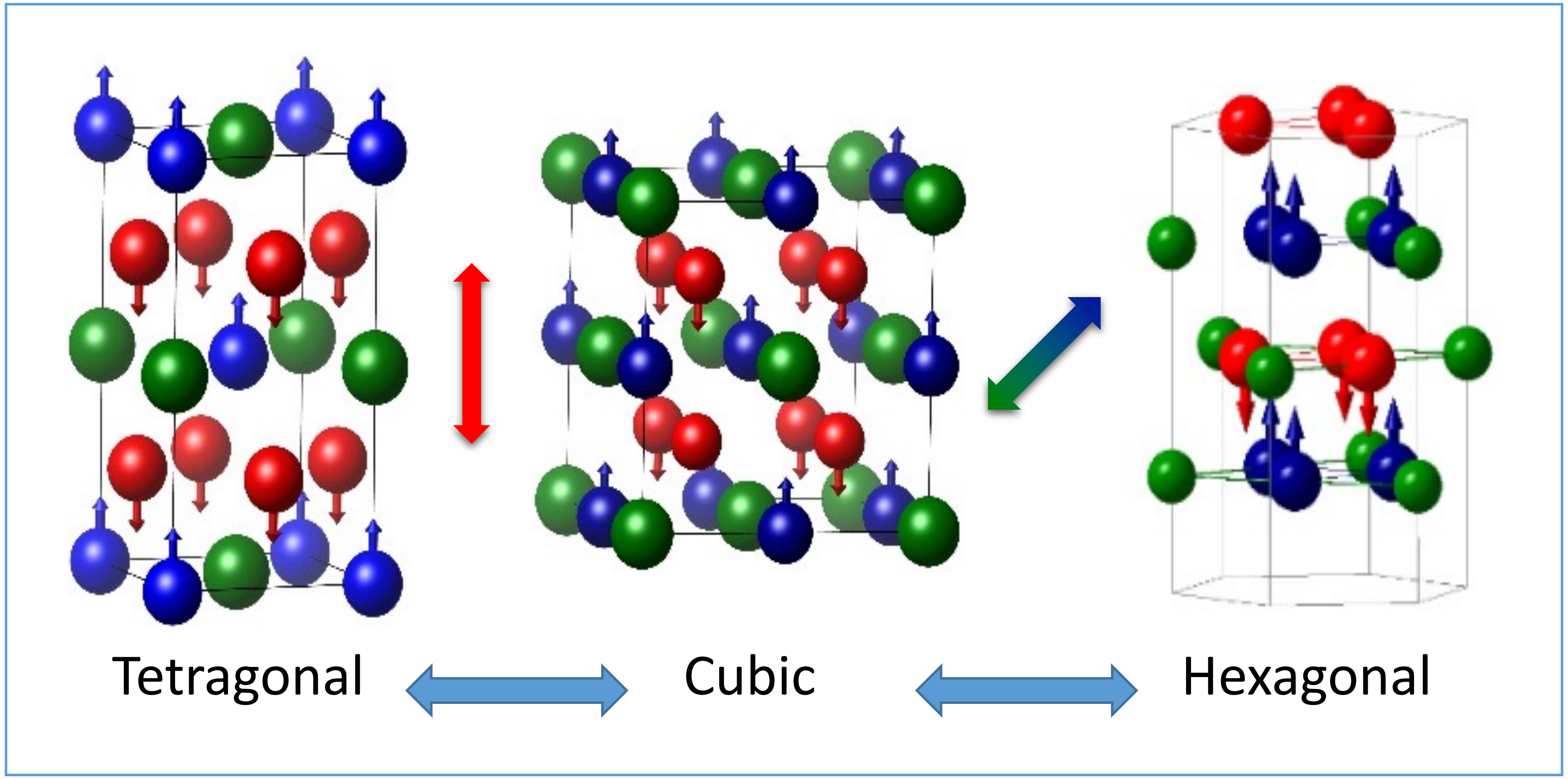

Mn_3Ga Mn_3Ge Mn_3Sn

Heusler compounds for STT MRAM

- Materials with low magnetic damping
- Materials with low magnetic moments
- Materials with high perpendicular anisotrop

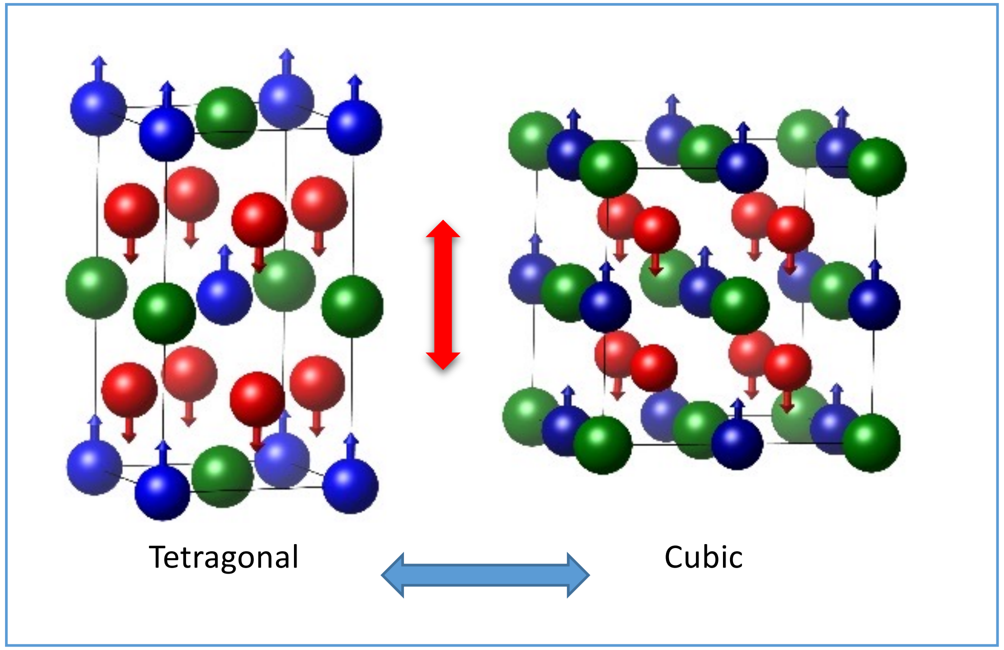

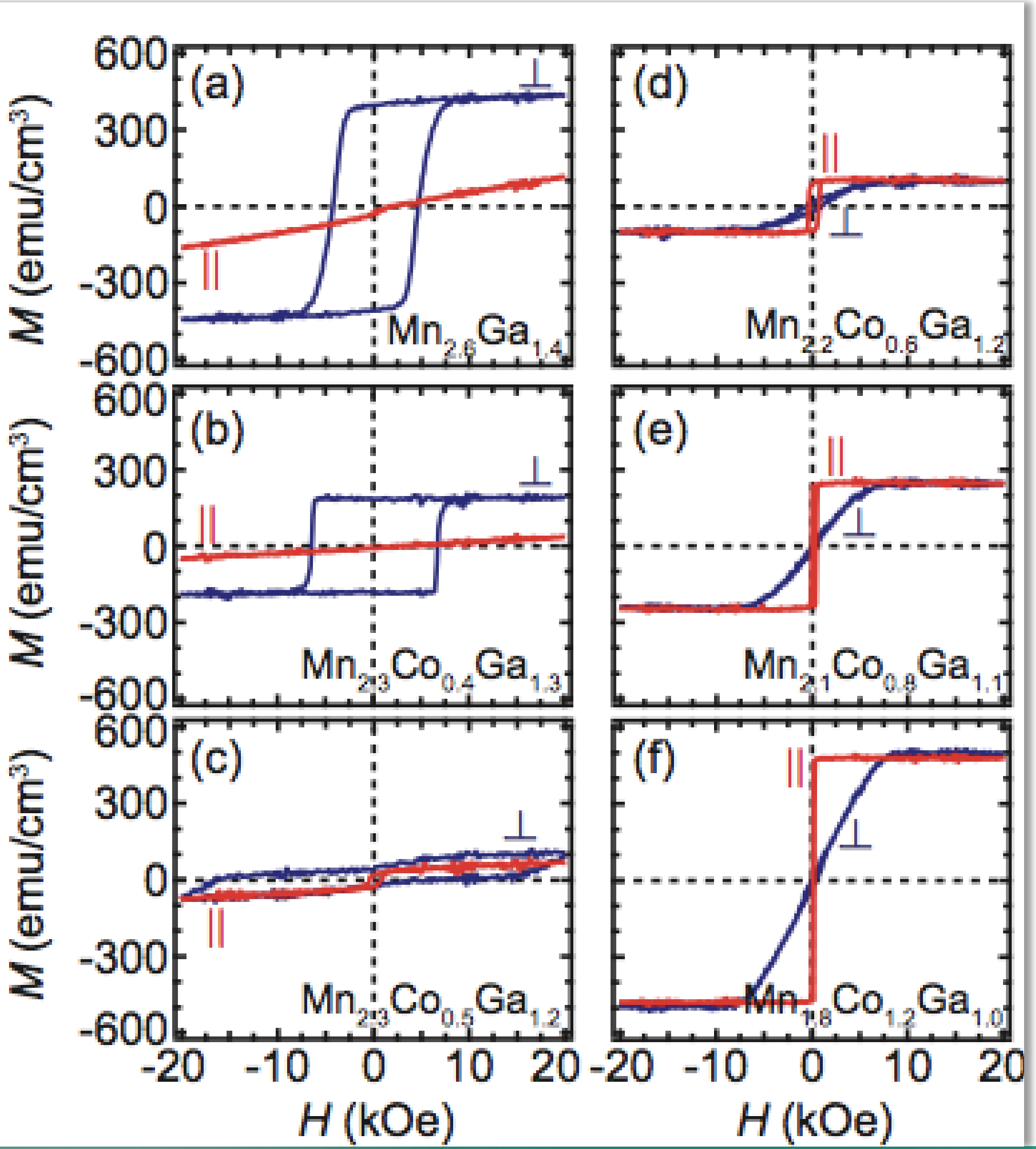

Mn_3Ga | $Co_{2-x}Mn_xGa$ | Co_2MnGa

Antiskyrmions in Heusler compounds

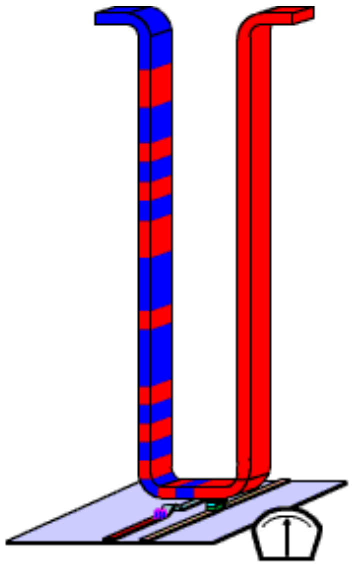

Stuart S. P. Parkin, et al.: *Magnetic Domain-Wall Racetrack Memory*, *Science* 320 (2008) 190–194

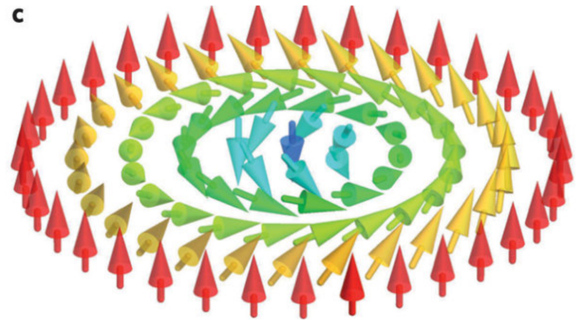

Skyrmions on the track

Albert Fert, Vincent Cros and João Sampaio

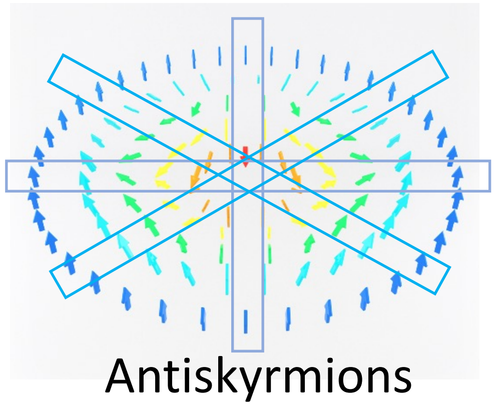

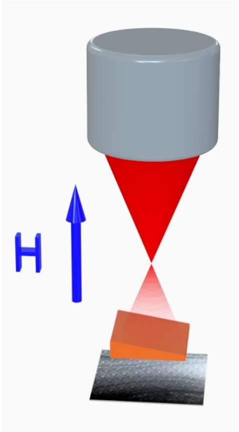

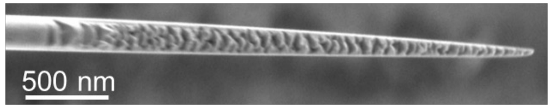

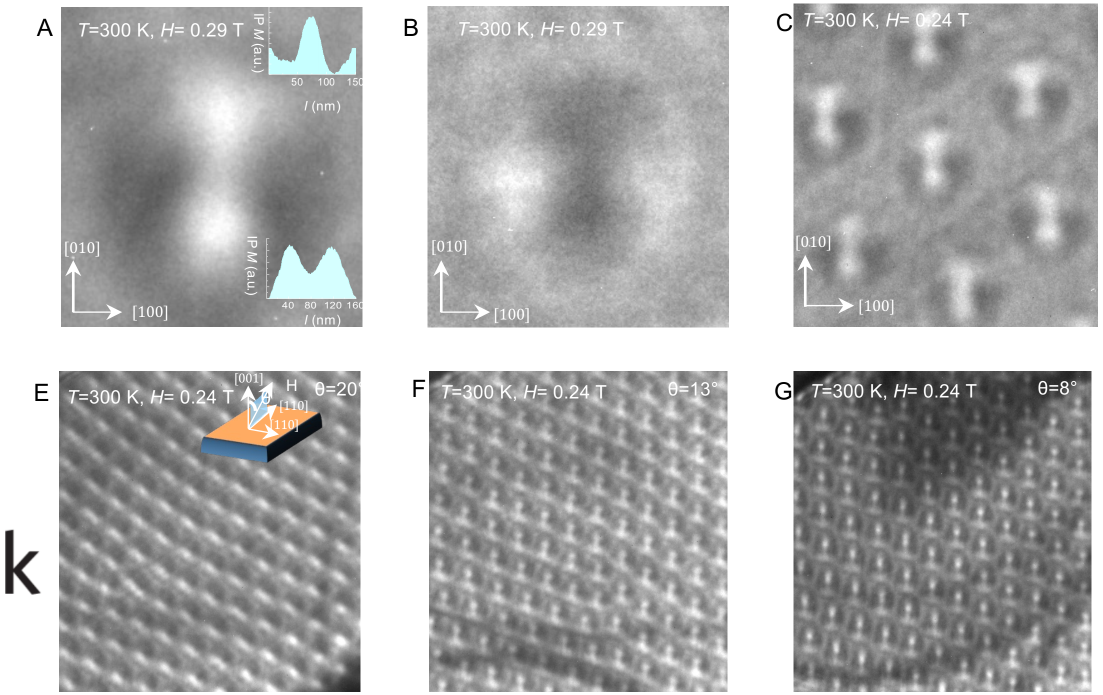

A. K. Nayak, et al., Nature 548 (2017) 561

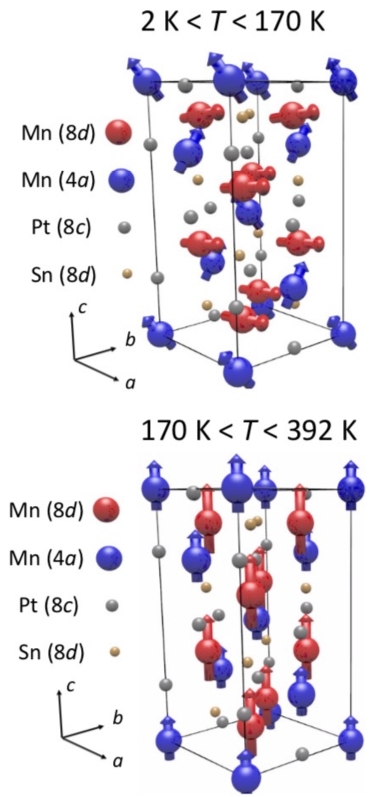

$Mn_{1,4}PtSn$

Heusler compounds

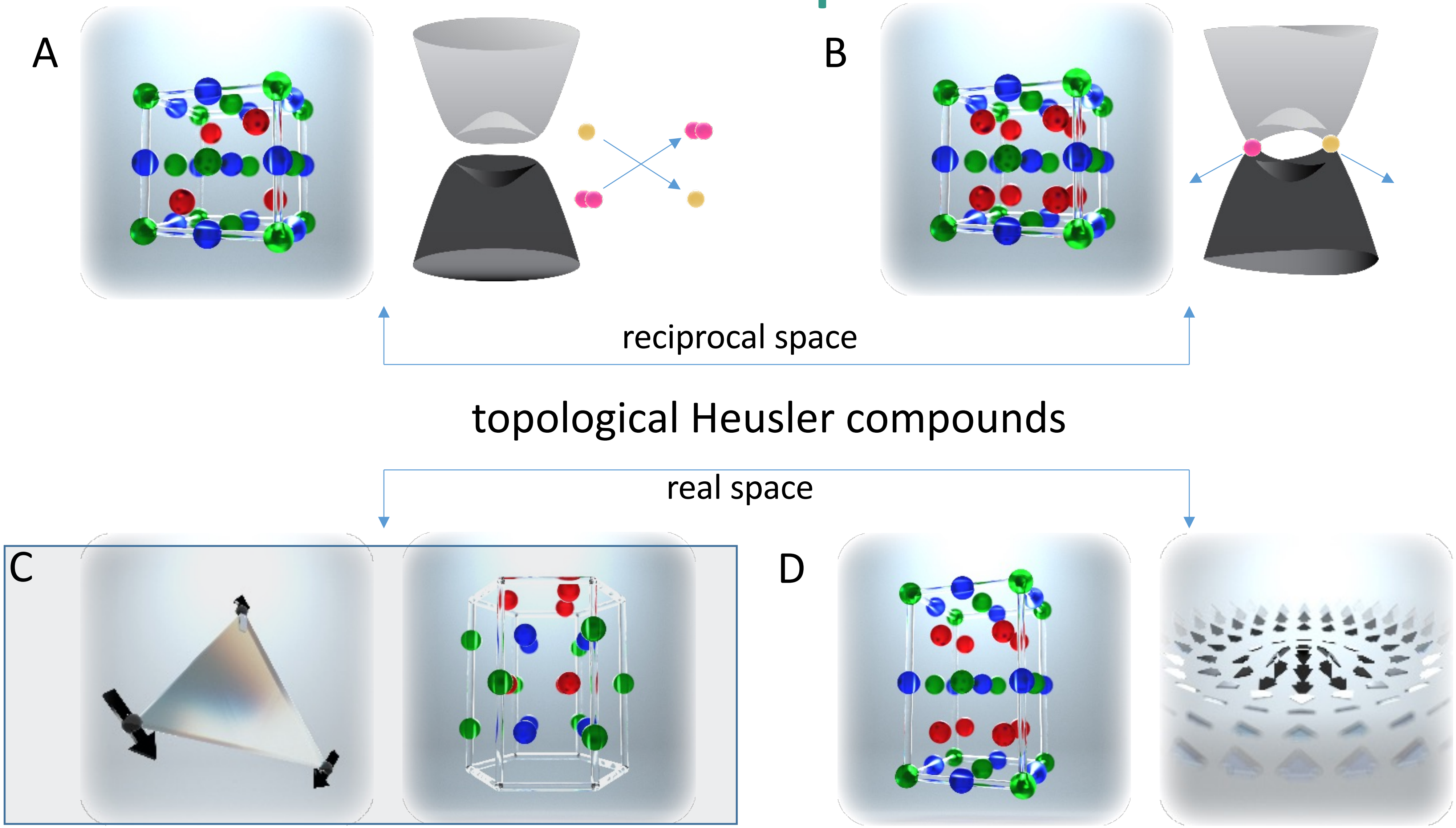

Kagome lattice

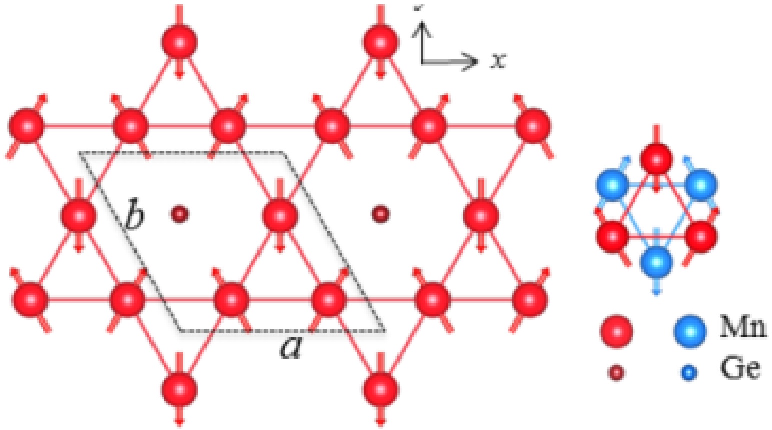

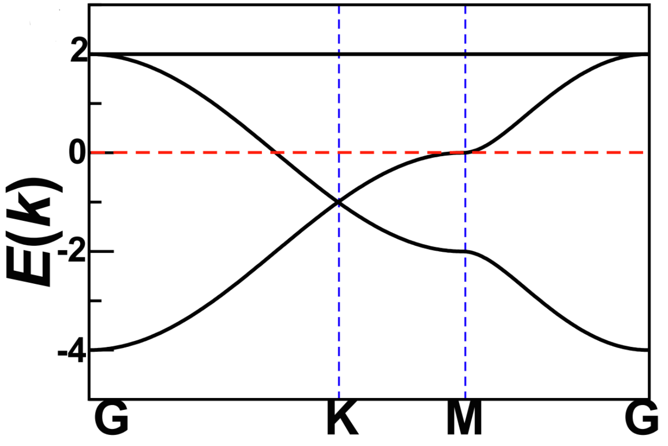

- Dirac cone,
- flat band, and
- van Hove singularity

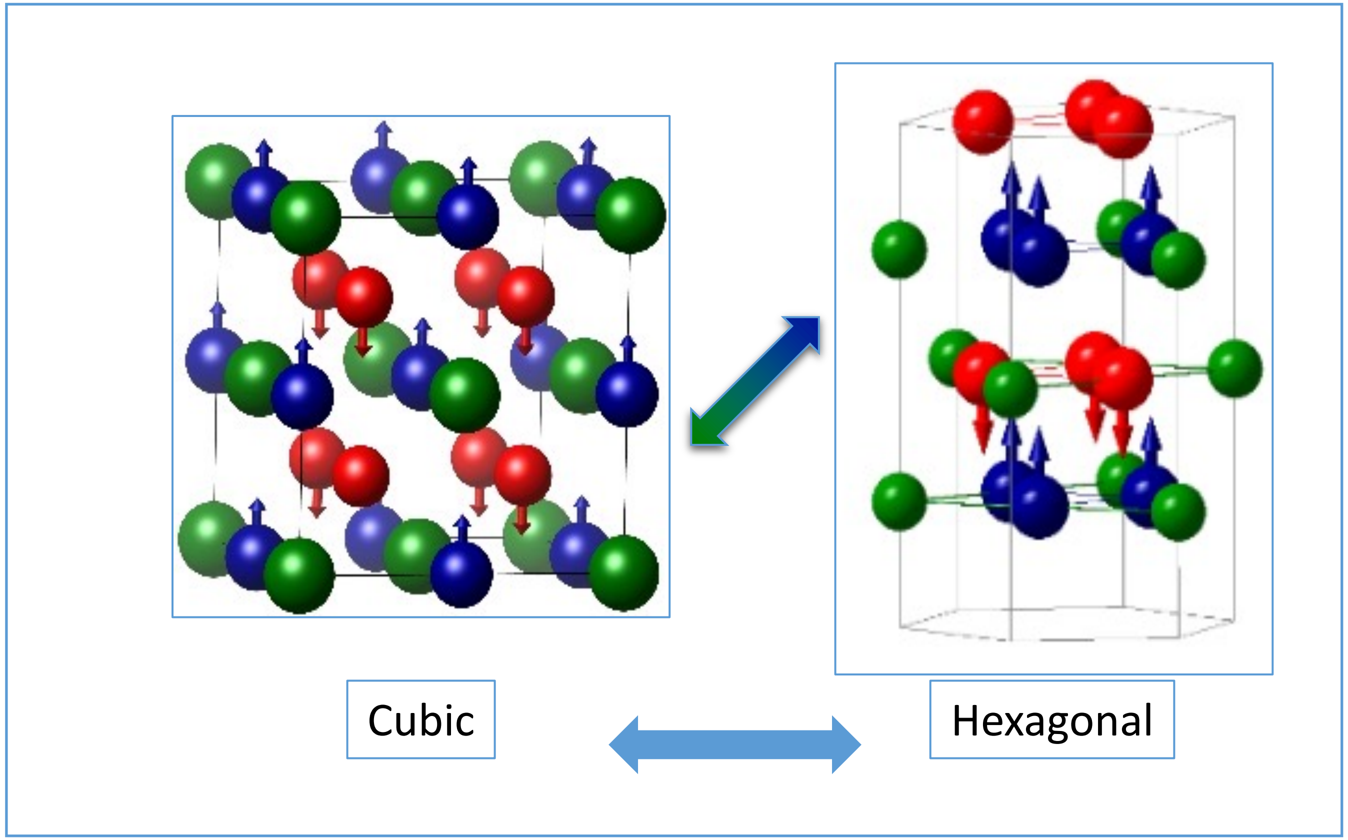

Mn_3Ga, Mn_3Ge, Mn_3Sn

Kübler, Felser EPL 108 (2014) 67001,

antiferromagnetic topological materials

Table 3 | The magnetic topological materials identified in this work

Categories	Properties	Materials
I-A	Non-collinear manganese compounds	Mn_3GaC, Mn_3ZnC, Mn_3CuN, Mn_3Sn, Mn_3Ge, Mn_3Ir, Mn_3Pt, Mn_5Si_3
I-B	Actinide intermetallic	$UNiGa_5$, $UPtGa_5$, $NpRhGa_5$, $NpNiGa_5$
I-C	Rare-earth intermetallic	$NdCo_2$, $TbCo_2$, $NpCo_2$, PrAg DyCu, NdZn, TbMg, NdMg, Nd_5Si_4, Nd_5Ge_4, Ho_2RhIn_8, Er_2CoGa_8, Nd_2RhIn_8, Tm_2CoGa_8, Ho_2RhIn_8, $DyCo_2Ga_8$, $TbCo_2Ga_8$, Er_2Ni_2In, $CeRu_2Al_{10}$, $Nd_3Ru_4Al_{12}$, $Pr_3Ru_4Al_{12}$, $ScMn_6Ge_6$, YFe_4Ge_4, $LuFe_4Ge_4$, $CeCoGe_3$
II-A	Metallic iron pnictides	LaFeAsO, $CaFe_2As_2$, $EuFe_2As_2$, $BaFe_2As_2$, Fe_2As, $CaFe_4As_3$, LaCrAsO, Cr_2As, CrAs, CrN
II-B	Semiconducting manganese pnictides	$BaMn_2As_2$ $BaMn_2Bi_2$, $CaMnBi_2$, $SrMnBi_2$, $CaMn_2Sb_2$, CuMnAs, CuMnSb, Mn_2As
II-C	Rare-earth intermetallic compounds with the composition 1:2:2	$PrNi_2Si_2$, $YbCo_2Si_2$, $DyCo_2Si_2$, $PrCo_2P_2$, $CeCo_2P_2$, $NdCo_2P_2$, $DyCu_2Si_2$, $CeRh_2Si_2$, UAu_2Si_2, U_2Pd_2Sn, U_2Pd_2In, U_2Ni_2Sn, U_2Ni_2In, U_2Rh_2Sn
II-D	Rare-earth ternary compounds of the composition 1:1:1	CeMgPb, PrMgPb, NdMgPb, TmMgPb
III-A	Semiconducting actinides/ rare-earth pnictides	HoP, UP, UP_2, UAs, NpS, NpSe, NpTe, NpSb, NpBi, U_3As_4, U_3P_4
III-B	Metallic oxides	Ag_2NiO_2, $AgNiO_2$, $Ca_3Ru_2O_7$, Double perovskite Sr_3CoIrO_6
III-C	Metal-to-insulator transition compounds	NiS_2, $Sr_2Mn_3As_2O_2$
III-D	Semiconducting and insulating oxides, borates, hydroxides, silicates and phosphate	$LuFeO_3$, $PdNiO_3$, $ErVO_3$, $DyVO_3$, $MnGeO_3$, $Tm_2Mn_2O_7$, $Yb_2Sn_2O_7$, $Tb_2Sn_2O_7$, $Ho_2Ru_2O_7$, $Er_2Ti_2O_7$, $Tb_2Ti_2O_7$, $Cd_2Os_2O_7$, $Ho_2Ru_2O_7$, Cr_2ReO6, $NiCr_2O_4$, MnV_2O_4, Co_2SiO_4, Fe_2SiO_4, $PrFe_3(BO_3)_4$, $KCo_4(PO_4)_3$, $CoPS_3$, $SrMn(VO_4)(OH)$, $Ba_5Co_5ClO_{13}$, FeI_2

Y Xu, et al., Nature 586 (2020) 702

antiferromagnetic materials

Ru₂MnSi

Ru

Mn

Ga

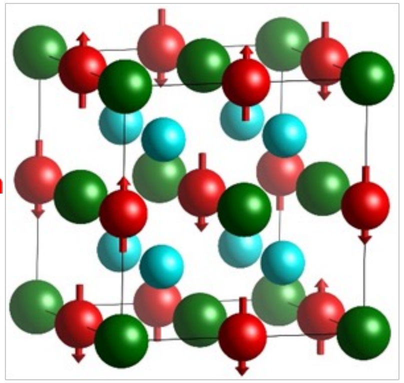

[Ru_2MnSi]

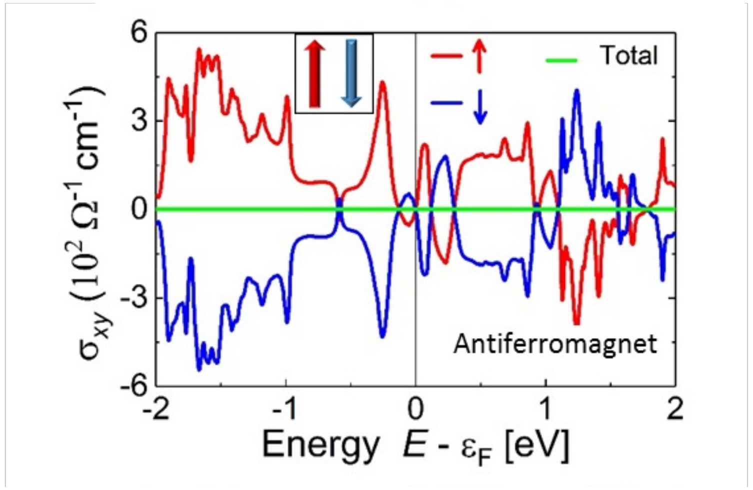

REVIEWS OF MODERN PHYSICS, VOLUME 82, APRIL–JUNE 2010

Anomalous Hall effect

Naoto Nagaosa

Department of Applied Physics, University of Tokyo, Tokyo 113-8656, Japan and Cross-Correlated Materials Research Group (CMRG), and Correlated Electron Research Group (CERG), ASI, RIKEN, Wako, 351-0198 Saitama, Japan

Jairo Sinova

Department of Physics, Texas A&M University, College Station, Texas 77843-4242, USA and Institute of Physics ASCR, Cukrovarnická 10, 162 53 Praha 6, Czech Republic

Shigeki Onoda

Condensed Matter Theory Laboratory, ASI, RIKEN, Wako, 351-0198 Saitama, Japan

A. H. MacDonald

Department of Physics, University of Texas at Austin, Austin, Texas 78712-1081, USA

N. P. Ong

Department of Physics, Princeton University, Princeton, New Jersey 08544, USA

(Published 13 May 2010)

$$\sigma^A_{xy}(\mu) = ie^2 \left(\frac{1}{2\pi}\right)^3 \int_k dk \sum_{E(n,k)<\mu} f(n,k,\mu)\Omega_{n,xy}(k),$$

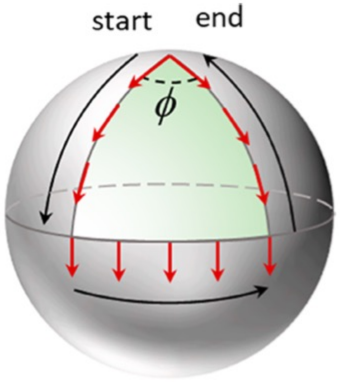

The anomalous Hall conductivity in an antiferromagnetic metal is zero

Berry curvature

Manna et al., Phys. Rev. X 8 (2018) 041045, arXiv:1712.10174

Manna et al., Nature Review Materials, 3 (2018) 244 arXiv:1802.02838v1

antiferromagnetic topological materials

Table 3 | The magnetic topological materials identified in this work

Categories	Properties	Materials
I-A	Non-collinear manganese compounds	Mn_3GaC, Mn_3ZnC, Mn_3CuN, Mn_3Sn, Mn_3Ge, Mn_3Ir, Mn_3Pt, Mn_5Si_3

Mn_3Ge, Mn_3Sn

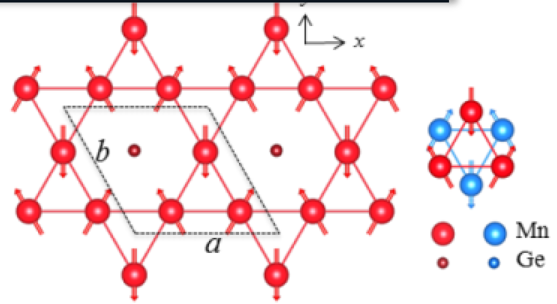

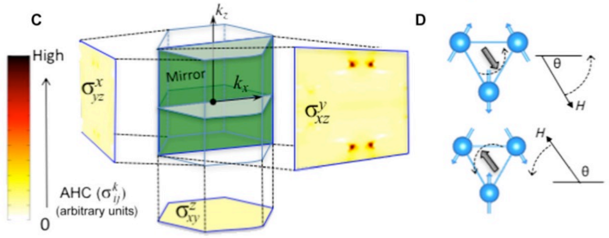

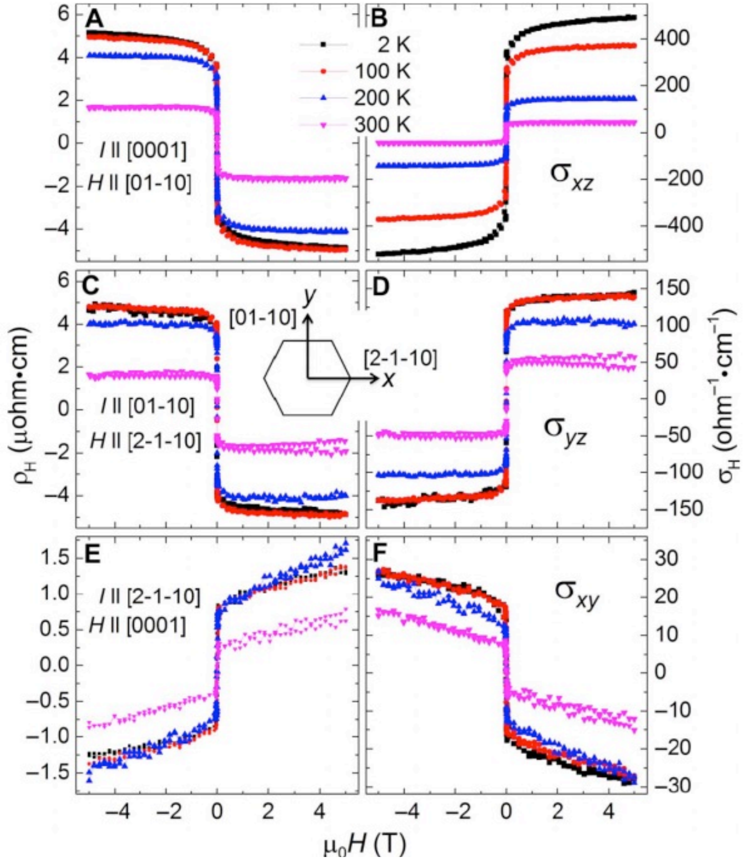

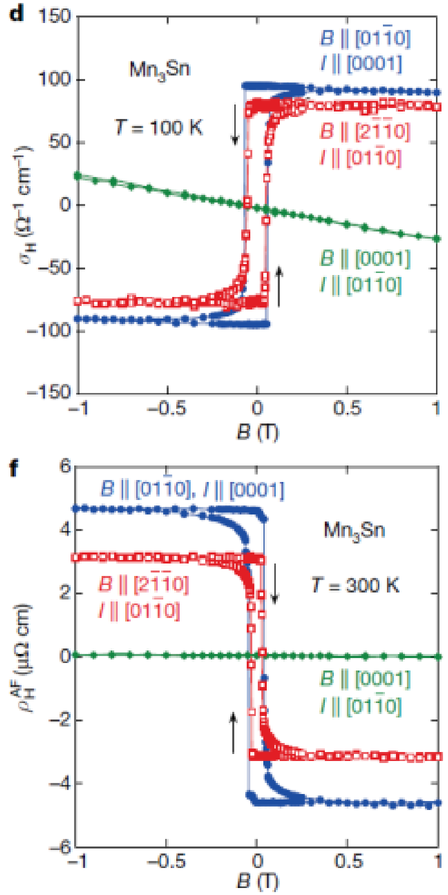

Chen, Niu, MacDonald, PRL112 (2014) 017205, Kübler, Felser EPL 108 (2014) 67001, Nayak et al., Science Advances 2 (2016) e1501870, Nakatsuji, et al., Nature, doi:10.1038/nature15723

Giant anomalous Nernst effect

PRL 119, 056601 (2017) PHYSICAL REVIEW LETTERS week ending 4 AUGUST 2017

Anomalous Nernst and Righi-Leduc Effects in Mn_3Sn: Berry Curvature and Entropy Flow

Xiaokang Li,[1] Liangcai Xu,[1] Linchao Ding,[1] Jinhua Wang,[1] Mingsong Shen,[1] Xiufang Lu,[1] Zengwei Zhu,[1,*] and Kamran Behnia[1,2,†]

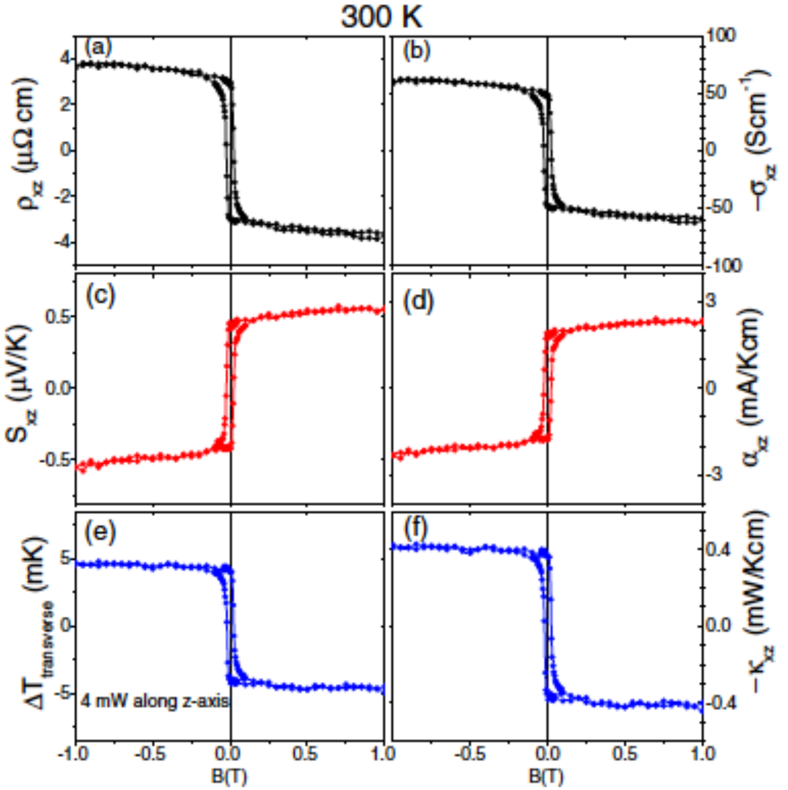

nature physics LETTERS
PUBLISHED ONLINE: 24 JULY 2017 | DOI: 10.1038/NPHYS4181

Large anomalous Nernst effect at room temperature in a chiral antiferromagnet

Muhammad Ikhlas[1†], Takahiro Tomita[1†], Takashi Koretsune[2,3], Michi-To Suzuki[2], Daisuke Nishio-Hamane[1], Ryotaro Arita[2,4], Yoshichika Otani[1,2,4] and Satoru Nakatsuji[1,4*]

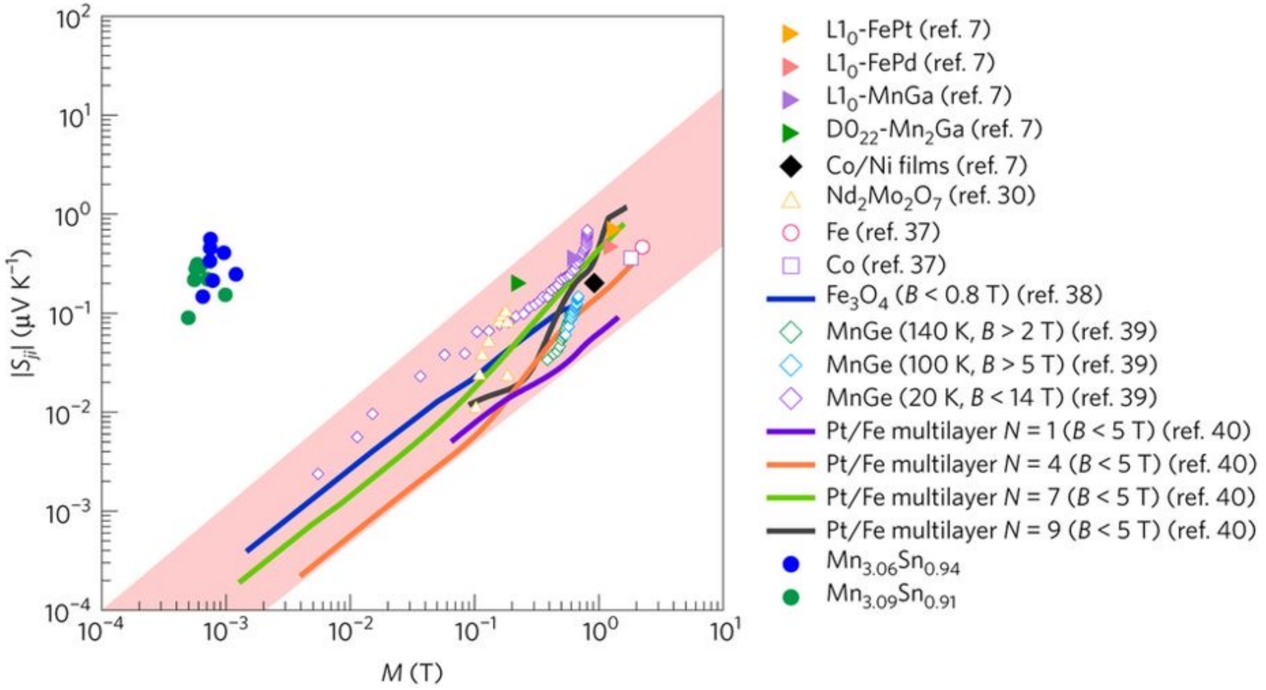

Magnetization dependence of the spontaneous Nernst effect for ferromagnetic metals and Mn_3Sn

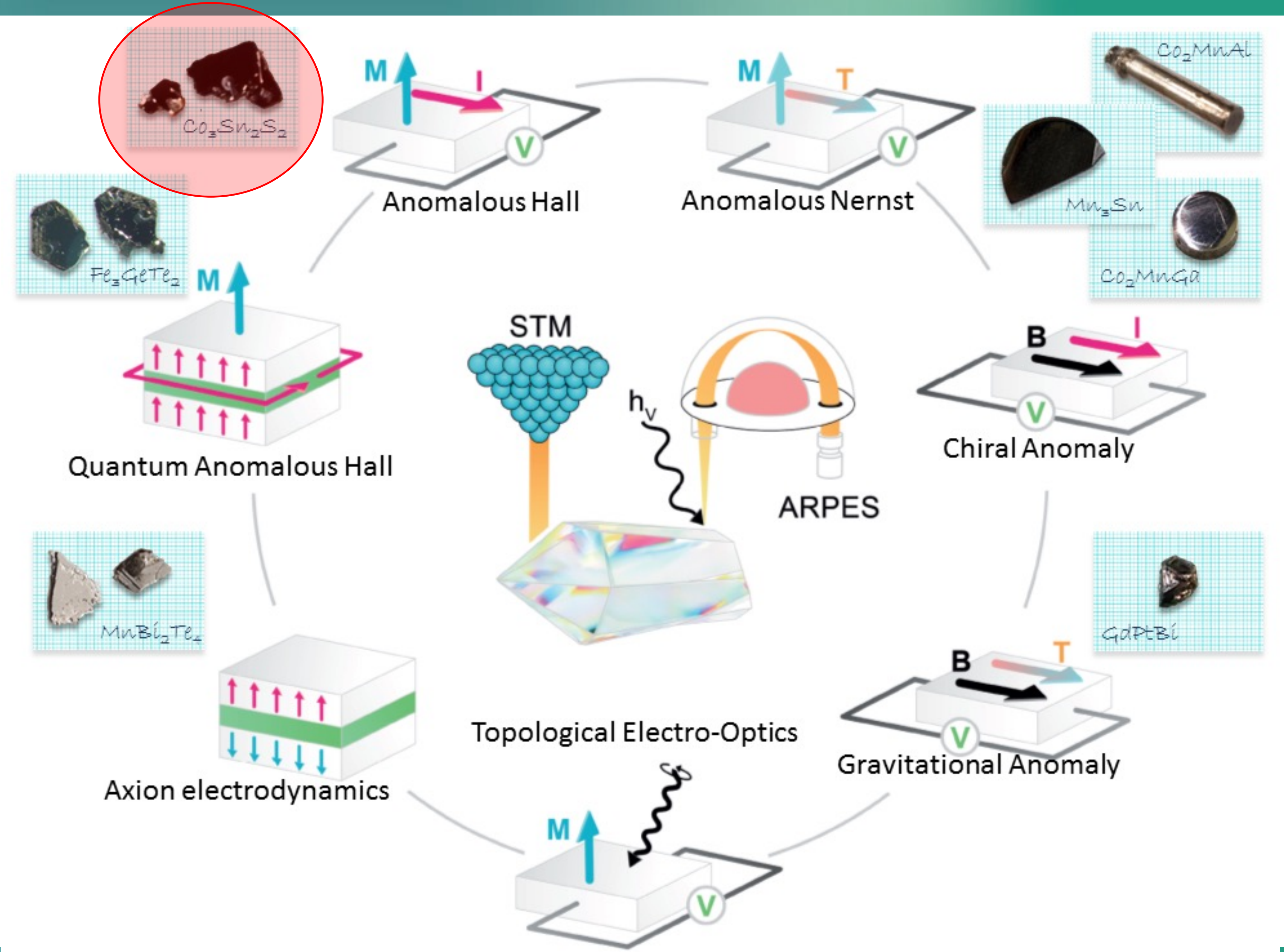
Co3Sn2S2
Fe3GeTe2
M
I
V
Anomalous Hall
T
Anomalous Nernst
Co2MnAl
Mn3Sn
Co2MnGa
Quantum Anomalous Hall
STM
hv
ARPES
B
Chiral Anomaly
MnBi2Te4
GdPtBi
Gravitational Anomaly
Axion electrodynamics
Topological Electro-Optics

Kagome lattice

Fe_2Sn_3

LETTER

doi:10.1038/nature25987

Massive Dirac fermions in a ferromagnetic kagome metal

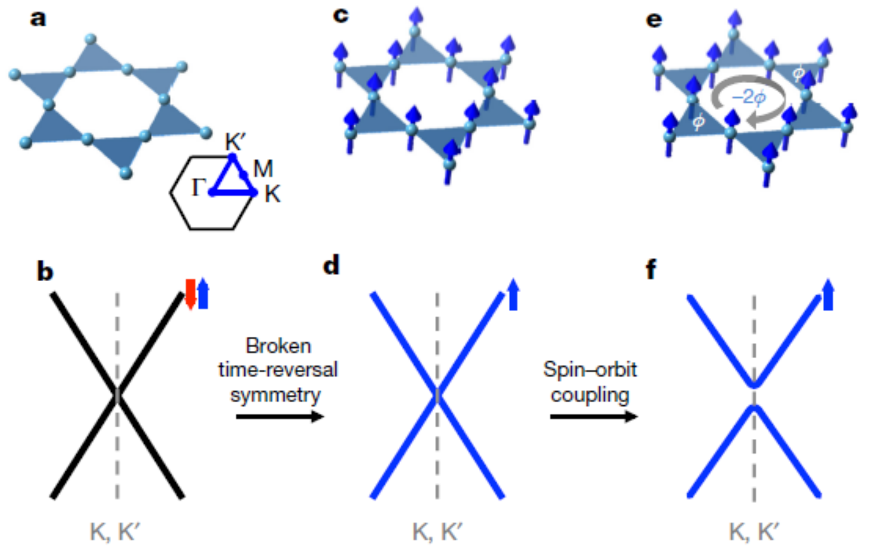

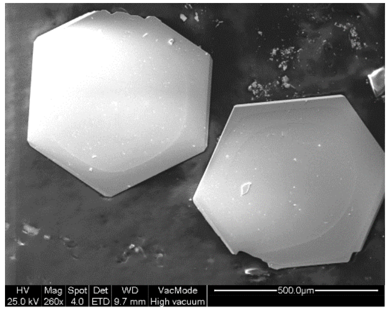

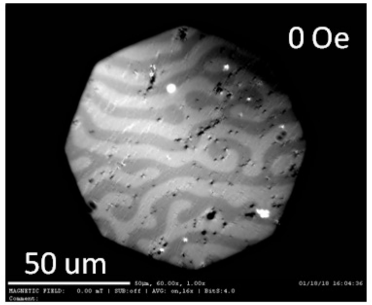

$Co_3Sn_2S_2$

Looking for Weyl fermions on a ferromagnetic Kagomé lattice with out of plane magnetisation.

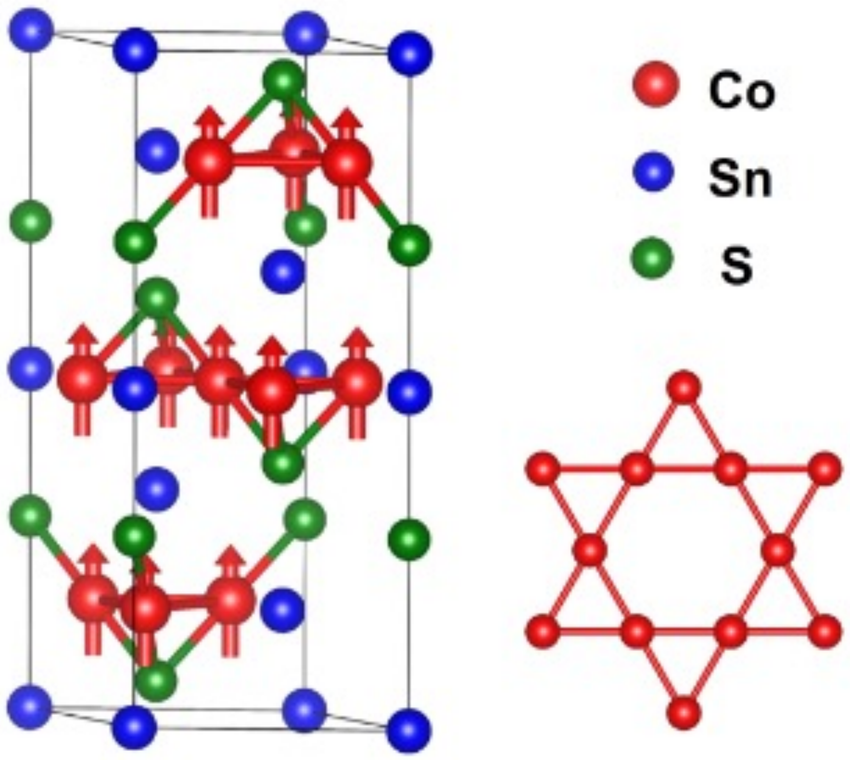

Nature, 2018, doi:10.1038/nature25987

Enke Liu, et al. Nature Physics 14 (2018) 1125 , preprint arXiv:1712.06722

Kagome lattice

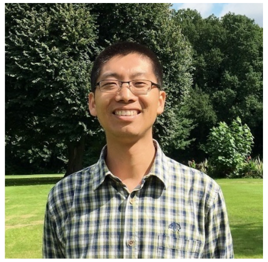

$Co_3Sn_2S_2$

half metallic

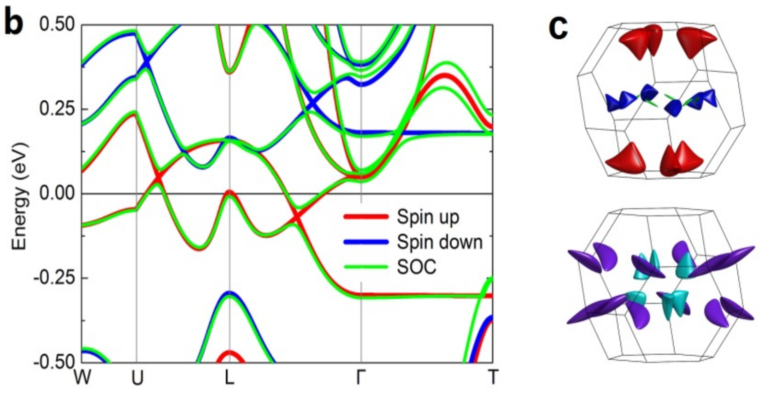

$Co_3Sn_2S_2$

chiral anomaly

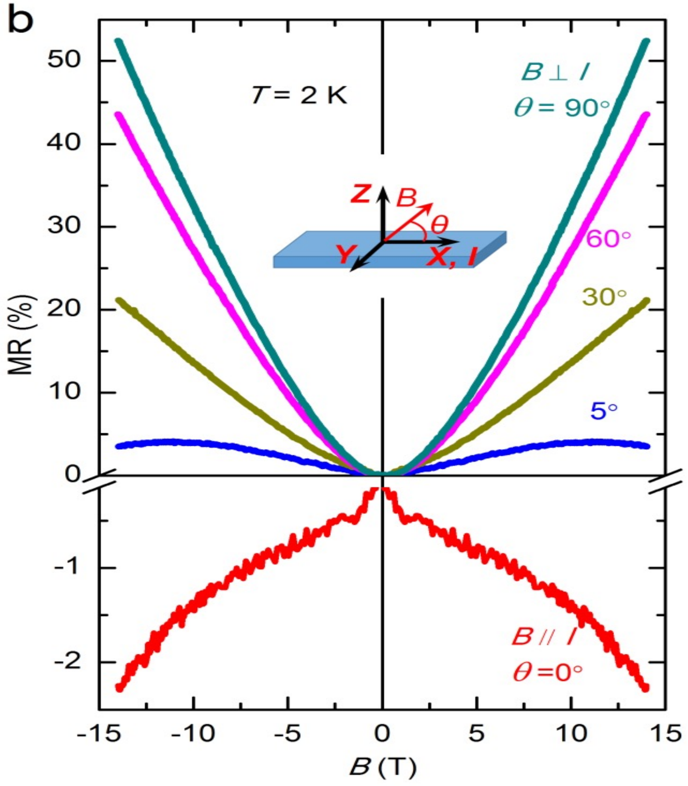

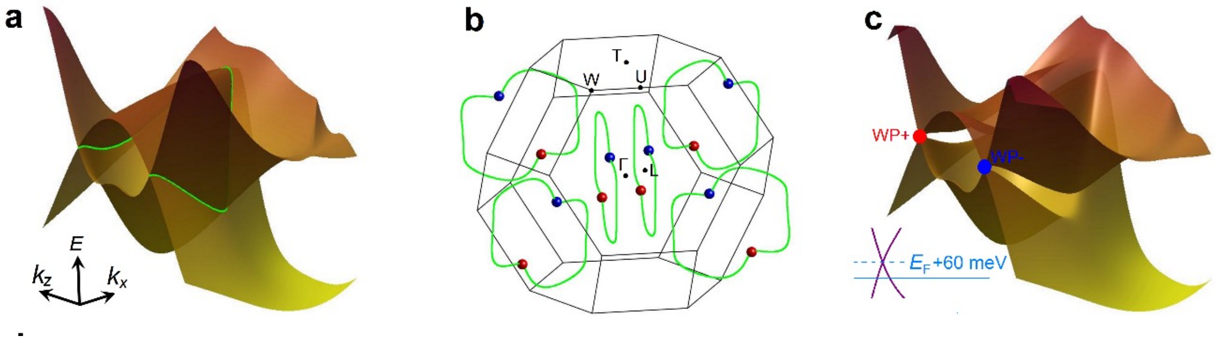

D. F. Liu, et al., Science 365 (2019) 1282

Liu, et al. Nature Physics 14 (2018) 1125 , preprint arXiv:1712.06722

Kagome lattice

$Co_3Sn_2S_2$

STM and ARPES confirms Weyl and Fermiarcs

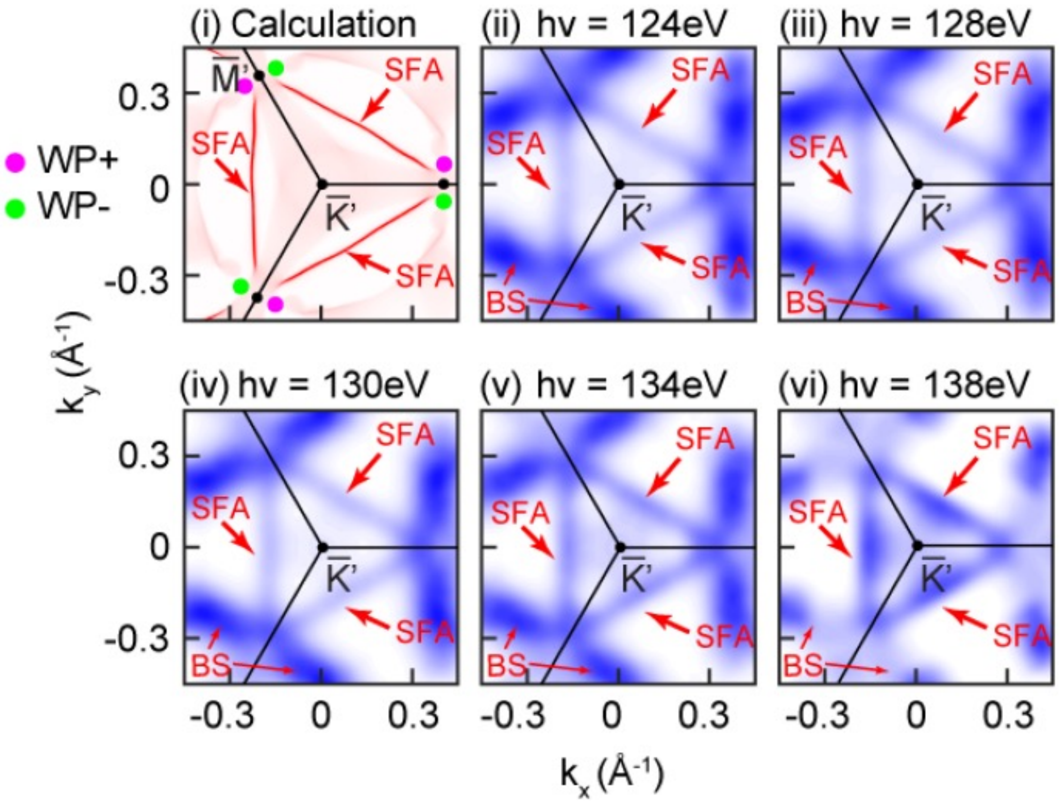

D. F. Liu, et al., Science 365 (2019) 1282

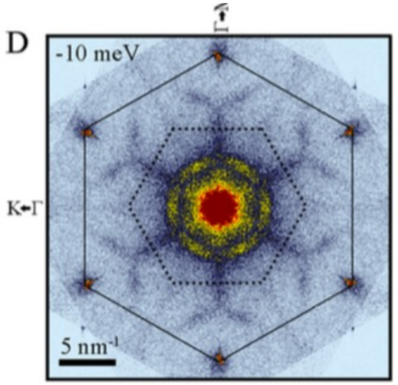

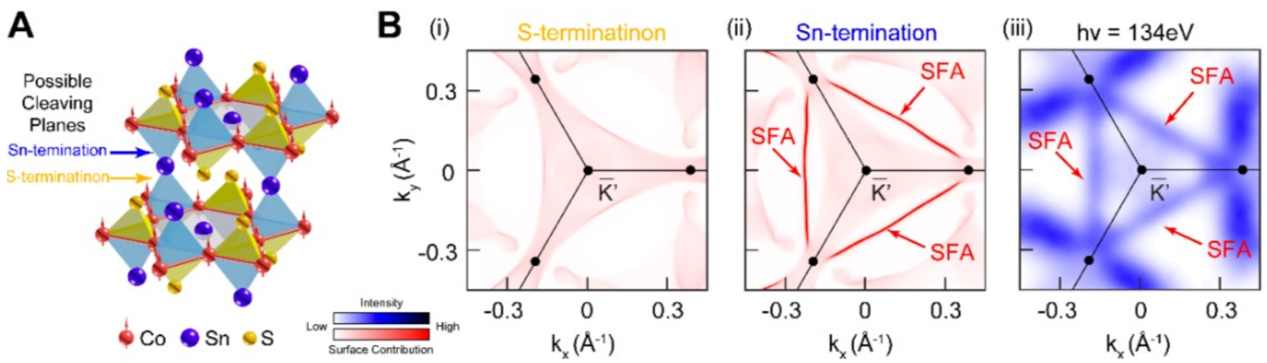

Morali et al., Science a365 (2019) 1286, preprint arXiv:1903.00509

Kagome lattice

$Co_3Sn_2S_2$

ARPES confirms Weyl and Fermiarcs

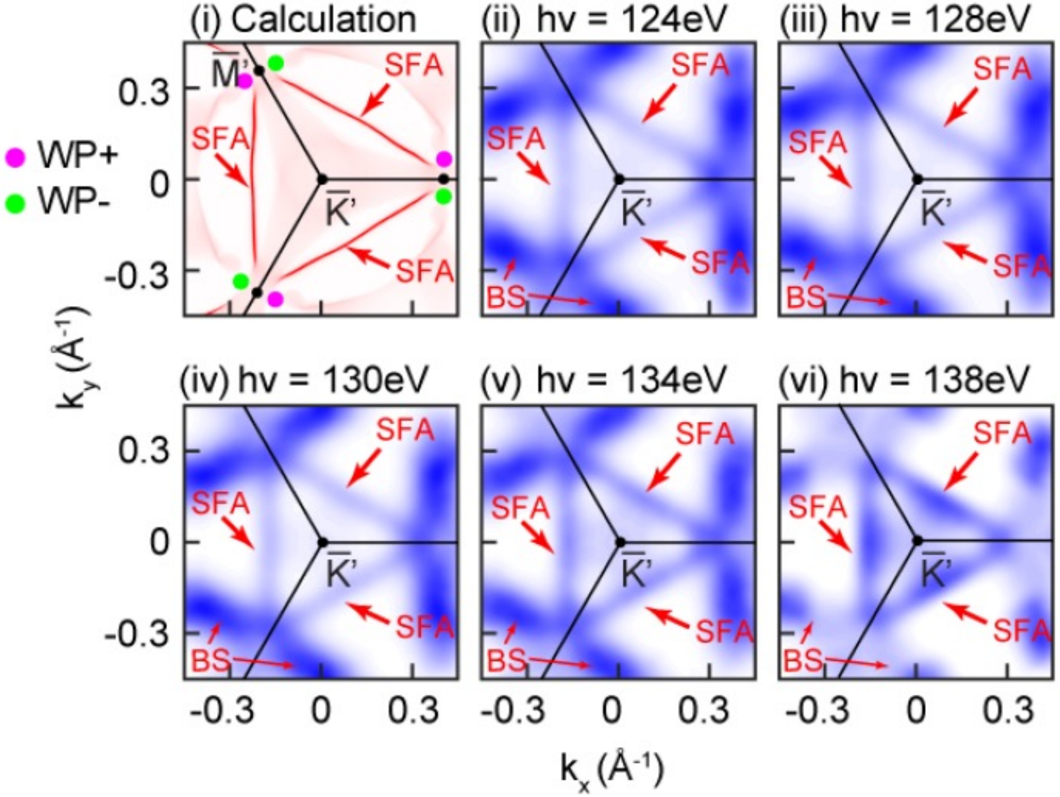

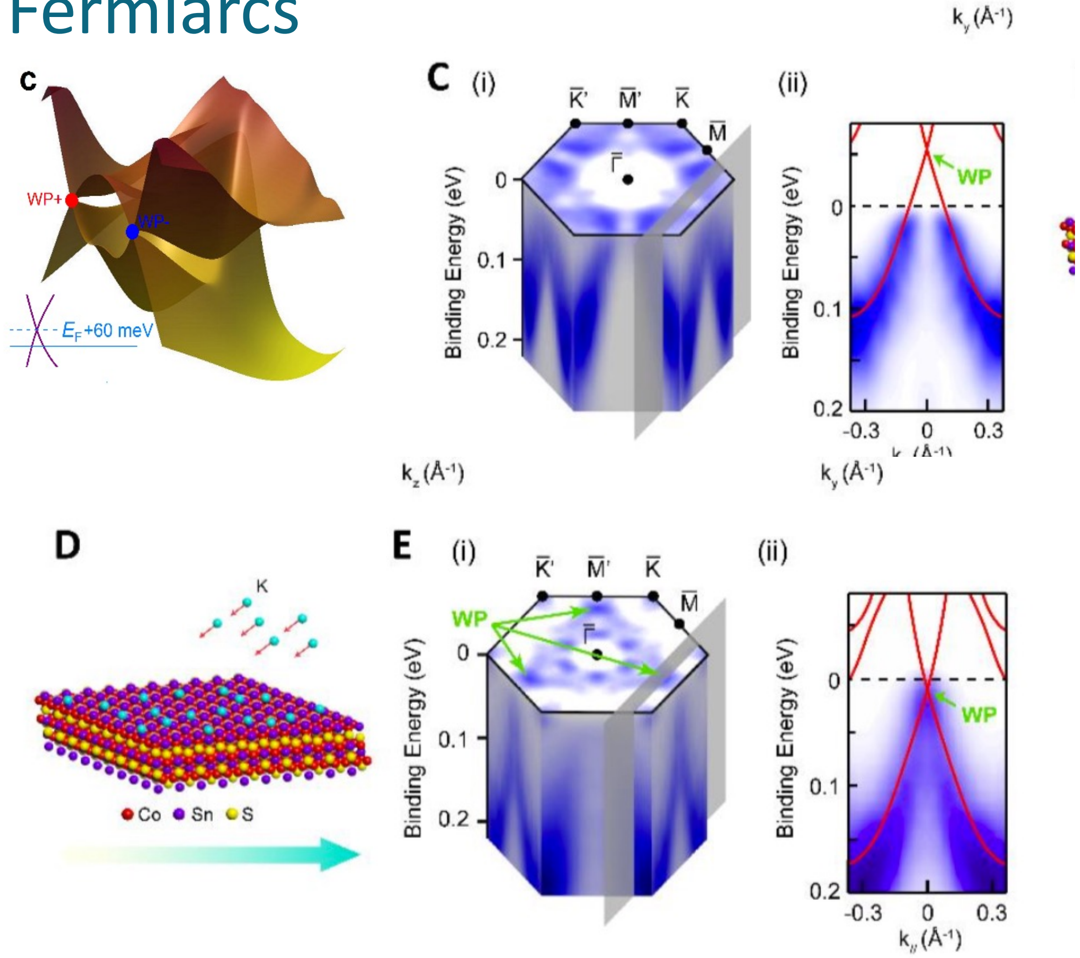

D. F. Liu, et al., Science 365 (2019) 1282

Giant anomalous Hall effect

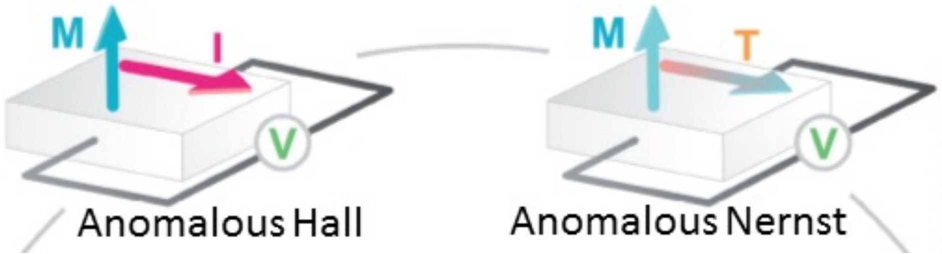

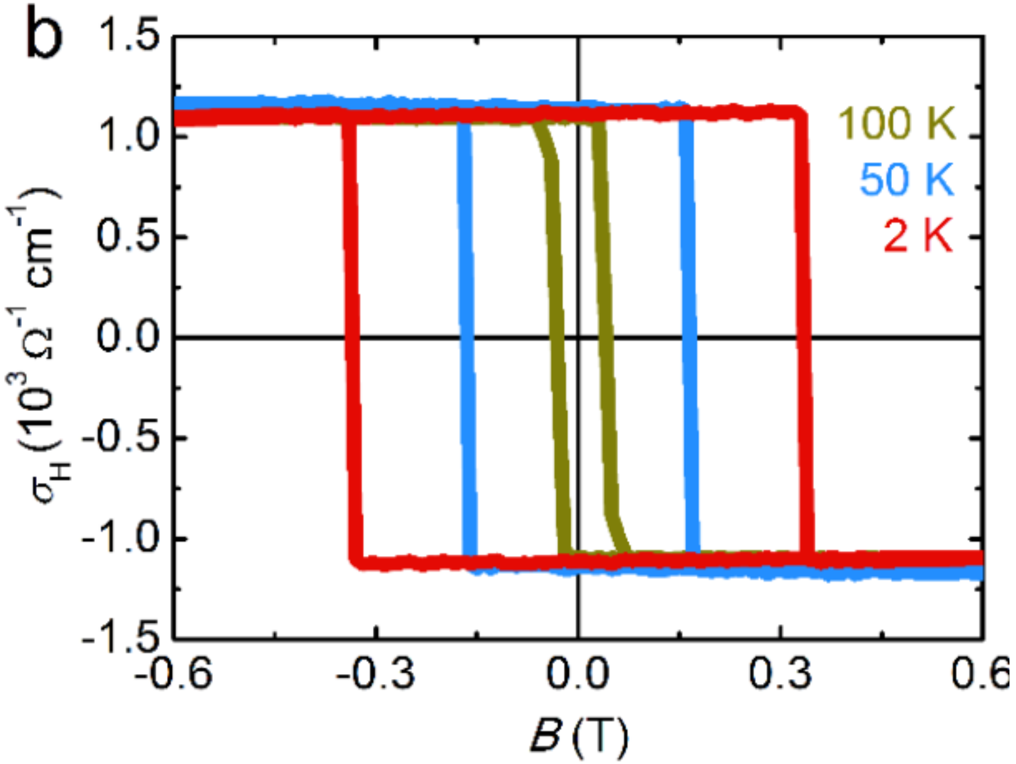

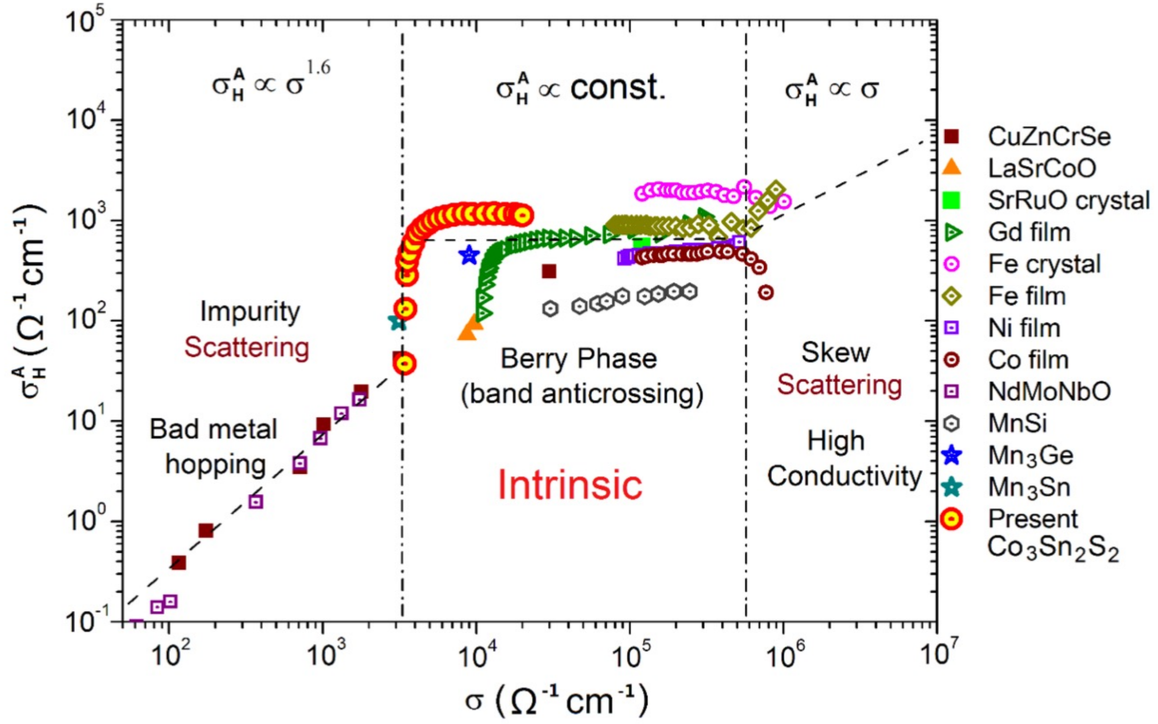

Naoto Nagaosa and Yoshinori Tokura 2012 Phys. Scr. 2012 014020

Liu, et al. Nature Physics 14 (2018) 1125 , Guin, et al. Adv. Mater. 2019, 1806622, arXiv:1712.06722, arXiv:1807.07843, arXiv:1806.06753

Giant anomalous Nernst effect

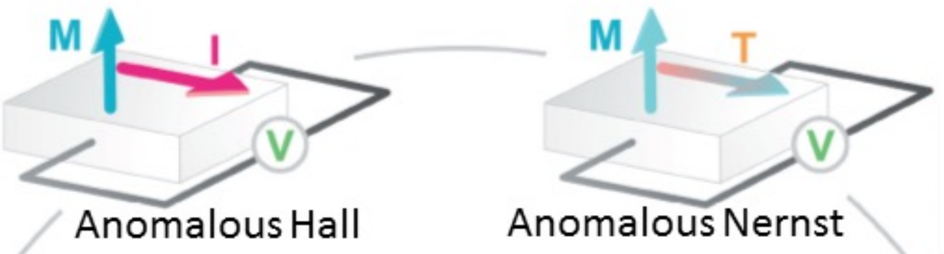

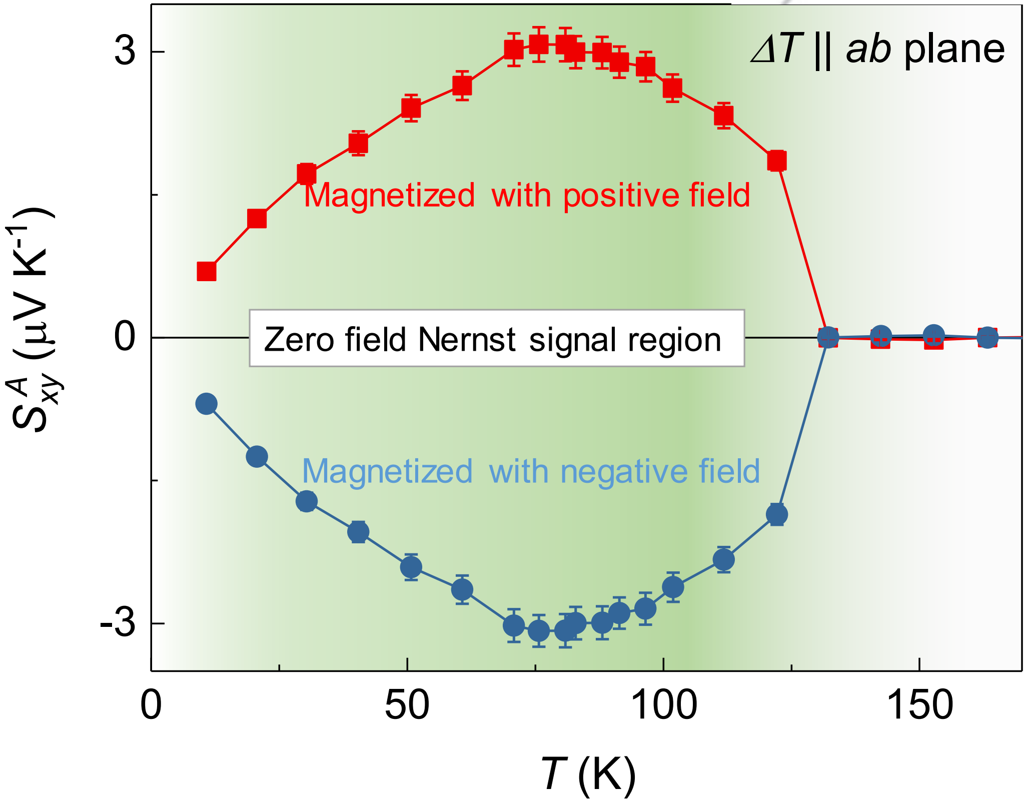

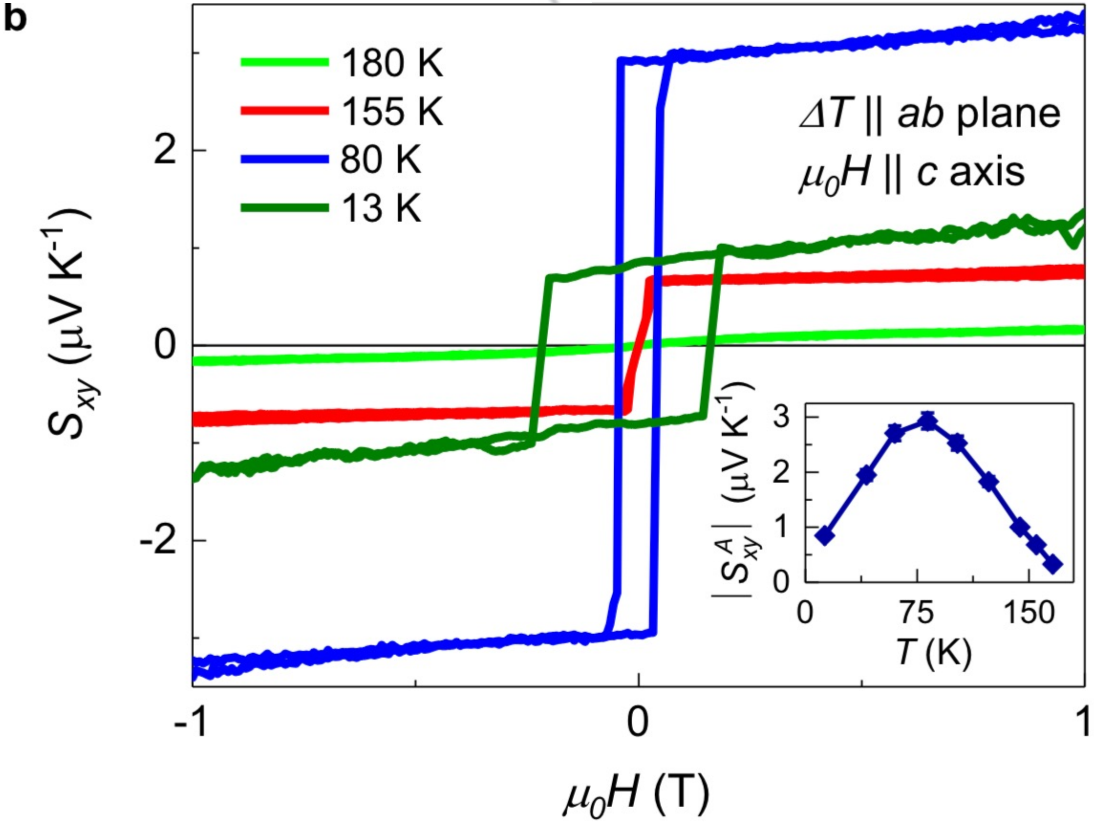

Guin, et al. Adv. Mater. 2019, 1806622, Liu, et al. Nature Physics 14 (2018) 1125 , arXiv:1712.06722, arXiv:1807.07843

Giant anomalous Nernst effect

magnetic Weyl semimetals as a recipe for large Nernst effects

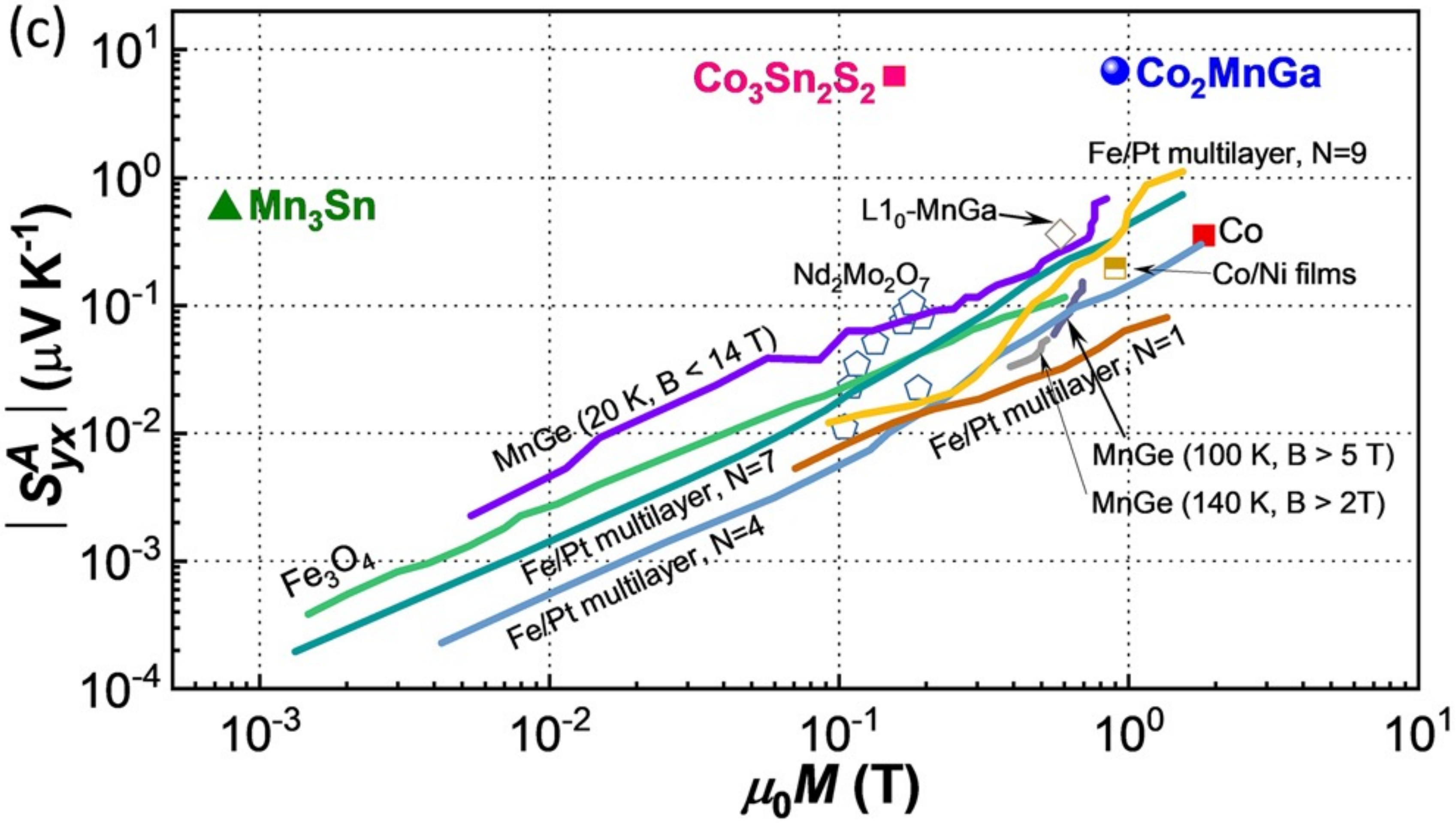

Guin, et al. Adv. Mater. 2019, 1806622, arXiv:1712.06722, arXiv:1807.07843, arXiv:1806.06753

from 3D to 2D quantum effects

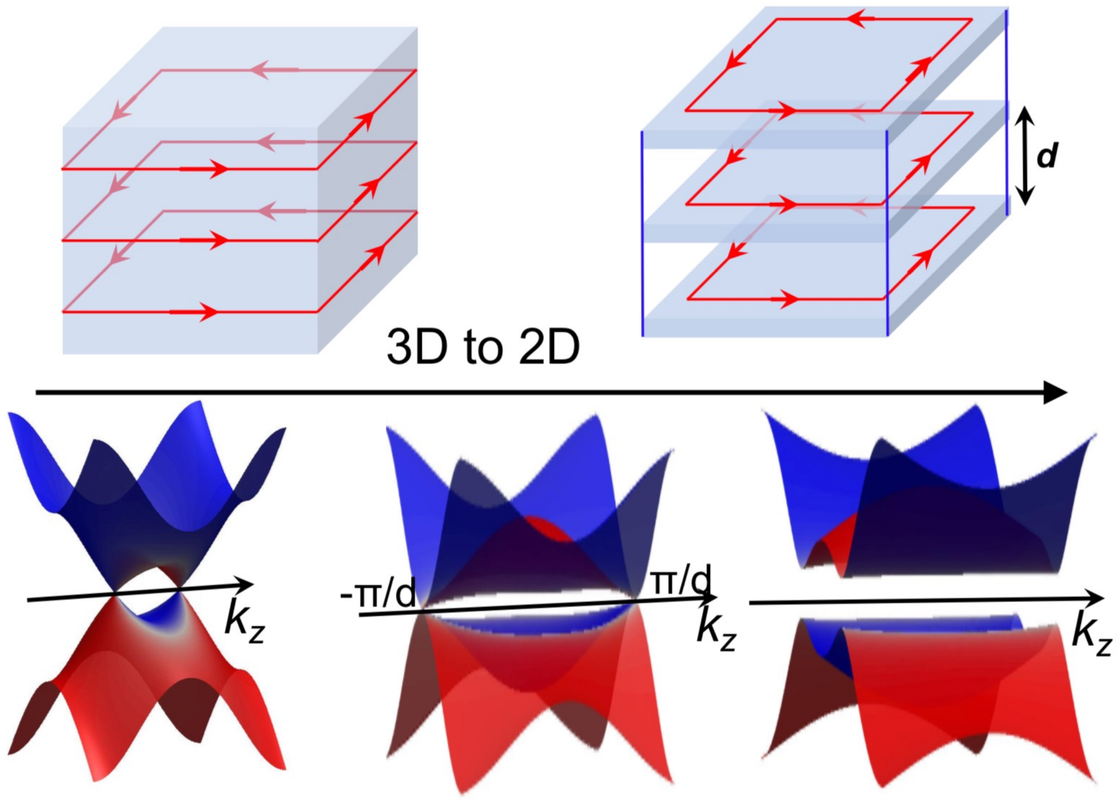

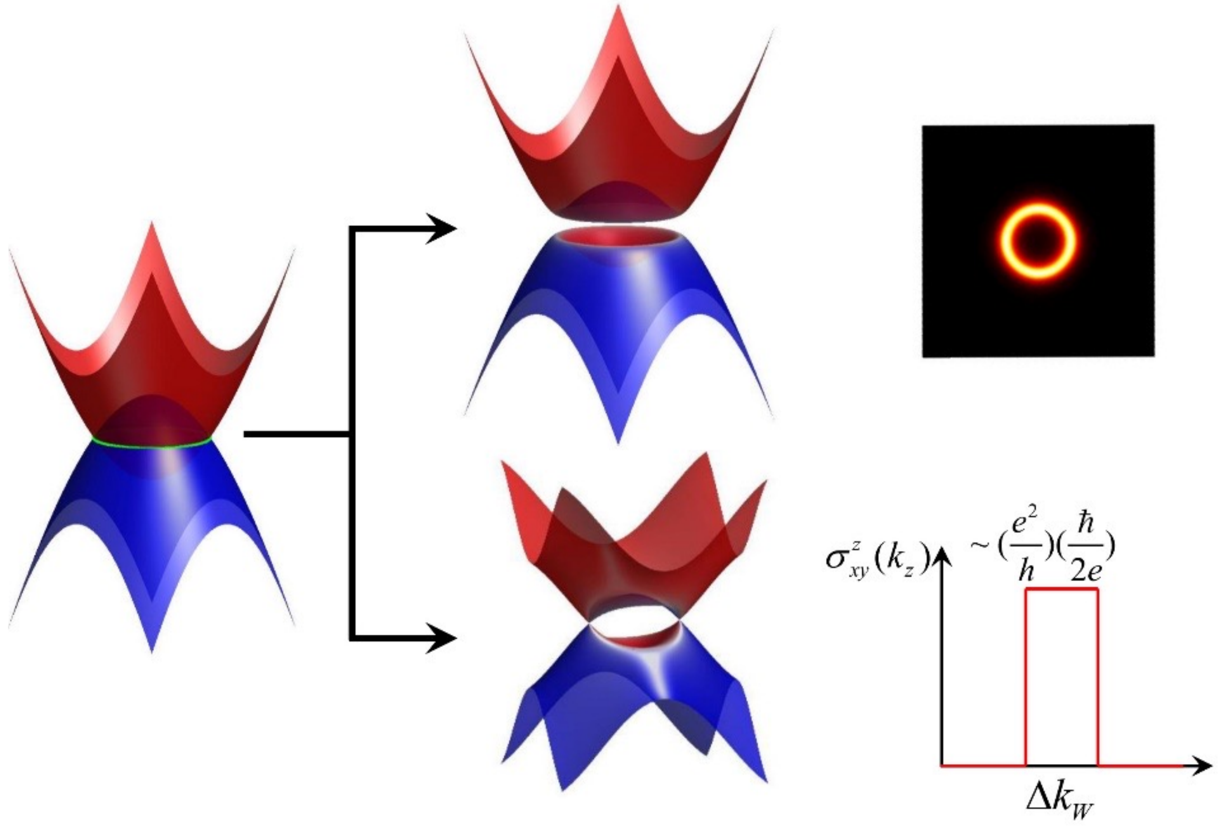

Satya N. Guin, et al. Chandra Shekhar, Andrea Damascelli, Yan Sun, and Claudia Felser, Advanced Materials DOI: 10.1002/adma.202006301

Quantum anomalous Hall effect?

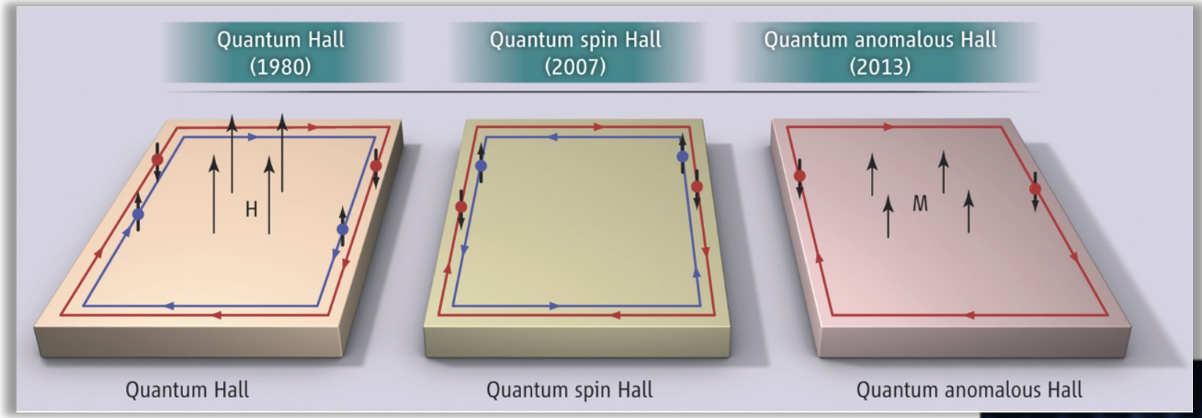

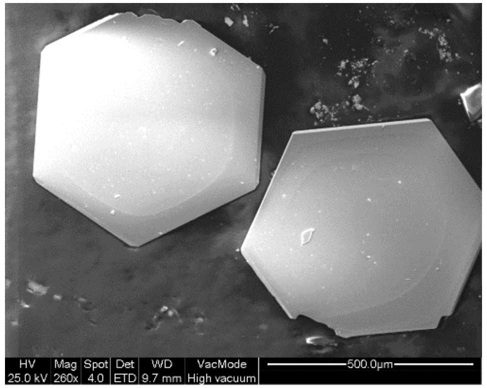

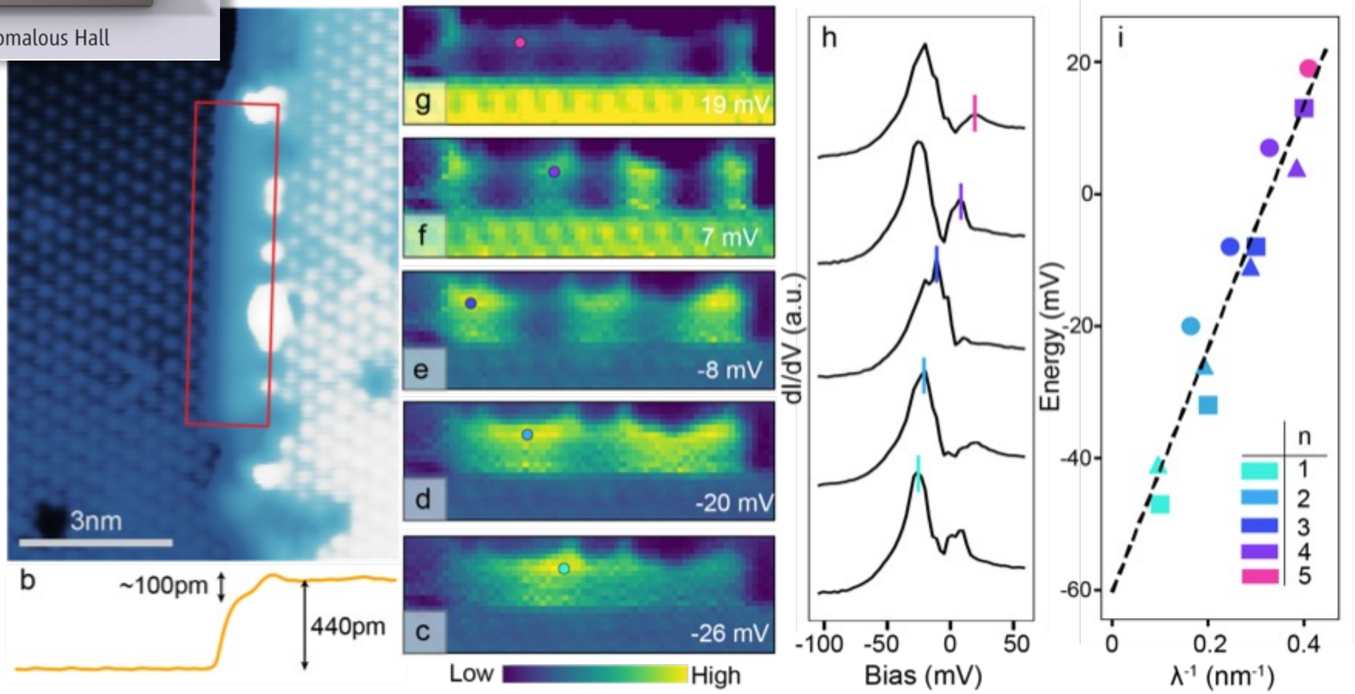

Sean Howard, Lin Jiao, Zhenyu Wang, Chandra Shekhar, CF, Taylor Hughes, Vidya Madhavan, preprint arXiv:1910.11205

Berry curvature design

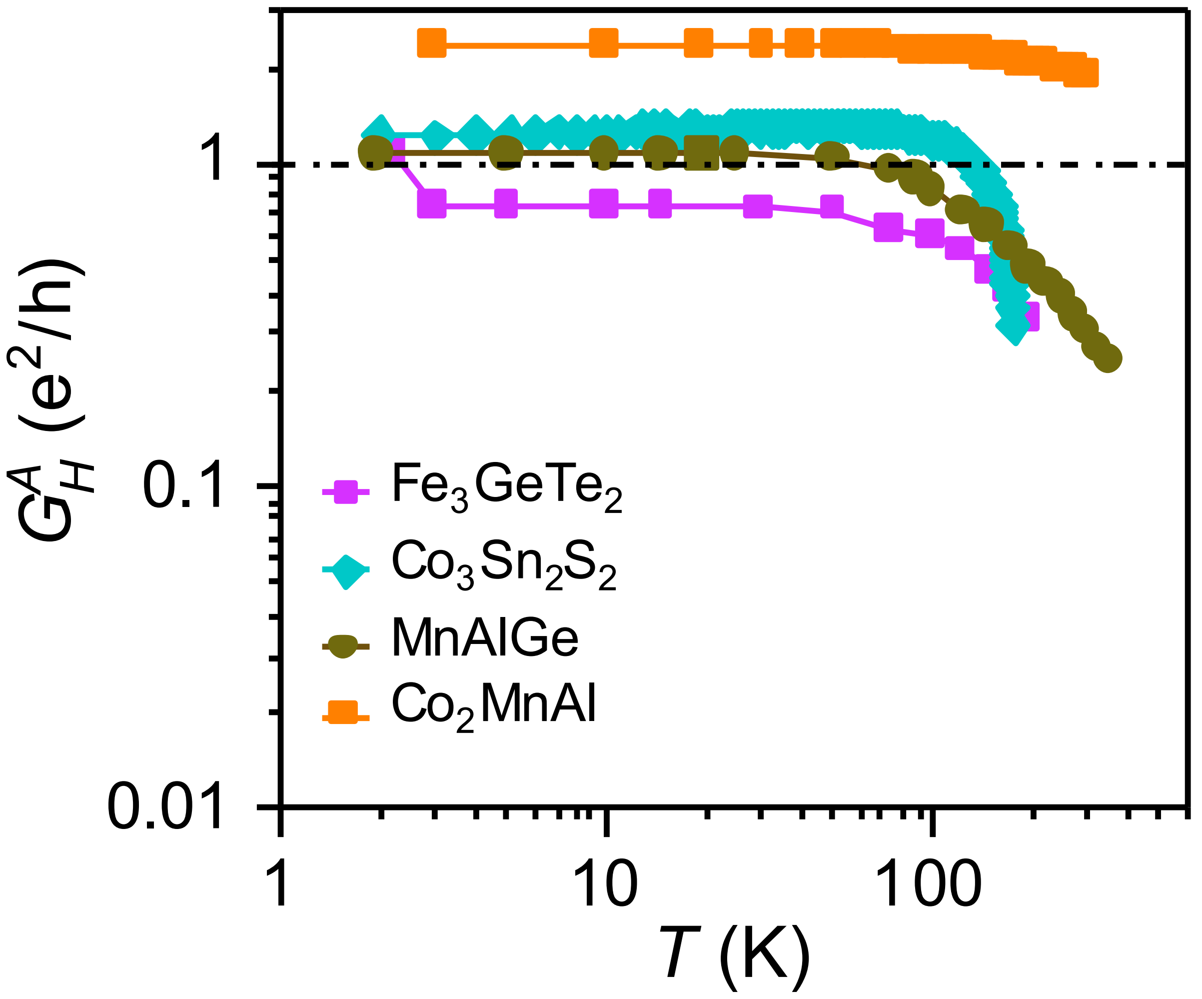

Qubit based on topology

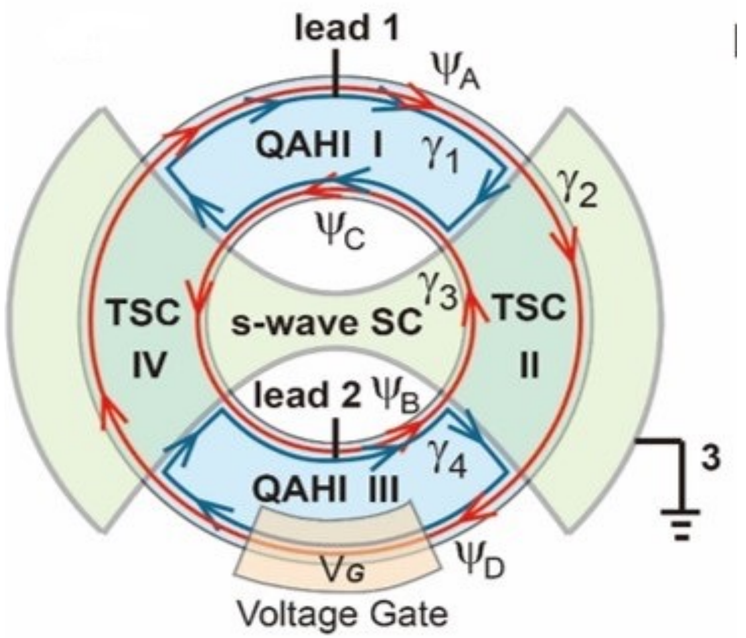

Lian, et al., PNAS 2018

Satya N. Guin, et al. Chandra Shekhar, Andrea Damascelli, Yan Sun, and Claudia Felser, Advanced Materials DOI: 10.1002/adma.202006301

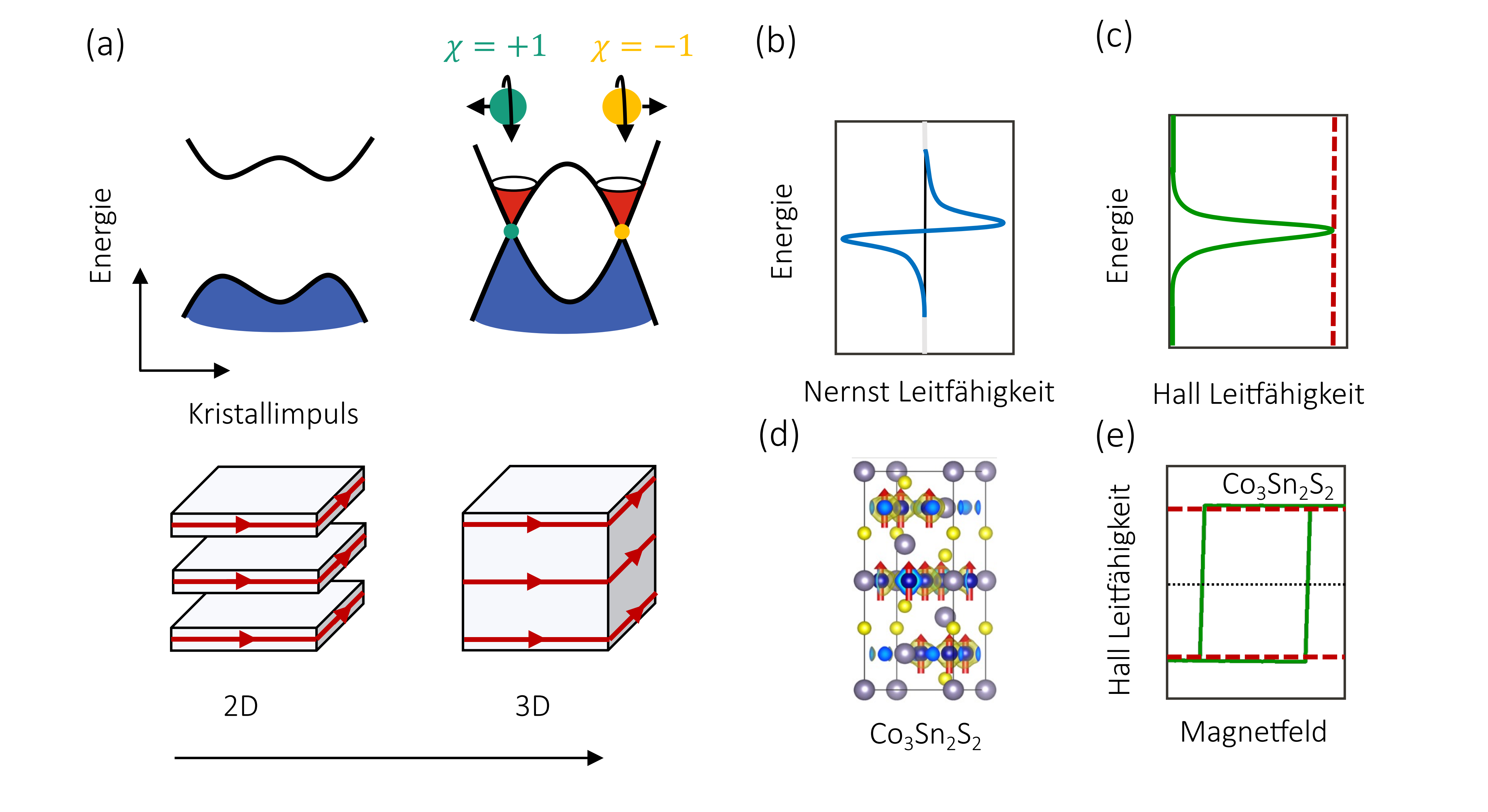
(a)
$\chi = +1$
$\chi = -1$
Energie
Kristallimpuls
2D
3D
(b)
Energie
Nernst Leitfähigkeit
(c)
Energie
Hall Leitfähigkeit
(d)
$Co_3Sn_2S_2$
(e)
$Co_3Sn_2S_2$
Hall Leitfähigkeit
Magnetfeld

antiferromagnetic topological materials

Table 3 | The magnetic topological materials identified in this work

Categories	Properties	Materials
I-A	Non-collinear manganese compounds	Mn_3GaC, Mn_3ZnC, Mn_3CuN, Mn_3Sn, Mn_3Ge, Mn_3Ir, Mn_3Pt, Mn_5Si_3
I-B	Actinide intermetallic	$UNiGa_5$, $UPtGa_5$, $NpRhGa_5$, $NpNiGa_5$
I-C	Rare-earth intermetallic	$NdCo_2$, $TbCo_2$, $NpCo_2$, PrAg DyCu, NdZn, TbMg, NdMg, Nd_5Si_4, Nd_5Ge_4, Ho_2RhIn_8, Er_2CoGa_8, Nd_2RhIn_8, Tm_2CoGa_8, Ho_2RhIn_8, $DyCo_2Ga_8$, $TbCo_2Ga_8$, Er_2Ni_2In, $CeRu_2Al_{10}$, $Nd_3Ru_4Al_{12}$, $Pr_3Ru_4Al_{12}$, $ScMn_6Ge_6$, YFe_4Ge_4, $LuFe_4Ge_4$, $CeCoGe_3$
II-A	Metallic iron pnictides	LaFeAsO, $CaFe_2As_2$, $EuFe_2As_2$, $BaFe_2As_2$, Fe_2As, $CaFe_4As_3$, LaCrAsO, Cr_2As, CrAs, CrN
II-B	Semiconducting manganese pnictides	$BaMn_2As_2$ $BaMn_2Bi_2$, $CaMnBi_2$, $SrMnBi_2$, $CaMn_2Sb_2$, CuMnAs, CuMnSb, Mn_2As
II-C	Rare-earth intermetallic compounds with the composition 1:2:2	$PrNi_2Si_2$, $YbCo_2Si_2$, $DyCo_2Si_2$, $PrCo_2P_2$, $CeCo_2P_2$, $NdCo_2P_2$, $DyCu_2Si_2$, $CeRh_2Si_2$, UAu_2Si_2, U_2Pd_2Sn, U_2Pd_2In, U_2Ni_2Sn, U_2Ni_2In, U_2Rh_2Sn
II-D	Rare-earth ternary compounds of the composition 1:1:1	CeMgPb, PrMgPb, NdMgPb, TmMgPb
III-A	Semiconducting actinides/ rare-earth pnictides	HoP, UP, UP_2, UAs, NpS, NpSe, NpTe, NpSb, NpBi, U_3As_4, U_3P_4
III-B	Metallic oxides	Ag_2NiO_2, $AgNiO_2$, $Ca_3Ru_2O_7$, Double perovskite Sr_3CoIrO_6
III-C	Metal-to-insulator transition compounds	NiS_2, $Sr_2Mn_3As_2O_2$
III-D	Semiconducting and insulating oxides, borates, hydroxides, silicates and phosphate	$LuFeO_3$, $PdNiO_3$, $ErVO_3$, $DyVO_3$, $MnGeO_3$, $Tm_2Mn_2O_7$, $Yb_2Sn_2O_7$, $Tb_2Sn_2O_7$, $Ho_2Ru_2O_7$, $Er_2Ti_2O_7$, $Tb_2Ti_2O_7$, $Cd_2Os_2O_7$, $Ho_2Ru_2O_7$, Cr_2ReO6, $NiCr_2O_4$, MnV_2O_4, Co_2SiO_4, Fe_2SiO_4, $PrFe_3(BO_3)_4$, $KCo_4(PO_4)_3$, $CoPS_3$, $SrMn(VO_4)(OH)$, $Ba_5Co_5ClO_{13}$, FeI_2

Y Xu, et al., Nature 586 (2020) 702

canting and anomalous Hall

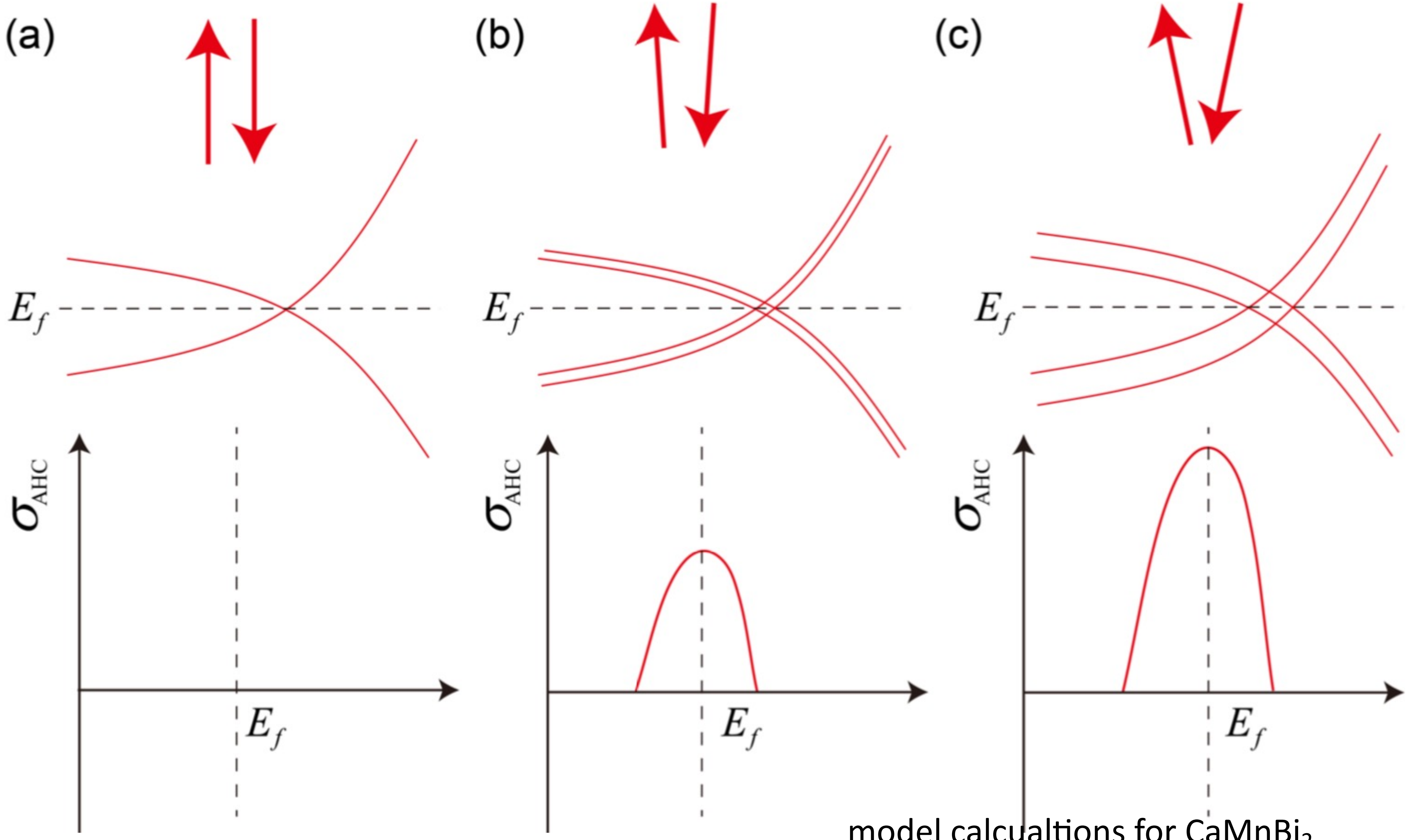

model calcualtions for $CaMnBi_2$

Congcong Le, Claudia Felser, and Yan Sun, Phys. Rev. B 104, 125145

non-collinear antiferromagnet $YbMnBi_2$

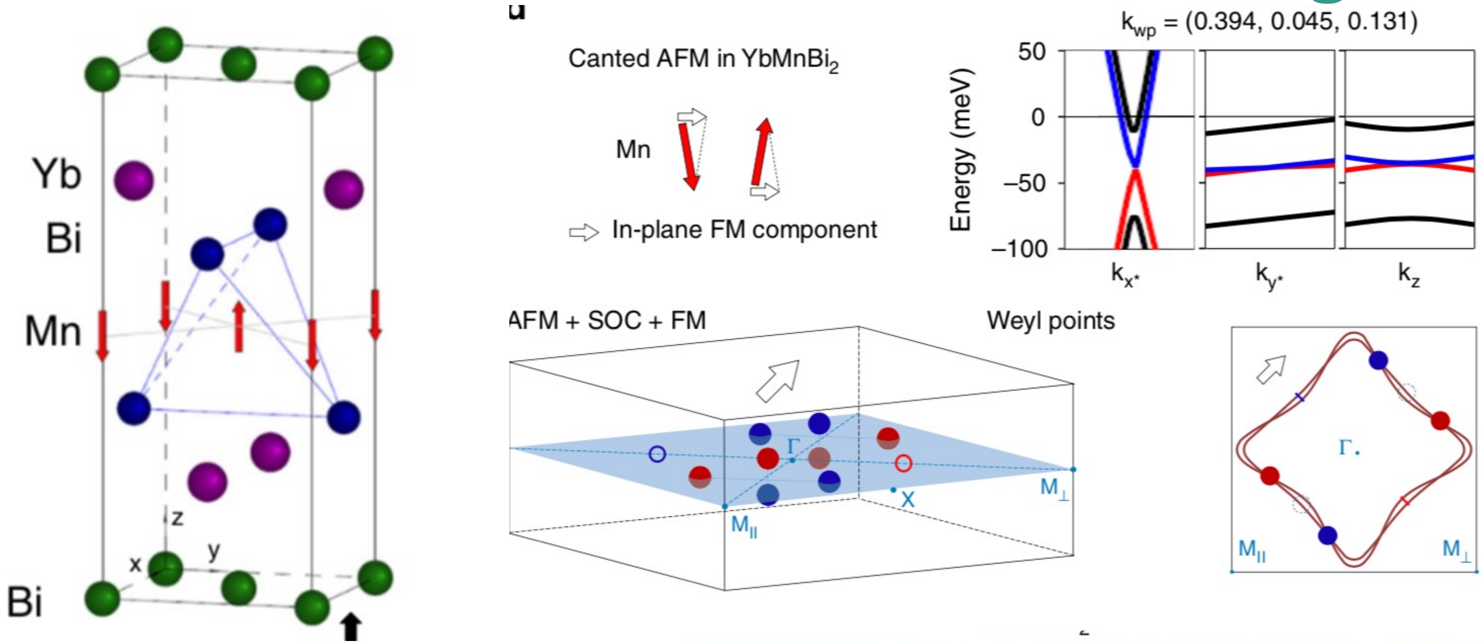

magnetic ordering below 290K
canted Mn atoms

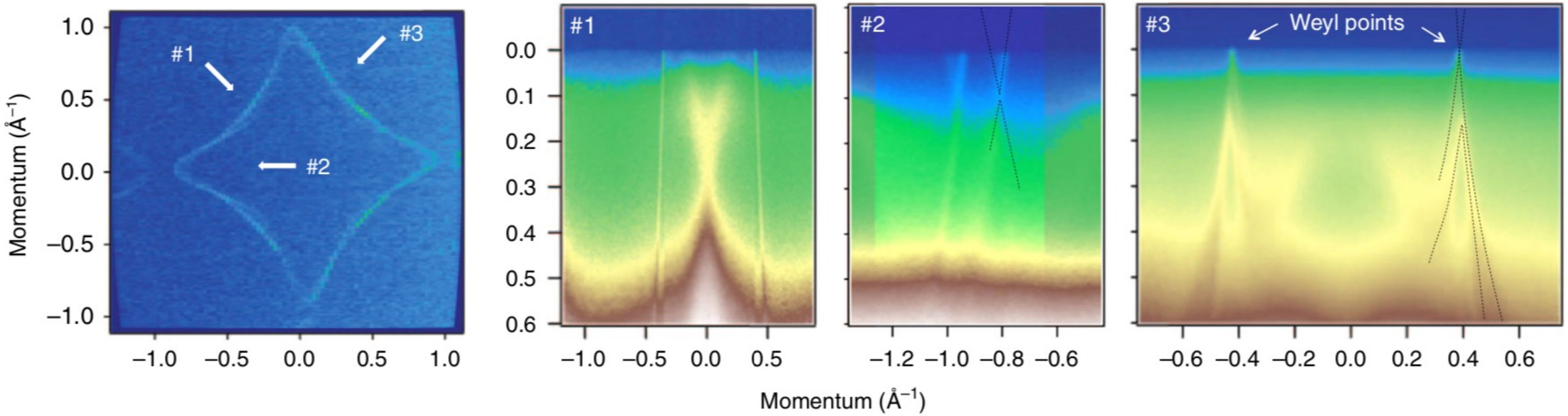

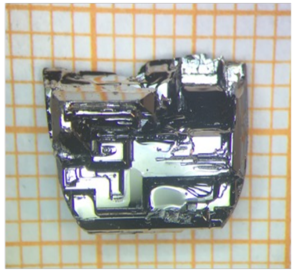

Sergey Borisenkoet al., Nature Communications 10 (2019) 3424

non-collinear antiferromagnet $YbMnBi_2$

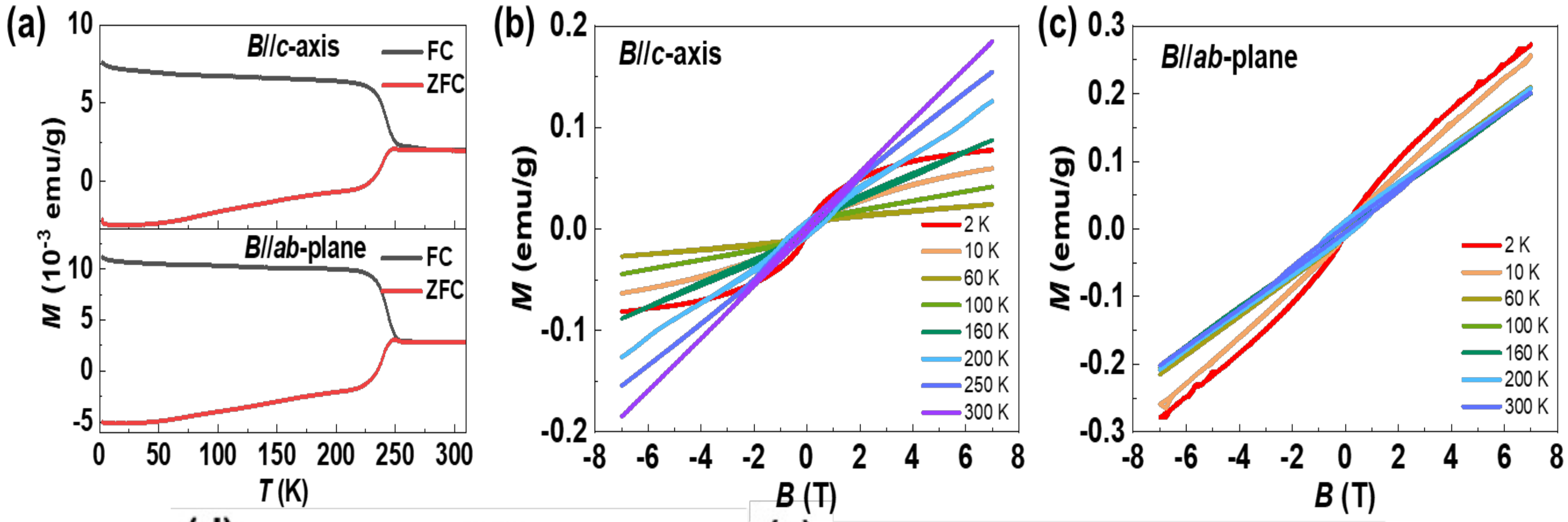

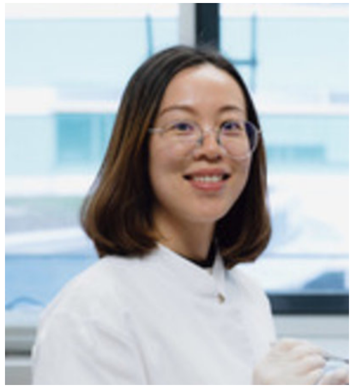

evidence for a small moment 0.0015 μ_B per Mn

nodal line

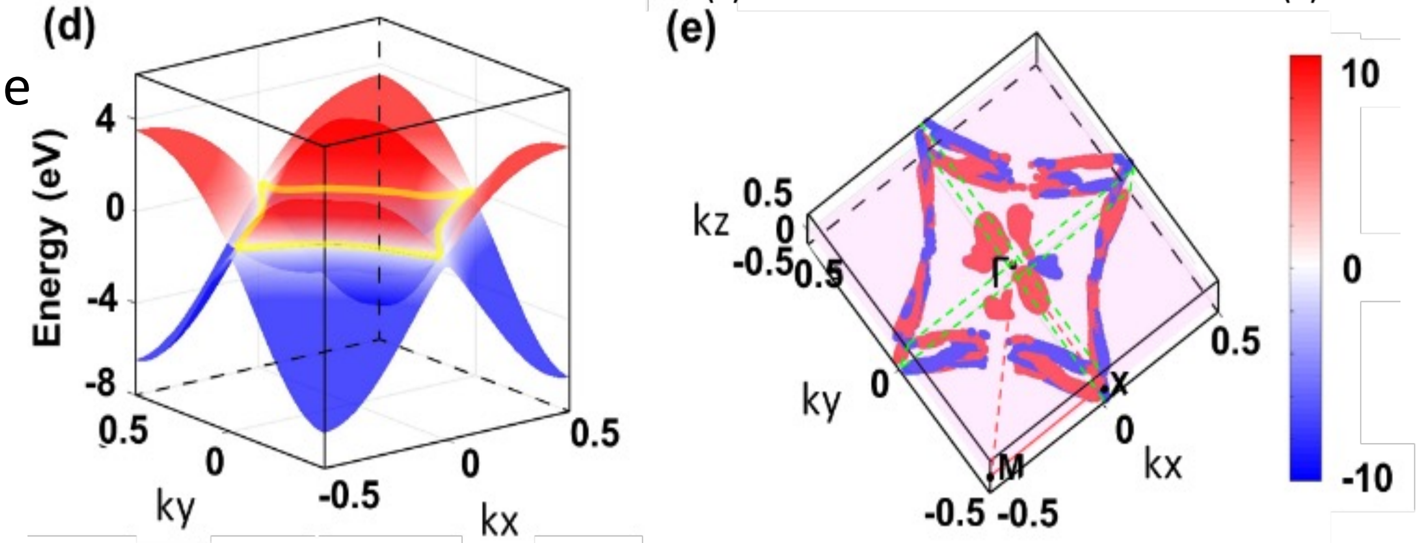

Berry curvature

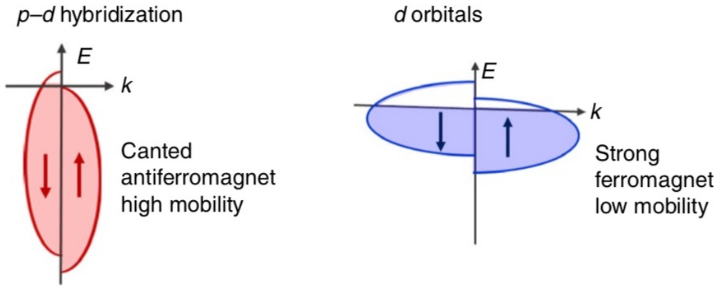

μ_m = 3.48 ×10 cm V s

Pan et al., Nature Materials **21**, 203–209 (2022), JP Heremans, S Watzman, N Trivedi, T Mccormick, C Felser, US Patent App. 16/157,522

non-collinear antiferromagnet $YbMnBi_2$

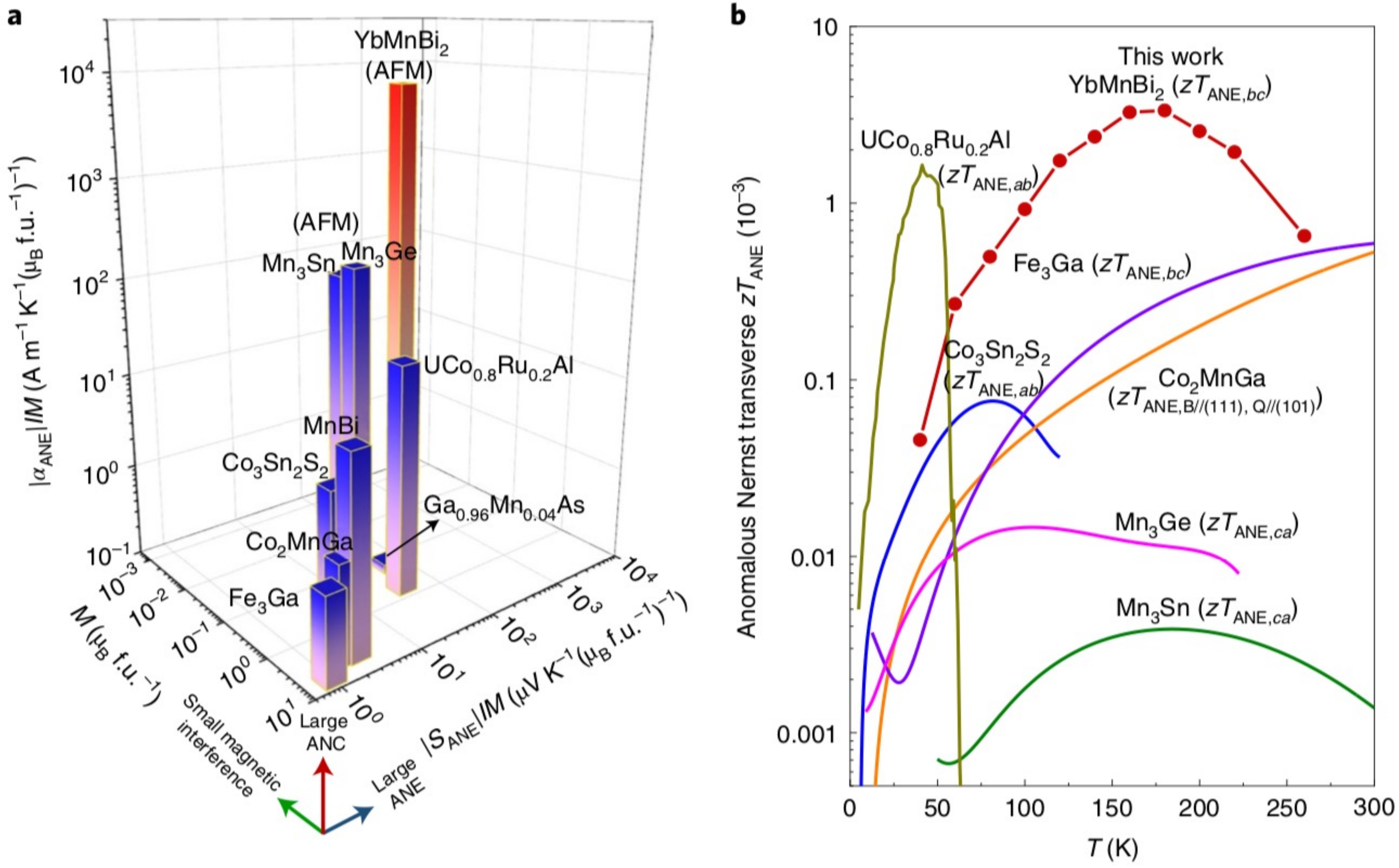

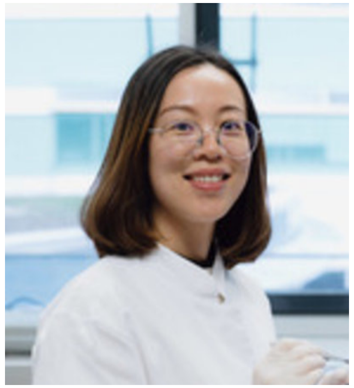

Pan et al., Nature Materials 21, 203–209 (2022), JP Heremans, S Watzman, N Trivedi, T Mccormick, C Felser, US Patent App. 16/157,522

chirality

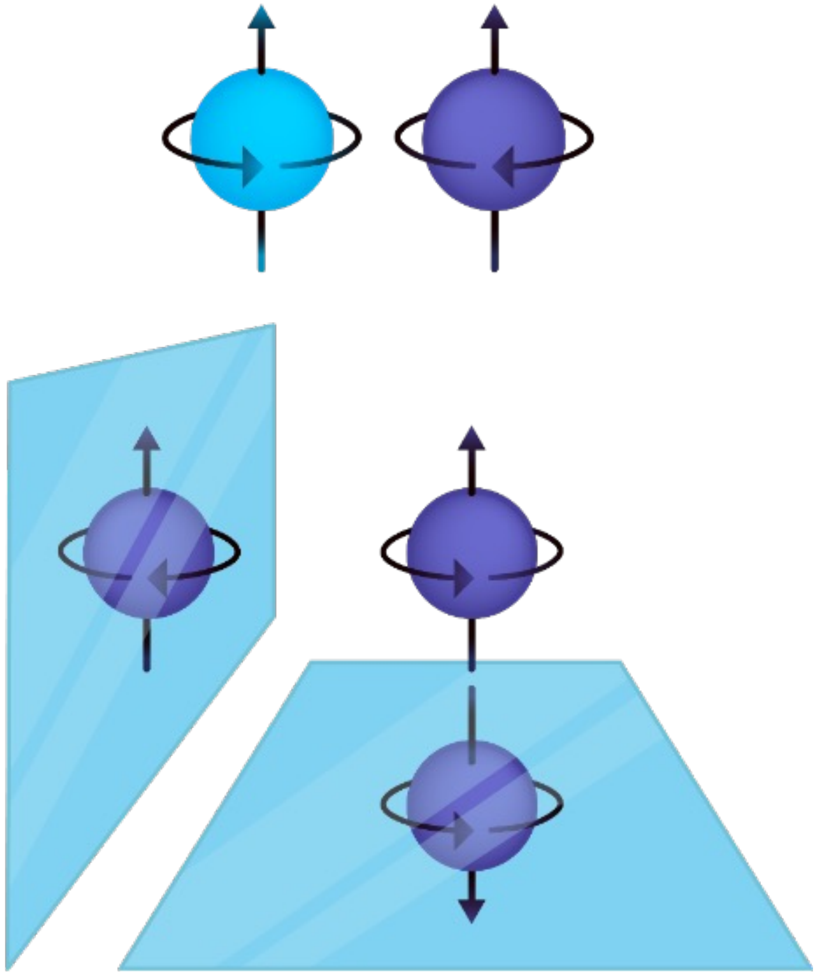

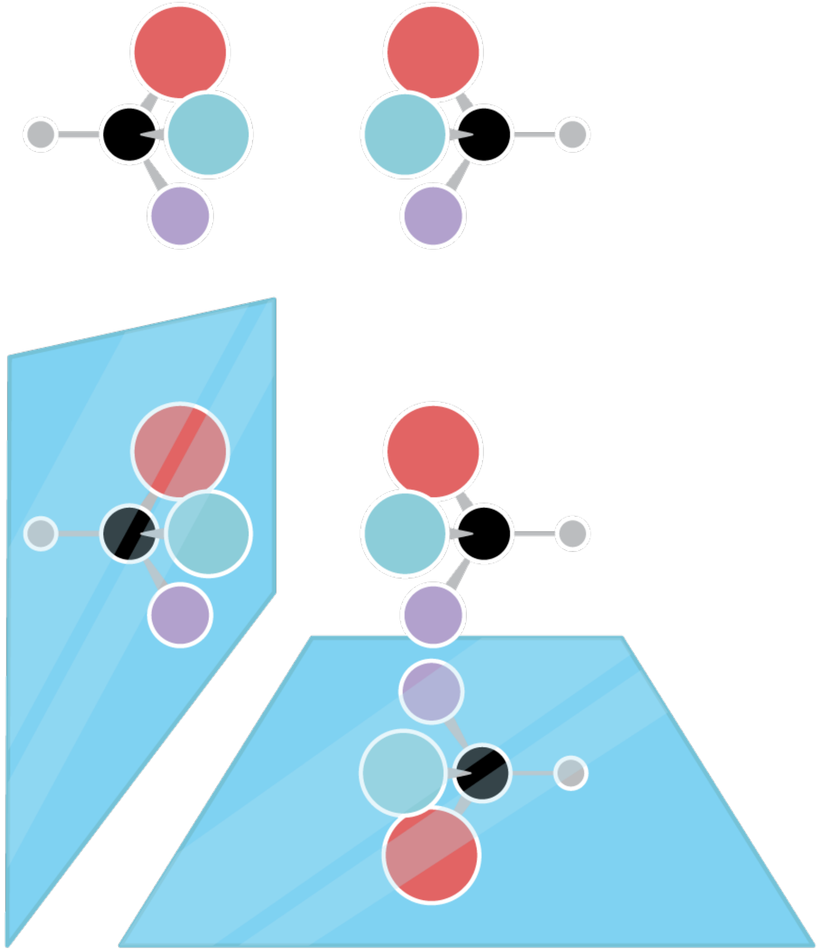

new fermions

RESEARCH

RESEARCH ARTICLE SUMMARY

TOPOLOGICAL MATTER

Beyond Dirac and Weyl fermions: Unconventional quasiparticles in conventional crystals

Barry Bradlyn,* Jennifer Cano,* Zhijun Wang,* M. G. Vergniory, C. Felser, R. J. Cava, B. Andrei Bernevig†

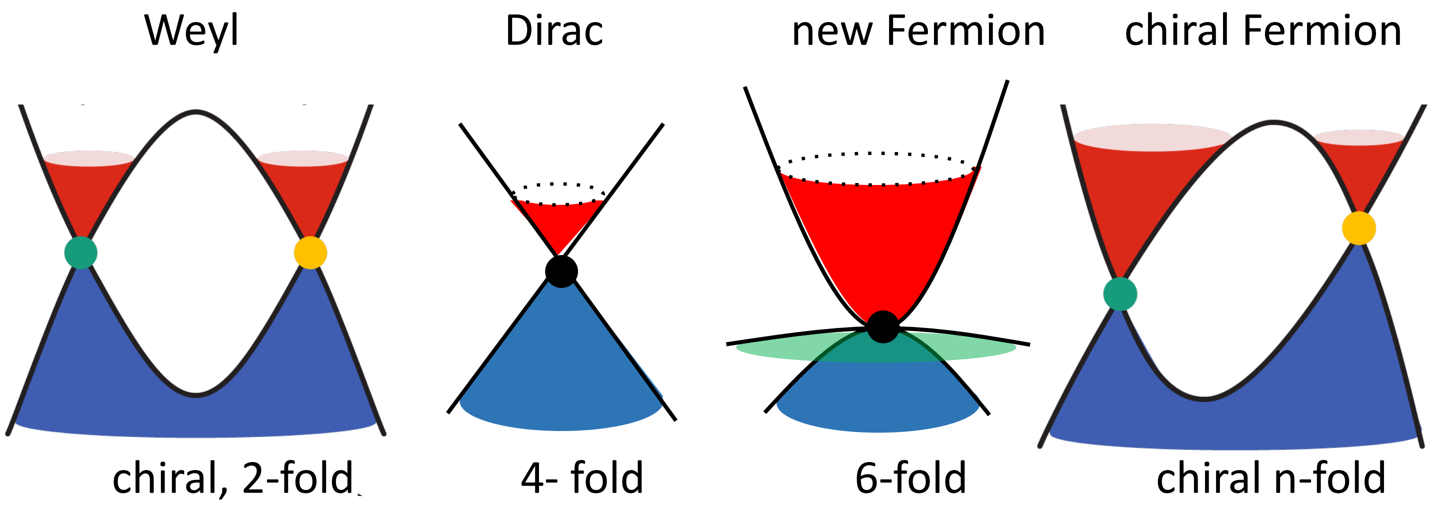

free fermionic excitations in solid-state systems that have
no high-energy counterparts.
Some of these new Fermions are even chiral

- Chiral Crystals
  B20, Skyrmions, CoSi, MnSi, PdGa, RhSi
- Superconductors
  A15 superconductors: Nb_3Sn, Li_2Pd_3B

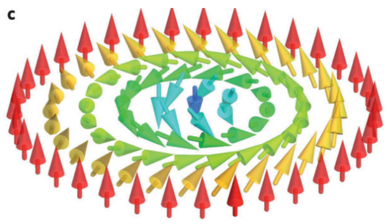

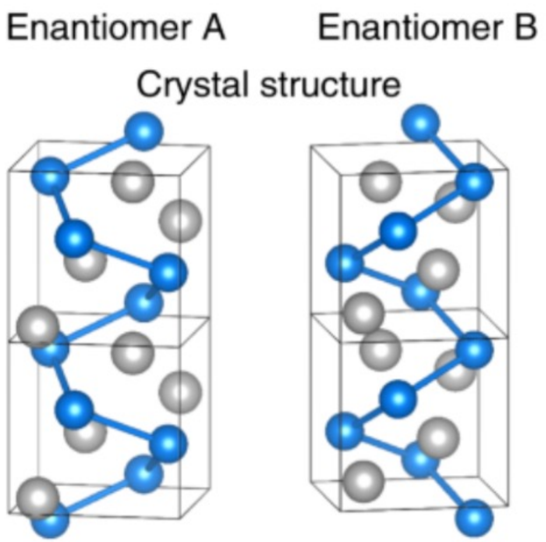

Bradlyn *et al.* Science **353**, (2016) 6299

chiral fermions

E SUMMARY

TOPOLOGICAL MATTER

Beyond Dirac and Weyl fermions: Unconventional quasiparticles in conventional crystals

Barry Bradlyn,* Jennifer Cano,* Zhijun Wang,* M. G. Vergniory, C. Felser, R. J. Cava, B. Andrei Bernevig†

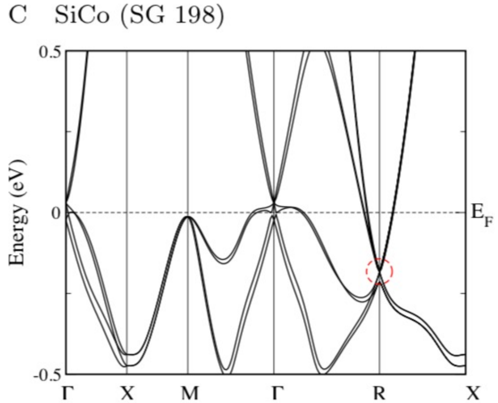

CoSi

chiral Fermion

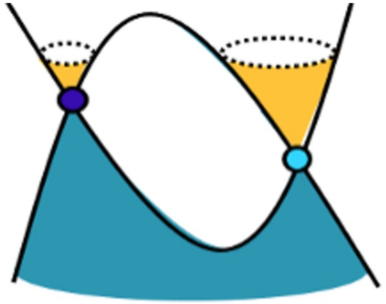

chiral n-fold

Bradlyn *et al.* Science **353**, (2016) 6299

ARTICLES
https://doi.org/10.1038/s41563-018-0169-3

Topological quantum properties of chiral crystals

Guoqing Chang[1,2,3,4,12], Benjamin J. Wieder[5,6,7,12], Frank Schindler[8,12], Daniel S. Sanchez[1], Ilya Belopolski[1], Shin-Ming Huang[9], Bahadur Singh[2,3], Di Wu[2,3], Tay-Rong Chang[10], Titus Neupert[8], Su-Yang Xu[1]*, Hsin Lin[2,3,4]* and M. Zahid Hasan[1,11]*

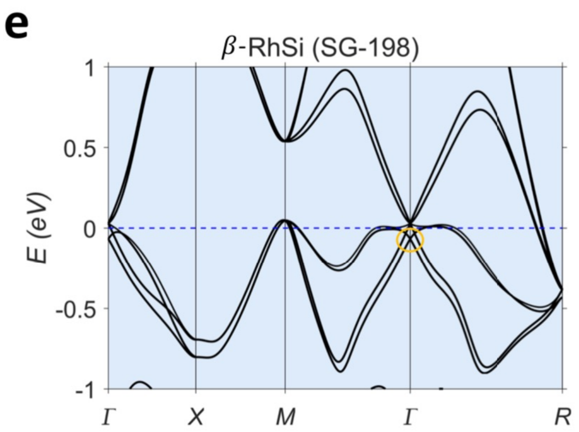

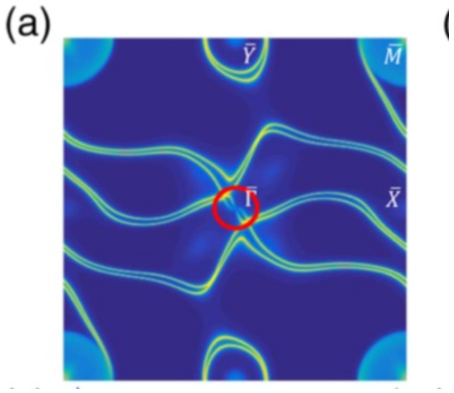

RhSi

Unconventional Chiral Fermions and Large Topological Fermi Arcs in RhSi

Guoqing Chang, Su-Yang Xu, Benjamin J. Wieder, Daniel S. Sanchez, Shin-Ming Huang, Ilya Belopolski, Tay-Rong Chang, Songtian Zhang, Arun Bansil, Hsin Lin, and M. Zahid Hasan

Phys. Rev. Lett. **119**, 206401 – Published 17 November 2017

Bringing order to the expanding fermion zoo

Carlo Beenakker Commentary

Heisenberg (1930): We observe space as a continuum, but we might entertain the thought that there is an underlying lattice and that space is actually a crystal. Which particles would inhabit such a lattice world? Werner Heisenberg *Gitterwelt* (lattice world) **hosted electrons that could morph into protons, photons that were not massless,** and more peculiarities that compelled him to abandon "this completely crazy idea"

chirality and topology

chiral crystals
optical activity
…

topological crystals
unusual surface states
large photogalvanic effect
…

new Fermions
largest Fermi arc
Quantized circular photogalvanic effect
…

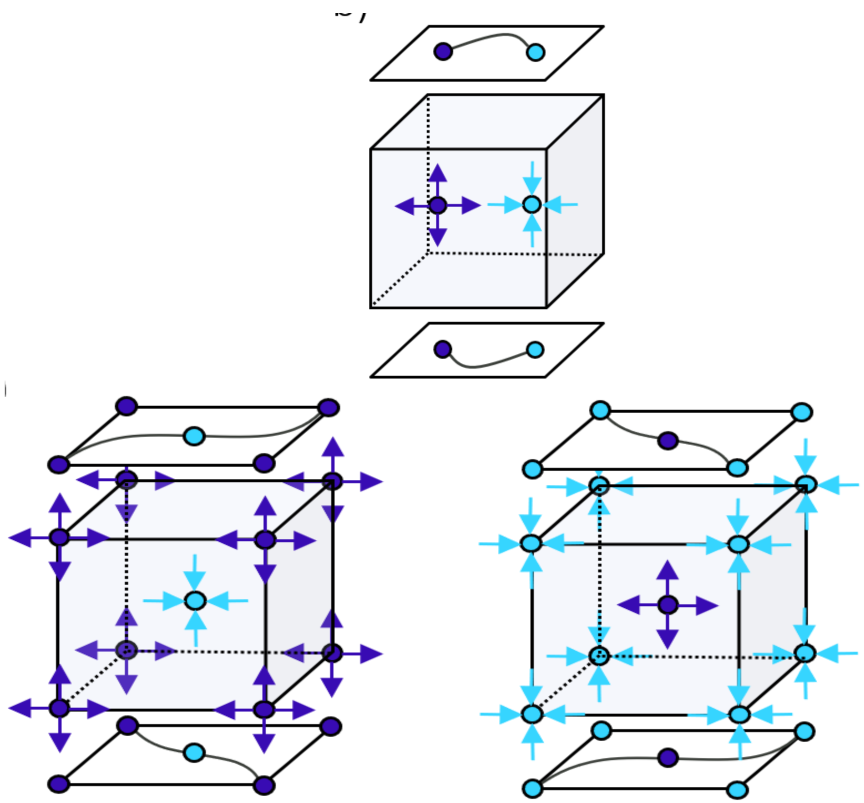

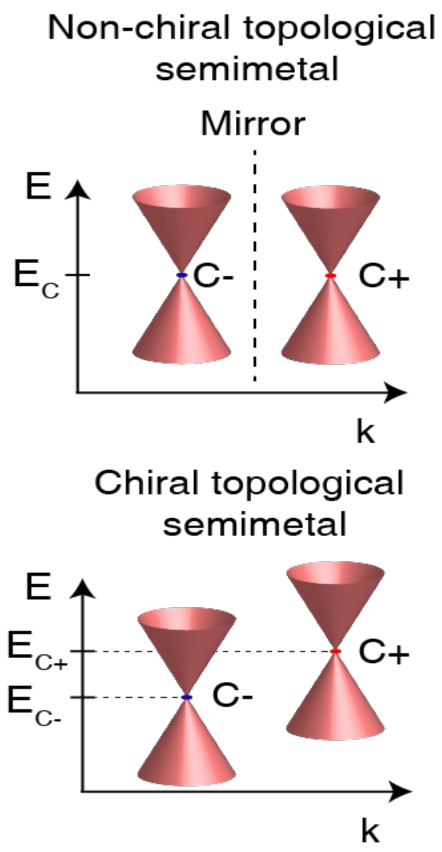

chirality and chiral anomaly

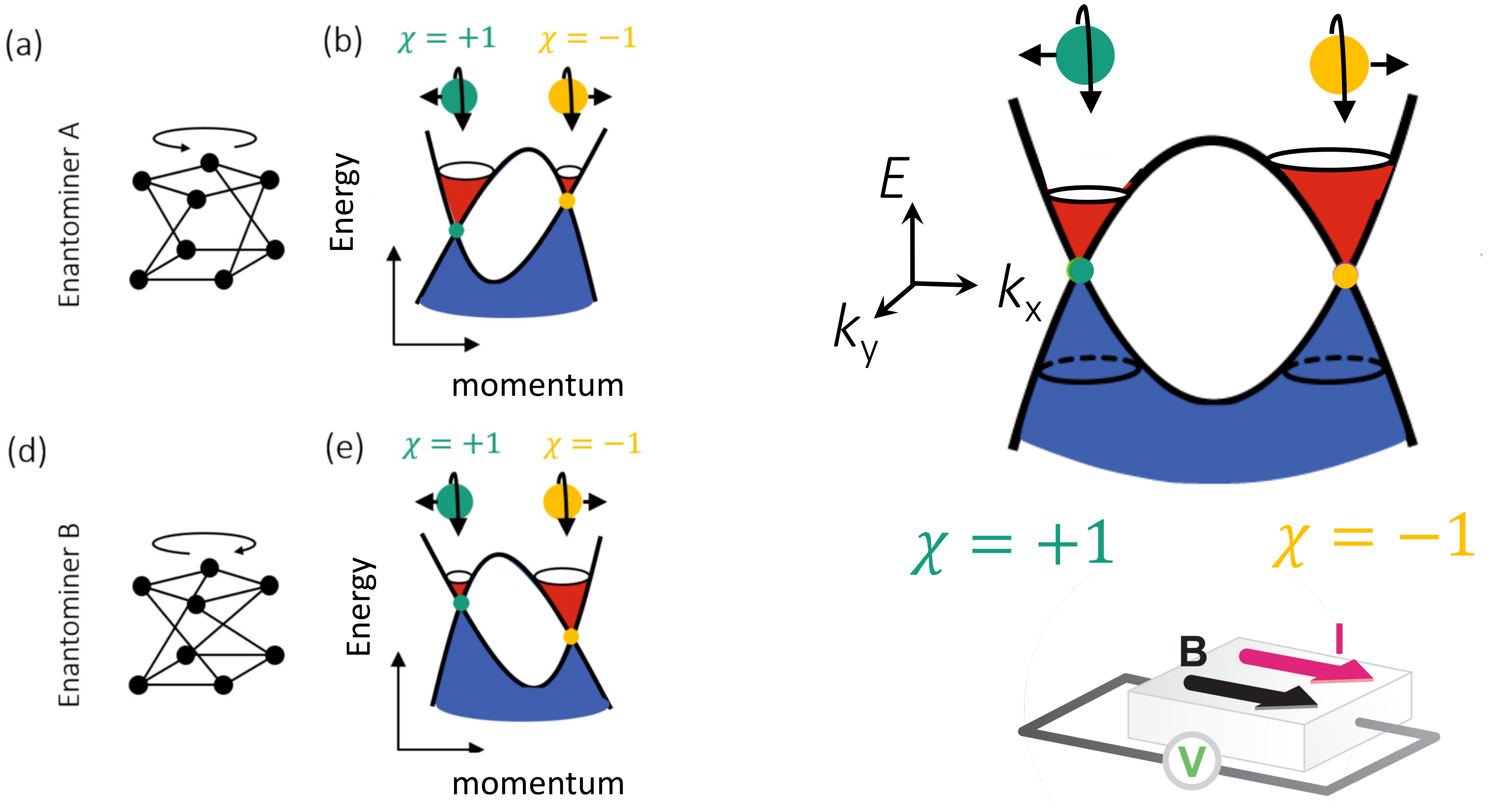

J. Gooth et al., Nature 547 (2017) 324 arXiv:1703.10682.
J. Gooth, J. Kübler, C. Felser, Physik Journal 20 (2021) 29.

chirality in chemistry

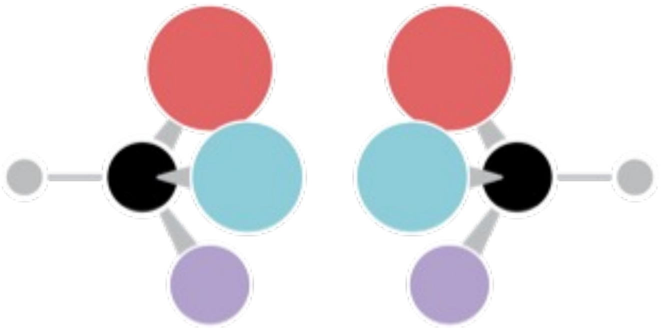

Molecules with different chiralities have different optical and catalytic properties

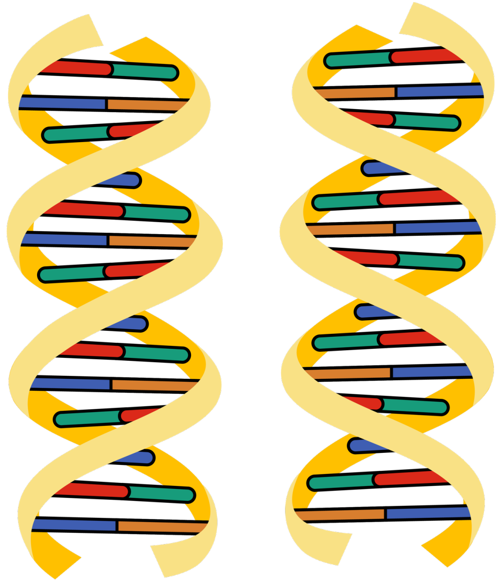

Lord Kelvin: An object or a system is *chiral* if it is distinguishable from its mirror image; that is, it cannot be superposed onto it.

In terms of point groups, all chiral molecules lack an improper axis of rotation (S_n)

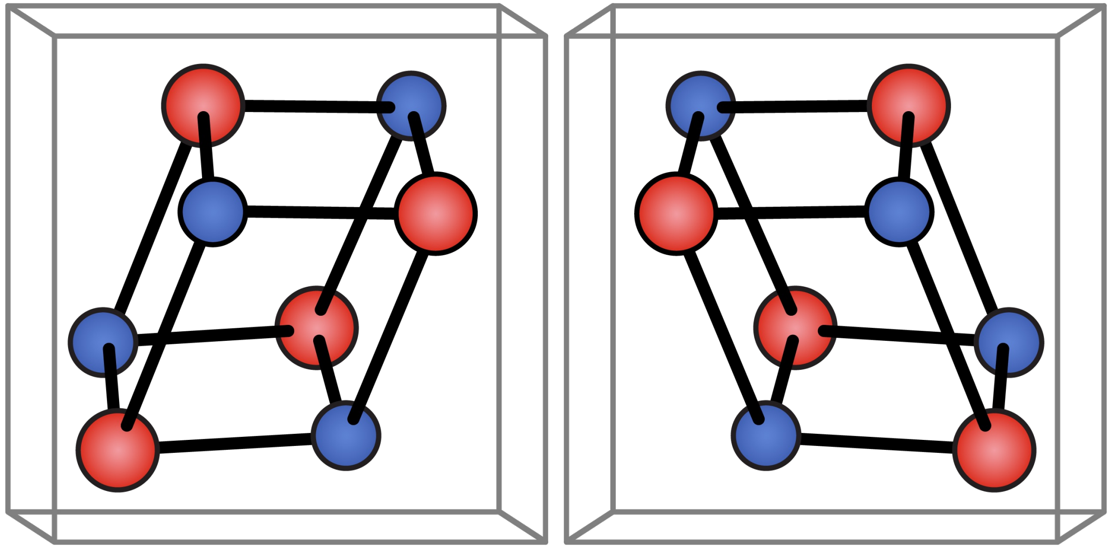

chirality in chemistry

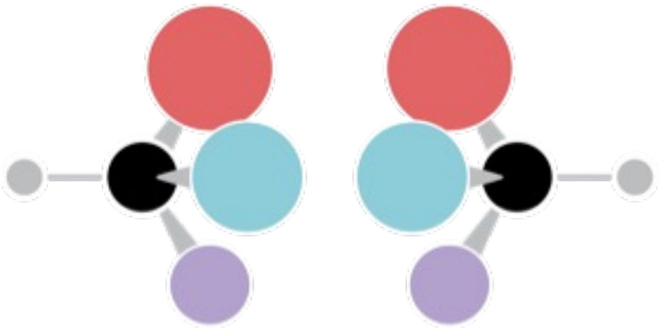

Molecules with different chiralities have different optical and catalytic properties

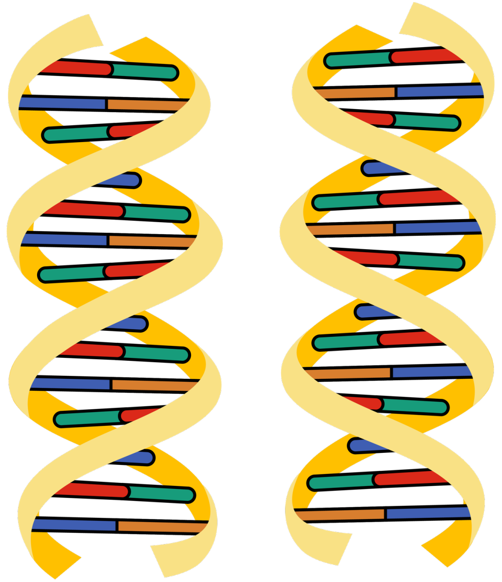

Chiral space groups contain symmetry operations of the first kind (rotation). There are 11 pairs of enantiomorphic space groups (e.g. P61 and P65) which are chiral. 43 achiral space groups can host a chiral crystal structure.

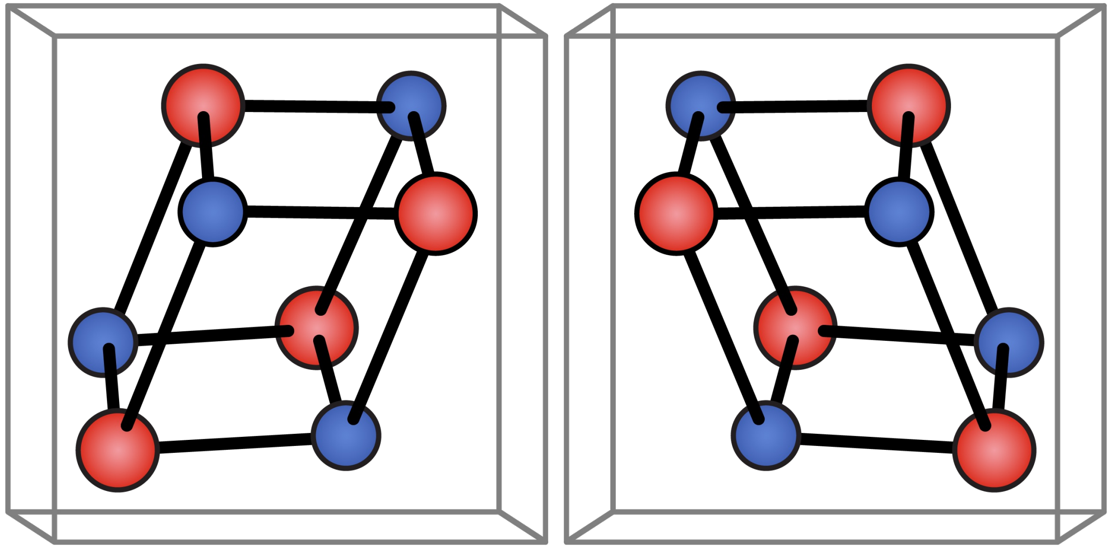

synthesis

RhSi

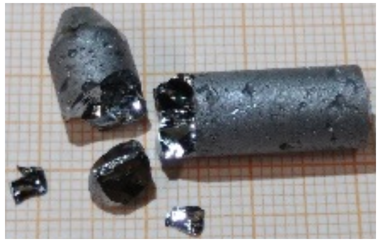

Flux +
Bridgman

CoSi

Chemical vapor transport
Bridgman, Flux

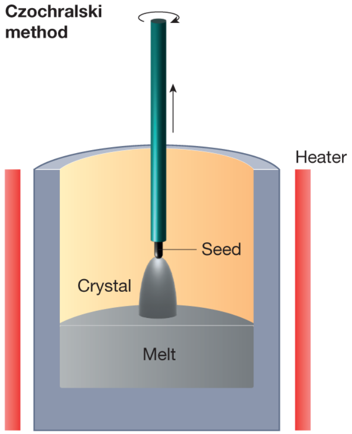

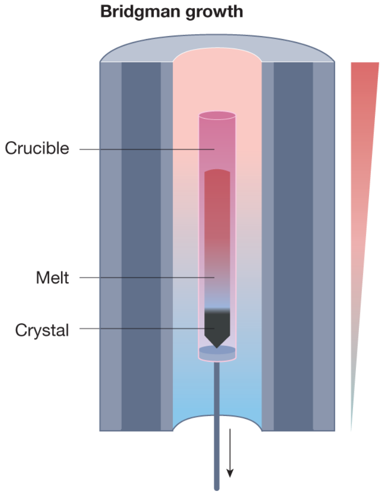

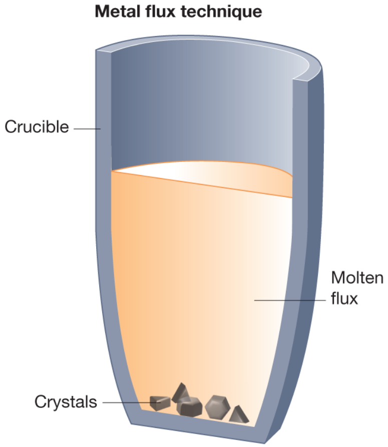

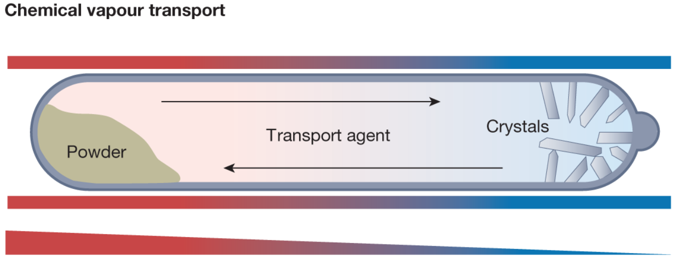

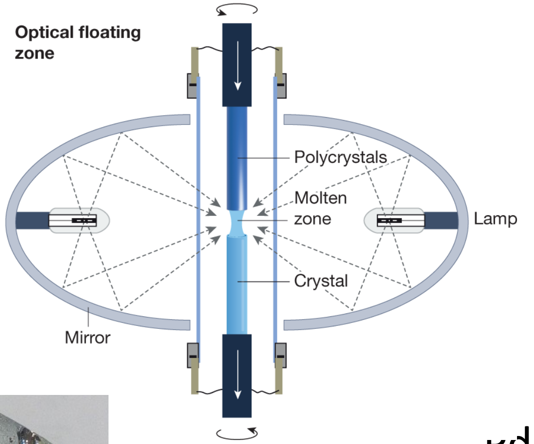

PtGa

Self-Flux

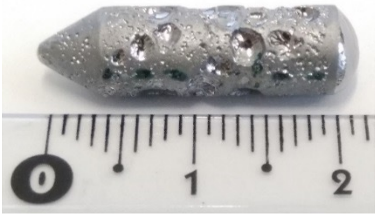

PdGa: Chiral-1, Right handed

Self-Flux

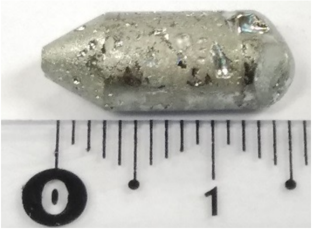

PtAl

Self-Flux

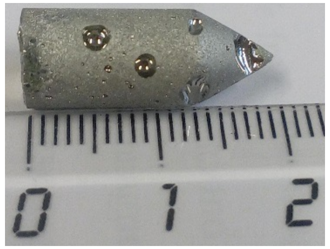

PdGa: Chiral-2, Left handed

Self-Flux

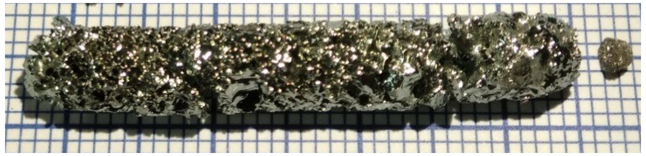

Nitesh Kumar, Satya N. Guin, Kaustuv Manna, Chandra Shekhar, and Claudia Felser, Chem. Rev. 121 (2021) 2780.

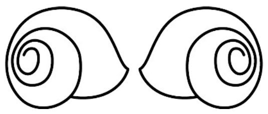

chiral crystals which host new fermions

Compounds with the B20 structure

Enantiomer A and Enantiomer B
Crystal structure

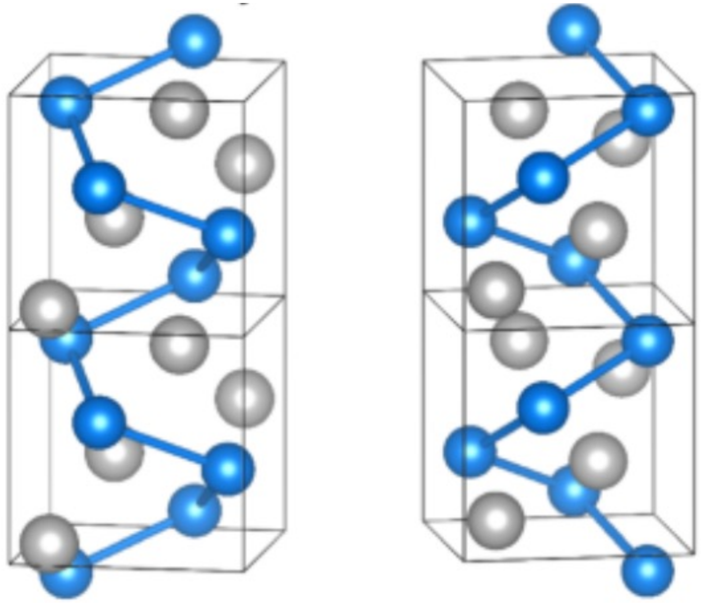

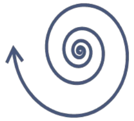

PdGa : Chiral-1, Right handed

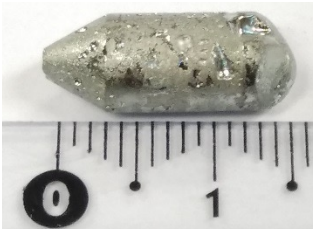

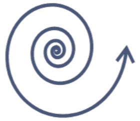

PdGa Chiral-2, Left handed

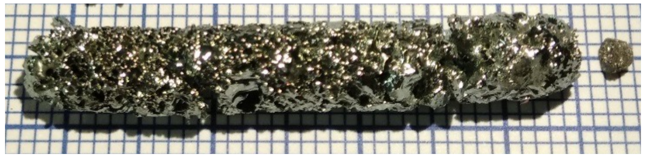

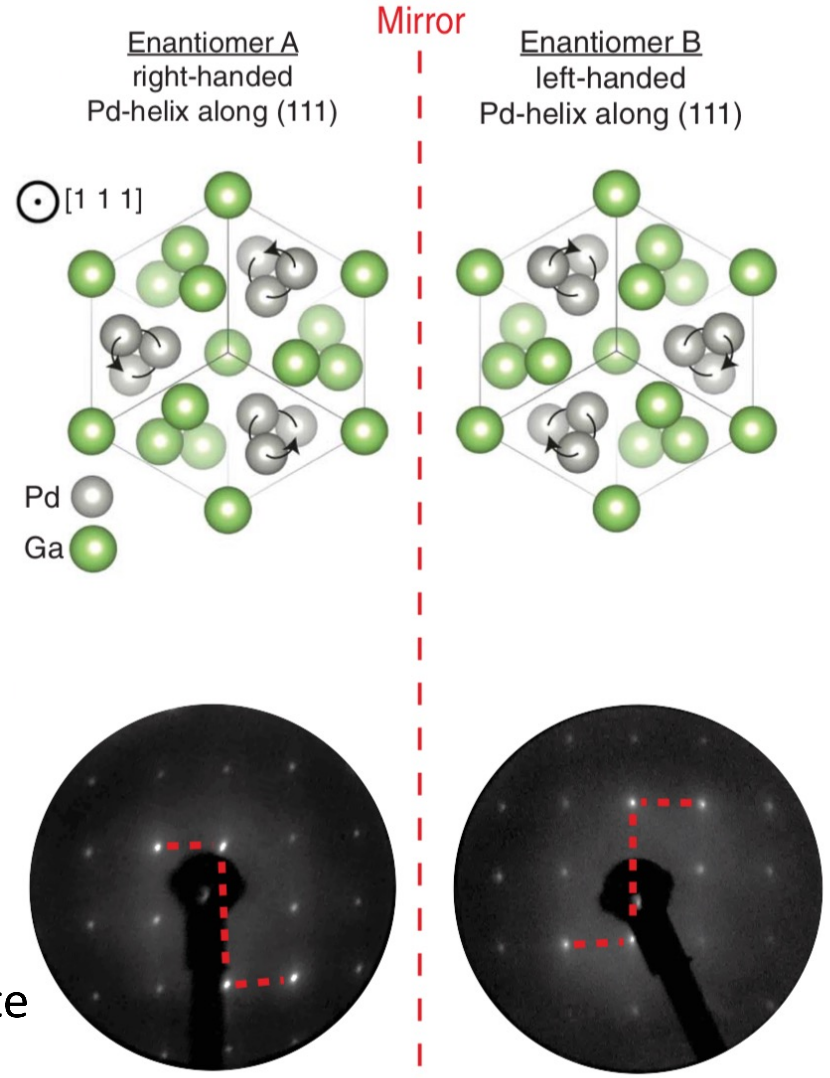

PdGa crystallizes in space group $P2_13$ (No. 198) 4- and 6- fold degenerate Fermions: more examples include CoSi, RhSi, PtAl, CoGe, RhGe, PtGa, PtAl and magnetic MnSi and FeGe

Schröter *et al.*, Nature Physics 2019, Schröder *et al.*, Science **369** (2020) 179, Sanchez *et al.* Nature 2019, Sessi *et al.*, Nature Communications **11** (2020) 3507

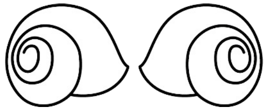

homochiral crystals

Compounds with the B20 structure

Enantiomer A and Enantiomer B
Crystal structure

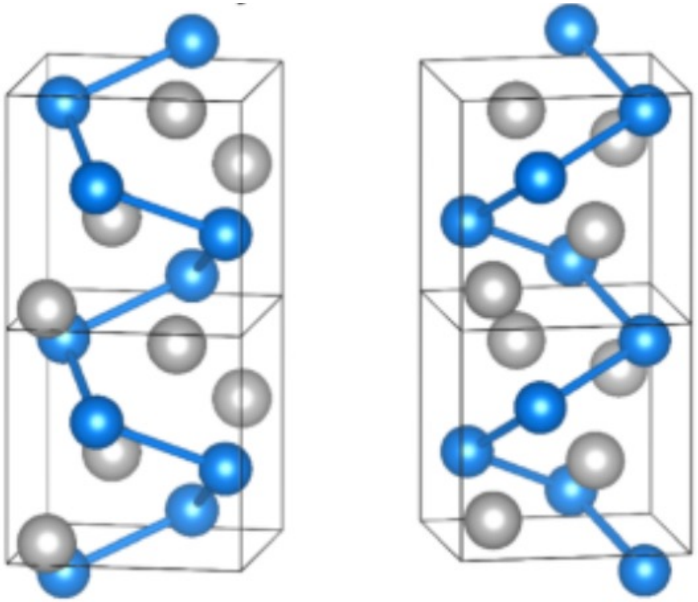

CoSi

Absolute Structure from Scanning Electron Microscopy

Ulrich Burkhardt[1*], Horst Borrmann[1], Philip Moll[1,2], Marcus Schmidt[1], Yuri Grin[1] & Aimo Winkelmann[3,4]

- *X*- ray (volume sensitive)
- electron backscatter diffraction (EBSD) (surface sensitive)

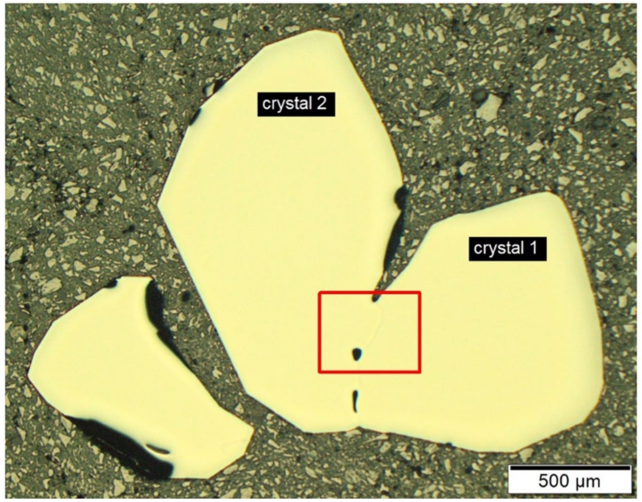

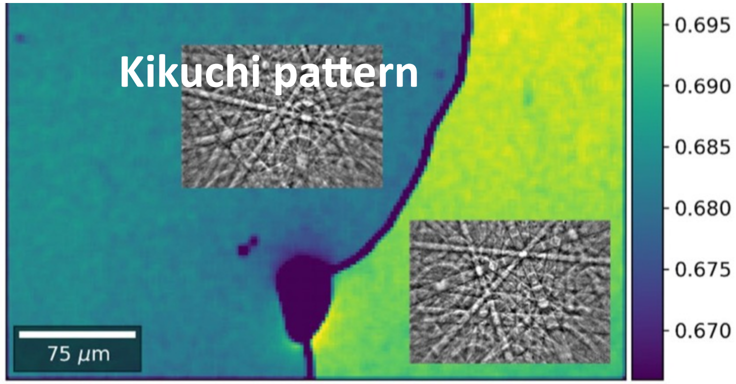

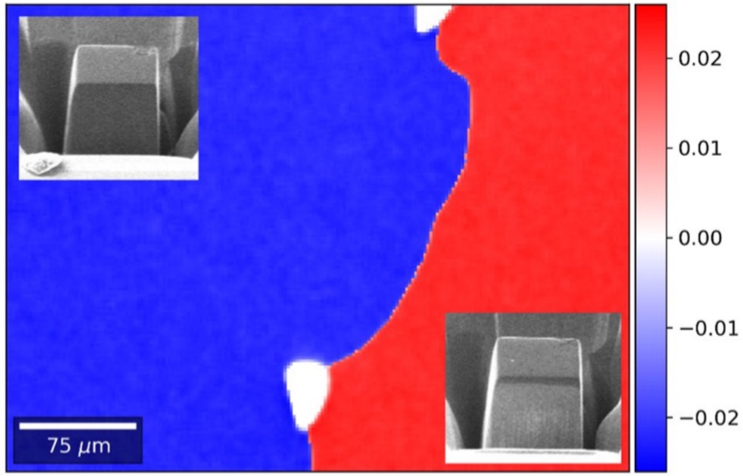

Fermions: more examples include CoSi, RhSi, PtAl, CoGe, RhGe, PtGa, PtAl and magnetic MnSi and FeGe

new fermions with chiral surface states

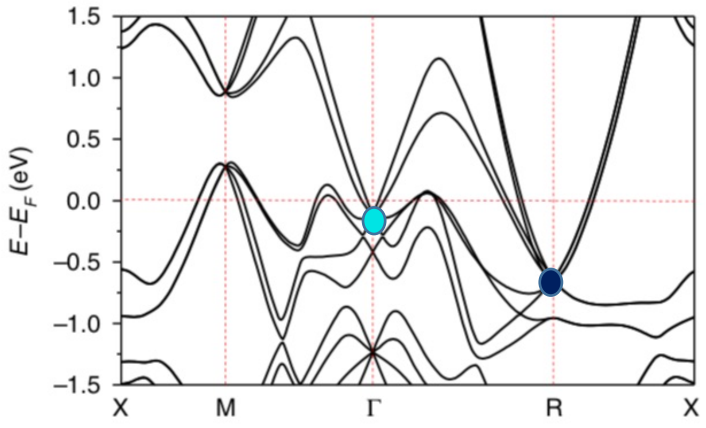

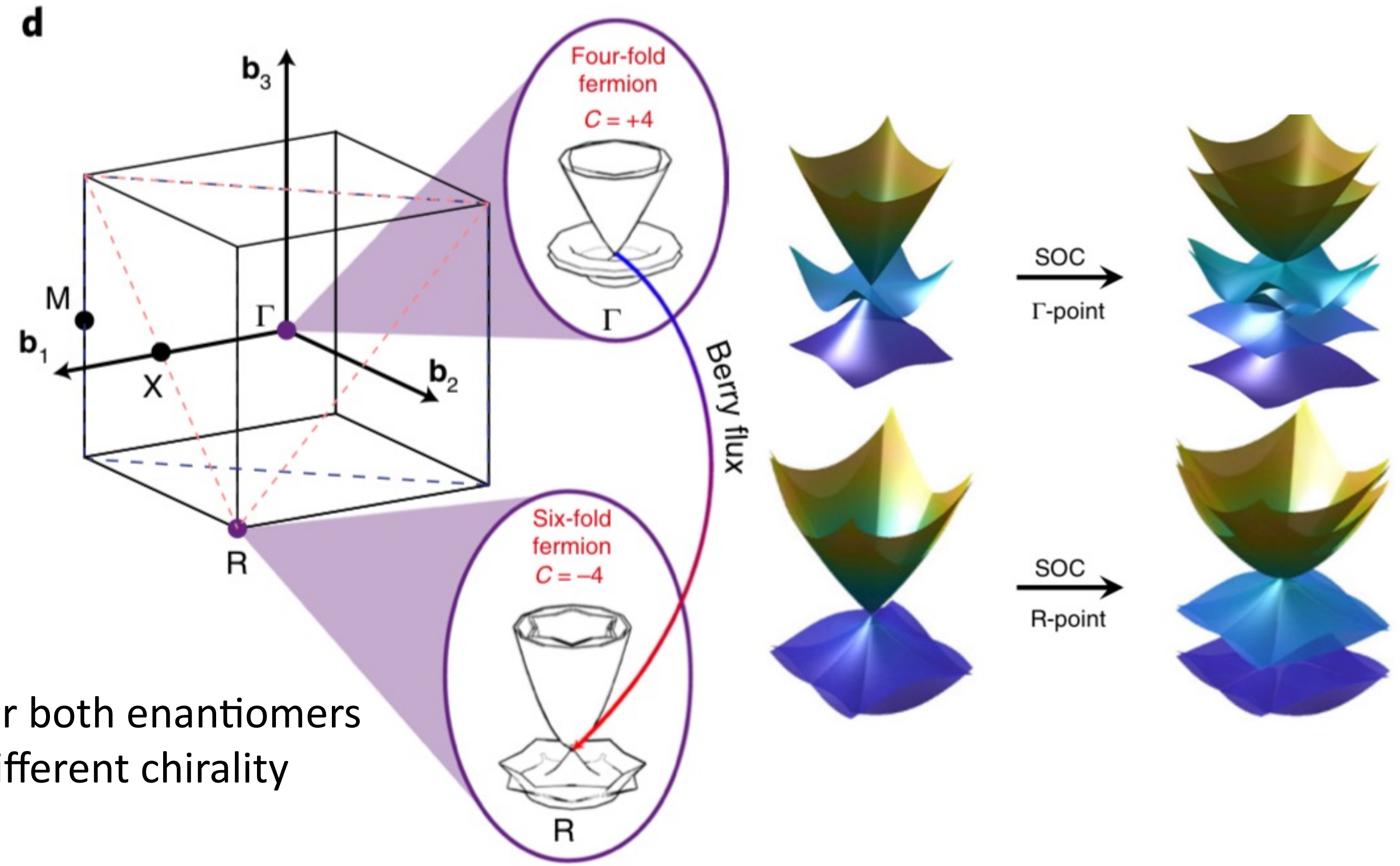

the band structure is the same for both enantiomers
however the Weyl points have different chirality

Schröter *et al*., Nature Physics 2019, Schröder *et al*., Science **369** (2020) 179, Sanchez *et al.* Nature 2019, Sessi *et al*., Nature Communications **11** (2020) 3507

new fermions with chiral surface states

PtAl

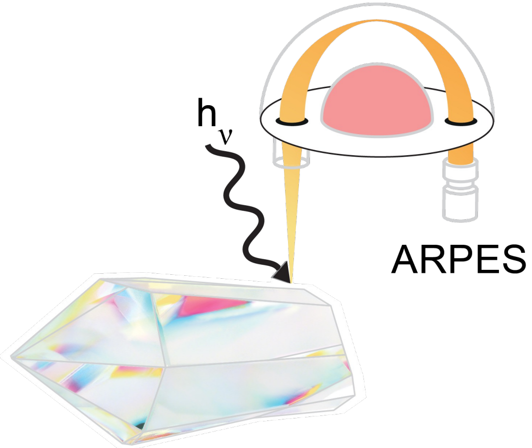

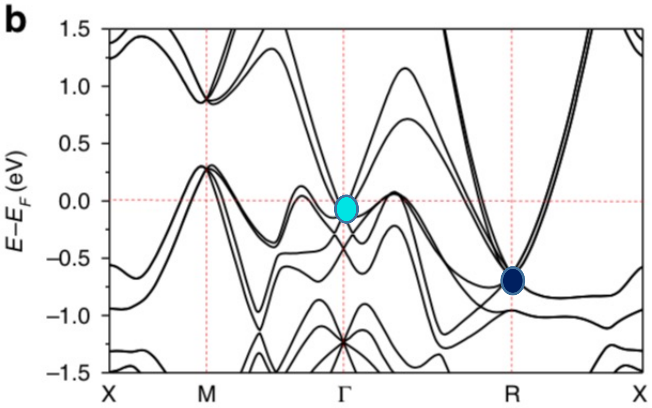

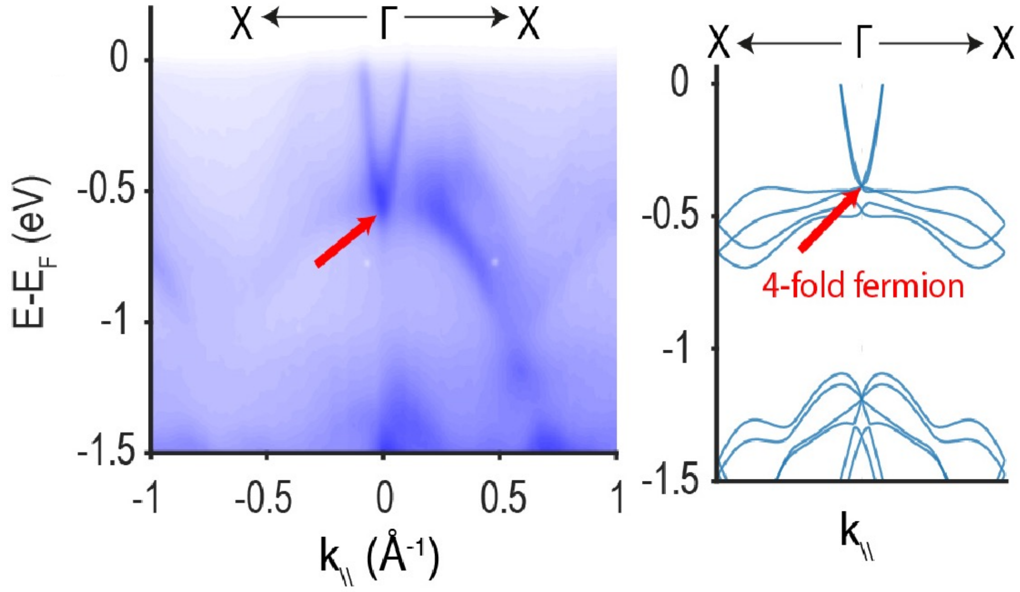

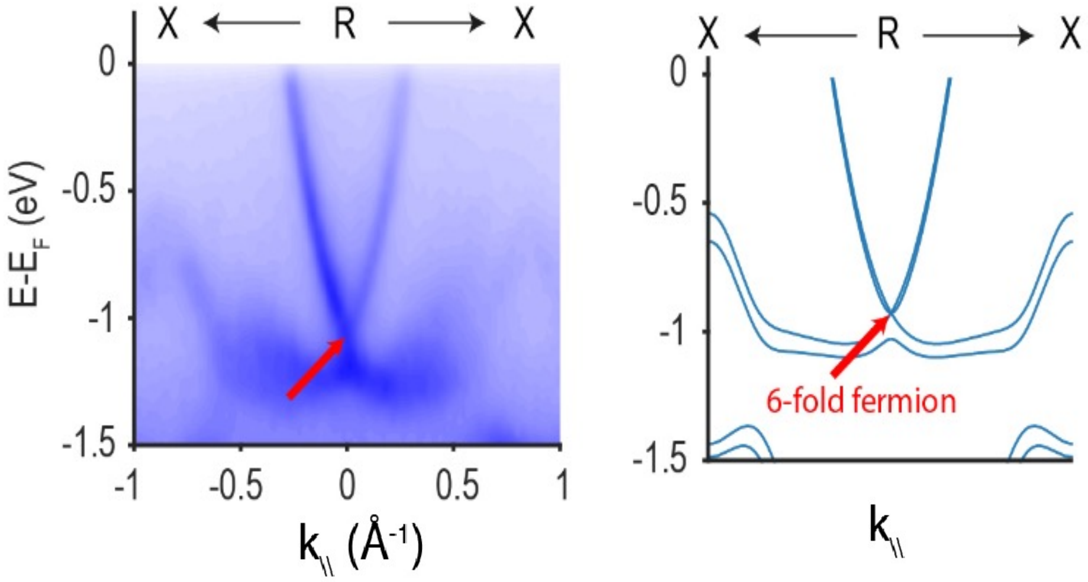

Schröter *et al*., Nature Physics 2019, Schröder *et al.,* Science **369** (2020) 179, Sanchez *et al.* Nature 2019, Sessi *et al*., Nature Communications **11** (2020) 3507

new fermions with chiral surface states

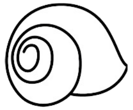

PdGa Chiral-1, Right handed

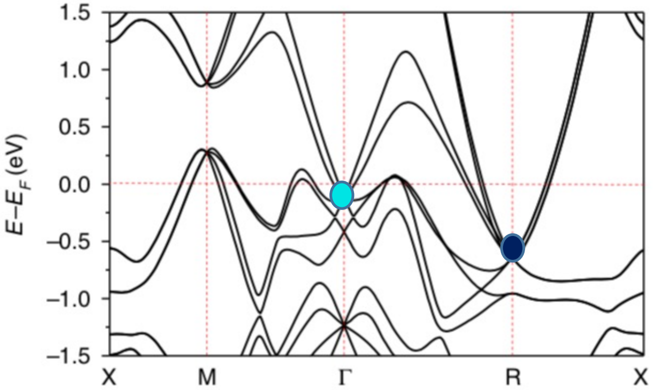

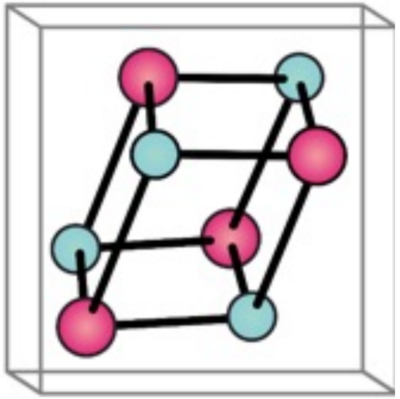

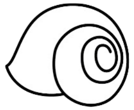

PdGa Chiral-2, Left handed

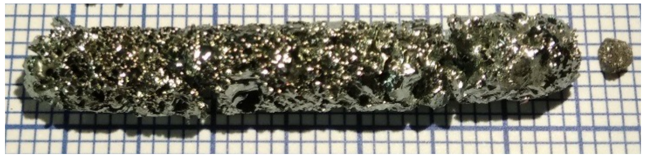

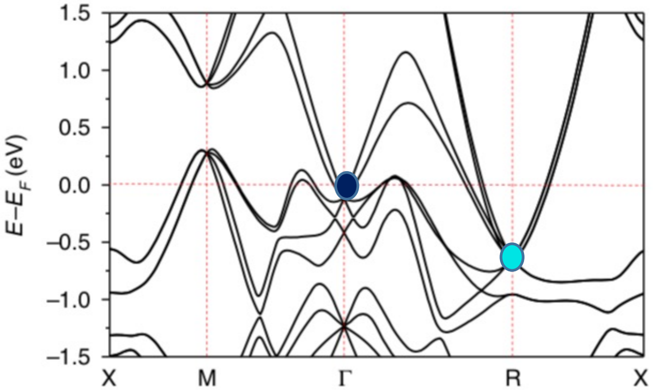

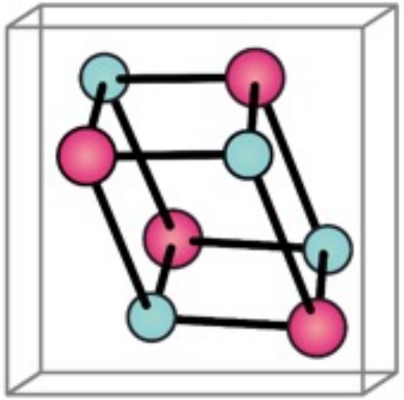

The crystal structure is **chiral,** the electronic structure is **identical**, however, the Weyl points and the Fermi arcs are **chiral**

Schröter *et al.*, Nature Physics 2019, Schröder *et al.*, Science **369** (2020) 179, Sanchez *et al.* Nature 2019, Sessi *et al.*, Nature Communications 11 (2020) 3507

new fermions with chiral surface states

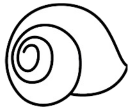

PdGa Chiral-1, Right handed

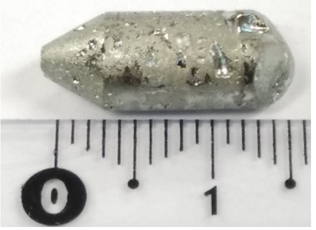

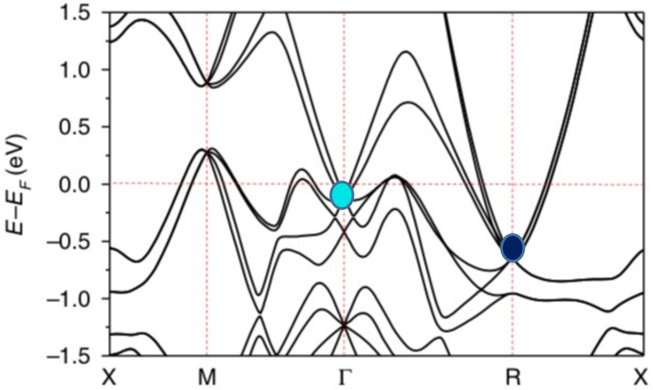

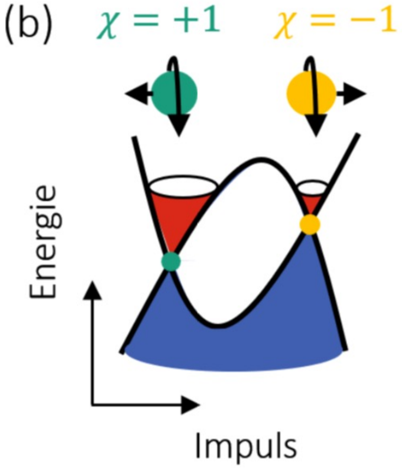

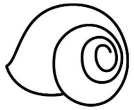

PdGa Chiral-2, Left handed

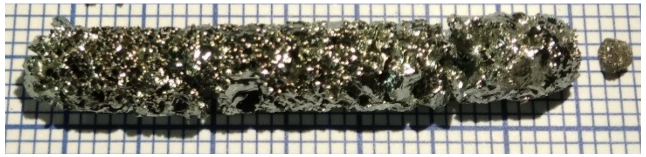

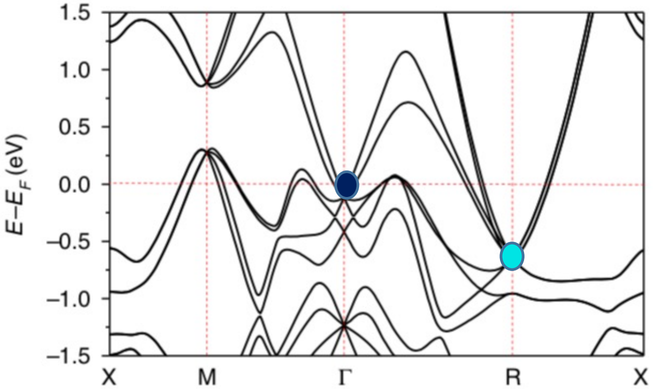

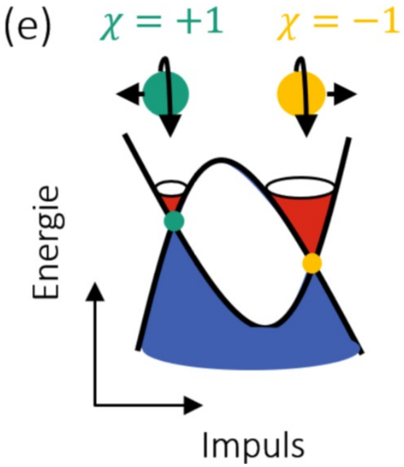

The crystal structure is **chiral,** the electronic structure is **identical**, however, the Weyl points and the Fermi arcs are **chiral**

Schröter *et al.*, Nature Physics 2019, Schröder *et al.*, Science **369** (2020) 179, Sanchez *et al.* Nature 2019, Sessi *et al.*, Nature Communications 11 (2020) 3507

chiral Fermions

Weyl electrons and the Fermi arc **chiral**

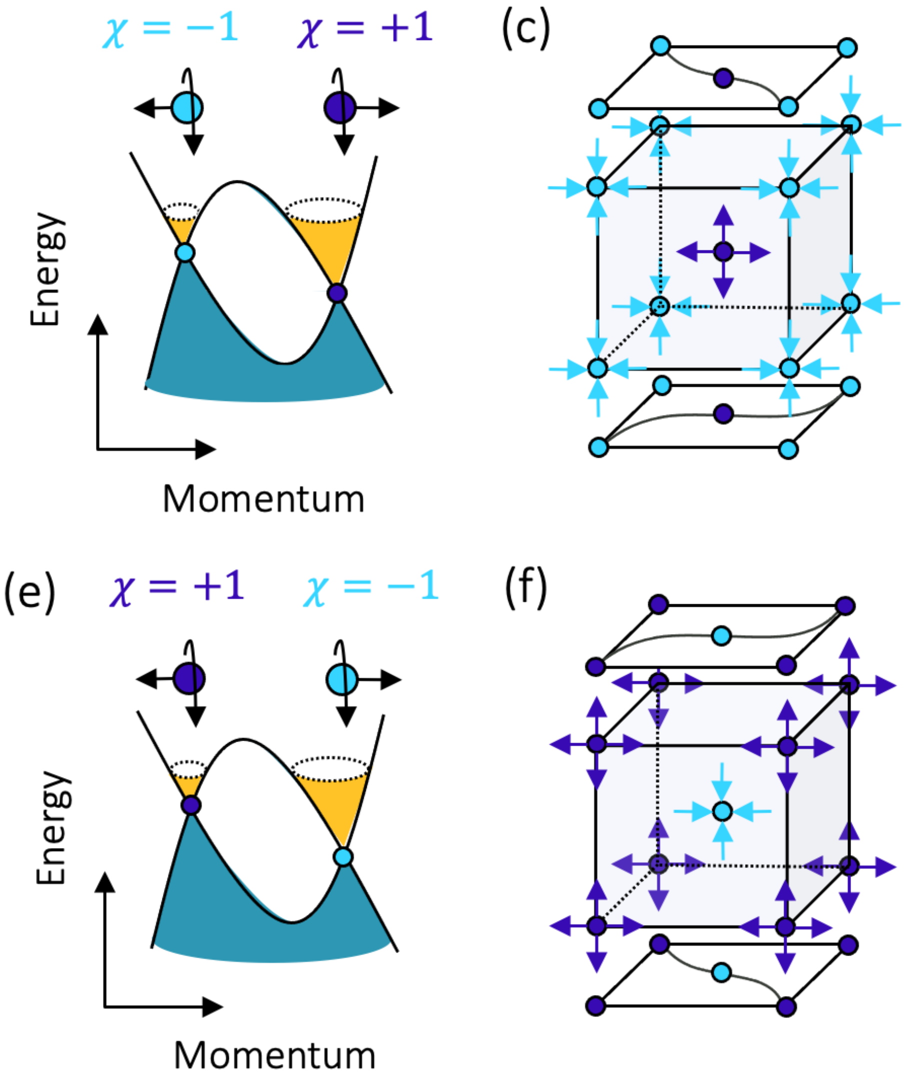

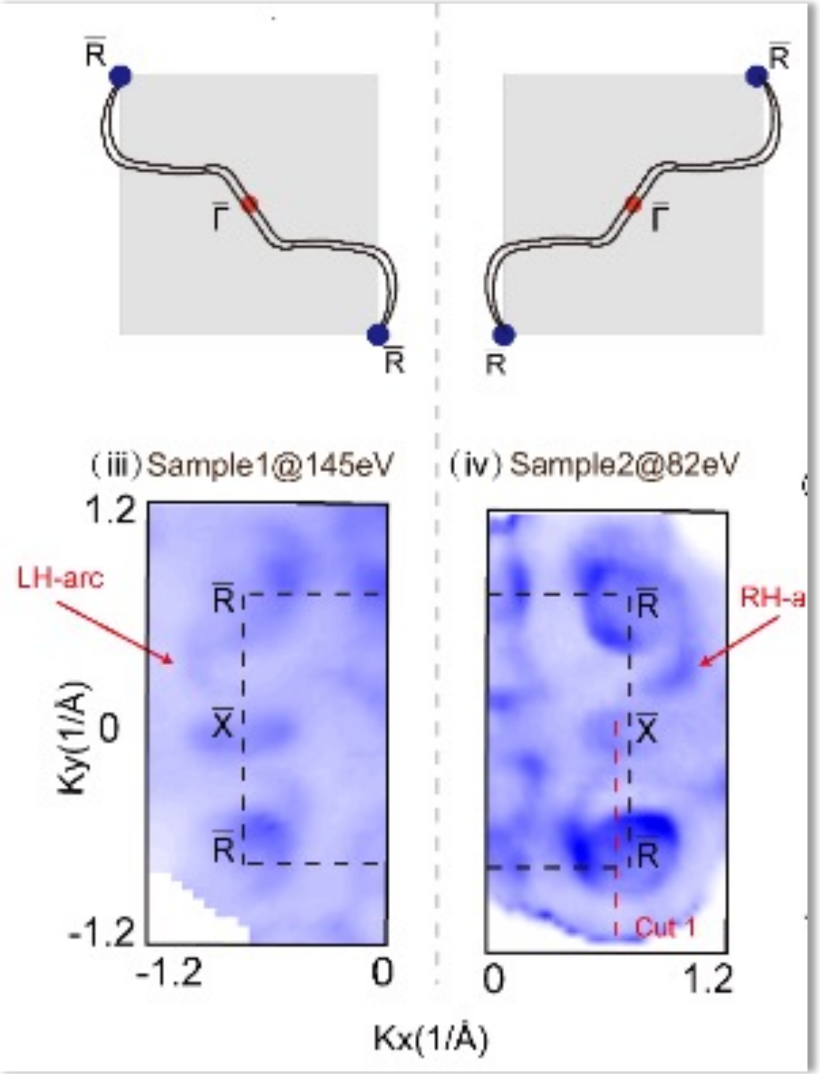

PdGa

Schröter et al., Nature Physics 15 (2019) 759, Schröter et al., Science 369 (2020) 179, Sanchez et al. Nature Nature 567 (2019) 500

new fermions with chiral surface states

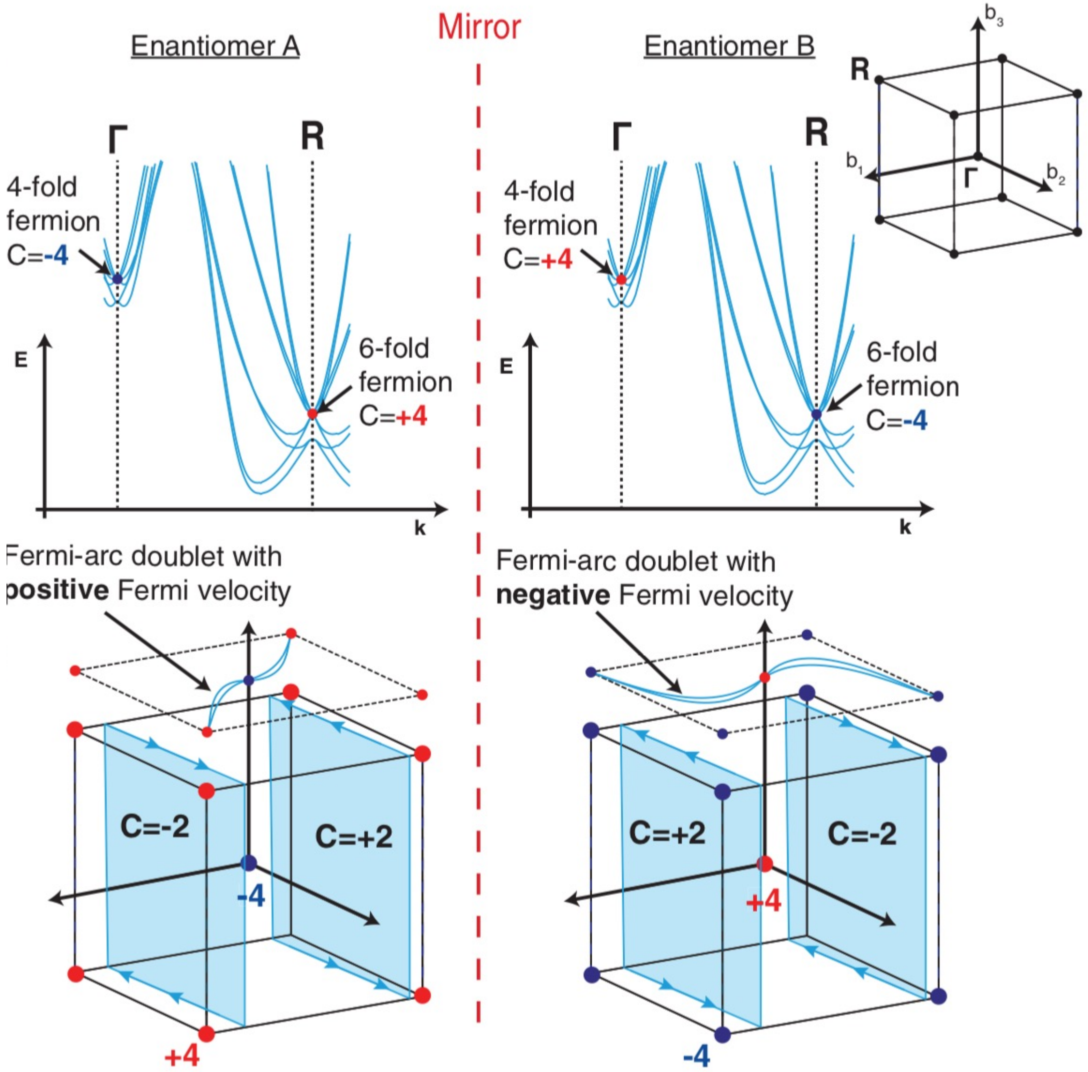

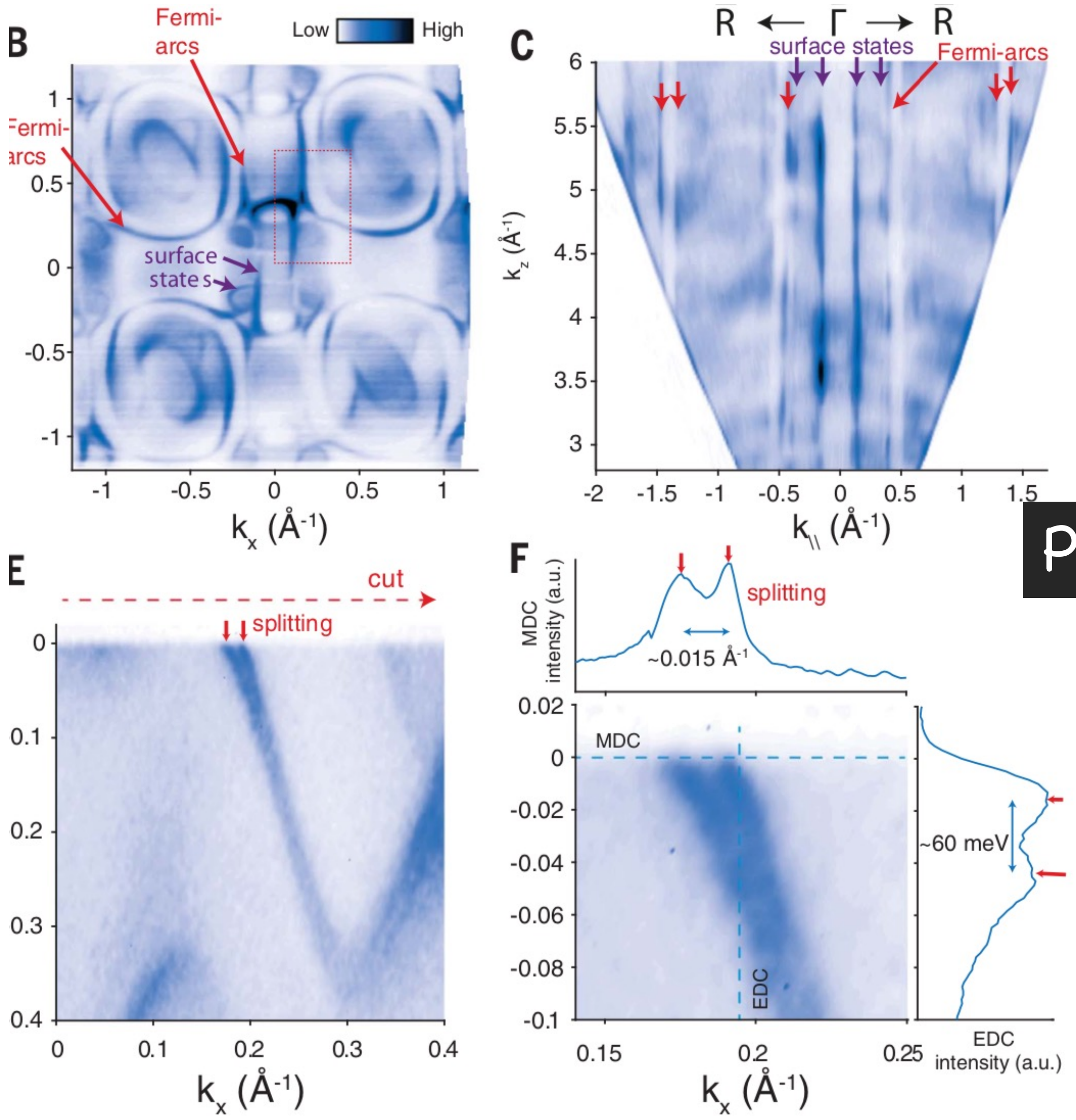

PdGa

Schröter *et al.*, Science **369**, 179–183 (2020)

new fermions with chiral surface states

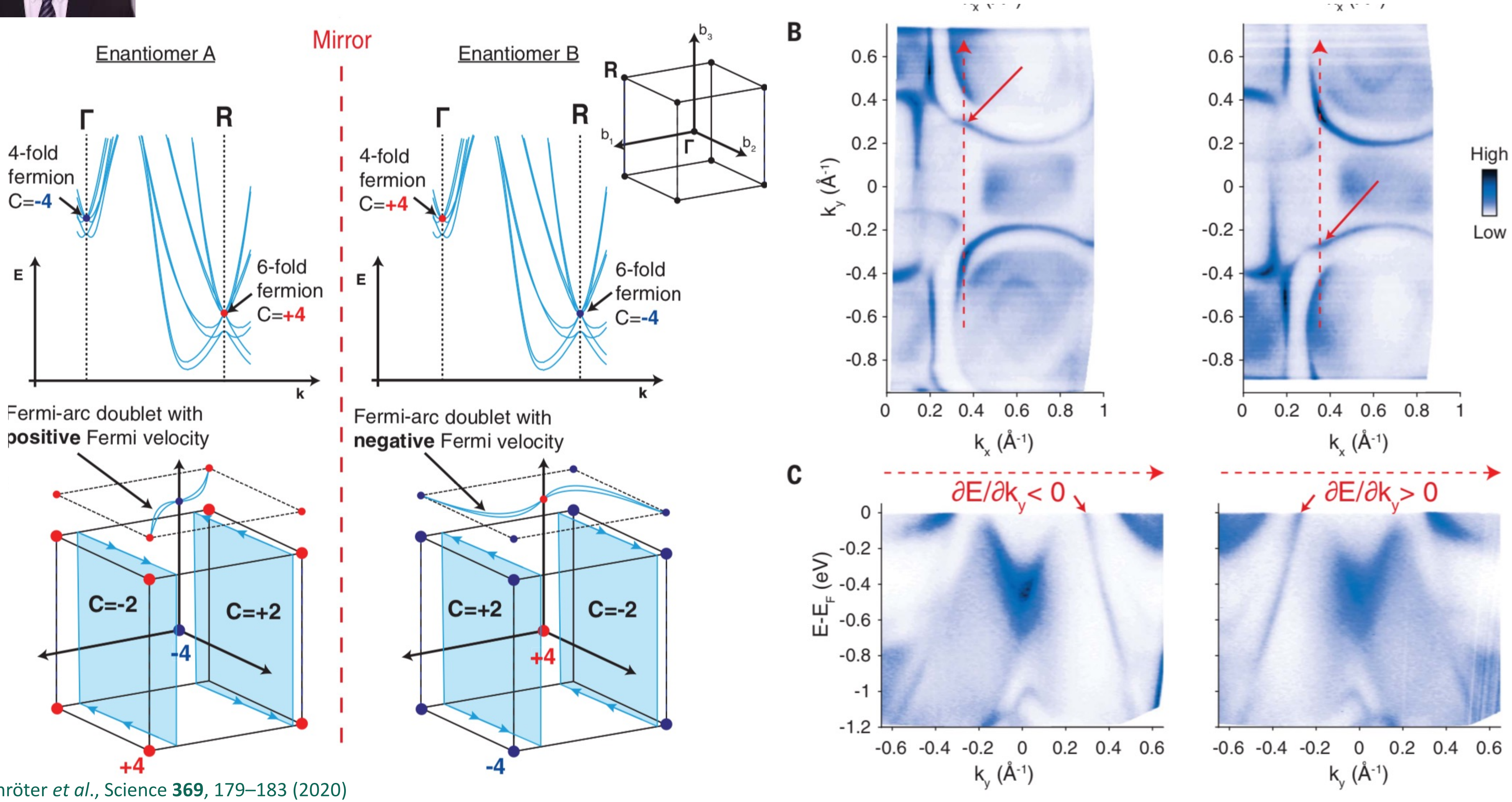

PdGa

Schröter *et al.*, Science **369**, 179–183 (2020)

new fermions with chiral surface states

RhSi

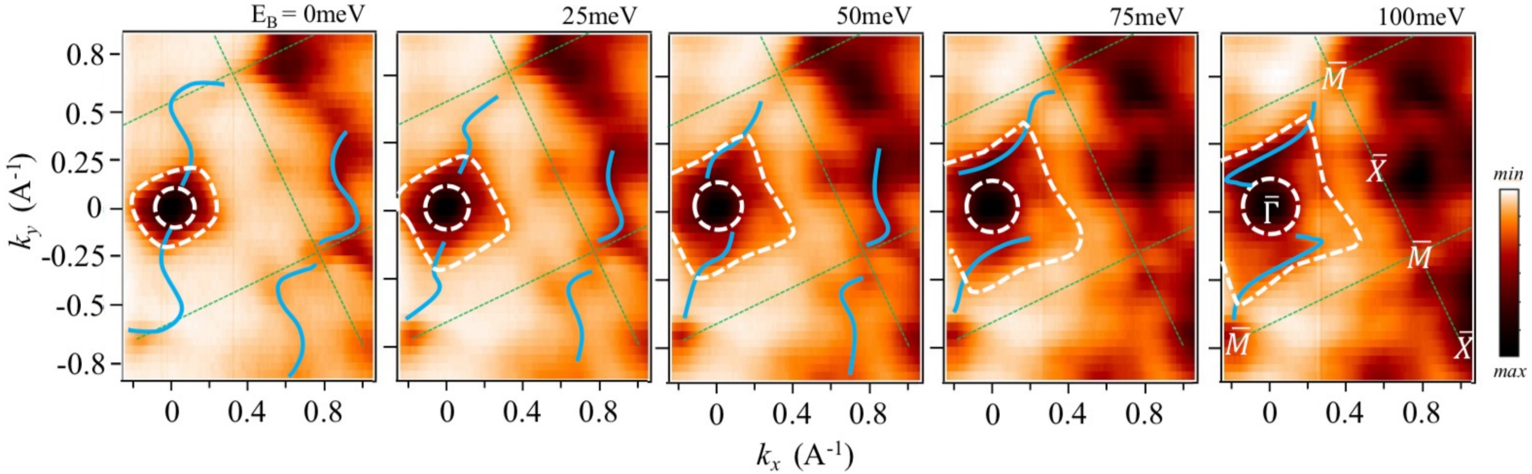

CoSi

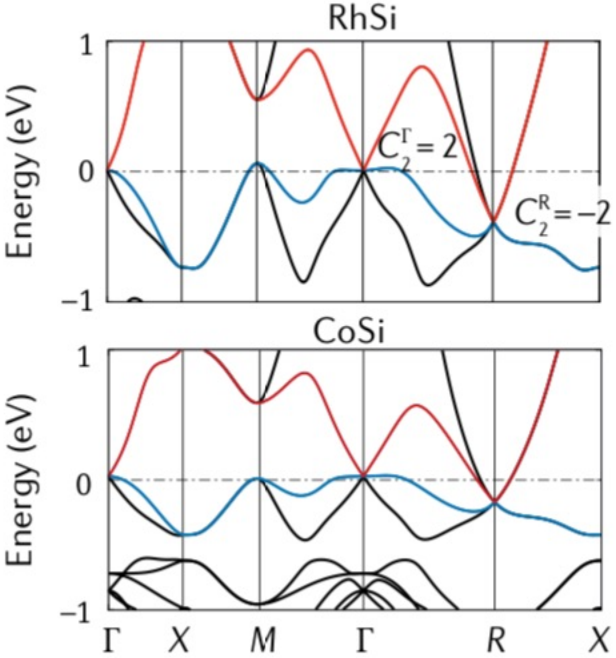

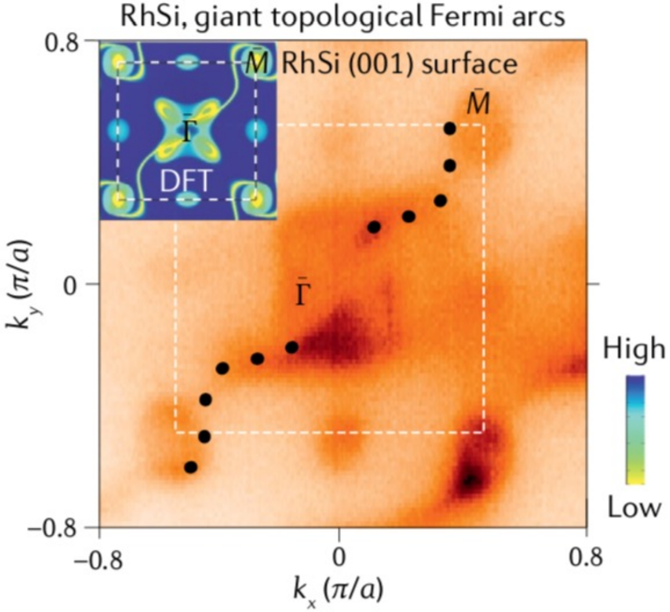

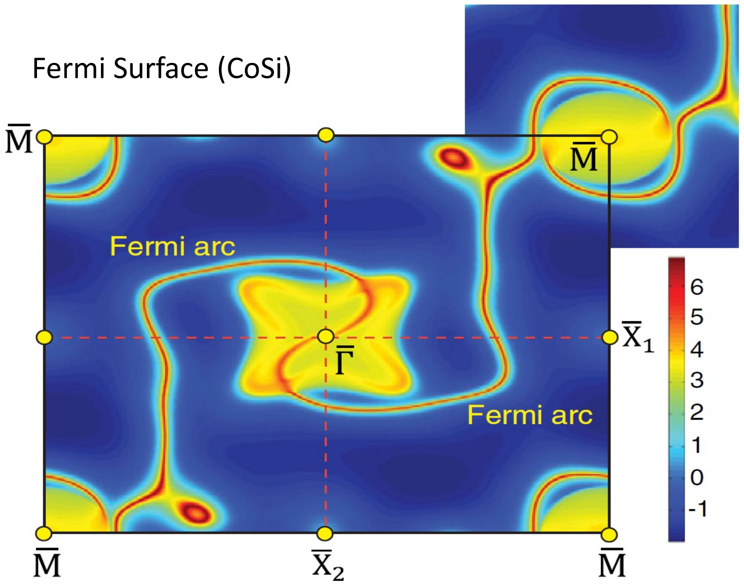

S. Sanchez, K. Manna *et al.* Nature **567**, 500 (2019).

quantum oscillations of PtGa

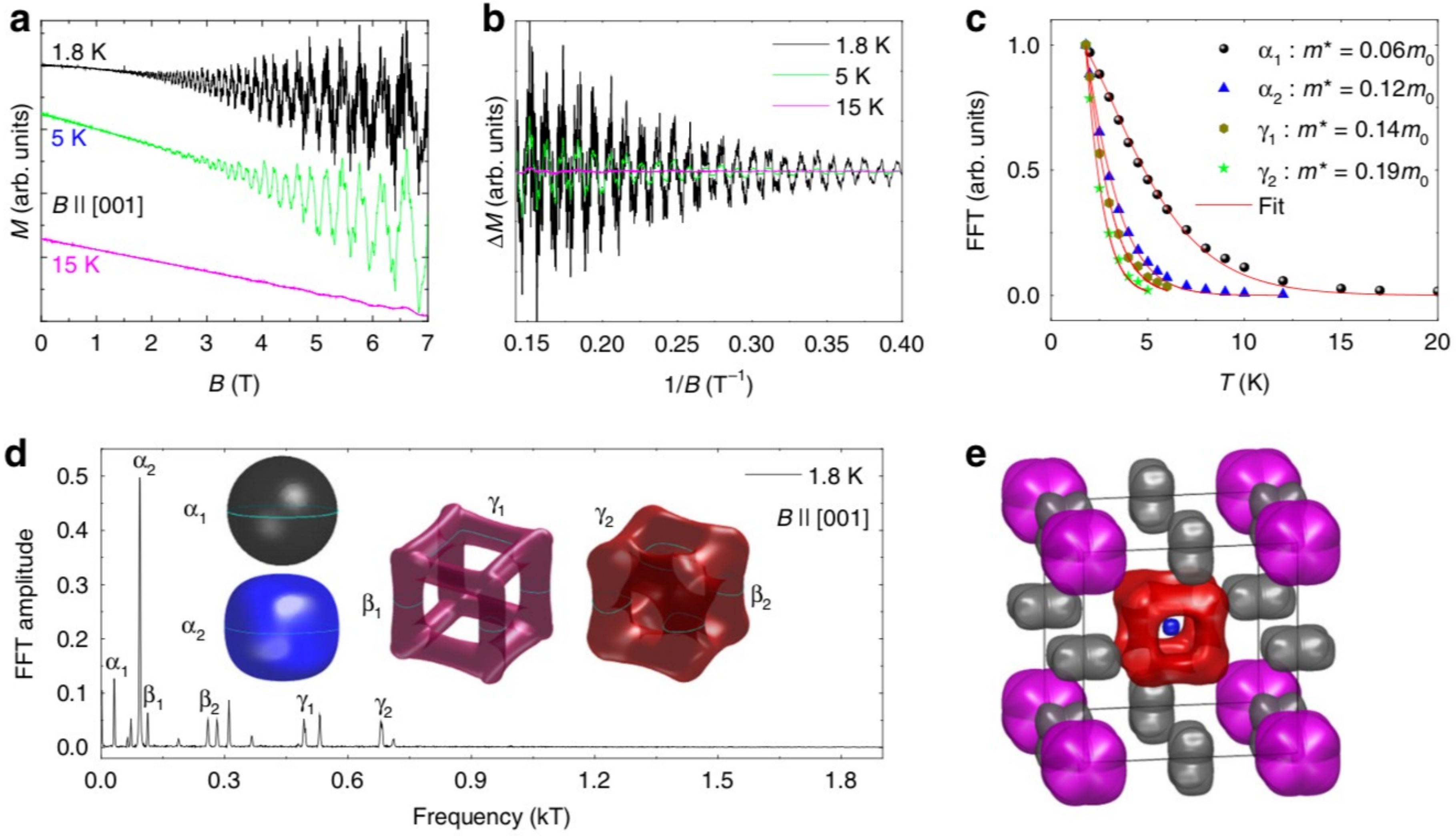

Yao et al., Nature Communications 11 (2020) 2033,

chiral surface states with STM

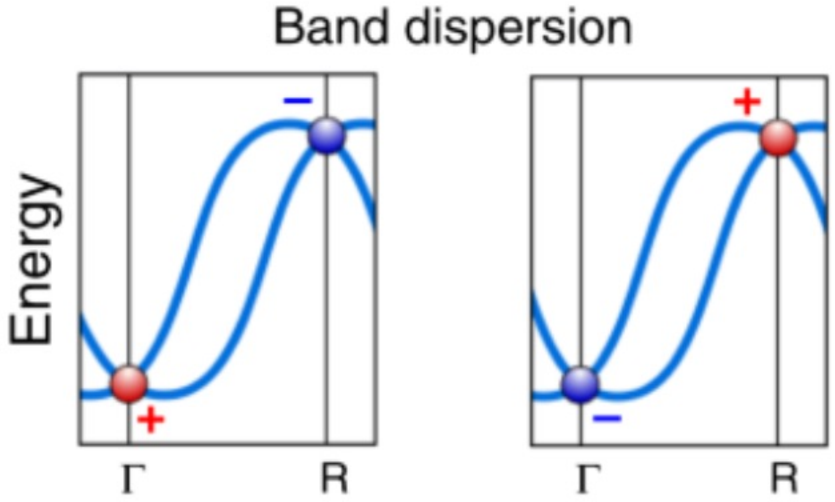

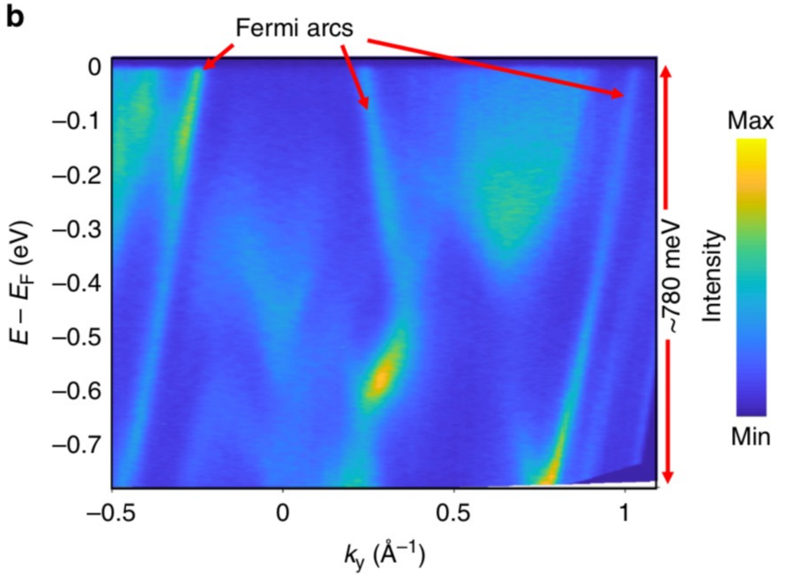

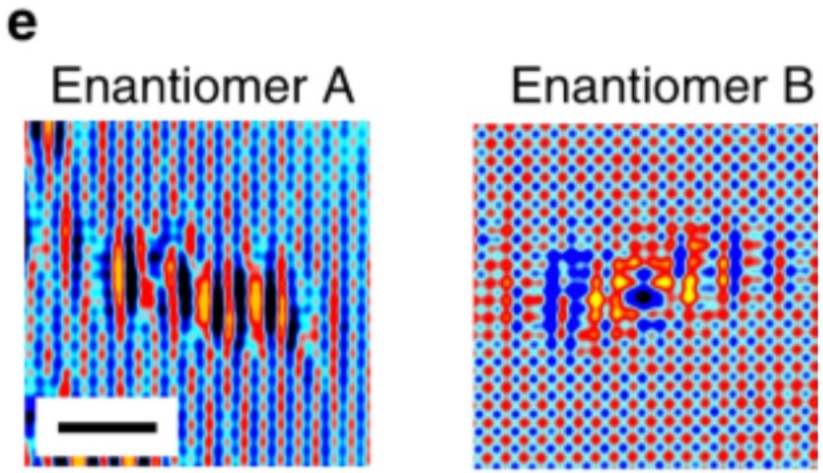

From STM investigations:
(i) the perturbation developing around native defects is chiral
(ii) the scattering vector associated with scattering events between opposite Fermi arcs is also chiral

Quasiparticle interference of two PdGa(001) enantiomers

PdGa

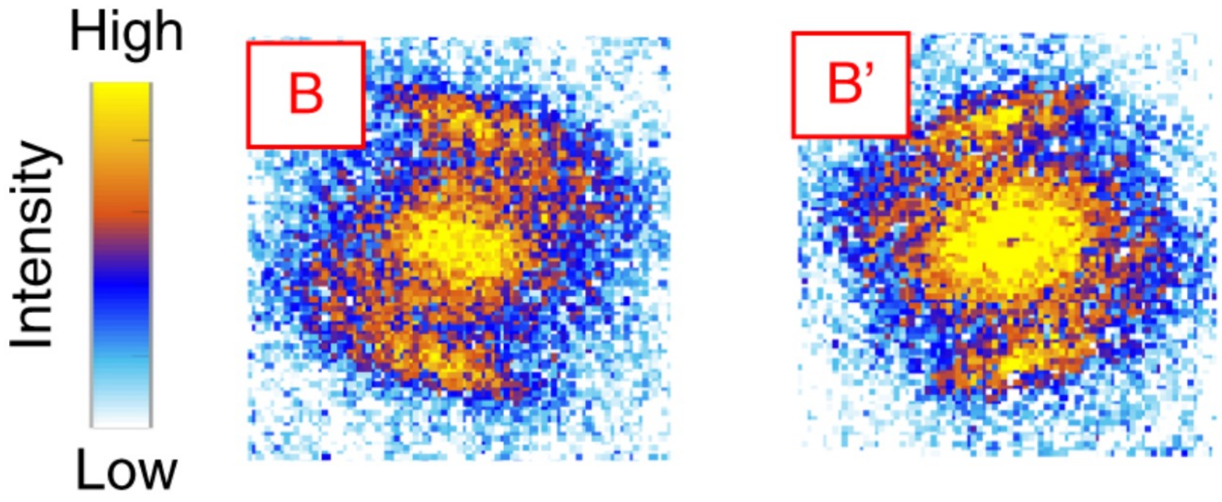

Quasiparticle interference of two PdGa(001) enantiomers

Sessi *et al.*, Nature Communications **11** (2020) 3507

chiral electrons in the bulk

With **circular polarized light** we can visualize the difference in the band structure

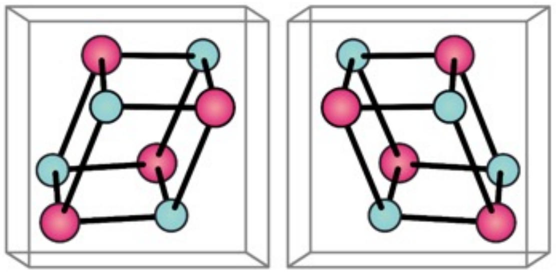

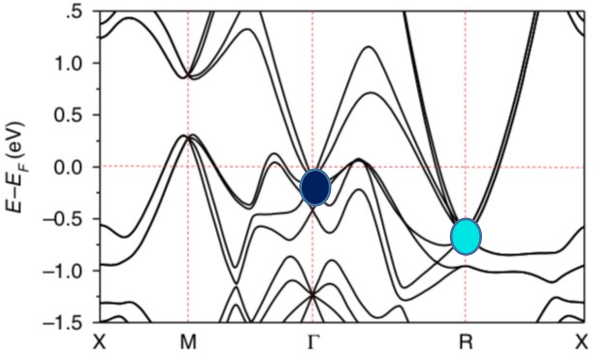

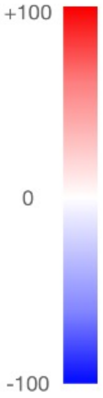

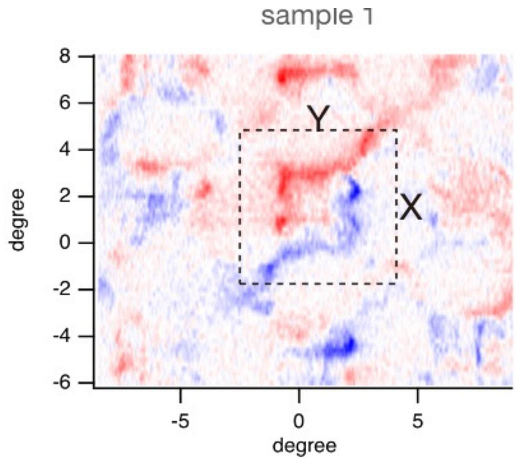

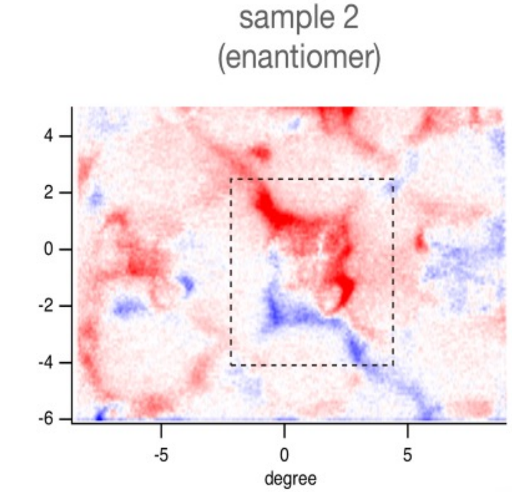

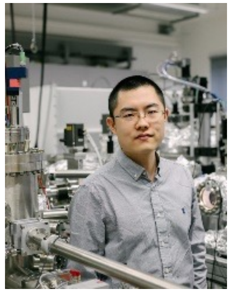

PdGa

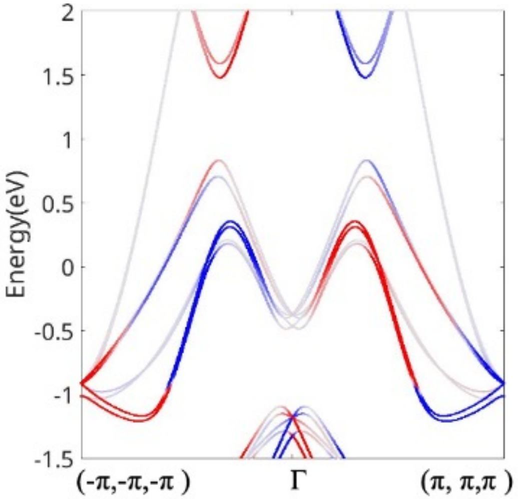

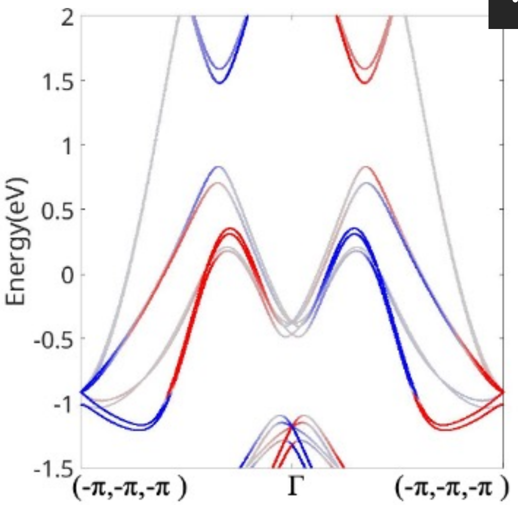

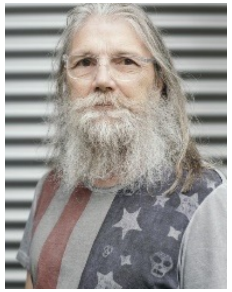

Orbital angular momentum, <111>

Yao et. al., to be published

Quantized circular photogalvanic effect

ARTICLE

Received 27 Dec 2016 | Accepted 18 May 2017 | Published 6 Jul 2017

DOI: 10.1038/ncomms15995 OPEN

Quantized circular photogalvanic effect in Weyl semimetals

Fernando de Juan[1,2,3], Adolfo G. Grushin[1], Takahiro Morimoto[1] & Joel E. Moore[1,4]

Prediction: Excitation of Weyl fermions –
a **current that is quantized** in units of material-independent fundamental constants over a range of photon energies

The rate of change of the difference in photocurrent generated by left-circularly and right-circularly polarized light, dj/dt, is quantized to the **Chern number**

Experiment: Frequency-independent plateau at low photon energy abruptly falls-off above 0.66 eV

RhSi

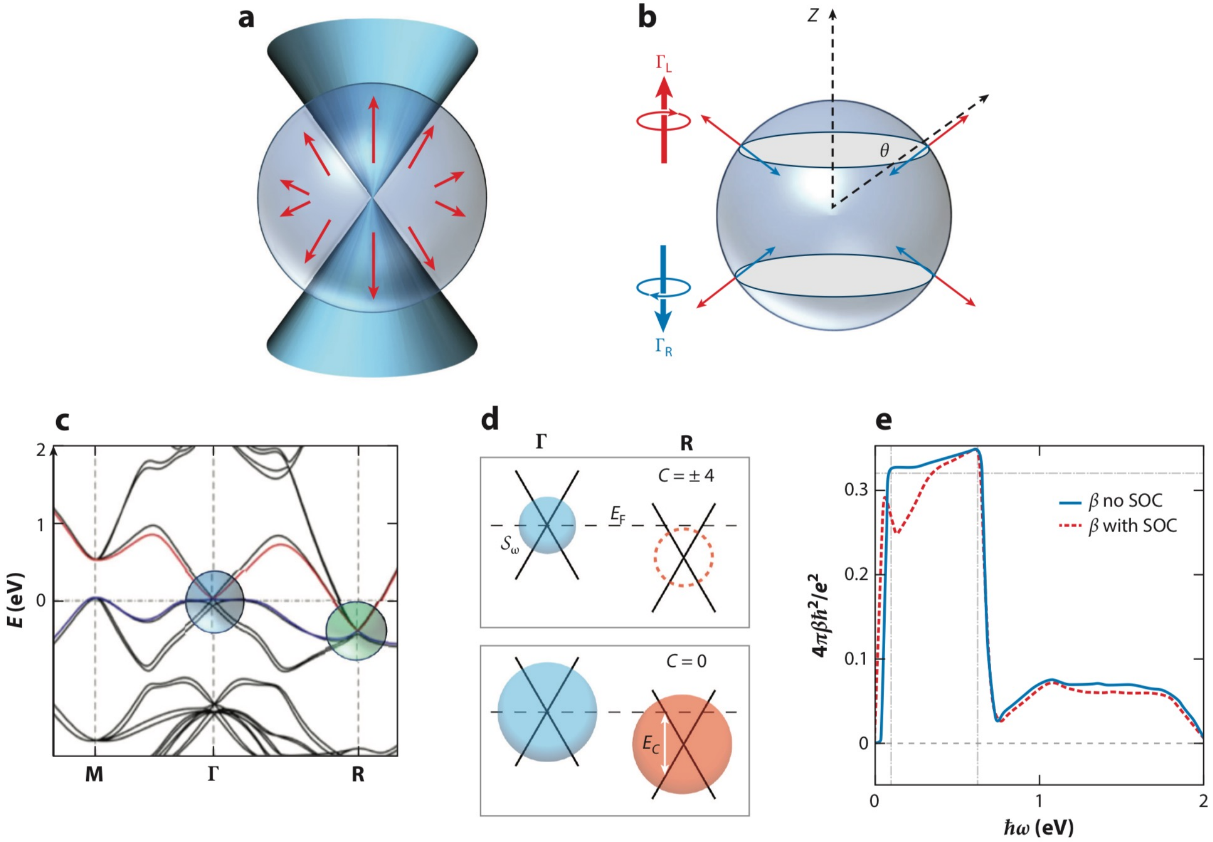

Rees et al., Science Advances 6 (2020) eaba0509, preprint arXiv:1812.04466

Quantized circular photogalvanic effect

ARTICLE

Received 27 Dec 2016 | Accepted 18 May 2017 | Published 6 Jul 2017 DOI: 10.1038/ncomms15995 OPEN

Quantized circular photogalvanic effect in Weyl semimetals

Fernando de Juan[1,2,3], Adolfo G. Grushin[1], Takahiro Morimoto[1] & Joel E. Moore[1,4]

Prediction: Excitation of Weyl fermions –
a **current that is quantized** in units of material-independent fundamental constants over a range of photon energies

The rate of change of the difference in photocurrent generated by left-circularly and right-circularly polarized light, dj/dt, is quantized to the **Chern number**

Experiment: Frequency-independent plateau at low photon energy abruptly falls-off above 0.66 eV

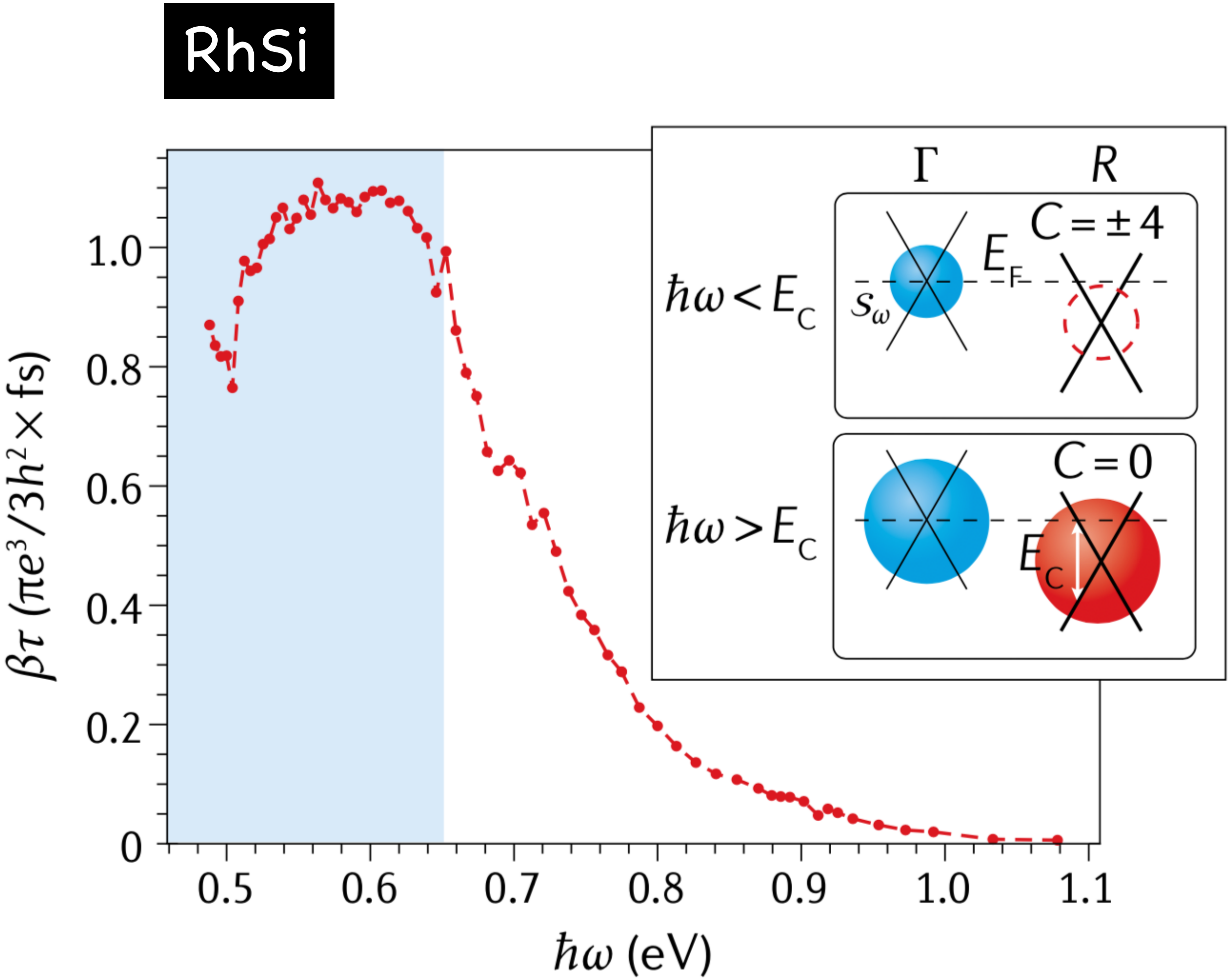

Rees et al., Science Advances 6 (2020) eaba0509, preprint arXiv:1812.04466

Quasi-symmetry-protected topology

a new concept of hidden or quasi symmetries: avoided crossings with small gaps but large Berry curvature in the electronic bands of the topological semimetal CoSi.

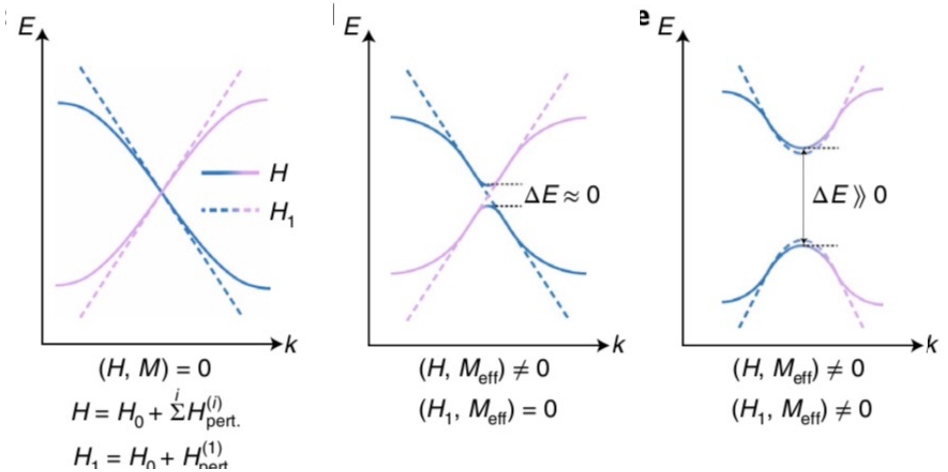

CoSi

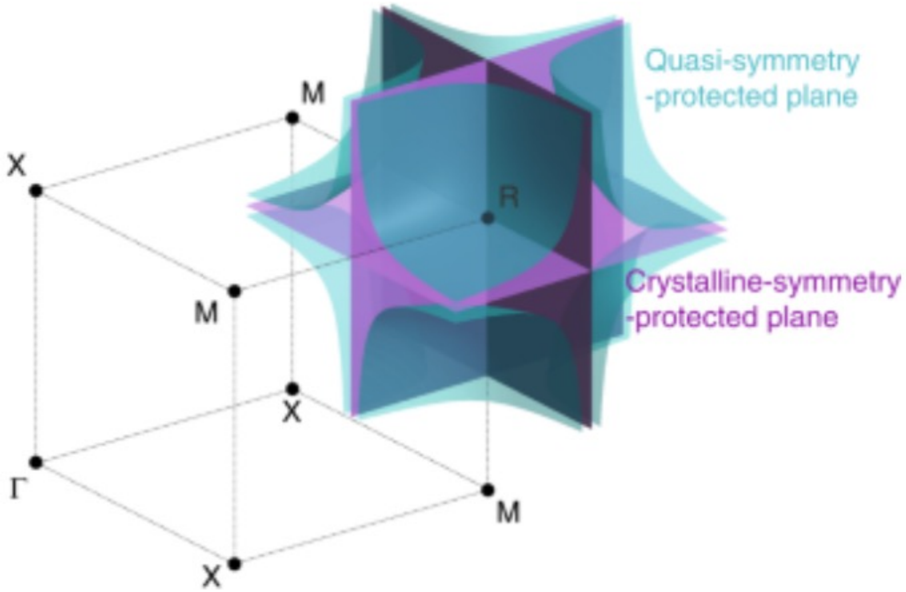

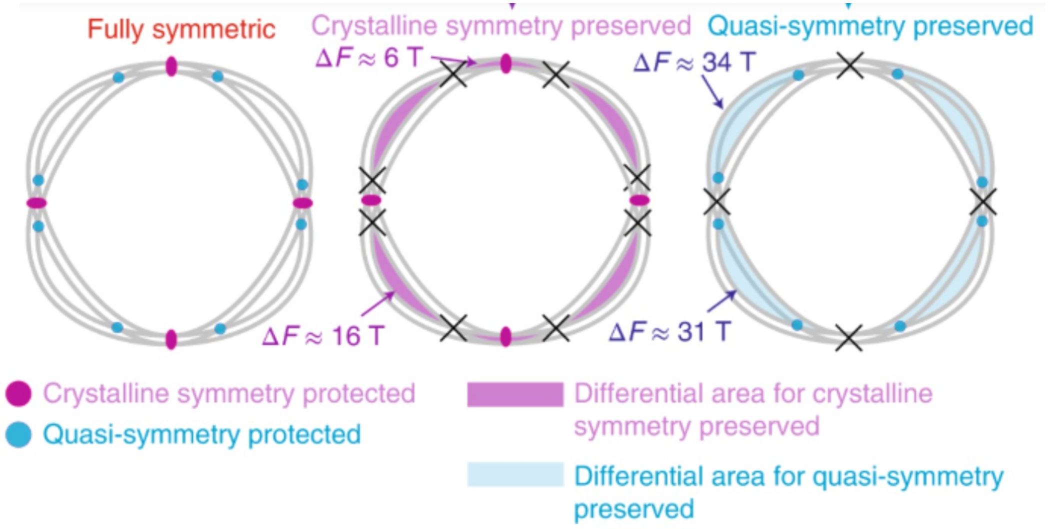

Chunyu Guo,et al. , Nature Physics online arXiv:2108.02279 and new and views from Marc A. Wilde and Christian Pfleiderer

chiral surface states in CoSi

RhSi and CoSi: with multiple helicoid arc saddle points: type-I and type-II van Hove singularities.

CoSi

Charge instability of topological Fermi arcs in chiral crystal CoSi

Zhicheng Rao[1,2,†], Quanxin Hu[1,2,†], Shangjie Tian[3,†], Shunye Gao[1,2], Zhenyu Yuan[1,2], Cenyao Tang[1,2], Wenhui Fan[1,2], Jierui Huang[1,2], Yaobo Huang[4], Li Wang[5], Lu Zhang[1,2], Fangsen Li[5], Huaixin Yang[1,2,6], Hongming Weng[1,2,6], Tian Qian[1,2,6], Jinpeng Xu[1,2,7*], Kun Jiang[1,2], Hechang Lei[3*], Yu-Jie Sun[8,1*] and Hong Ding[1,6,7]

Chirality locking charge density waves in a chiral crystal

Geng Li[1,2,3,4#], Haitao Yang[1,2#], Peijie Jiang[1,2#], Cong Wang[5#], Qiuzhen Cheng[1,2], Shangjie Tian[5], Guangyuan Han[1,2], Chengmin Shen[1,2], Xiao Lin[1,2], Hechang Lei[5*], Wei Ji[5*], Ziqiang Wang[6*], Hong-Jun Gao[1,2,3,4*]

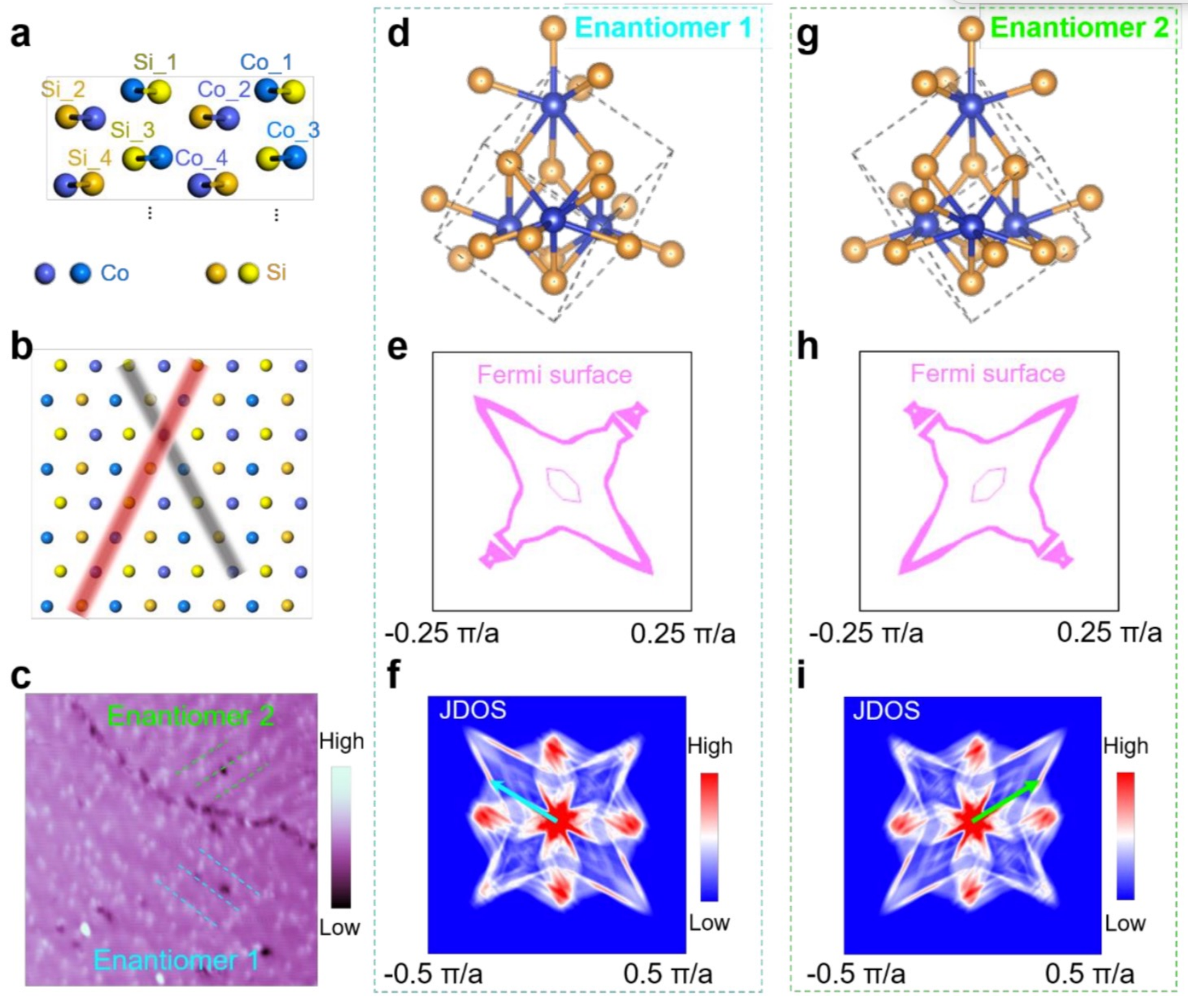

chiral surface states in CoSi and RhSi

RhSi and CoSi: with multiple helicoid arc saddle points: type-I and type-II van Hove singularities.

$Ni_xRh_{1-x}Si$

Tunable topologically driven Fermi arc Van Hove singularities

Daniel S. Sanchez *,[1,2] Tyler A. Cochran *,[1] Ilya Belopolski,[1,3] Zi-Jia Cheng,[1] Xian P. Yang,[1] Yiyuan Liu,[4] Tao Hou,[5] Xitong Xu,[4] Kaustuv Manna,[6,7] Chandra Shekhar,[6] Jia-Xin Yin,[1] Horst Borrmann,[6] Alla Chikina,[8] Jonathan D. Denlinger,[9] Vladimir N. Strocov,[8] Weiwei Xie,[10] Claudia Felser,[6] Shuang Jia,[4] Guoqing Chang †,[5] and M. Zahid Hasan †[1,11,12]

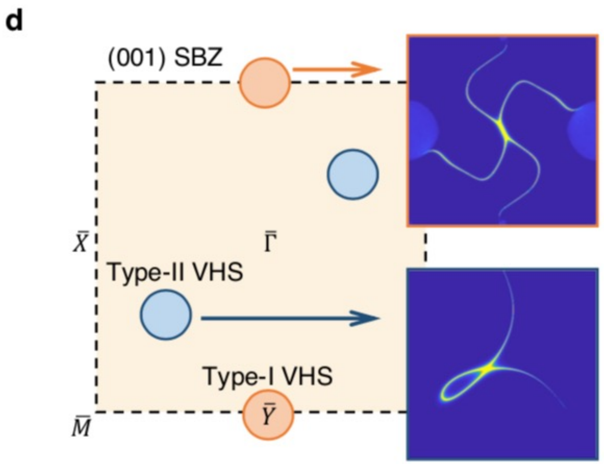

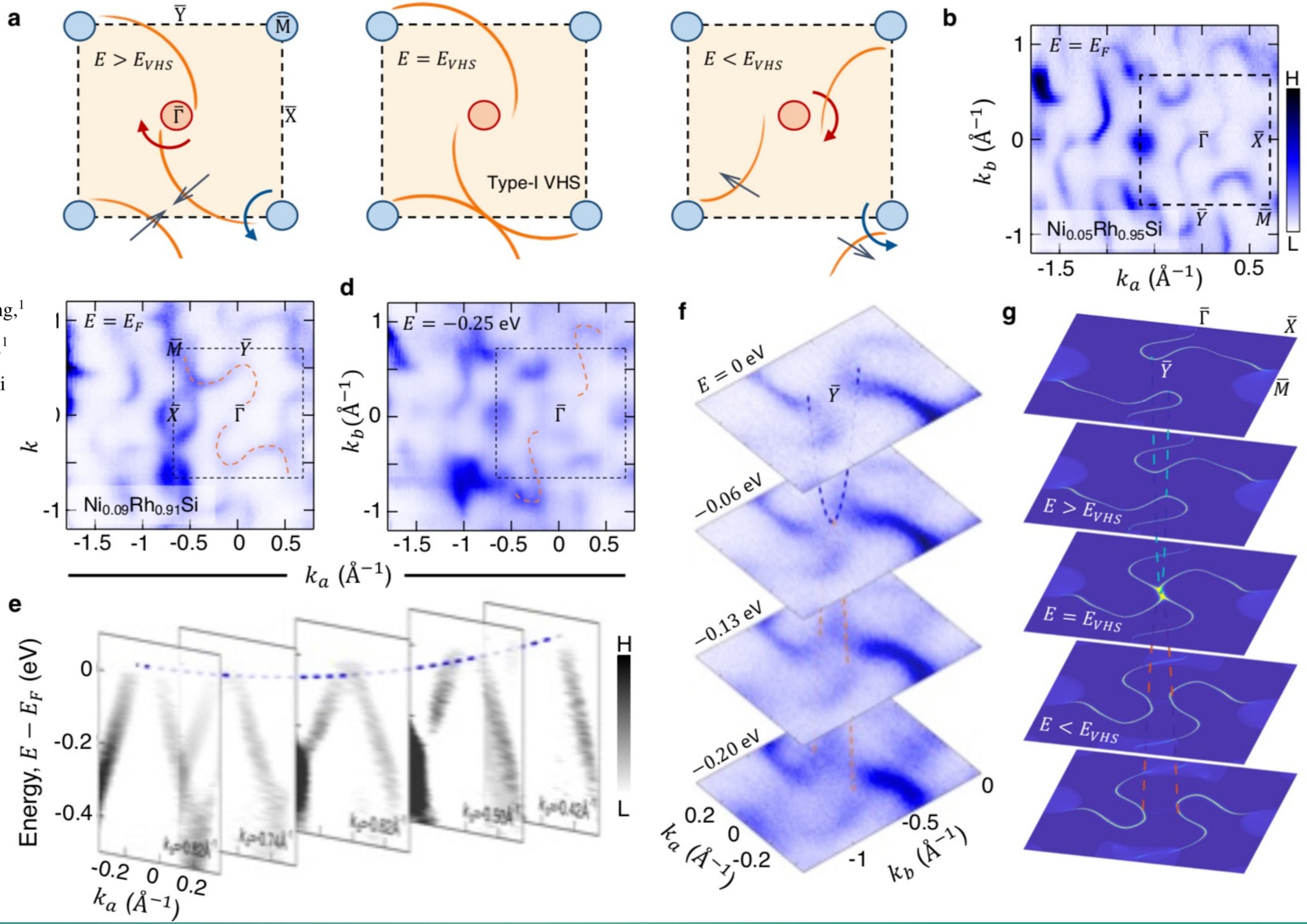

new catalysist with chiral surface states

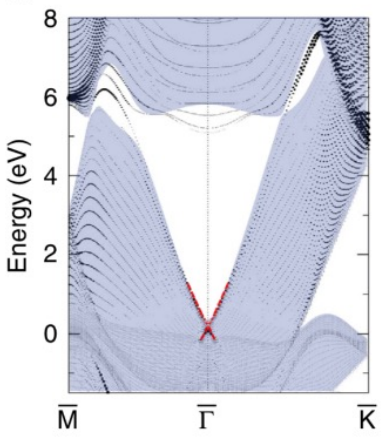

Surface State of Platinum

B. Yan, et al. Nat. Commun. 2015, 6, 10167.

better than Pt for hydrogen evolution reaction (HER) and IrO_2 (OER, oxygen evolution reaction)

Pt and IrO_2 are topological
relativistic effects and spin orbit coupling

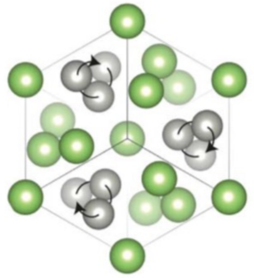

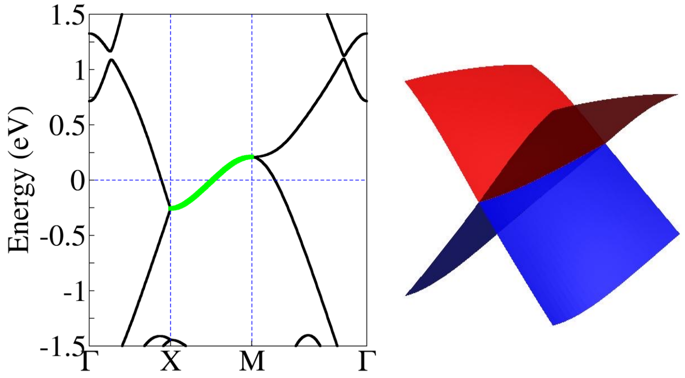

Nodal line in IrO_2

X. Xu et al. Phys. Rev. B 99 (2019) 195106

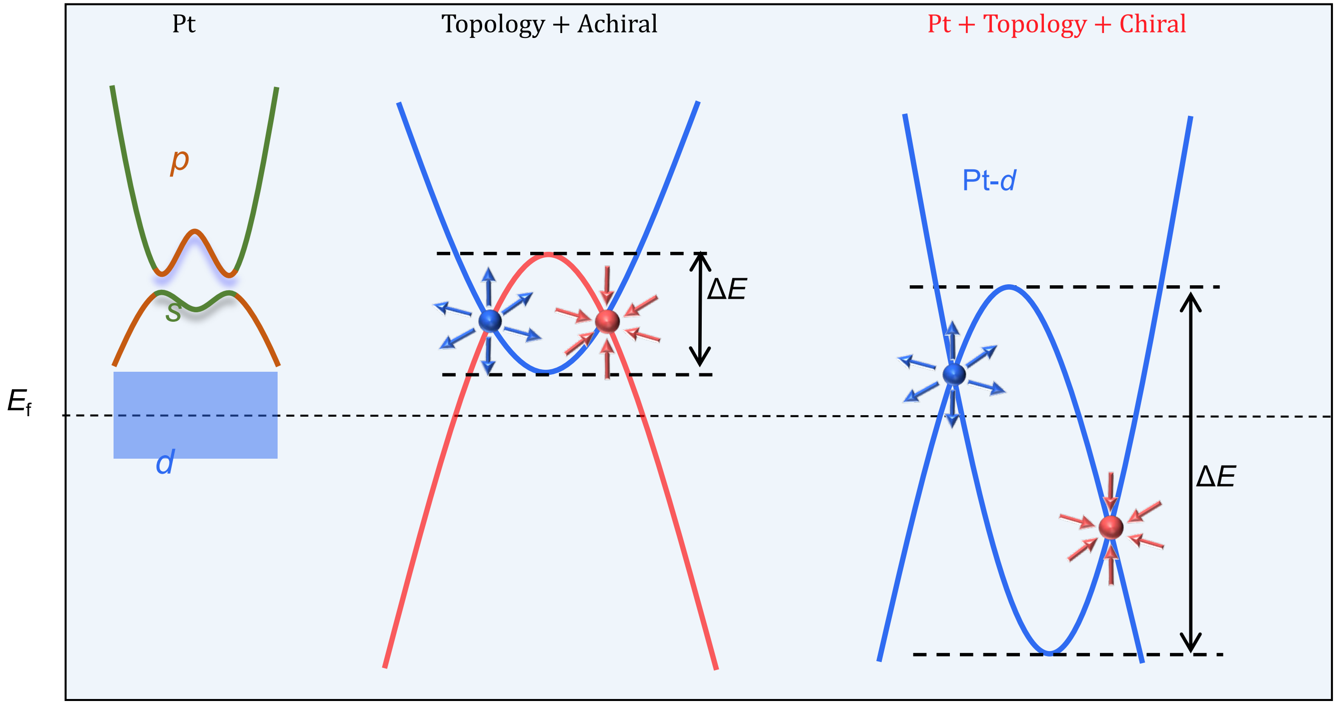

Q. Yang, et al, Adv. Mater., 2020, 32,1908518.
Chiral crystals for Water electrolysis and fuel cells, European patent, 19211719.0, submission 27.11.2019

new catalysist with chiral surface states

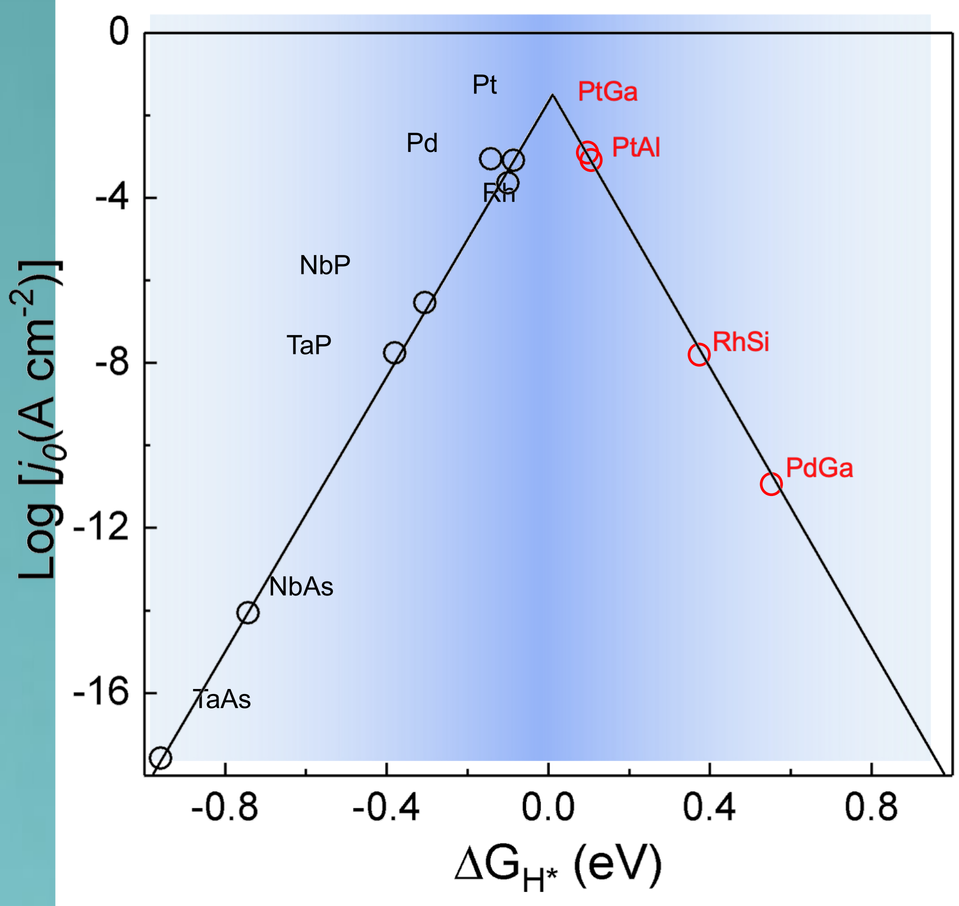

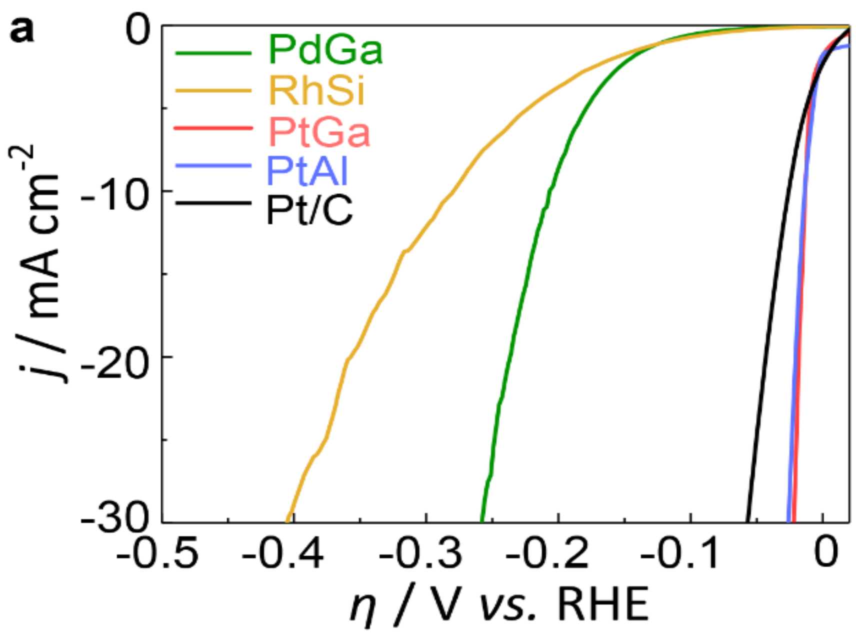

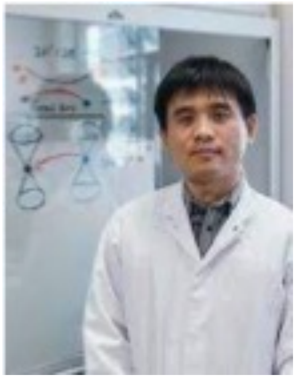

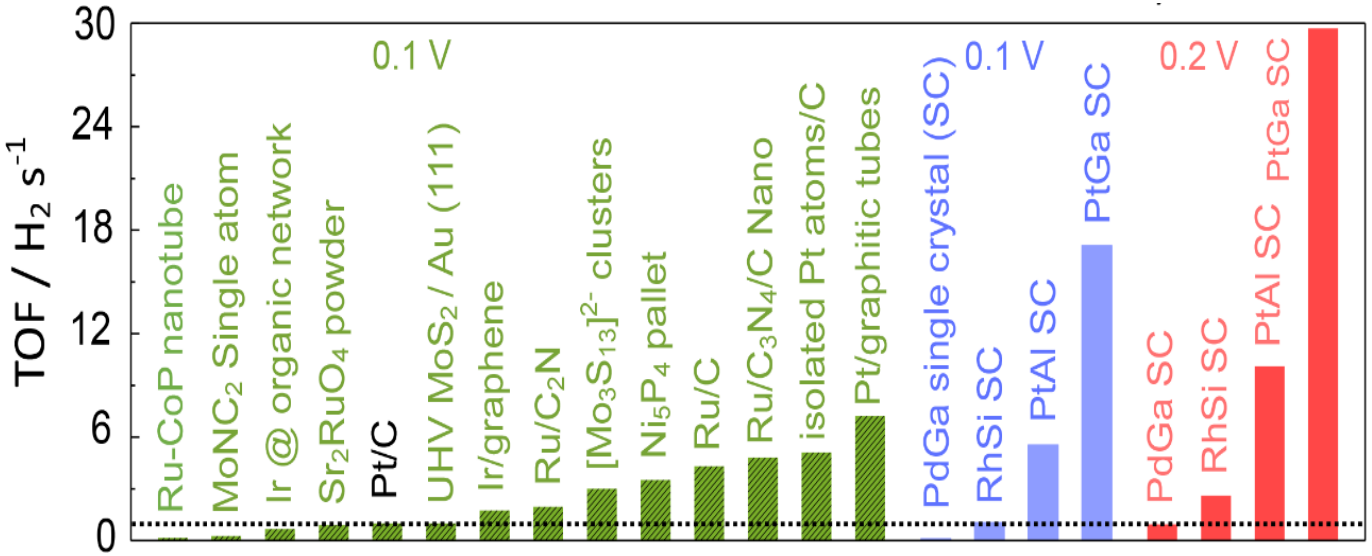

Qun Yang, et al. Advanced Materials 32 (2020) 1908518

absorption and oxidation of chiral molecules

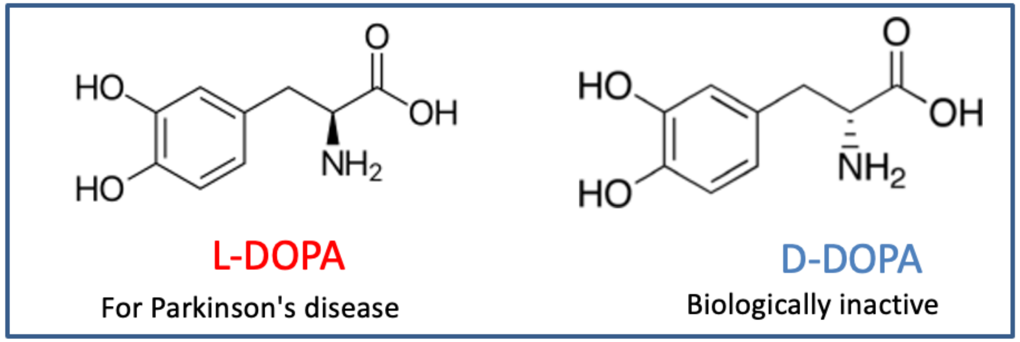

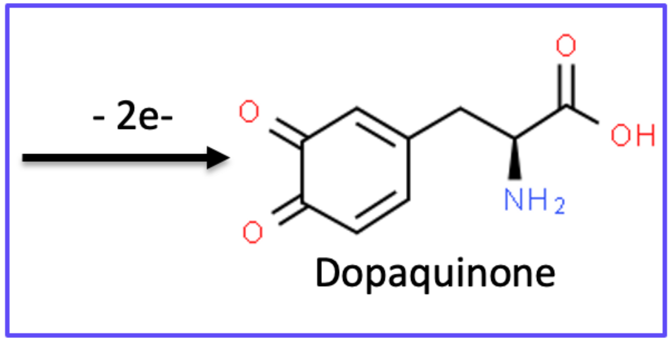

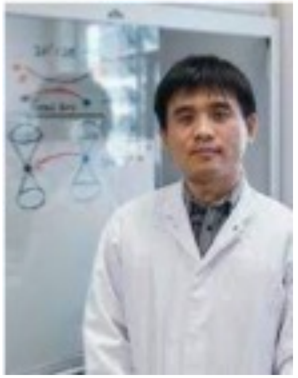

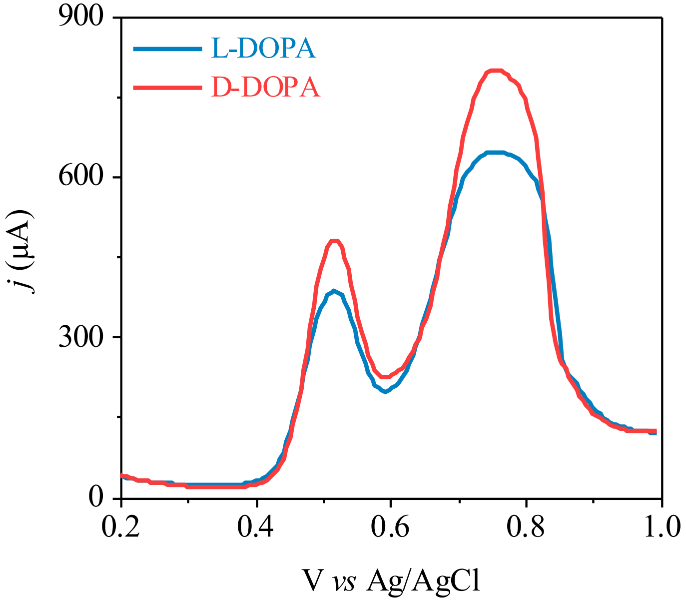

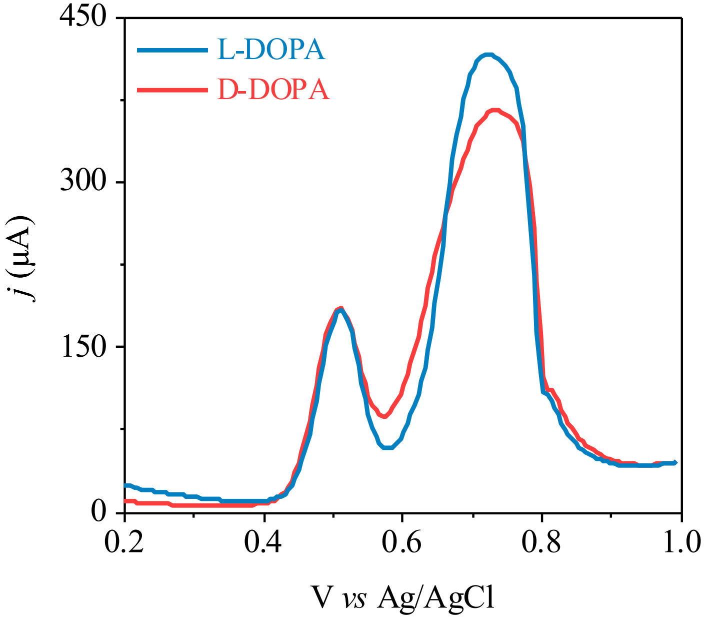

oxidation of Dopa on the surface of PdGa
all the measurement conditions are kept the same except the chirality of the PdGa crystal
D-DOPA and L-DOPA show different oxidation behaviors, depending on the chirality of PdGa

electrons – molecules, surfaces and crystals

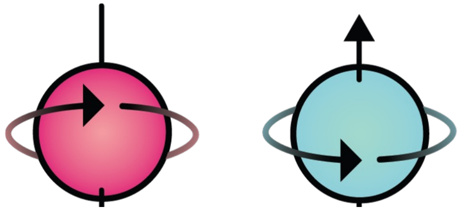

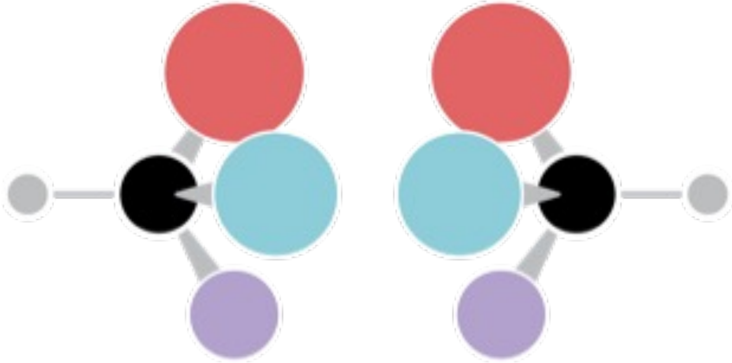

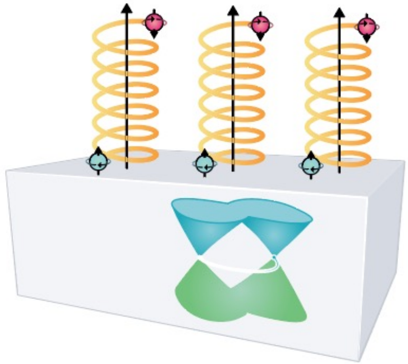

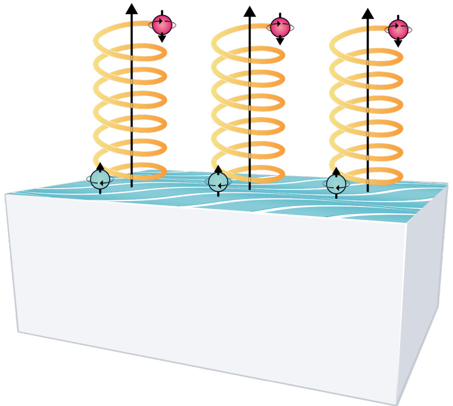

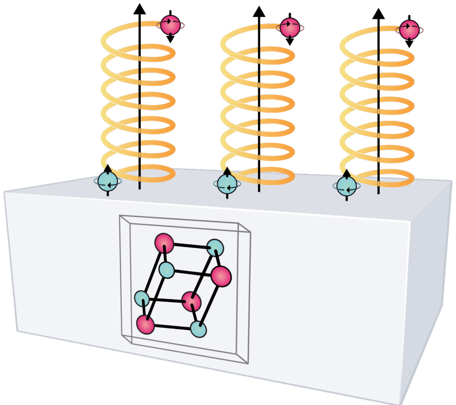

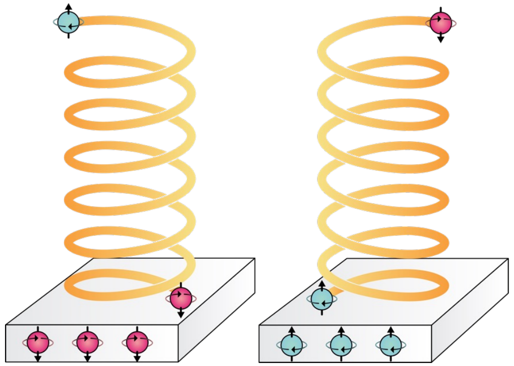

physics meets chemistry

parity violation

Vacuum state

elementary particles

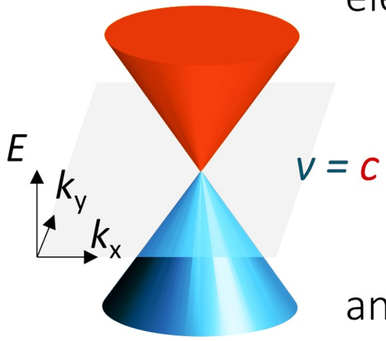

$v = c$

anti-particles

vacuum dispersion

Dirac semimetal

'electrons'

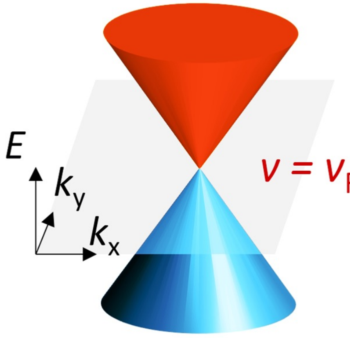

$v = v_F \approx 0.001\,c$

'holes'

band structure

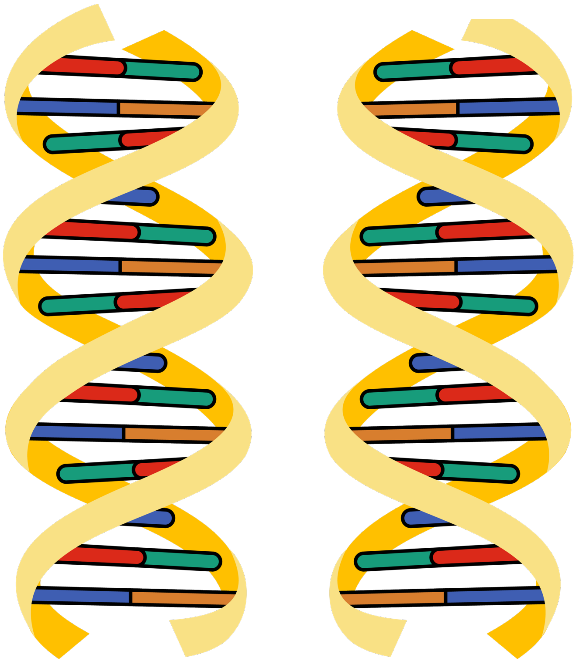

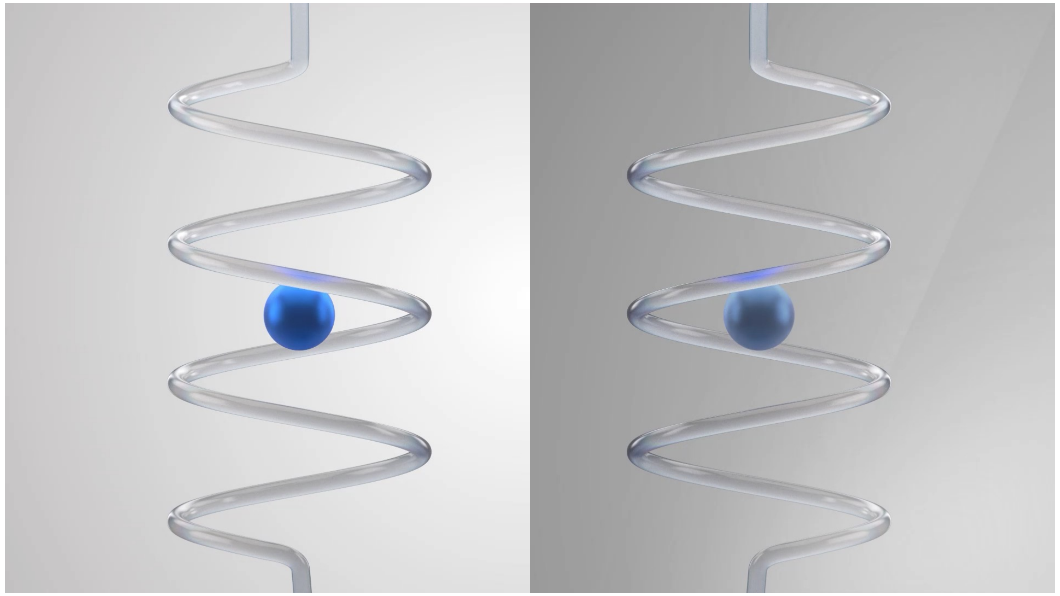

Wu experiment

β-decay

direction of electrons

chirality in Charge density wave systems

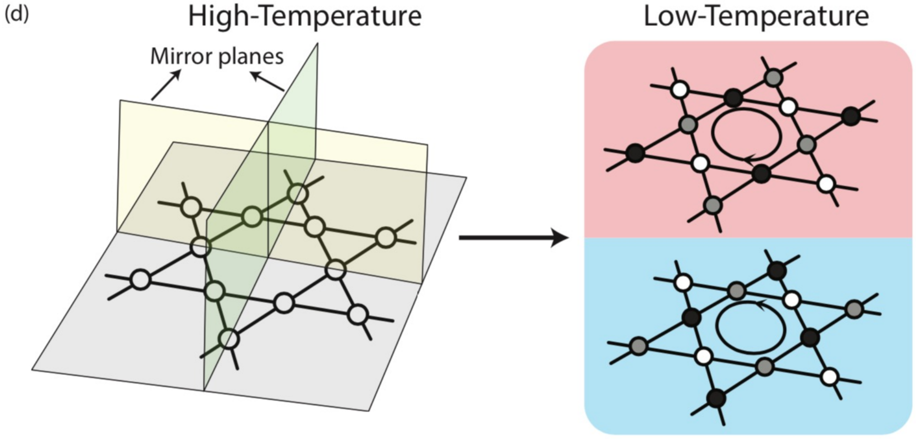

Switchable chiral transport in charge-ordered CsV_3Sb_5

Chunyu Guo*,[1] Carsten Putzke,[1,2] Sofia Konyzheva,[1] Xiangwei Huang,[1] Martin Gutierrez-Amigo,[3,4] Ion Errea,[3,5,6] Dong Chen,[7] Maia G. Vergniory,[5,7] Claudia Felser,[7] Mark H. Fischer*,[8] Titus Neupert†,[8] and Philip J. W. Moll‡[1,2]

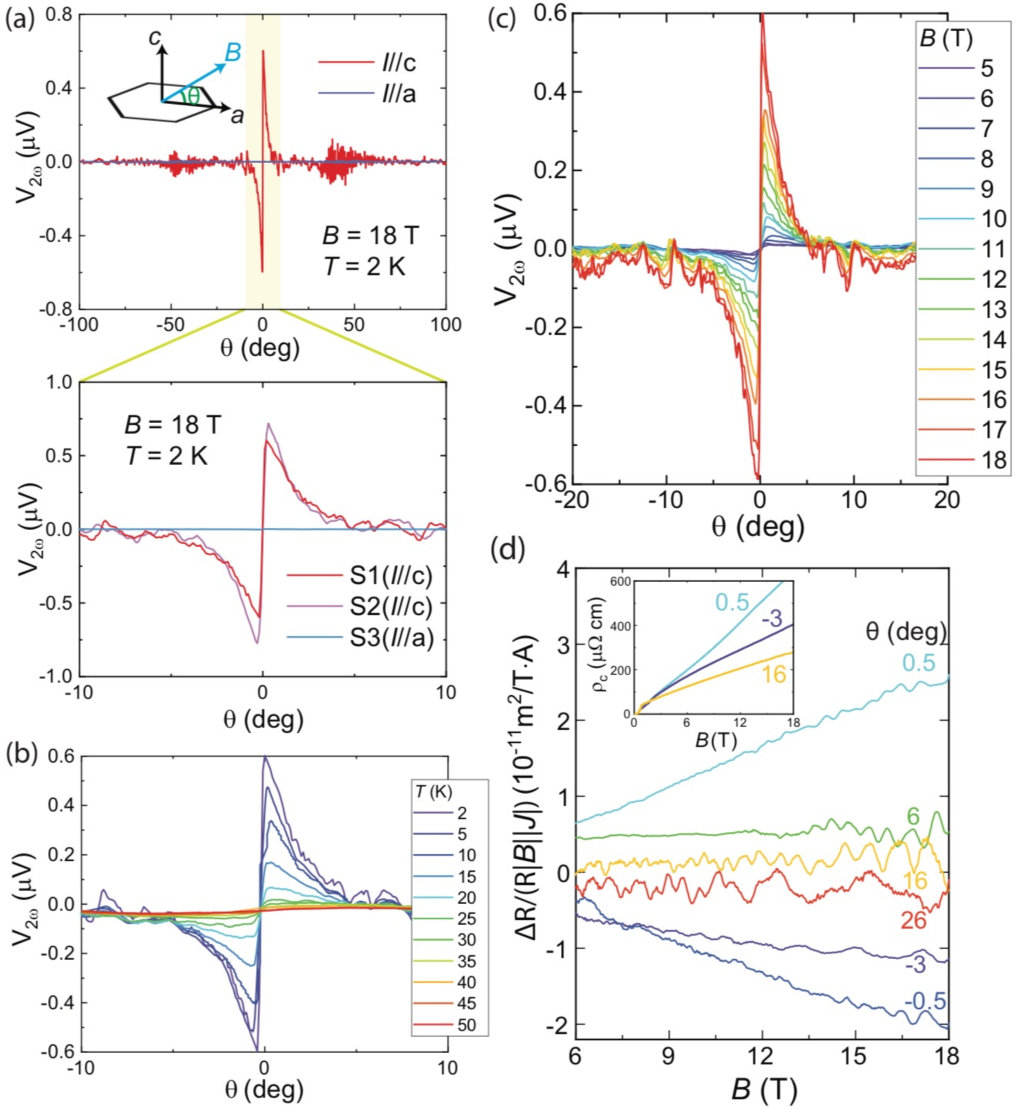

Guo et al., Nature accepted, preprint arXiv:2203.09593

chirality in Charge density wave systems

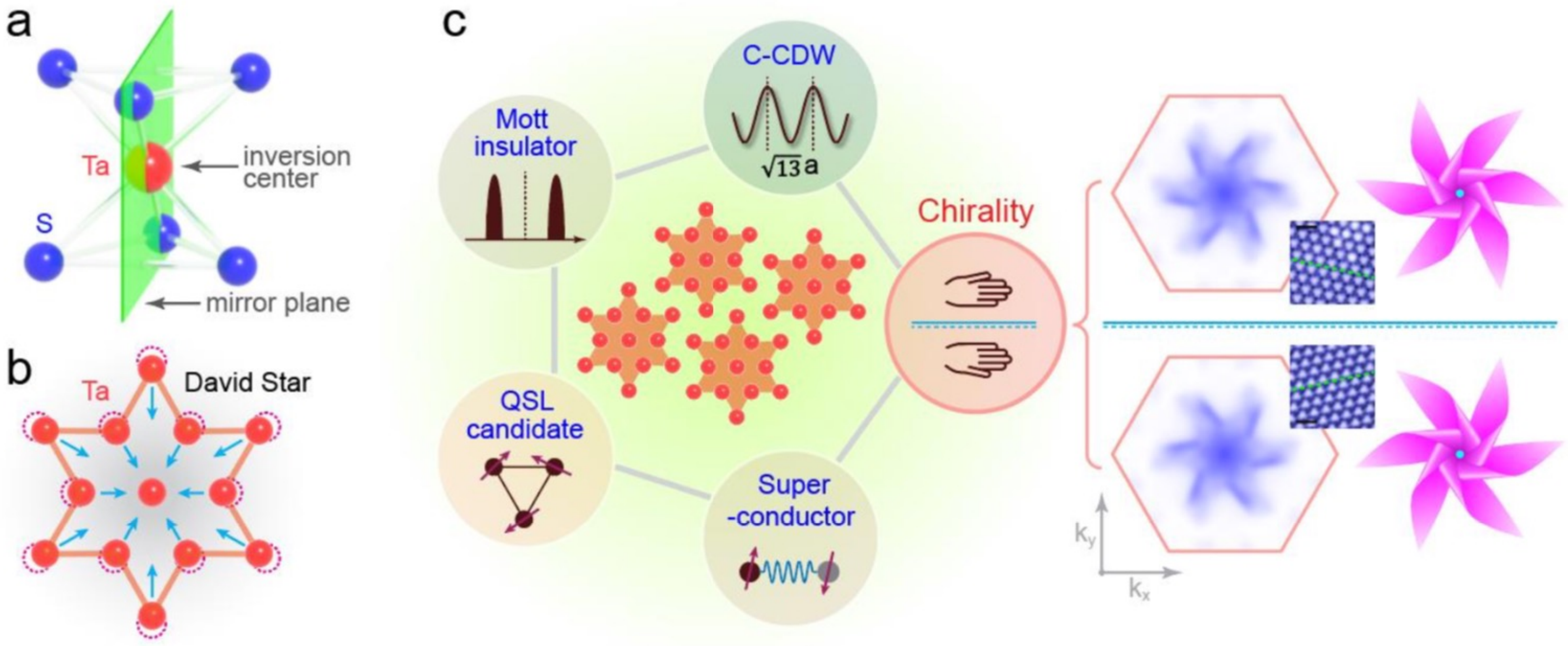

TaS_2

Visualization of Chiral Electronic Structure and Anomalous Optical Response in a Material with Chiral Charge Density Waves

H. F. Yang[1*], K. Y. He[2*], J. Koo[3*], S. W. Shen[1], S. H. Zhang[1], G. Liu[2], Y. Z. Liu[3], C. Chen[1,4], A. J. Liang[1,5], K. Huang[1], M. X. Wang[1,5], J. J. Gao[6], X. Luo[6], L. X. Yang[7], J. P. Liu[1,5], Y. P. Sun[6,8,9], S. C. Yan[1,5], B. H. Yan[3†], Y. L. Chen[1,4,5,7†], X. Xi[2,9†], and Z. K. Liu[1,5†]

summary

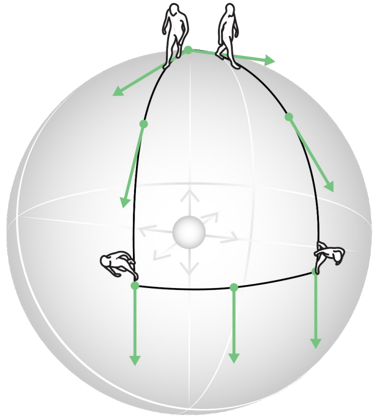

Berry Phase

- topologically protected surfaces edge or edge states in crystals
- new quantum effects in crystals
- in semimetals one observes giant effects in response of magnetic, electric field, light etc.
- Fermi arcs
- arcs extended over the recirpoken space in chiral crystals
- high mobilities, free electron path lengths up to mm
- giant Nernst effect and magnetic Seebeck effect
- giant photovoltaic effect - quantized
- Weyl semimetals as model systems for high energy and astrophysics
- Parity violation E*B in Weyl semimetals
- chiral anomaly
- axial graviation anomaly
- topological catalysis

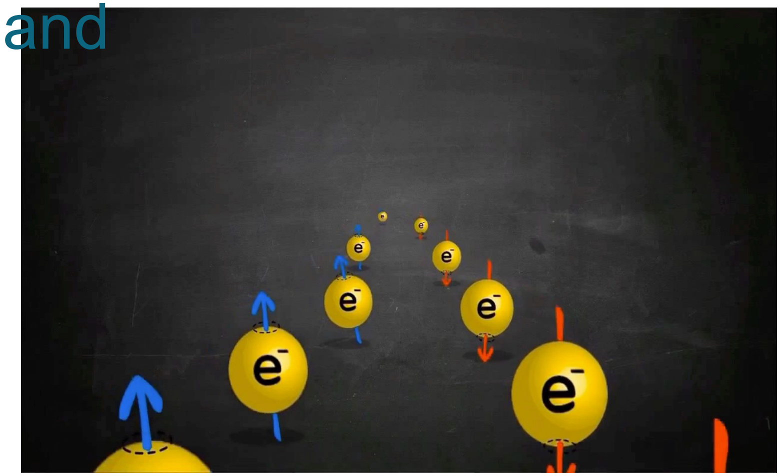

summary

- more than **25% of all inorganic compounds are topological**
- quantum simulator for high energy and astro-physics
- paramagnetic Weyl semimetals, which break inversion: **chiral anomaly** in thermal and electrical transport
- chiral new Fermions: giant Fermi arcs, strong **Berry curvature effects**, new chiral optical effects

outlook

- chirality and magnetism
- **beyond the single particle picture** – topology in correlated materials
- experiments and understanding of **3D quantum Hall** effects
- connect chiral molecules and catalysis with Berry curvature
    - the interplay between chiral structure/surface state/orbital moment

potential applications

- energy conversion
    - catalysis …
- spintronics
- quantum computing

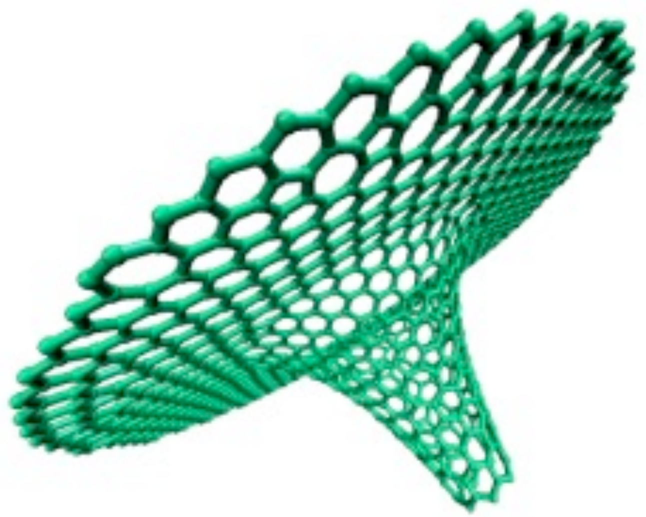

arXiv:1511.07672v1

Vision

- Crystal growth of both enantiomers of topological chiral compounds
  - interfaces, grain boundaries, chiral phonons, magnons, …
  - Investigation of the interplay between structure, chiral surface state, orbital angular momentum, spin momentum locking …
  - strain and magnetic field

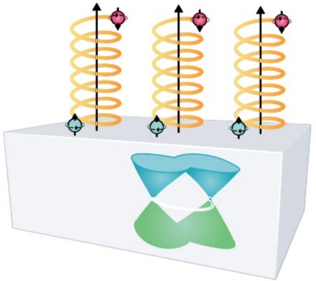

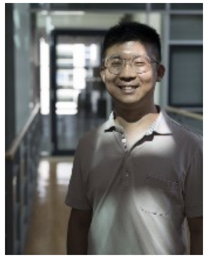

- Chiral electrons, chiral Fermions, chiral surfaces and **catalysis**
  - enhanced light matter interaction and magnetic field

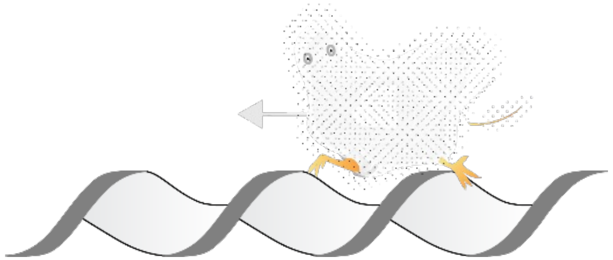

- Non local transport in chiral crystals
  - spin polarized currents over μm

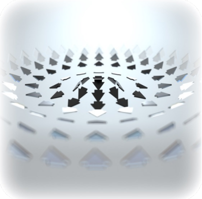

- Chirality plus magnetism, correlations, superconductivity
  - Skyrmions, Antiskyrmions …

Potentielle Anwendungen

New Konzepte zur Energiekonversion

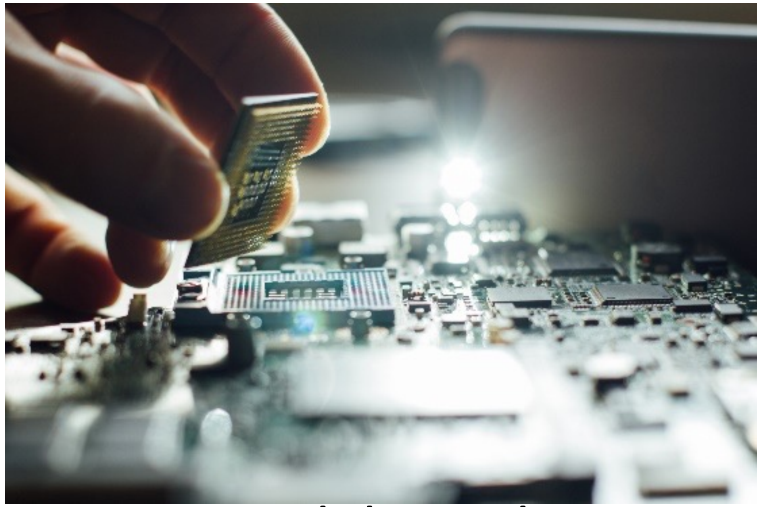

Neue Elektronik – Spin

Verlustfreier Elektronentransport

IBM

Microsoft

Google

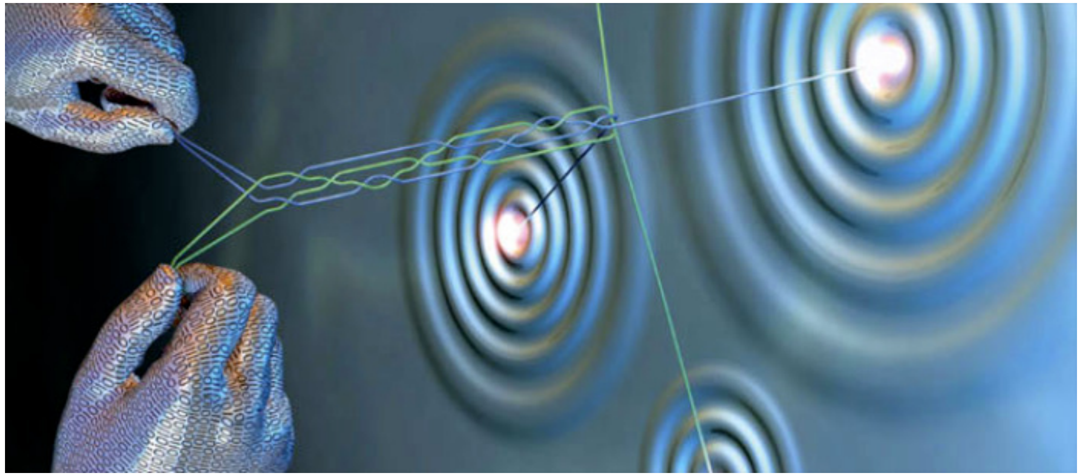

Ultraschnelle Quantencomputer

Thank you!

Johannes Gooth

Niels Schröter

Andrei Bernevig

Maia Vergniory

erc

Alexander von Humboldt
Stiftung/Foundation

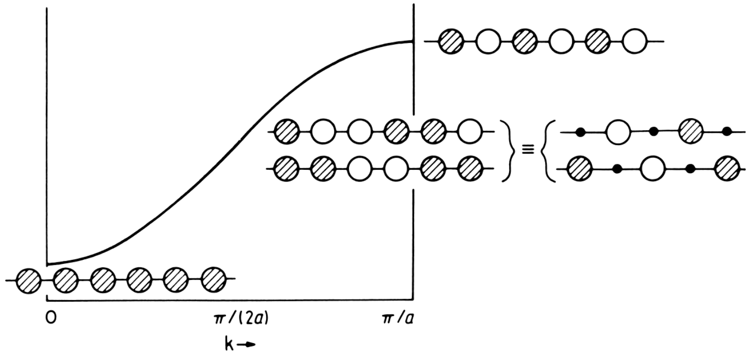

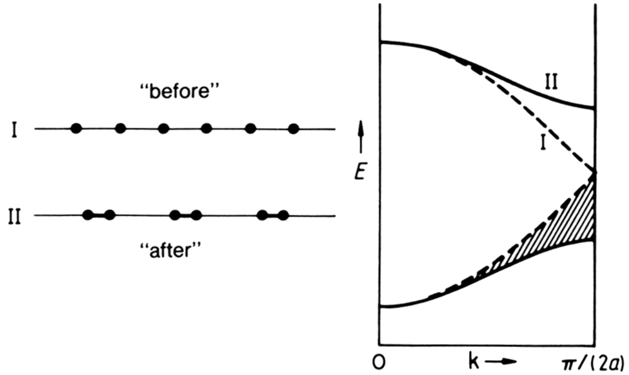

a‘= 2a
k= π/2a

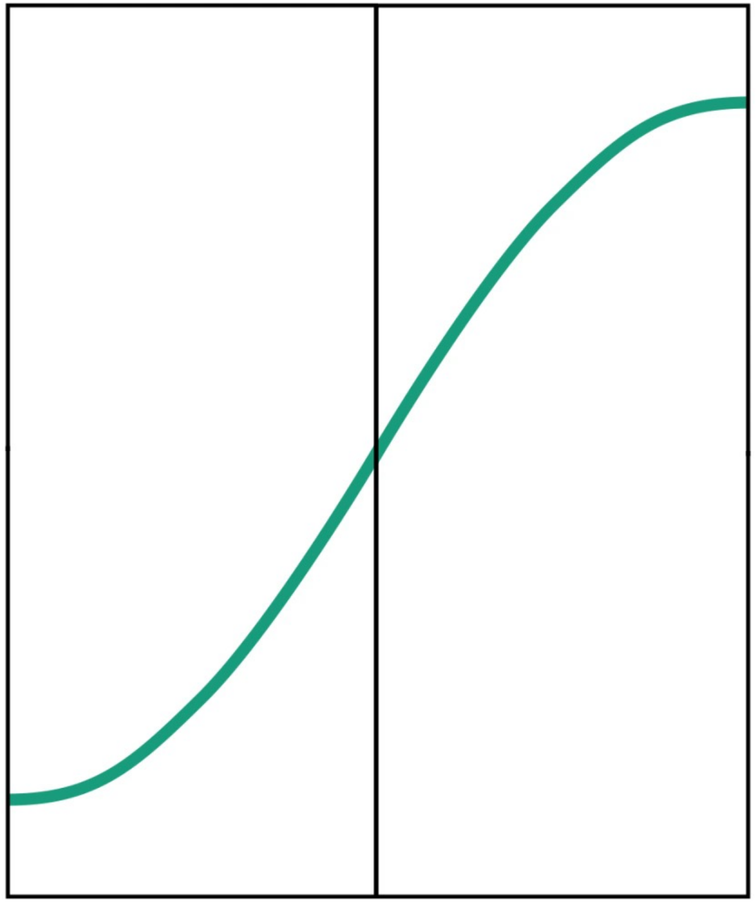

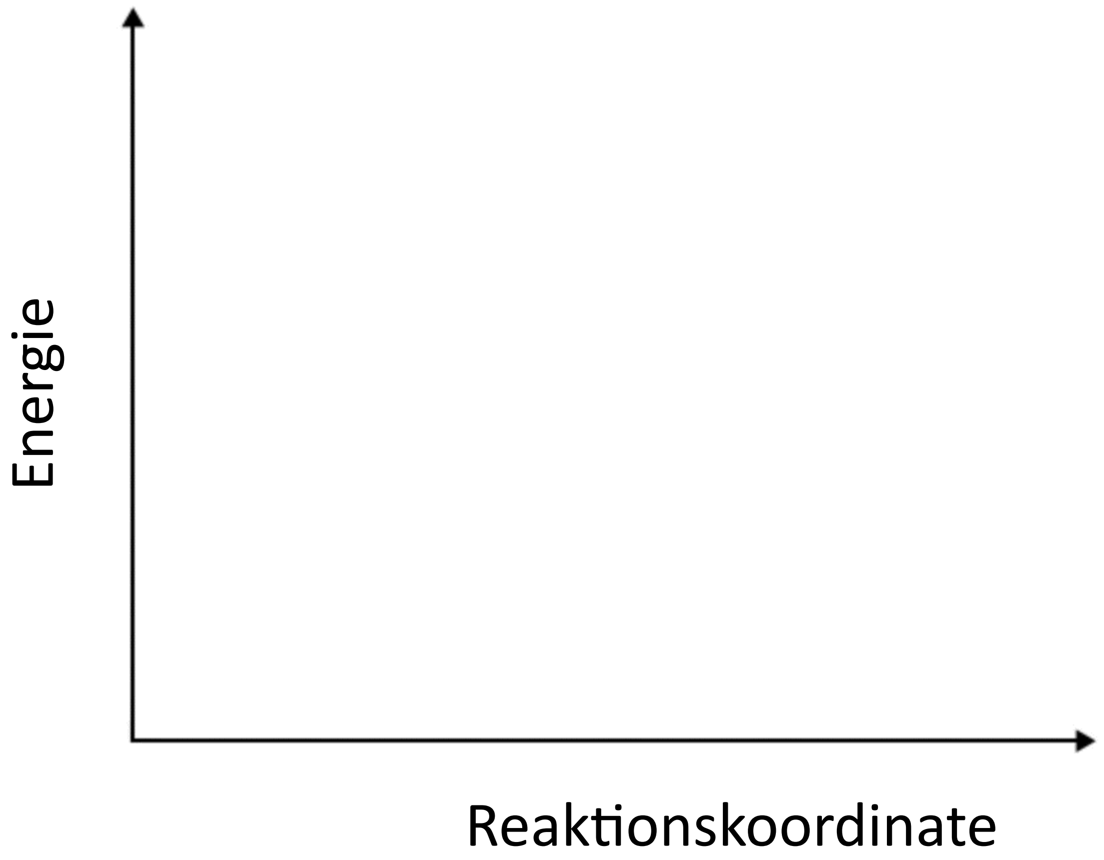
Energie
Reaktionskoordinate

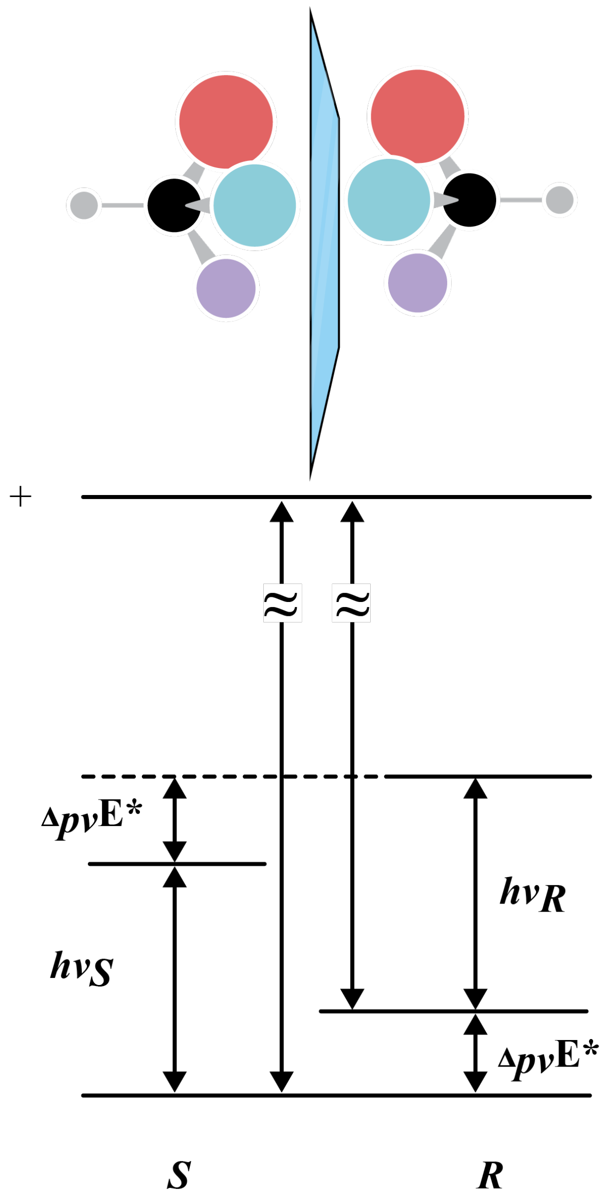

ΔpvE*
hνS
hνR
ΔpvE*
S
R